Proteomic characterization of host-pathogen interactions using human cell lines infected with *Staphylococcus aureus* HG001 as a model

I n a u g u r a l d i s s e r t a t i o n

zur
Erlangung des akademischen Grades eines
Doktors der Naturwissenschaften (Dr. rer. nat.)
der
Mathematisch-Naturwissenschaftlichen Fakultät
der
Ernst-Moritz-Arndt-Universität Greifswald

vorgelegt von
Kristin Surmann
geboren am 07.02.1985
in Leipzig

Greifswald, 17.10.2014

Dekan: Prof. Dr. Klaus Fesser.....

1. Gutachter: Prof. Dr. Uwe Völker.....

2. Gutachter: Prof. Dr. Jan Maarten van Dijl.....

Tag der Promotion: 15.12.2014.....

CONTENT

ABBREVIATIONS

(m/v)/(m/m)/(v/v)	(mass to volume)/(mass to mass)/(volume to volume)
ABC	ammonium bicarbonate
ACN	acetonitrile
AQUA	absolute quantification
ATP/ADP/AMP	adenosine-tri-/di-/monophosphate
Au/FeOx	gold/ferric oxide
AUC	area under the curve
B. pertussis	*Bordetella pertussis*
BLAST	basic local alignment search tool
BR	biological replicate
BSA	bovine serum albumin
c	concentration
CBB/CCD/CCS	Coomassie Brilliant Blue/colloidal Coomassie stock/colloidal Coomassie solution
CCB	cacodylate buffer
CE	collision energy
CFP/GFP/YFP	cyan/green/yellow fluorescent protein
CFU	colony forming units
CID/HCD	collision induced dissociation/higher energy collisional dissociation
CSF	colony stimulation factor
CV	coefficient of variation
DDA/DIA	data dependent/independent analysis
DMEM	Dulbecco's Modified Eagle's medium
DMSO	dimethylsulfoxide
DTT	dithiothreitol
e.g.	for example
Em/Ex	emission/excitation
eMEM/pMEM	eukaryotic/prokaryotic minimal essential medium
ESI	electrospray ionization
FACS	fluorescence assisted cell sorting
FBS	fetal bovine serum
FC	fold change
FDR	false discovery rate
FITC	fluorescein isothiocyanate
FSC/SSC	forward/side scatter
FWHM	full width at half maximum
GA	glutaraldehyde
GC/LC-MS	gas/liquid chromatography-mass spectrometry
GF	growth factor
HAc	acetic acid
HEPES	4-(2-hydroxyethyl)-1-piperazineethanesulfonic acid
IAA	iodoacetamide
Ig	immunoglobulin
IL	interleukin
IPA	Ingenuity Pathway Analysis
LSU/SSU	large/small ribosomal subunit
m/z	mass to charge
MeOx	o-methylhydroxylamin-hydrochlorid
MOI	multiplicity of infection

MRM/SRM	multiple/single reaction monitoring
MRSA/VRSA	methicillin resistant *S. aureus*/vancomycin resistant *S. aureus*
MSCRAMM	microbial surface component recognizing adhesive matrix molecules
MS	mass spectrometry
MSTFA	N-methyl-N-tri-methylsilyltrifluoracetamide
nanoLC-MS/MS	nano flow liquid chromatography coupled to tandem mass spectrometry
NCBI	National Center for Biotechnology Information
NEAA	non-essential amino acids
NP	nanoparticles
OD	optical density
p.i.	post-infection
PBS	phosphate buffered saline
PCA	principal component analysis
PE	phycoerythrin
PFA	paraformaldehyde
PMT	photomultiplier tube
POD	peroxidase
PVA	polyvinyl alcohol
qRT-PCR	quantitative real time polymerase chain reaction
RBITC	rhodamine B isothiocyanate
RP	reversed phase
RT	retention time
S. aureus	*Staphylococcus aureus*
SAg	super antigen
SCV	small colony variants
SDS	sodium dodecyl sulfate
SILAC	stable isotope labeling in of amino acids cell culture
t	time
TCA	tricarboxylic acid cycle
TCEP	tris-2-carboxyethyl-phosphine
TCS	two component system
TEM	transmission electron microscopy
TFA	trifluoroacetic acid
TNF	tumor necrosis factor
TPP	trans-proteomic pipeline
trypsin-EDTA	trypsin-ethylenediaminetetraacetic acid
TSB	tryptic soy broth
TSB-T	tris-buffered saline-Tween
TSP	3-trimethylsilyl-[2,2,3,3-D4]-1-propionic acid
TSS	toxic shock syndrome
UT-buffer	urea thiourea buffer
XIC	extracted ion chromatogram

ZUSAMMENFASSUNG DER DISSERTATION

Infektionskrankheiten, besonders Lungeninfektionen, gehören noch immer zu den häufigsten Todesursachen weltweit. Erschreckenderweise werden immer noch viele der tödlichen Keime im Krankenhaus erworben. Dies gilt auch für Industrienationen mit hohen Hygienestandards. Der bedeutendste humanpathogene Erreger von nosokomialen Infektionen ist *Staphylococcus aureus*. Er besiedelt die Haut und Schleimhäute von etwa 20-30% der Menschen ohne dabei Krankheiten auszulösen. Wenn dieses Bakterium jedoch in den Körper eindringen kann, ist es fähig, eine Reihe von Krankheiten zu verursachen, welche vor allem bei Personen mit geschwächtem Immunsystem lebensbedrohliche Folgen haben können. Das Krankheitsspektrum umfasst leichtere Hautinfektionen wie Furunkel, ebenso wie toxinvermittelte Erkrankungen. Zudem können Infektionen mit *S. aureus* auch die Organe betreffen und schwere Krankheiten wie Lungenentzündung, Nierenentzündung, Knochenentzündungen oder Endokarditis bis hin zu Sepsis auslösen. Erschwerend kommt hinzu, dass sich einige hochpathogene Stämme entwickelt haben, die gegen den Großteil der derzeit verfügbaren Antibiotika resistent sind. Die Vielzahl der Stämme mit unterschiedlichsten Eigenschaften und Anpassungsmöglichkeiten ist auch ein Grund dafür, dass bis jetzt noch kein erfolgreich einsetzbarer Impfstoff für Menschen auf dem Markt ist. Daher ist es dringend notwendig neue effektive Strategien für Vorbeugung und Therapie zu entwickeln.

Um all dies zu bewerkstelligen ist das Verständnis des Zusammenspiels von Erreger und Wirt auf molekularer Ebene unabdingbar. *S. aureus* ist mit einer Vielzahl an Faktoren ausgerüstet, die es ihm erlauben in Gewebe einzudringen und sich dort zu verbreiten. Früher wurde angenommen, dass *S. aureus* ein ausschließlich extrazellulärer Krankheitserreger ist. Mittlerweile ist bekannt, dass dieses Pathogen auch in unterschiedlichste nicht-professionell phagozytierende Wirtszellen wie zum Beispiel Epithelzellen eindringen und dort längere Zeit überdauern oder sich sogar vermehren kann. Damit kann es der direkten Eliminierung durch das Immunsystem entkommen. Viele Virulenzfaktoren, welche entweder mit der Zellwand oder der Membran assoziiert sind oder in die Umgebung sezerniert werden, helfen dem Pathogen hierbei. Verschiedene Proteine dienen der Anheftung der Bakterien an unterschiedliche Wirtszellmoleküle, die den ersten Schritt der Aufnahme von *S. aureus* durch die Wirtszelle darstellt. Weiterhin besitzt dieser Erreger ein großes Repertoire an Toxinen, welche die Membranen der Wirtszellen zerstören können. Andere bakterielle Enzyme werden zur Akquirierung von Nährstoffen, wie zum Beispiel Eisen, aus der Umgebung innerhalb des Wirts benötigt. Wiederum andere Proteine helfen *S. aureus* sich gegen das Immunsystem und harsche Bedingungen wie oxidativen Stress zu schützen.

Jedoch ist auch die infizierte Zelle nicht völlig hilflos. Nachdem die Bakterien als Fremdkörper erkannt und aufgenommen werden konnten, befinden sie sich umschlossen von einer Membran in einem sogenannten Phagosom. Dieses kann mit der Zeit mit anderen Wirtsorganellen, den Lysosomen verschmelzen. Letztere schleusen saure Proteasen in die Phagosomen ein, wodurch die

darin enthaltenen Bakterien lysiert und unschädlich gemacht werden können. Auch die Bildung von reaktiven Sauerstoffspezies ist eine Abwehrreaktion der eukaryotischen Zelle. *S. aureus* ist in der Lage, sich zum einen an die Bedingungen im Phagosom anzupassen und sich durch Phänotypänderung innerhalb der Zelle als sogenannte „*small colony variants*“ zu „verstecken“. Zum anderen sind einige Stämme in der Lage mit Hilfe von bestimmten Proteinen, den phenollöslichen Modulinen, die Phagosomenmenbran zu zerstören und sich anschließend im Zytoplasma auszubreiten und damit die Wirtszelle zu töten. Letztere kann in diesem Fall allerdings auch die Apoptose, den selbstverursachten Zelltod der Eukaryoten mitsamt den enthaltenen Bakterien durch spezielle Proteasen, den Caspasen, auslösen, wodurch eine weitere Ausbreitung der Infektion auf Nachbarzellen verhindert werden kann. Zusätzlich können auch Epithelzellen genau wie Immunzellen im Zellverband bzw. Organismus über kleine Moleküle, die sogenannten Zytokine, miteinander kommunizieren und somit Abwehrketten der angeborenen Immunantwort und damit eine schnelle Antwort auf die Bakterien hervorrufen. Darunter sind sowohl pro- als auch anti-inflammatorische Prozesse zu verstehen, die zum einen zur Eliminierung der Bakterien führen zum anderen aber auch überschießende Abwehrreaktionen des Organismus verhindern sollen. Schwere Erkrankungen treten dann auf, wenn die Immunantwort auf die Bakterien aus dem Gleichgewicht gebracht wird.

Um die Wechselwirkungen von Wirt und Erreger zu analysieren, stehen verschiedene Techniken der Molekularbiologie zur Verfügung. Zelllinienmodelle helfen die Grundlagen der Anpassung beider Partner an die Infektion zu untersuchen, indem diese mit Bakterien inkubiert werden. Dabei können Änderungen der Genexpression auf den Ebenen der Transkripte, der Proteine und der Metabolite unterschieden werden. Proteine sind dabei die Schlüsselmoleküle, die die Anpassungen der Zellen, die in der genetischen Ebene programmiert werden, direkt ausführen. Sie können bewirken, dass sich der Stoffwechsel und die Virulenz der Bakterien entsprechend den Bedingungen der Umgebung einstellen. Heutzutage sind die Genomsequenzen für viele Organismen von Bakterien bis zum Menschen bekannt. Damit lassen sich auch die möglichen Proteine vorhersagen. Tatsächlich produzierte Enzyme einer Zelle oder eines Organismus können inzwischen mit hochauflösenden Massenspektrometern identifiziert und quantifiziert werden. Da eukaryotische Zellen wesentlich größer als prokaryotische Zellen sind, überwiegen die Wirtsproteine stark in den oben beschriebenen Infektionsmodellen. Außerdem wird nur ein Bruchteil der Eukaryotenzellen im Modell von den Bakterien befallen. Um die Anpassung der infizierten Wirtszellen oder Bakterien detailliert anschauen zu können, müssen die jeweils gewünschten Subgruppen aus dem Infektionsmodell angereichert werden. Bei einer bereits etablierten Methode werden *S. aureus* Zellen verwendet, welche mittels genetischer Manipulation das grün-fluoreszierende Protein (GFP) synthetisieren. Mit dessen Hilfe ist es möglich, im Durchflusszytometer Bakterien aus zuvor mechanisch lysierten Wirtszellen anzureichern. In dieser Doktorarbeit wurde dieses Protokoll verwendet um den Einfluss von verschiedenen Wirtzellen unterschiedlicher Herkunft (menschliche Lunge oder Niere) auf die Anpassung der Bakterien zu untersuchen. In diesen Versuchen konnte gezeigt werden, dass die

Bakterien ihr Wachstum in der Wirtszelle verlangsamen und einige Abwehrmechanismen wie zum Beispiel eine verstärkte Eisenaufnahme oder Verteidigung gegen oxidativen Stress induzieren. Außerdem war offensichtlich, dass sich die Bakterien intrazellulär in einem Milieu mit leicht reduziertem Sauerstoffangebot wiederfinden und sich dementsprechend anpassen.

In einem weiteren Projekt dieser Arbeit wurde GPF aber auch verwendet um intakte bakterienhaltige Wirtszellen von nicht-infizierten Eukaryoten ebenfalls mittels Durchflusszytometrie abzutrennen. Für die Wirtszellen wurde gezeigt, dass einige Signalwege betroffen sind. Zytokine als Botenstoffe an das Immunsystem wurden verstärkt produziert und der programmierte Zelltod trat nur zu Beginn der Infektion auf.

Da es nicht immer möglich ist Bakterien gentechnisch zu modifizieren, zum Beispiel wenn klinische Isolate untersucht werden sollen, wurde zusätzlich ein neues Protokoll zur Anreicherung von *S. aureus* aus infizierten Zellen entwickelt. Dieses nutzt Nanopartikel, welche einen Gold- oder Eisenoxidkern besitzen und mit fluoreszierenden Farbstoffen markiert sind. Werden Bakterien mit diesen Partikeln vorinkubiert, können sie entweder ebenfalls mittels Durchflusszytometrie oder im Falle des Eisenoxids über einen starken Magneten von Wirtszellkomponenten separiert werden. Dieses Protokoll konnte erfolgreich für eine infizierte Lungenzellline angewendet werden. Wie bereits zu Beginn dieser Einführung angesprochen, sind auch viele von Bakterienseite sezernierte Proteine für die Virulenz von *S. aureus* verantwortlich. Alle zuvor beschriebenen Protokolle, die der Anreicherung von Bakterien und Abtrennung von eukaryotischen Zellbestandteilen dienen, konzentrieren sich allerdings nur auf die Bakterienzelle. Im Verlauf des Experiments werden sekretierte Proteine weggespült. Wie eingangs erwähnt, werden Bakterien mittels Phagozytose in die Wirtszelle aufgenommen und einige *S. aureus* Stämme können auch für längere Zeit in den Phagosomen verweilen. Mittels Fluoreszenzmikroskopie konnte gezeigt werden, dass dies auch für den hier verwendeten *S. aureus* Stamm HG001 der Fall ist. Da zu erwarten ist, dass die Virulenzproteine direkt in die Phagosomen sekretiert werden, wurde ein weiteres Protokoll entwickelt, welches diese Kompartimente der Wirtzelle zusammen mit den darin enthaltenen Bakterien und sekretierten Proteinen vom Rest der Eukaryotenzelle abtrennt. Zusätzlich wurde eine hochsensitive Technik der Massenspektrometrie angewendet, die so genannte „*multiple*“ oder auch „*single reaction monitoring*“ (MRM/SRM) Methode, welche zielgerichtet ausgewählte Proteine in einem hohen dynamischen Bereich analysieren kann und somit das Problem der hochabundanten humanen Proteine und der vergleichsweise sehr geringen Zahl bakterieller Proteine umgeht. Es konnte gezeigt werden, dass sich mit diesem Versuchsaufbau verschiedene vorher nicht zugängliche Proteine nachweisen lassen. Auch deren Regulation wurde untersucht und festgestellt, dass viele Virulenzfaktoren innerhalb der Wirtszelle induziert werden, aber auch dass einige Toxine weniger produziert werden um möglicherweise den programmierten Zelltod des Wirts und damit das eigene Untergehen zu verhindern. Neben der experimentellen Seite sind auch Auswerte- und Interpretationsstrategien der komplexen Proteindaten gefragt um Rückschlüsse aus den Versuchen

zu ziehen. Auch dazu wurde ein Beitrag in dieser Arbeit geleistet, indem zum einen verschiedene Auswertealgorithmen kombiniert wurden und deren Interpretation durch Optimierung der funktionellen Annotierungen in der Datenbank verbessert wurde. Diese neuen Informationen, die eine bessere Auswertung von Stoffwechselwegen erlauben, haben auch Einzug in die neu vorgestellt AureoWiki Plattform gefunden. Nachdem diese vielfältigen Methoden zahlreiche neue Einblicke in das Wechselspiel von *S. aureus* und humanen Wirtszellen brachten, wurde noch ein weiterer intrazellulärer Krankheitserreger, *Bordetella pertussis,* der Verursacher von Keuchhusten, in Zusammenarbeit mit einer argentinischen Arbeitsgruppe massenspektrometrisch nach Internalisierung durch Makrophagen analysiert. Dabei wurden einige Gemeinsamkeiten zu internalisierten *S. aureus* Zellen wie zum Beispiel reduzierte Proteinsynthese, verstärkte Produktion von eisenakquirierenden Enzymen sowie eine Umstellung des Virulenzfaktorrepertoires beobachtet.

Zusammenfassend bietet diese Arbeit dank der neuentwickelten Methoden und deren Anwendung auf verschiedene Infektionsmodelle einen umfassenden Überblick über das Zusammenspiel von pathogenen Bakterien und infizierten Wirtszellen, welcher nach Anwendung im größeren Maßstab oder gar in *in vivo* Versuchen einen wesentlichen Beitrag zum Verständnis dieses gefährlichen Erregers leisten kann.

SUMMARY OF DISSERTATION

Infections, especially pneumonia, are still among the most prevailing causes of death. Alarming numbers of pathogen induced infections are acquired in hospitals. This is still true for industrial countries with high standards in hygiene. One of the most important causes of nosocomial infections is *Staphylococcus aureus*. It colonizes the skin and mucous membranes of about 20-30% of the human population symptom-free. As soon as this bacterium invades the organism and tissues, it is able to cause a broad range of infections which can be life-threatening especially in immune-deprived patients. The spectrum of diseases comprises mild skin infections such as furuncles as well as toxin-mediated diseases. Furthermore, *S. aureus* can harm organs and initiate severe infections such as pneumonia, nephritis, osteomyelitis, endocarditis, and even septicaemia. Development of strains with resistance against many antibiotics available at the moment complicates this situation. The variety of strains with their various properties is one reason why no successful vaccine has been introduced to the market, yet. Therefore, efficient strategies for prevention and therapy of these dangerous infections are urgently needed.

To accomplish this goal, understanding the interplay between pathogen and host on molecular level is indispensable. *S. aureus* is armed with a multitude of factors allowing intrusion into and spreading inside organs and tissues. Earlier it was assumed that *S. aureus* is an exclusively extracellular pathogen. Recently, it became clear that it can be internalized by different non-professional phagocytic host cells and persists there for long time and even replicates. This property helps the pathogen to hide from the immune system. Invasion is triggered by several virulence factors which are associated with the cell wall or membrane or secreted into the environment. The first step is mediated by various proteins which help the bacteria to attach to host cells prior to uptake. Furthermore, this pathogen possesses a huge repertoire of toxins which destroy host cell membranes. Other bacterial enzymes are required for acquisition of nutrients such as iron from the host. Again, other proteins enable *S. aureus* to protect against host defense and connected harsh conditions such as oxidative stress.

However, also the infected cell is adapting. After the bacteria were recognized as intruders, they are taken up and engulfed by a membrane, in the so-called phagosome. Phagosomes can mature and fuse with lysosomes. These compartments provide acid proteases which lyse and destroy enclosed bacteria. Also production of reactive oxygen species is a defense mechanism of eukaryotic cells. Some *S. aureus* strains are able to adapt to the conditions inside the phagosome and prevent fusion with lysosomes. By phenotype switching into so-called small colony variants they can hide inside the host. Other strains are capable to destroy the phagosomal membrane with the help of certain proteins, the phenol soluble modulins, which enable them to replicate inside the cytoplasm and then kill host cells. However, the host itself can activate a programmed cell death, apoptosis, which will eliminate infected host cells together with enclosed bacteria. This mechanism is triggered

by special proteases, the caspases, and should prevent spreading of the infection to adjacent cells. In addition, epithelial cells as well as immune cells are able to communicate with other cells among the tissue or organism with the help of small molecular cytokines and thus, activate a fast innate immune response to the bacteria. These reactions comprise pro- and anti-inflammatory processes which should on the one hand eliminate bacteria but on the other hand avoid excessive reactions of the immune system. Imbalanced immune response implicates severe diseases.

Host-pathogen interactions can be analyzed by a broad range of molecular biological techniques. Cell lines which are infected with pathogens help to investigate the basics of the adaptation of both partners to internalization. Adaptive changes in the gene expression can be differentiated on the level of transcripts, proteins or metabolites. However, proteins are the key players which accomplish the adaptations that are programmed at the genetic level. They can ensure that metabolism and virulence of the bacteria are adjusted to the new environment. Nowadays, genome sequences for several organism including humans and many bacteria are known. Having that information at hand, the proteins potentially produced can be predicted. However, the enzymes and structural proteins actually synthesized, posttranslational modifications included, can only be identified and quantified using high precision mass spectrometers. Since eukaryotic cells are by far larger than prokaryotic cells, host proteins often prevail in infection models. Furthermore, usually only a small percentage of eukaryotic cells will really carry bacteria. In order to analyze solely the infected host or the internalized pathogen in detail, subpopulations of interest need to be enriched in internalization models. In an already established approach, genetically manipulated *S. aureus* cells are employed which constitutively express the green-fluorescent protein (GFP). These GFP-expressing bacteria can be isolated by fluorescence activated flow cytometry from previously mechanically lysed host cells.

In this thesis, this protocol was applied to investigate the effect of several human cell lines deriving from different organs (human lung and kidney) on the adaptation of internalized bacteria. Results from these experiments revealed reduced bacterial growth rates inside host cells and increased levels of *S. aureus* proteins that enable iron acquisition or defense against oxidative stress. Moreover, it was obvious that the bacteria have to adapt to decreased intracellular oxygen supply.

In a subproject, GFP-expressing bacteria were additionally applied to separate intact host cells which carry bacteria after incubation from those which do not. For the host side it was shown that some signaling pathways were affected, cytokine secretion was enhanced, and programmed cell death was only indicated early after infection.

Since it is not always possible to genetically modify bacteria, for example when clinical isolates should be investigated, an additional bacterial enrichment protocol was developed. Therein, gold or iron-oxide core nanoparticles which were labeled with fluorescent dyes were utilized to label the bacteria. After pre-incubation of *S. aureus* with these particles they can be enriched by fluorescence activated flow cytometry or – in the case of the iron-oxide core – with a strong magnet from infected

host cell debris. This protocol was successfully employed for an infected human bronchial epithelial cell line.

As already mentioned, besides cellular bacterial proteins also many secreted factors are responsible for virulence of *S. aureus*. The beforehand described bacterial enrichment protocols only concentrate on intracellular, membrane or surface-exposed bacterial proteins. Proteins which were secreted during internalization into the host environment are washed away. It is already well established that *S. aureus* cells are taken up inside the host by phagocytosis and persist for longer time inside the phagosomes. This assumption was confirmed for the herein applied strain *S. aureus* HG001 by fluorescence microscopy. Since it was expected that the virulence factors are directly secreted into the phagosome, a protocol was developed which allows isolation of this compartment together with the enclosed bacteria and secreted proteins. Additionally, a more sensitive mass spectrometry (MS) technique, single or multiple reaction monitoring (SRM/MRM) was employed, which analyzes targeted proteins in a high dynamic range. This minimized further the problem of analyzing comparatively low amounts of bacterial proteins against a high abundance of host proteins. Several proteins which were not detected earlier could now be covered with this approach. Analysis of regulation of secreted virulence factors and other targeted proteins indicated that many virulence factors [*e.g.* extracellular fibrinogen binding protein (Efb), secretory staphylococcal antigen precursor (SsaA2)] were increased in level during internalization but others (*e.g*. leukocidin s subunit HlgC) were produced in lower levels, maybe in order to prevent apoptosis and the connected death of bacteria. In addition to the experimental part, also sophisticated strategies for data analysis and interpretation are important for understanding the data generated with internalization models. For this purpose, different analysis algorithms were combined and functional interpretation was improved by optimization of database annotations for the utilized strain. This new information allowed better understanding of metabolic pathways and was implemented into the newly introduced AureoWiki platform. Besides *S. aureus*, another intracellular human pathogen, *Bordetella pertussis*, the leading cause of whooping cough, was investigated upon internalization by macrophages using MS in collaboration with partners from Argentina. The data generated revealed similarities to the adaptation reactions already noted for internalized *S. aureus* such as reduced protein biosynthesis, enhanced production of proteins involved in iron acquisition, and modulation of virulence factors.

To summarize, this thesis provides – by using newly developed methods – new insights into the interaction of pathogenic bacteria and infected host cells that can contribute to a better understanding of the pathophysiology of *S. aureus* as an important pathogen.

INTRODUCTION

Staphylococcus aureus

S. aureus is a Gram-positive coccus with the size of 0.5-1.5 *µ*m. Its name derives from its ability to form grape-like structures (Greek: *staphyle* for “bunch of grapes”) and the golden or yellow color of the colonies (Latin: *aurum* for “gold”). The latter property is caused by the carotenoid staphyloxanthin which has also antioxidant activity (Marshall and Wilmoth, 1981). Besides pigmentation *S. aureus* differs from other members of the staphylococcal family also by expression of coagulase and deoxyribonuclease as well as on its ability to ferment mannitol (Lowy, 1998). These bacteria are immobile and do not form spores. Further, they are quite resistant against many environmental factors, such as heat, salt, oxidative stress or detergents (Chaibenjawong and Foster, 2011, Weber et al., 2004, Bruins et al., 2007, Amado et al., 2013). *S. aureus* is protected by a thick cell wall consisting of peptidoglycan linked to N-acetylmuramic acid by a pentaglycine bridge. Formation of microcapsules composed of polysaccharides around the cell reduces phagocytosis (O'Riordan and Lee, 2004). *S. aureus* is normally a commensal known to colonize about 20-30% of the healthy human population without any symptoms (Wertheim et al., 2005). However, it is also an opportunistic pathogen and able to lead to a wide range of infectious diseases (Figure 1). It was first described to be involved in abscess formation by Alexander Ogston in 1882 (Lowy, 1998, Ogston, 1882). Besides milder skin infections and toxin-induced diseases [*e.g.* toxic shock syndrome (TSS)] further organs and tissues can be affected resulting in *e.g.* pneumonia, osteomyelitis, emesis, endocarditis or septicemia (Wertheim et al., 2005). Interestingly, it was observed that individuals which carry *S. aureus* have a significant higher risk of acquiring an infection with this pathogen compared to non-carriers. However, infections in non-carriers show often a more severe progress of the disease (Wertheim et al., 2004). The authors suppose that the immune system of carriers could be adapted to their *S. aureus* strain which might result in a more adequate response to infection. Some *S. aureus* infections can be treated with antibiotics such as β-lactam antibiotics. However, since decades more and more resistance of *S. aureus* strains was observed. First, an increased spreading of methicillin-resistant *S. aureus* (MRSA) strains was

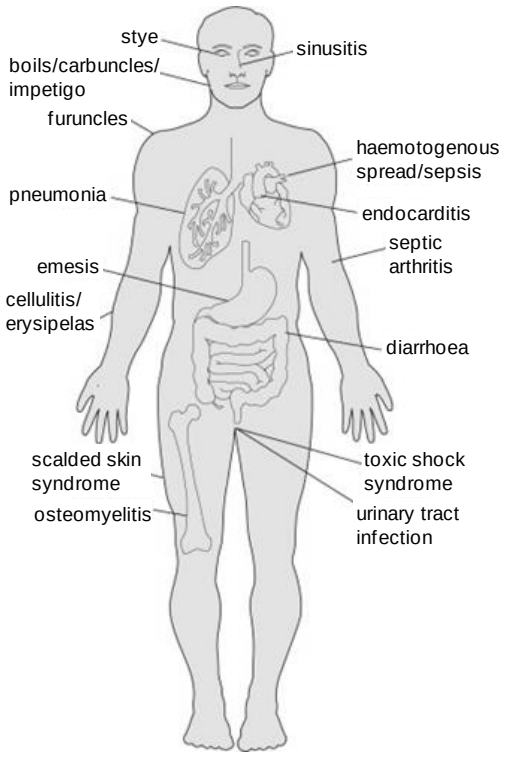

Figure 1. Infectious diseases caused by *S. aureus.* *Modified after Wertheim and colleagues (Wertheim et al., 2005).*

reported (Appelbaum, 2006a). Those cases were treated with vancomycin. Soon after treatment, vancomycin-resistant *S. aureus* (VRSA) strains were isolated from patients, interestingly together with vancomycin-resistant enterococci. Thus, *in vivo* transfer of the *vanA* gene, whose expression was found to be involved in resistance, between the species could have occurred (Appelbaum, 2006b, Périchon and Courvalin, 2009). Both strains, MRSA and VRSA, were prevailing causes of severe diseases acquired in hospitals. Also the highly pathogenic community-acquired MRSA strains infecting people outside of hospitals are an important cause of live-threatening diseases (Jungk et al., 2007, Mediavilla et al., 2012).

Thus, there is need for effective treatments of *S. aureus* infections. The focus lies on gaining knowledge leading to development of effective antibiotics or vaccines which could probably reduce the number of MRSA cases in hospitals (Hogea et al., 2014). It is still a challenge to develop an effective vaccine which would prevent severe infections due to complex interactions of *S. aureus* with the host immune system (Lindsay, 2007). Therefore, intense research concentrates on the understanding of this bacterium and its virulence especially during contact with host cells. Originally, *S. aureus* was regarded as extracellular pathogen. However, several more recent studies showed that this pathogen can be internalized by non-professional phagocytic cells and some were already reviewed in 2009 (Garzoni and Kelley, 2009). This requires new techniques and strategies to investigate the consequences of *S. aureus* invasion into host cells. This thesis aims to contribute to understanding of especially those processes occurring after internalization of *S. aureus* by host cells.

S. aureus strain HG001

Research with *S. aureus* has established that the different strains display extensive differences in the virulence factor repertoire far beyond resistance against antibiotics. Thus, the choice of a certain strain influences the outcome of experiments, *e.g.* in host-pathogen interaction studies. Most importantly, pathogenicity depends on expression of global regulators of virulence factors. The *S. aureus* strain HG001 used in this study is a derivative of the strain NCTC8325 (RN1) (Herbert et al., 2010). Its genome was fully sequenced in 2006 (Gillaspy et al., 2006). The parental strain NCTC8325 was isolated from a patient suffering from sepsis in 1960. Mutants and derivates of NCTC8325 such as NCTC8325-4 are widely employed in the scientific community working on *S. aureus* (Moreilhon et al., 2005, Hirschhausen et al., 2010). NCTC8325 has functional regulatory genes *agr, sarA*, and *sae*, but defects in the genes *rsbU* and *tcaR*. These defects were repaired by Herbert and coworkers in the group of Friedrich Götz, and several derivatives are now available (Herbert et al., 2010). In strain HG001 *rsbU* is repaired but it still contains a mutation in *tcaR* (activator of protein A transcription). The regulatory protein RsbU positively regulates activation of the important alternative sigma factor B (SigB) (Giachino et al., 2001). Since many crucial virulence factors are also under control of *sigB,* the HG001 strain with a functional copy of *rsbU* was used throughout this study.

Virulence factors and host adaptation strategies of S. aureus

For effective infection and persistence, *S. aureus* needs to overcome the barrier of the skin, invade host cells, survive in the environment, and resist the human or animal immune system. A massive cell wall and the polysaccharide capsule, which is present in many strains, reduce phagocytosis (O'Riordan and Lee, 2004). The antioxidant staphyloxanthin contributes to intracellular survival by reduction of the impact of phagosomal activity (Olivier et al., 2009). Furthermore, *S. aureus* possesses an enormous repertoire of secreted and surface-attached virulence factors (Figure 2).

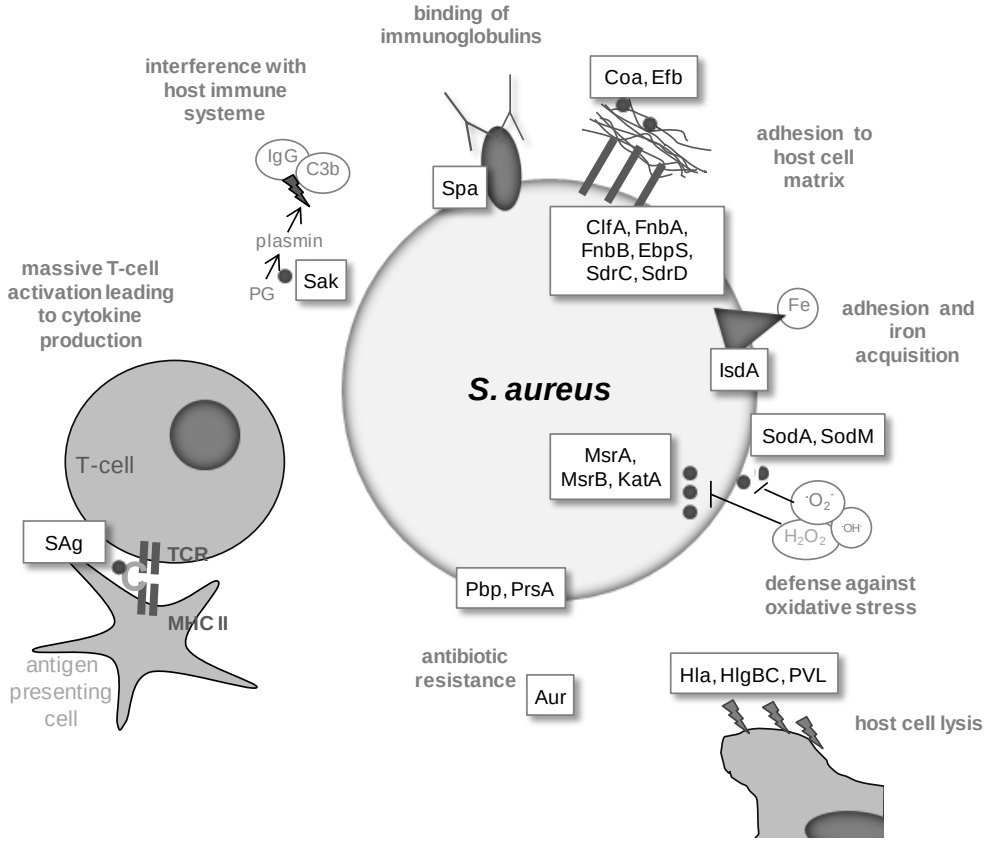

Figure 2. Virulence factors of *S. aureus*. *Some selected virulence factors and their main functions are illustrated in this scheme. The cell surface attached adhesins clumping factor A (ClfA), fibronectin binding protein A and B (FnbA, FnbB), elastin binding protein (EbpS), and serine proteases C and D (SdrC, SdrD) bind host cell components. Also secreted proteins such as coagulase (Coa) and extracellular fibrinogen binding protein (Efb) enable adhesion to host cells. Iron-regulated surface determinant protein IsdA binds to host molecules and promotes iron acquisition from eukaryotic cells. Defense against reactive oxygen species is mediated by the secreted superoxide dismutases SodM and SodA, and the cytosolic proteins catalase (KatA) and methionine sulfoxide reductases (MsrA, MsrB). Secreted pore-forming toxins such as α-hemolysin (Hla), γ-hemolysin (HlgBC), and Panton-Valentin-leukocidin destroy eukaryotic cell membranes. Secreted aureolysin (Aur), cell bound penicillin-binding protein (Pbp), and foldase protein PrsA contribute to resistance against antimicrobial substances. S. aureus is further able to influence the host immune system. Protein A, an enzyme of the bacterial surface, binds the Fc part of immunoglobulins. Secreted superantigens (SAg) cause massive activation and proliferation of T-cells leading to cytokine production. Staphylokinase (Sak) is secreted by the bacteria and mediates transformation of plasminogen (PG) to plasmin, which causes lysis of fibrin and degrades IgG and C3b, and thus, allows spreading of S. aureus in host tissue. The figure was adapted from previous publications (Gordon and Lowy, 2008, Nizet, 2007). TCR (T-cell receptor), MHC II (major histocompatibility complex class II molecules), Fe (iron), H_2O_2 (hydrogen peroxide), $^{\cdot}O_2^-$ (superoxide anion), $^{\cdot}OH$- (hydroxyl anion).*

As first step of an infection, *S. aureus* has to attach to host cells (Gordon and Lowy, 2008). Adhesion to host matrix molecules is mediated by secreted as well as cell wall-bound proteins. The so-called microbial surface components recognizing adhesive matrix molecules (MSCRAMMs) allow bacteria to attach to extracellular host cell matrix molecules such as fibronectin, fibrinogen or collagen. Among others, fibronectin binding proteins A and B (FnbA, FnbB), elastin-binding protein (EbpS), and clumping factor A and B (ClfA, ClfB) which bind fibrinogen (Clarke et al., 2009, Hair et al., 2010) belong to this group. Clumping factor A also interacts with the complement and inhibits phagocytosis (Hair et al., 2010). MSCRAMMs such as FnbA and B have further been shown to contribute to biofilm formation in certain *S. aureus* strains (McCourt et al., 2014). Also the serine-aspartic acid repeat proteins SdrC and SdrD have been shown to contribute to adherence of *S. aureus* to nasal epithelial cells (Corrigan et al., 2009). Other surface-attached adhesins are represented by the iron-regulated surface determinant proteins (IsdA, IsdB, IsdC, and IsdH) which bind host cell fibronectin and fibrinogen (Clarke et al., 2009, Kim et al., 2010). As these proteins also bind hemoglobin, they fulfill another important function in *S. aureus* virulence by acquisition of iron as survival strategy inside the host (Mazmanian et al., 2003). They have been reported as possible targets for vaccination (Kim et al., 2010). By binding von Willebrand factor also staphylococcal protein A (Spa) functions as MSCRAMM (Hartleib et al., 2000). In addition, Spa possesses high affinity to the Fc part of the heavy chain of immunoglobulins (Ig), preferably IgG. Thus, *S. aureus* is secured from opsonization by specific antibodies which would lead to phagocytosis by the host (Dossett et al., 1969). Non-MSCRAMM staphylococcal surface protein SasG was described to bind to nasal epithelial cells and contribute to biofilm formation without binding fibronectin or similar molecules (Corrigan et al., 2007).

But also secreted proteins such as the staphylococcal coagulase (Coa) or the extracellular fibrinogen binding protein (Efb) can mediate adhesion between *S. aureus* and host cell molecules (Ko et al., 2011). Secreted Coa binds prothrombin by formation of a stoichiometric complex. This marks the start of the coagulation cascade by converting fibrinogen to fibrin (Hendrix et al., 1983). By binding to fibrinogen Efb inhibits the innate immune response through blocking of platelet aggregation and preventing neutrophil adherence to immobilized fibrinogen (Ko et al., 2011). The secreted autolysin (Atl) is responsible for correct separation of bacterial cells during replication. Accordingly, *atl* deletion mutants were reported to form enlarged clusters of *S. aureus* cells (Heilmann et al., 1997). Atl binds to host molecules such as vitronectin and therefore enables also attachment to and internalization by non-professional phagocytic cells and contributes to virulence (Hirschhausen et al., 2010, Heilmann et al., 1997). Further, Atl plays a crucial role in the secretion of usually cytosolic proteins (Pasztor et al., 2010).

Besides Spa, also immunoglobulin G (IgG)-binding protein Sbi which was likewise found secreted enables *S. aureus* to bind the Fc region of host IgG and its antigen-specific Fab region when Sbi is linked to the bacterial surface and thereby abating host defense (Smith et al., 2011). Staphylokinase

(Sak), a secreted virulence factor, mediates the transformation of host plasminogen to the active serine protease plasmin which is responsible for fibrinolysis (Silence et al., 1995) and degrades IgG and C3b of the host immune system and thereby enables spreading of *S. aureus* (Rooijakkers et al., 2005).

The adaptive immune system is influenced by harmful secreted toxins such as the toxic shock syndrome toxin-1 (TSST-1) as well as different types of staphylococcal enterotoxins, which were discovered in various clinical isolates. These so-called superantigens (SAg) are highly heat stable and also partly resistant to proteolytic enzymes. SAgs induce enormous unspecific and oligoclonal activation of T-cells leading to proliferation, cytokine secretion, and symptoms of septic shock (Thomas et al., 2007). Other toxins secreted by *S. aureus* can cause severe damage to cell membranes ending in host cell death. Among them are hemolysins and leukocidins like for example α-hemolysin (Hla), the bicomponent gamma-hemolysin (HlgAB, HlgBC) or the Panton-Valentine-leukocidin (PVL) (Vandenesch et al., 2012). Employing their cytolytic activity they are able to form pores leading to host cell death (DuMont and Torres, 2014). Hla binds to host cell membranes and builds heptameric transmembrane pores (Song et al., 1996). Gamma-hemolysin is pore-forming in a complex of each one slow (S) (HlgA or HlgC) and one fast (F) subunit (HlgB) which were named according to their different electrophoretic migration pattern (Vandenesch et al., 2012). The Panton-Valentine leukocidin (PVL), a β-pore-forming toxin, is derived from a bacteriophage which infects *S. aureus* and increases its virulence. This toxin consists of the two subunits LukS-PV and LukF-PV. The toxin-dimer is highly leukotoxic (König et al., 1997). PVL was reported to attack host cell mitochondria, causing alterations in the mitochondrial proteins. As a consequence, apoptosis *via* activation of caspase-3 and caspase-9 was observed (Genestier et al., 2005).

S. aureus owns some proteins which allow resistance to antimicrobial substances. The membrane associated protein export protein PrsA which is responsible for accurate folding of many proteins also influences the virulence of *S. aureus*. Disruption of *prsA* was observed to change sensitivity to glycopeptides and dramatically decreased the resistance to methicillin in strain *S. aureus* COL (Jousselin et al., 2012). The surface attached penicillin binding proteins (PBP) participate in cell wall biosynthesis of *S. aureus*. These peptidases catalyze cross-linking of peptide chains in the peptidoglycan scaffold but can be inhibited by β-lactam antibiotics such as penicillin. *S. aureus* possesses several PBPs. Another version of the normal PBP2, PBP2a, is encoded by the *mecA* gene only in MRSA strains. This protein is still able to form cross-linking in the presence of methicillin and thus, helps the bacteria to overcome antibiotic treatment (Chambers, 1997). However, recently Dave and coworkers described neutral β-lactams which are able to inactivate some classes of resistance-associated PBPs including PBP2a (Dave et al., 2014). Also the secreted metalloproteinase aureolysin (Aur) contributes to *S. aureus* resistance against antimicrobial peptides. This protein was described to cleave the human bactericidal peptide cathelicidin LL-37 which usually degrades staphylococci which do not express aureolysin (Sieprawska-Lupa et al., 2004).

S. aureus not only destroys host cells but requires strategies to survive inside this new environment which is likely characterized by limited nutrient supply compared to culture media as well as limited oxygen conditions or oxidative stress caused by molecules produced as host defense. Thus, the bacteria require strategies to acquire nutrients from the host cells. As already mentioned, several surface attached proteins function in iron acquisition [IsdA, IsdB, IsdC, and IsdH (Clarke et al., 2009, Kim et al., 2010)]. Since the preferred iron source of *S. aureus* is hemoglobin (Skaar et al., 2004b), this pathogen owns heme-degrading enzymes such as IsdG and IsdI (Skaar et al., 2004a).

S. aureus can also fight against oxidative stress. It possesses proteins which reduce damage caused by reactive oxygen species such as hydrogen peroxide, hydroxyl-anion or superoxide ions. It expresses for example the superoxide dismutases SodA and SodM which reduce superoxide and the catalase katA which converts hydrogen peroxide to water and oxygen (Karavolos, et al., 2003). Also methionine sulfoxide reductases contribute to tolerance to oxidative stress. They catalyze reduction of oxidized methionine (Singh and Moskovitz, 2003). In *S. aureus* MsrA was found specific for the S-enantiomer of oxidized methionine and MsrB for the R-enantiomer (Moskovitz et al., 2002, Singh and Moskovitz, 2003). For the extracellular pathogen *Streptococcus pneumoniae* it was shown recently, that methionine sulfoxide reductase influences virulence and is crucial to protect against uptake and killing of the bacterium by macrophages in a mouse model of infection (Saleh et al., 2013).

Further, secreted lipases play an important role in *S. aureus* virulence. The strain HG001 encodes two lipases with the *lipA* and the *geh* gene (Hu et al., 2012). Hu and colleagues observed that a mutation in the lipase gene of *S. aureus* resulted in decreased biofilm formation (Hu et al., 2012). Biofilm formation can also be regarded as a virulence strategy of *S. aureus*. It describes a microbial community which is attached to a surface. Colonization of intra-vascular medical devices such as catheters often leads to severe infections, as this biofilm protects the bacteria from the immune cells and antimicrobials. Biofilm formation starts with detachment followed by cell-to-cell adhesion and replication, maturation, and finally, again detachment (Otto, 2013). *S. aureus* biofilms are characterized by an exopolysaccharide, the poly-N-acetyl glucosamine (also called polysaccharide intercellular adhesion), which is encoded by the *ica* gene and mediates the adhesion between the bacteria of a biofilm (Cramton et al., 1999). Assembling of a biofilm is managed by quorum sensing mechanisms among the *S. aureus* cells to control gene expression (Kong et al., 2006).

A newly described group of virulence factors of *S. aureus* are the phenol-soluble modulins (PSM). They were also reported to contribute to biofilm formation and have pro-inflammatory properties (Otto, 2014). Recently, PSMα was shown to be responsible for phagosomal escape and prevention of phagolysosomal digestion and, as consequence, cytosolic replication of bacteria (Grosz et al., 2014).

Since several virulence factors are secreted into the environment and thus, might have a high impact on the outcome of infections *in vivo*, it is important but still challenging to capture them from infected organs and tissues, and study their properties. Many virulence factors are differentially

expressed in different growth phases (Ziebandt et al., 2004, Gordon and Lowy, 2008) and might also be influenced by the environment such as nutrient starvation or internalization. The expression is controlled by a broad range of global transcriptional regulators. An overview of selected important regulators and their function is provided in Table 1. Among them are two component systems (TCS), alternative sigma factors, and transcription factors (Novick, 2003). More regulators were discovered in recent studies, and also strain dependent differences were observed (Ibarra et al., 2013).

Table 1. Regulons of *S. aureus* (adapted from Novick, 2003). *TCS (two component system).*

regulator	type	role	reference
agrACDB/rna III	TCS	regulation of extracellular and cytoplasmic proteins	(Novick et al., 1993)
saePQRS	TCS	regulation of extracellular proteins	(Giraudo et al., 1999)
arlRS	TCS	regulation of autolysis and accessory genes	(Fournier et al., 2001)
svrA	membrane protein	required for expression of *agr*	(Garvis et al., 2002)
srrAB	TCS	regulation of certain accessory proteins at low oxygen partial pressure	(Yarwood et al., 2001)
sigB	alternative sigma factor	late exponential phase, regulates accessory genes	(Kullik et al., 1998)
sarA	transcription factor	important for *agr* induction, pleiotropic receptor	(Heinrichs et al., 1996)
sarS	transcription factor	activation of transcription of *spa* and other surface proteins	(Tegmark et al., 2000)
sarT	transcription factor	repression of transcription of *hla* and other exoproteins	(Schmidt et al., 2001)
sarR	transcription factor	transcription factor for *sarA* and probably *sarS*	(Manna and Cheung, 2001)
rot	transcription factor	transcription factor for hla and other exoproteins	(McNamara et al., 2000)

Additionally, *S. aureus* is able to persist inside host cells for long time by changing its phenotype (Kahl, 2014). The so-called small colony variants (SCVs) are characterized by slower growth, formation of smaller colonies on agar plates, and reduced hemolysis (Proctor et al., 2006). Diverse mechanisms can cause this phenotype (Kahl, 2014). Well-characterized variants are those with deficiencies in the electron-transport chain caused by defects in hemin or menadione synthesis (Kohler et al., 2003, Kohler et al., 2008). SCVs are described to persist longer inside host cells (von Eiff 2001), produce less toxins but more adhesins, and are more resistant to antibiotics than the wild-type (Tuchscherr et al., 2011, Sendi and Proctor, 2009, Moisan et al., 2006, Vaudaux et al., 2002). They induce an attenuated host defense response compared to wild-type bacteria with decreased cytokine production (Tuchscherr et al., 2010). It was also shown that *S. aureus* is able to switch the phenotype from SCV to wild-type within a mouse model of chronic infection (Tuchscherr et al., 2011).

Host defense mechanism to S. aureus infection

Humans and animals are often exposed to microorganism such as bacteria. Several defense mechanisms were developed during evolution to prevent damage caused by closer contact to pathogens or invasion of tissues and cells. The skin protects the organism as a continuous barrier, mucus should eliminate foreign matter, and low pH for example in the stomach kills many microorganisms before they can enter the bloodstream in the small intestine.

However, some bacteria are able to overcome these barriers. When these invading bacteria are detected by the host organism or tissue, several molecular defense mechanisms are put into play.

The first and immediate response is given by the innate immune system after recognition of so-called pathogen-associated molecular pattern, a cascade of molecules which activates supporting macrophages and neutrophils to eliminate the bacteria. After this first response, the host is able to "remember" antigen patterns of the specific pathogen to respond more effectively to a repeated infection of the same organism, referred to as adaptive immune response.

For effective defense, infected cells and immune cells need to communicate. These interactions are mediated by the so-called cytokines; a group of low molecular-weight proteins playing an important role in response to infection. They are secreted and direct the cells of the adaptive immune response to the site of infection and enhance host defense (Janeway and Medzhitov, 2002). Cytokines are expressed by various cell types and function already in picogram or nanogram range after binding to specific cell surface receptors (Nicod, 1993). This class can be divided into interleukins (IL, *e.g.* IL1-13), colony stimulating factors (CSF), tumor necrosis factor (TNF, *e.g.* TNFα,β), interferons (IFN), chemokines (*e.g.* IL-8), and growth factors (GF, *e.g.* endothelial GF, insulin-like GF) (Whicher and Evans, 1990, Nicod, 1993). They influence cell maturation, differentiation or activation. Further, they alarm the inflammatory response, modulate function of immune cells and serve as chemotactic agents (*e.g.* IL-8) for leukocytes (Stadnyk, 1994, Whicher and Evans, 1990). Many of these cytokines (*e.g.* IL-1α, IL-1β, IL-6, IL-8, IFNγ, TNFα) fulfill pro-inflammatory functions. However, it is also necessary to avoid uncontrolled systemic reactions of the normally auto- or parakrine operating molecules which could lead to life-threatening septic shock. Some cytokines with anti-inflammatory impact such as IL-4 and IL-10 suppress this effect (Whicher and Evans, 1990, Stadnyk, 1994).

Taken together, cytokines are secreted by professional and non-professional phagocytic cells when stimulated, and mediate activation and inactivation of compounds of the innate immune system. This discrimination between the two types of cells depends on the effectiveness of phagocytosis (Rabinovitch, 1995). Professional phagocytes express more specific receptors on their surface such as immunoglobulin or complement receptors allowing them to detect foreign matter compared to non-professional phagocytic-cells. Classified to this group are for examples neutrophils, monocytes or macrophages which are able to kill and eliminate invading pathogens, in general by phagocytosis and subsequent elimination with lytic enzymes. However, it has been observed since a while that also

non-professional phagocytic cells, such as epithelial cells, fibroblasts or other cells are able to take up and eliminate particles including bacteria. In that case, uptake is often mediated by receptors of extracellular matrix molecules, comprising for example receptors of fibronectin or laminin (Rabinovitch, 1995).

Internalization of S. aureus by non-professional phagocytic cells

S. aureus was generally regarded as an extracellular pathogen. However, in the last years, it became clear that this pathogen can be internalized by non-professional phagocytic cells such as endothelial cells, mesothelial cells, epithelial cells, osteoblasts or keratinocytes (Ellington et al., 1999, Kintarak et al., 2004, Haslinger-Löffler et al., 2005, Sinha and Herrmann, 2005, Haslinger-Löffler et al., 2006, Garzoni et al., 2007, Schmidt et al., 2010b, Fraunholz and Sinha, 2012). *S. aureus* is taken up by non-professional phagocytic cells in a zipper-like mechanism (Fraunholz and Sinha, 2012) as described below.

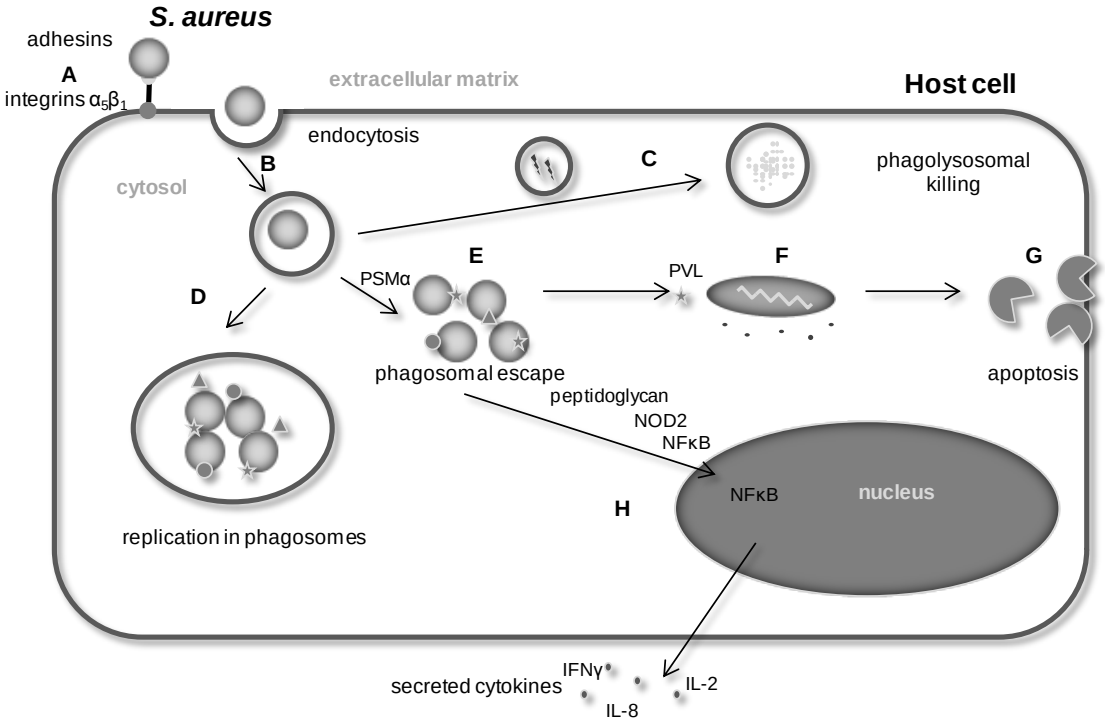

Figure 3. Possible intracellular fates of *S. aureus*. *A) S. aureus and host cells bind via extracellular matrix (e.g. fibronectin, fibrinogen) with staphylococcal adhesins (e.g. FnBP, Emp). B) After recognition and binding of bacteria the membrane composition is altered and bacteria are taken up by endocytosis in phagosomes. C) Phagosomes can mature and fuse with lysosomes which contain acid hydrolases leading to subsequent killing of engulfed bacteria. D) Some S. aureus strains can escape from phagosomes mediated by PSMα. E) Secreted S. aureus toxins like PVL can lead to release of cytochrome C from mitochondria, resulting in activation of caspase-9 which (F) further activates other caspases causing programmed cell death (apoptosis). G) Cytoplasmic peptidoglycan is recognized by NOD2 leading to NFκB activation and production of cytokines which are secreted into the culture medium for communication with other cells and recruitment of the immune cells. H) S. aureus can also survive, replicate, and secrete proteins inside phagosomes. Figure adapted after Fraunholz & Sinha (Fraunholz and Sinha, 2012).*

Once being internalized, *S. aureus* encounters the phagosomal maturation events aiming at final degradation of the endocytosed material. Several possible fates of *S. aureus* inside non-professional phagocytic host cells have been described (Figure 3) (Fraunholz and Sinha, 2012). Before uptake, the pathogen and the potential host cell have to bind to each other. *S. aureus* possesses several, mainly cell wall-associated proteins. Among them are the above introduced adhesins (*e.g.* ClfA, FnbAB, SdrC, SdrD), which can attach to extracellular matrix of the host cells, such as fibronectin, fibrinogen, lamin or collagen. The corresponding receptors on the host cell surface are the integrins, especially integrin $\alpha_5\beta_1$ (Figure 3A). Subsequent fibronectin-bridging between bacterial adhesins and host's integrins mediates the uptake of staphylococci (Sinha et al., 2000). This contact leads to reformation of the extracellular matrix and the actin cytoskeleton (Agerer et al., 2005). *S. aureus* is engulfed by the membrane and transferred into the cell by endocytosis (Figure 3B). The vacuole containing *S. aureus* is referred to as phagosome. There are three general fates for internalized *S. aureus*: fusion of phagosomes with lysosomes and subsequent killing of bacteria (Figure 3C), persistence of *S. aureus* within phagosomes (Figure 3D), and outbreak of bacteria from phagosomes leading to cytosolic replication and probable host cell death by apoptosis (Figure 3E-H).

Phagosomes mature and can fuse with lysosomes. The influx of acid hydrolases and reactive oxygen species will kill engulfed bacteria (Figure 3C). Phagosomes comprise specific groups of proteins. Among them are Rab-GTPases. These small GTPases are involved in phagosomal maturation meaning reformation of the phagosomal composition by several reactions. The main stages in the maturation process of a phagosome are the early endosome, the late endosome which fuses with lysosomes, and finally, the phagolysosome which is able to kill bacteria with a bunch of lytic enzymes like proteases and glucosidases. Also V-type ATPases support pathogen elimination by causing a low pH inside the phagosomal lumen which activates acid hydrolases. Typical markers for different stages of ripening phagosomes are RAB5 and early endosome antigen-1 (EEA1) for the early endosome, RAB7 and the mannose-6-phosphate receptors (MPRD, MPRE) for the late endosome. Late endosomes fuse with lysosomes which contain lytic enzymes. The fusion finally leads to killing of bacteria by cathepsins (endoproteases), galactosidases or peptidases.

As a second option, it was shown that *S. aureus* can reduce phagolysosomal activity and persist or even replicate within these structures (Figure 3D) (Melvin et al., 2011, Olivier et al., 2009).

If phagolysosomal killing is not successful, host cells can eliminate intracellular pathogens by autophagocytosis. In that process cytoplasmic components together with the bacteria are degraded. However, Schnaith and colleagues observed that *S. aureus* is able to induce autophagy triggered by *agr* and subsequently escape from those autophagosomes, replicate in the cytosol, and induce host cell death (Schnaith et al., 2007). Some *S. aureus* strains can escape the phagosomal compartment (Figure 3E). Recently, the phenol soluble modulin α was discovered to be responsible for the outbreak from phagosomes (Grosz et al., 2014). Avoiding phagolysosomal lysis, the bacteria replicate inside the cytosol. They secrete virulence factors into their environment to survive by enabling

intracellular spreading and acquisition of nutrients. It was shown that some *S. aureus* toxins such as the Panton-Valentin-Leukocidin (PVL) can lead to release of cytochrome C from mitochondria (Figure 3F) (Genestier et al., 2005). Cytosolic cytochrome C can activate caspases *via* several signal cascades (Figure 3G) (Genestier et al., 2005). The interference of apoptosis activated by proteolytic caspases during infection with *S. aureus* is discussed controversially in literature. Bantel and colleagues proposed staphylococcal hemolysin A to be responsible for caspase-3, -8, and -9 activation in lymphocytes and monocytes leading to apoptosis (Bantel et al., 2001). Koziel and coworkers also observed early induction of caspase-3 in macrophages which triggered apoptosis but *S. aureus* seemed to induce cytoprotective mechanisms by expression of anti-apoptotic genes preventing programmed cell death and supporting its intracellular survival (Koziel et al., 2009).

Intracellular *S. aureus* cells can lead to cytokine production (Figure 3F). Thereby, cytoplasmic *S. aureus* peptidoglycan is recognized by NOD2, which activates NFκB and results in secretion of cytokines (Kapetanovic et al., 2007). Also other studies showed that *S. aureus* components like peptidoglycan or alpha-hemolysin activate cytokine expression in non-professional phagocytes like epithelial cells (Cheon et al., 2008, Räth et al., 2013). To summarize, the interplay of *S. aureus* and host cells is very complex and thus, needs sophisticated strategies to elucidate host-pathogen interaction of molecular level.

Studying infections with human cell lines

In order to investigate the impact of *S. aureus* upon eukaryotic cells and organisms, it is possible to apply animal models and infect for example mice, primary cells or immortalized human cell lines. Using animal models, complex reactions of many tissues and organs of the whole animal are expected and can be studied after killing and dissection of the animal to analyze several organs or the plasma. Animal studies have been widely performed to explore *S. aureus* mediated infections. For example, Ventura and colleagues investigated in pneumonia-model *post-infection* (*p.i.*) events in mouse lungs infected with *S. aureus*. Dose-dependent clearance of infection by the mouse immune system or replication of *S. aureus* and death of mice were observed. Several pro-inflammatory cytokines (*e.g.* TNF-α, IL-1β, IL-6) were induced in the infected mice 6 h *p.i.*, and anti-inflammatory cytokines (*e.g.* IL-10, IL-12p70) were not increased significantly. In addition, the authors observed alterations in the host proteome, including increase of proteins involved in inflammation and coagulation as response to 6 h infection with *S. aureus*. Bacterial proteins were not accessible in this study (Ventura et al., 2008a).

However, even if it is possible to investigate the proteome response of the mouse, innate and adaptive immune responses differ between human and mice. Thus, in order to transfer results from mice to human, mouse models have to be adapted (Kim et al., 2010). Therefore, human cell lines might be an alternative choice. Especially when the responses of a single type of cells or of human cells are of interest, it is advisable to utilize human cell lines. Further, for basic analyses in early

studies which not yet justify killing of many animals, cell lines are favorable. Primary cells might be preferred since they directly derive from living organism and thus, are probably closer to nature. However, due to restricted availability (especially for human cells) and reproducibility of primary cells immortalized cell lines are widely employed in many experiments. Numerous studies prove the benefit of investigating infections of cell lines with pathogens such as *S. aureus* or its virulence factors (Almeida et al., 1996, Below et al., 2009, Cheon et al., 2008, Eichstaedt et al., 2009, Garzoni et al., 2007, Gierok et al., 2014, Giese et al., 2009, Haslinger-Löffler et al., 2006, Schmidt et al., 2010b, Wang et al., 2013).

However, the choice of the host cells might influence the response of the pathogen. Eisenreich and colleagues reviewed properties and metabolic responses of host cell lines and animal models for infection with several pathogens (*Salmonella enterica serovar Typhimurium*, *Mycobacterium tuberculosis*, *Listeria monocytogenes*, *Chlamydia spp., Coxiella burnettii*, and *Legionella pneumophilia*) (Eisenreich et al., 2013). The authors indicate that proteome adaptation of immortalized cell lines to infection might differ from that observed for primary cells and particularly from the proteomic reaction to pathogens in *in vivo* infection models and might even show the opposite result. Further, they describe that differences in the response to infection might originate from the type of cell line. Most human differentiated cells behave different than tumor cells. On metabolic level the so-called “aerobic glycolysis” or “Warburg effect” which displays decreased respiration and increased lactate production (Diaz-Ruiz et al., 2011) is known in tumor cells but does not occur in normal differentiated cells. Nevertheless, tumor cells, among them the A549 cell line (see below), are commonly used in research institutions. Furthermore, Eisenreich and coworkers pointed out that the media used for cell line cultivation are mostly rich media containing many metabolites in high concentrations which results in altered expression of nutrient transporters and proteins involved in central pathways (Levine and Puzio-Kuter, 2010). In the future it might be advisable to develop model systems consisting of more than one type of cell line, for example epithelial cells and neutrophils as part of the innate immune system which are in contact *via* cytokines in nature (Eisenreich et al., 2013). However, until now immortalized human cell lines are valuable model systems for studying infections since they allow easy reproduction of experiments and their results and many sampling points compared to animal models. These properties are especially necessary at early stages of basis research on a scientific question as they give insight into reaction of human cells.

In the study presented here, three different human cell lines representing non-professional phagocytic cells were employed (Figure 4). The human bronchial epithelial S9 cell line originated from a patient suffering from cystic fibrosis. These cells were immortalized with the adeno-12-SV-40-virus (Zeitlin et al., 1991). In contrast to the isolated mother cell line (IB3-1) the S9 cells are repaired and express a functional cystic fibrosis conductance regulator (CFTR)-channel (Flotte et al., 1993, Egan et al., 1992). This cell line was used for first time-resolved proteome analyses of internalized

S. aureus HG001 cells applying the internalization workflow developed in our group (Schmidt et al., 2010b) and later for follow-up studies of the intracellular behavior of an isogenic mutant and in the context of a new sampling protocol (Pförtner et al., 2014, Depke et al., 2014). Also the impact of pure *S. aureus* alpha-hemolysin on S9 cells was already studied extensively (Räth et al., 2013, Hermann et al., 2014, Gierok et al., 2014, Eichstaedt et al., 2009). Räth and colleagues comparatively investigated the influence of this toxin on cytokine production of S9, 16HBE14o-, and A549 cells (Räth et al., 2013).

The A549 cell line, applied as second cell line within this thesis, comprises alveolar epithelial cells derived from a human lung cancer (Lieber et al., 1976). Type II pneumocytes can differentiate to type I pneumocytes and produce surfactant. A549 cells have been shown to secrete several cytokines, for example the chemokine IL-8 (Cheon et al., 2008). With these cytokines they are able to recruit monocytes, lymphocytes or neutrophils to infiltrate the alveolar tissue and thereby enhance the immune response (Rosseau et al., 2000). Like S9 cells, A549 cells grow in monolayers in culture plates. Several studies investigating host-pathogen effects using A549 cells were performed for various bacteria or fungi (Bergmann et al., 2013, Aval et al., 2013, Wu et al., 2013, de Astorza et al., 2004, García-Pérez et al., 2003). Also the interaction of *S. aureus* or its toxins with A549 cells was studied (Wang et al., 2013, Liang et al., 2009), but not yet on proteome level. The A549 host proteome was already investigated following virus infection (Munday et al., 2010b, Munday et al., 2010a, Dove et al., 2012). In the frame of this thesis the A549 cells served as host model for simultaneous analysis of host's and pathogen's proteome from the same time-resolved setting.

Third, the HEK 293 cell line consists of adenovirus type 5-transformed human embryonic kidney cells. These cells with mainly epithelioid character do not form monolayers and are harder to handle in cell culture as they easily detach from culture plates. Further, the size of these cells can vary strongly in culture and also heterokaryons can be observed (Graham et al., 1977). This cell line is also an established cell culture model for infections with *S. aureus* (Sinha et al., 1999, Cucarella et al., 2002, Maya et al., 2012). As these kidney cells represent a different organ than the lung, the behavior of *S. aureus* inside this cell line was interesting to study in order to find common and different patterns of adaptation to host milieu.

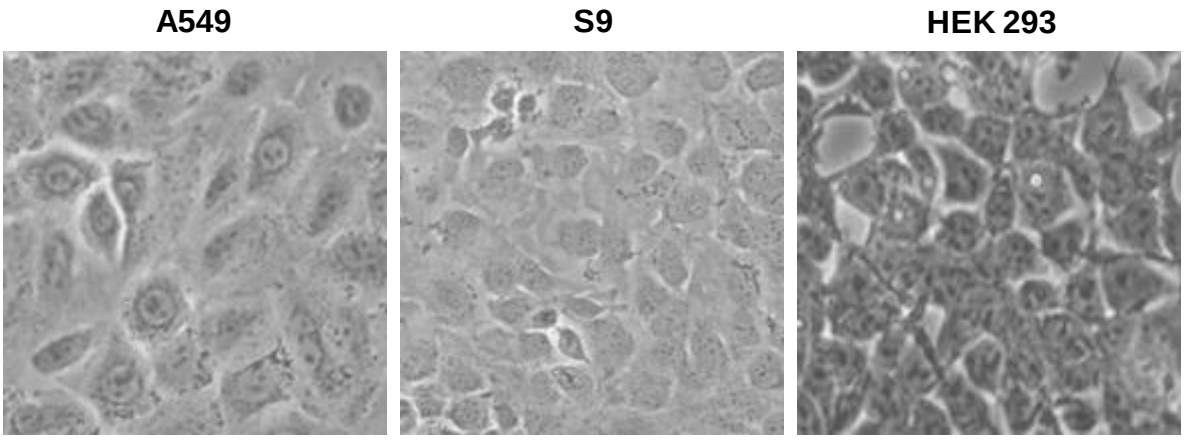

Figure 4. Human cell lines cultivated in 10 cm diameter tissue culture plates. *Human alveolar epithelial A549 cells, human bronchial epithelial S9 cells, and human embryonic kidney HEK 293 cells were observed with a microscope with a 20x objective (Nikon Eclipse TS100, Nikon GmbH, Düsseldorf, Germany).*

Host interactions with pathogens such as *S. aureus* can be studied in different ways. Some groups treat host cells with sterile bacterial culture supernatant or purified proteins in order to investigate the impact of secreted virulence factors or selected proteins (Gierok et al., 2014, Räth et al., 2013); these proteins are sometimes bound to the surface of beads in the size of *S. aureus* (Joost et al., 2011, van den Berg et al., 2011). Others centrifuge and wash *S. aureus* pre-cultures prior to exposure to cells (Grosz et al., 2014), and another option uses complete bacterial culture, combining bacterial cells and supernatant to infect the host cells (Schmidt et al., 2010b). *In vivo,* pathogens attack host cells with secreted factors but also their cellular proteins play a role, thus, the third option was preferred in this study. This means, the cell lines were infected with diluted bacterial culture containing bacteria and the culture medium with the secreted proteins of *S. aureus*. In order to avoid artificial effects caused by the medium shift from bacterial culture to cell culture medium, a new medium was utilized which was developed for cultivation of host and pathogen with a high similarity between bacterial and eukaryotic medium (Schmidt et al., 2010b).

Functional genomics approaches for the analysis of host-pathogen interactions

Interactions between *S. aureus* and host cells likely involve complex changes on the molecular level of both partners. Thus, changes during interaction are expected for transcription, protein synthesis, and metabolism which in principle can all be captured comprehensively by integrated OMICs approaches (Figure 5). Despite their great potential, opportunities in understanding molecular correlations are accompanied by challenges regarding sample preparation and setup of infection models. This might probably explain the low number of transcriptome, proteome or metabolome studies that have been performed so far to analyze the adaptation of *S. aureus* to the host environment upon internalization.

On the lowest level the genes contain information for all mechanisms controlling a cell or organism which are possible in theory. Genome sequencing and genome wide association studies using single nucleotide polymorphisms are common techniques to investigate the entity of all genes of an organism or cell, the genome. Gene activity and expression are represented by RNA. The according entirety of RNA of a cell or organism, the transcriptome, is typically analyzed by reverse transcription in combination with polymerase chain reaction (PCR) experiments whereby quantitative real-time PCR (qRT-PCR) is a common method used to quantify only single selected transcripts. Global high-throughput transcriptome analysis is accomplished on the base of expression levels of mRNAs with DNA microarray technology and RNA-sequencing. Also for *S. aureus* infections transcriptome studies have been performed (Garzoni et al., 2007, Date et al., 2014). Garzoni and colleagues observed an altered transcriptome profile of *S. aureus* 6850 in the initial hours after internalization by A549 (Garzoni et al., 2007). In another study the transcriptional adaptations of methicillin-resistant *S. aureus* USA300 were analyzed in human abscesses and infected murine kidneys (Date et al., 2014). The authors observed for both models up-regulation of genes coding for divers proteases and toxins as well as peptide and iron transporters. Further, the impact of two global virulence regulators agrB and saeRS *in vivo* was examined.

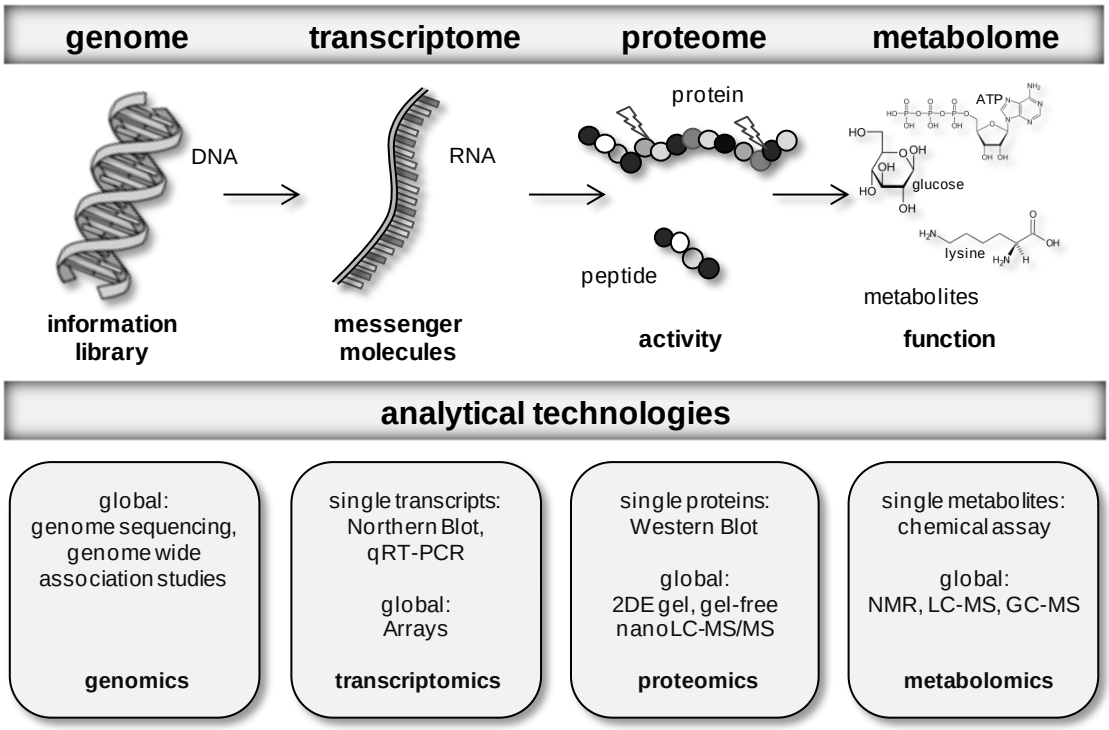

Figure 5. Levels of functional genomics. *The genome comprises all genetic information of a cell or organism. The transcriptome represents the messenger molecules that were transcribed. Activity of the cells is accomplished by the proteome and the products of enzyme reactions are summarized in the metabolome.*

Enzymes and other proteins accomplish vital processes. The proteome comprises all translated proteins. The first study which used this term was published in 1995 (Wasinger et al., 1995). Proteomics, in turn, describes the analysis of proteins at a large-scale. This became possible with sequencing of the human genome and genomes from other organism (Pandey and Mann, 2000). The availability of genome sequences allowed annotation of until then unknown genes and paved the way for dynamic analyses, such as expression, modification, and protein-interactions (Cho et al., 2004). Classical methods characterizing protein abundance include Western Blot analyses, which use antibodies to identify and quantify selected proteins. Global proteomics analysis can be achieved with gel-based or gel-free techniques. In gel-based approaches, complex protein mixtures are pre-fractionated with gel electrophoresis. Gel-free methods employ immediate protease digestion of the proteins and liquid chromatography based on different affinities of molecules to stationary and mobile phase. A commonly employed protease is trypsin, which cleaves peptide bonds C-terminal after lysine and arginine (Olsen et al., 2004, Eng et al., 1994). Gel-based approaches require higher amounts of sample than gel-free methods. Peptides resulting from tryptic digestion are analyzed in a mass spectrometer. Obtained spectra are compared in database searches utilizing search algorithms such as SEQUEST (MacCoss et al., 2002, Eng et al., 1994) or MASCOT (Perkins et al., 1999) with theoretical positive mass spectra calculated from theoretical peptide masses. Such databases are generated by *in silico* translation of DNA-codes in amino acid sequences followed by *in silico* hydrolysis of theoretical proteins using defined criteria (tryptic digestion after arginine and lysine). Then, all theoretical possible peptides from such database are compared with the acquired data sets. The obtained peptides are associated to corresponding proteins.

Finally, results from biological processes are reflected by the metabolome, the entirety of small endogenous or exogenous substances which are produced by a cell, tissue or organism. Usually, metabolome analyses are accomplished with ^{1}H-NMR (nuclear magnetic resonance spectroscopy), GC-MS, and LC-MS (Liebeke et al., 2012, Dörries and Lalk, 2013, Gierok et al., 2014). Techniques for identification and quantification of intracellular and extracellular metabolites require fast sample processing and control of the energy charge (Atkinson, 1968, Meyer et al., 2010). The energy charge represents the ratio relation between adenosine-triphosphate (ATP), adenosine-diphosphate (ADP), and adenosine-monophosphate (AMP). According to Atkinson, for living cells this value amounts between 0.8 and 0.95 (Atkinson, 1968). Metabolome analyses of infected host cells or internalized bacteria are challenging, as it is still not possible to distinguish host metabolites from secreted bacterial metabolites. Thus, within this study the complementing metabolite pool of non-infected host cell lines was determined to illustrate the nutrients available for *S. aureus* in each cell line at the start of internalization.

Prerequisites for proteome analysis of host-pathogen interactions

Proteomic analyses of bacteria are often hampered by the relatively low number of bacteria accessible in an infection approach. Such studies are even more complicated as the exceeding number of interfering human host proteins challenges identification of low abundant bacterial proteins. Miller and colleagues analyzed the adaptation of *S. aureus* to co-cultivation with THP-1 macrophages but confined the study to non-adherent, non-internalized bacteria (Miller et al., 2011). In this comparative study the authors report that the *S. aureus* NCTC8325 proteome is altered dramatically even after contact to eukaryotic cells. For example, the stringent response was induced, the alternative sigma factor SigB was activated, and the capability of oxidative stress response and virulence factor production in presence of macrophages was increased (Miller et al., 2011). Interestingly, these findings are in contrast to transcriptome data published by Garzoni and colleagues (Garzoni et al., 2007). The authors observed significant changes in gene expression pattern of *S. aureus* 6850 only after internalization by A549 cells but not after contact of to the epithelial cells (non-adherent bacteria) in comparison to bacteria which were cultivated in pure cell culture medium (Garzoni et al., 2007). Because different strains and different host cell types were employed in both studies and as proteomic and transcriptomic data are likely to differ, it is hard to compare both studies. To obtain reliable data of proteins actually changed upon internalization in comparison to the control, more proteome investigations of control samples with non-adherent bacteria are required.

Efforts were made to analyze host and bacterial proteins out of an infection setting (Attia et al., 2013, Ventura et al., 2008a). However, Ventura and coworkers analyzed the proteome of infected murine lungs and did not access *S. aureus* proteins with sufficient confidence (Ventura et al., 2008a). In a more recent study, Attia and colleagues detected only 22 staphylococcal proteins in infected abscess tissue. Among them were secreted virulence factors, IsdA, and proteins involved in gluconeogenesis (Attia et al., 2013). As these few numbers cannot describe the manifold adaptation mechanism, global proteome analysis of internalized bacteria requires enrichment of bacteria as well as highly sensitive mass spectrometers and sophisticated data analysis. Different separation techniques are available such as differential centrifugation (Xia et al., 2007, Abu Kwaik et al., 1993), immunomagnetic separation (Twine et al., 2006) or fluorescence assisted cell sorting using green fluorescent protein (GFP) or similar proteins (Becker et al., 2006, Jehmlich et al., 2010). Even if all three methods were already applied successfully, method optimization is still necessary in order to increase sampling speed and reproducibility, allow analysis of pathogens which demand for higher safety levels, and to reduce host contamination (Schmidt and Völker, 2011).

Digestion efficiency, which is also a critical point in proteome analysis, can be enhanced by previous breaking of disulfide bonds by reduction and alkylation prior to protease digestion. Further, uncontrolled modifications of free reactive cysteine molecules are prevented in that step. Addition of detergents such as RapiGest increases the number of detected proteins (Vowinckel et al., 2013).

However, the RapiGest concentration should not exceed than 0.1% as higher concentrations can inactivate trypsin. The compatibility of the sample and proteome analysis to RapiGest treatment has to be checked for each approach. For *S. aureus* it is also possible to apply the antibiotic lysostaphin which is produced by *S. simulans* (Recsei et al., 1987). This glycyl-glycine endopeptidase hydrolyzes the pentaglycine bridges of the cell wall (Kumar, 2008). By degradation of the cell wall, cytosolic proteins are more accessible to trypsin. Thus, the tryptic digestion protocol of *S. aureus* could be optimized by previous cell disruption adding lysostaphin (Pförtner et al., 2013). A first proteome study of sorted internalized bacteria was performed in 2010 (Schmidt et al., 2010b). Out of 3-6 million constitutively GFP-expressing *S. aureus* HG001 pMV158GFP cells internalized by S9, 591 bacterial proteins were identified and 367 could be quantified by nano liquid chromatography (nanoLC) coupled to tandem mass spectrometry (MS/MS) using the stable isotope labeling of amino acids in cell culture method (Schmidt et al., 2010b, Ong et al., 2002). By optimizing the digestion protocol and applying more sensitive mass spectrometers together with sophisticated data analysis more identified proteins are expected.

For a comprehensive understanding of the metabolism of a cell or organism it is absolutely necessary that gene and protein functions are known and updated as soon as new information are available. Some organisms are less annotated than others for example when they are newly discovered or sequenced. This is also true for some *S. aureus* strains. Often closely related strains with similar gene sequences exist that were investigated more extensively. The pan-genome of *S. aureus* comprises all genes which are found in different strains of this species and consists of the core-genome which covers the genes which are present in all strains of the *S. aureus* species and the dispensable genes which are in contrast present in only some strains and contribute to the diversity of a species (Medini et al., 2005). The proteome annotation of strain *S. aureus* HG001 was improved by comparison of annotation in other strains as part of this thesis.

A more recent strategy of protein identification uses spectral libraries obtained from actual detectable spectra from previous measurements. The advantage of it lies in increased accuracy due to direct comparison of sample spectra and the spectra in the library. With that it is also possible to exactly analyze complex samples of different organism, as for example bacteria carrying host cells. Comparison with spectral library allows identification of for example low abundant *S. aureus* protein within the background of human proteins and, at the same time false positive results are avoided. A tool which allows creating of these libraries is the recently introduced SpectraST (Lam et al., 2007).

Quantitative proteomics techniques to unravel host-pathogen interactions

In order to characterize the adaptation to internalization, it is essential to be able to quantify changes in the proteome composition of host and pathogen to be able to compare for example adaptation over time or different conditions (*e.g.* infected *vs.* non-infected host cells). In order to do so, techniques for relative or absolute quantification come into consideration. Relative quantification is applied for the comparison of protein amount over time or under different conditions. In these cases the point of interest lies in increased or decreased protein abundance compared to reference samples, and knowledge about absolute amounts of molecules is not necessary. However, for system biology approaches absolute quantification of proteins is essential. Knowledge about the number of molecules per cell allows modeling with bioinformatics approaches for conclusions about regulatory interaction of proteins. Analyses of protein complex stoichiometry or determination of composition of two component systems as well as protein-protein-interaction studies require knowledge of exact numbers of molecules.

In the last years, more sophisticated techniques were developed and widely applied by microbiologists in order to gain better understanding of the proteins, the “players of life”. Several methods were established, employed, and reviewed (Otto et al., 2014, Bantscheff et al., 2012). The development of LC-MS devices paved the way from protein driven analyses like Western Blotting, a target based quantification technique for single proteins, and 2DE-gel analysis, a top-down technique, developed in 1975 by Klose and O’Farrell (O'Farrell, 1975, Klose, 1975), which already allowed proteome analyses of organism to complex bottom-up proteomics on the level of peptides. Gel-free analyses are less limited by physicochemical properties of proteins such as pI or size, and by application of the proper solvent gradient, also hydrophobicity does not play a critical role. The combination of highly resolving liquid chromatography together with sensitive mass spectrometers, gel-free proteomics represents an excellent tool to investigate bacterial and human proteins from complex mixtures by efficient separation on peptide level and high accurate identification of mass to charge (m/z) ratios. In this study, three important techniques of gel-free quantitative proteomics were employed: stable isotope labeling of amino acids in cell culture (SILAC) method, label free quantification, and multiple reaction monitoring (MRM).

The SILAC method (Ong et al., 2002) was developed as a practicable approach for relative quantification of proteins (Figure 6). By cultivating bacteria or cell lines in medium containing heavy isotope labeled amino acids, for example $^{13}C_6$ arginine and $^{13}C_6$ lysine (6.02 Da more than $^{12}C_6$ arginine or $^{12}C_6$ lysine), a reference sample can be marked with only heavy peptides after incorporation in some replication cycles. It is required for the SILAC method that targeted bacteria or cells are auxotrophic for the SILAC amino acid used, meaning preferred uptake of amino acids over *de novo* synthesis (Dreisbach et al., 2008). It is further essential to check complete incorporation prior to the experiment. For cell lines a labeling time of five doublings should result in complete labeling (Ong et al., 2002). A method for rapid determination of the incorporation rate of heavy amino acids was presented by Schmidt and coworkers (Schmidt et al., 2007).

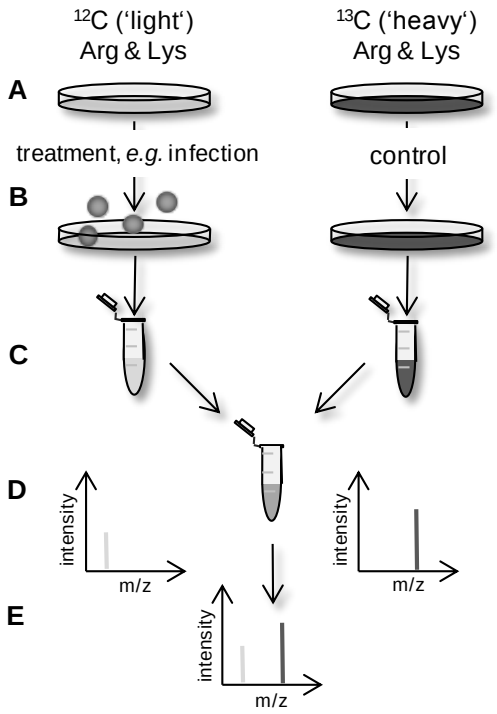

Figure 6. Principal setup of a SILAC experiment. *(A) One group of cells is cultivated in medium containing $^{12}C_6$ ("light") arginine (Arg) and lysine (Lys). In parallel, control cells are cultured in medium with $^{13}C_6$ ("heavy") amino acids. (B) Cells in light medium are treated with a stimulus (e.g. infection), control cells are not treated. (C) Cells are sampled in parallel and equal amounts are mixed. (D) After protease digestion samples are analyzed together by nanoLC-MS/MS and (E) quantified by the ratios of intensities from "light" and "heavy" sample.*

In a typical SILAC experiment, a reference sample is grown in heavy medium; in light medium a special treatment is applied. Afterwards, both conditions are mixed 1:1 on level of number of cells or on protein level. In the study presented here, intact $^{12}C_6$ labeled A549 cells after infection with *S. aureus* or mock infection with sterile medium were mixed with equal number of $^{13}C_6$ arginine or lysine control cells prior to protease digestion according to Figure 6. After digestion of these equal mixtures, proteins are measured by nanoLC-MS/MS, and protein amounts are compared based on the peak areas or intensities of light and heavy peptides eluting at the same retention time. When light and heavy versions of the proteins and corresponding peptides appear to the same extend, those proteins are not influenced by the specific condition or treatment. When the heavy peptides occur in higher intensities, their level is increased in the reference sample; prevail the light peptides, their level is increased in under the specific experimental condition. Changes in the proteome upon a certain treatment can also be monitored using the pulse-chased SILAC method with exchange of different labeled media within one setting (Fierro-Monti et al., 2013, Schmidt et al., 2010b).

Label-free quantification also allows relative quantification of complex protein data sets but requires more careful sample processing and special care in data acquisition and analysis.

There are different strategies to interpret label-free data. A widely employed quantification method is the spectral counting approach. The method starts with the assumption that more abundant proteins lead to a higher number of peptide spectrum matches. Since the size of a protein additionally influences the number of detected peptides and their according spectra, the protein length or molecular mass is taken into account to calculate the spectral abundance factor as ratio of number of spectra and the protein size. Further, this factor is normalized by the total number of spectra from one sample to avoid run-to-run variations due to sample preparation and data acquisition (Zybailov et al., 2006, Foerster et al., 2013, Gokce et al., 2011).

A more accurate way of label-free quantification is comprised by calculating areas under the curve (AUC) of peaks (Chelius and Bondarenko, 2002). Classical shotgun analysis (data dependent analysis, DDA) quantifies peaks on MS1 level as soon as they exceed a certain threshold. Since accuracy and reliability of a measurement depend on the exclusion time for selected peptides low abundant peptides show inaccurate values if a too broad exclusion time window is applied. In the recently introduced SWATH-MS approach or data independent analysis (DIA) masses of peptide-relevant m/z range (400-1200 m/z) are scanned in 25 m/z windows, and all ions in that range are fragmented. Peptides are quantified on MS2 level based on the peak areas of extracted ion chromatograms (XIC) (Gillet et al., 2012). Therefore, previously acquired spectral libraries and high resolution mass spectrometers are required (Gillet et al., 2012). According to Vowinckel and colleagues, both techniques are almost comparable regarding the number of identified proteins. However, applying the SWATH-MS method, the number of precisely quantified peptides (CV <15%) increased clearly compared to the DDA method (Vowinckel et al., 2013). Furthermore, the authors point out that sample preparation influences precision, sensitivity, and throughput of label-free quantification. They suggest preferring gel-free analysis and employing digestion protocols yielding high digestion efficiencies and low rates of missed cleavages to improve the quantitative results.

Multiple reaction monitoring (MRM) or single reaction monitoring (SRM) is a targeted analysis of a peptide (precursor) and fragment (product) pair (referred to as transition) performed mostly on a triple quadrupole mass spectrometer. It allows highly sensitive and selective quantification of even low abundant molecules of interest (Figure 7). Therefore, this method found increasing application in quantitative protein studies (Gallien et al., 2011). Proteotypic peptides (Mallick et al., 2007) are selected for each protein, and monitoring of several transitions for each proteotypic peptide allows exact identification.

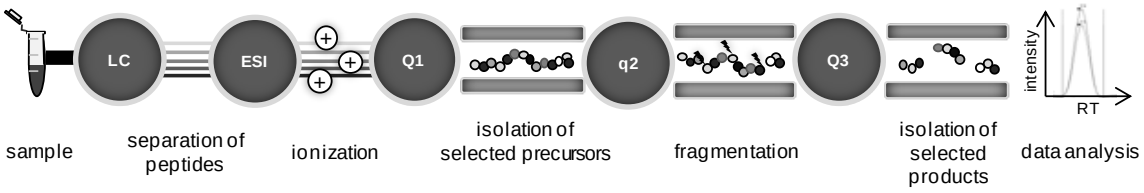

Figure 7. Principle of MRM. *Peptides are separated using liquid chromatography (LC) and subsequently ionized using electro spray (ESI). In a first quadrupol (Q1) targeted precursors are analyzed by their mass-to-charge (m/z) ratio. After fragmentation through collision with an inert gas like nitrogen (q2), the targeted fragment products are again analyzed in a second quadrupol (Q3). Signals are detected and can be analyzed.*

Absolute quantification (AQUA) (Gerber et al., 2003) of proteins by MRM is often performed by adding known amounts of stable isotope-labeled reference peptides to a sample comprising unknown amounts of a molecule of interest. Furthermore, AQUA provides a basis for the determination of the protein stoichiometry in protein complexes (Schmidt et al., 2010a). Another approach is the so-called QconCAT (Beynon et al., 2005) strategy which is based on the heterologous expression of a protein consisting of concatenated proteotypic peptides for quantification of different proteins of interest encoded by a QconCAT gene. The latter method requires hydrolysis of the QconCAT protein to obtain standard peptides for quantification. This brings the advantage that the QconCAT is spiked into the sample prior to digestion and is treated under the same conditions as the sample proteins. Another strategy uses tagged heavy standard peptides of interest which offer advantageous quantification. Like in the QconCAT strategy these standard peptides are added to the samples prior to protease digestion to remove a defined C-terminal tag required for quantification during factory process. Again, this procedure allows a similar treatment of the heavy standard peptides and the natural occurring peptides during sample preparation prior to quantification and therefore limits bias due to sample preparation (Surmann et al., 2014a). The ratio of the areas or intensities of sample peptide and corresponding heavy standard are used to calculate absolute amounts of the biological peptide. When a big set with a large number of proteins has to be quantified, it is possible to combine MRM of selected anchor proteins with 2DE-gels to absolutely quantify entire samples (Maass et al., 2011). When no heavy labeled standard for quantification is available, external standard curves with a non-labeled standard which is less cost extensive can be created in order to calculate the protein

amount in correlation to the measured area or intensity. However, this technique is easily tampered with run-to-run biased differences. Therefore, stable reproducible nanoLC-MRM runs are mandatory. Also interference between sample peptides can be expected in complex mixtures leading to intensities different to pure peptide dilutions. Standard curves are always recommended, in label-free as well as in spike-in approaches, to elucidate the limit of quantification and detection, and the linear range in which the quantification is reliable. In cases of label-free quantification, external standard curves can be used, in addition, to ensure exact identification of proteins whose intensities or areas can afterwards be relatively compared between different conditions or points in time. Actually standard-free targeted quantification by MRM was applied in the literature as this is a cheaper alternative when large numbers of proteins in a complex mixture have to be quantified. This points to the need for even more careful sample processing and data acquisition. Possible proteotypic peptides are scanned by MRM within the sample and have to be verified with spectra obtained by high accurate nanoLC-MS/MS approaches in parallel. Finally, measured peak areas or intensities are normalized to cellular reference proteins within the sample (Bluemlein and Ralser, 2011).

AIM OF THE STUDY

Infections with *S. aureus* play an important role for human health. Although normally infectious diseases can be treated efficiently with antibiotics, more and more resistances are observed. The spreading of resistant and highly virulent strains causes a high rate of mortality and morbidity due to *S. aureus* infections. Therefore, a better understanding of the behavior of *S. aureus* during interactions with the host is necessary to design more effective therapies or vaccines which could prevent severe infections. Additional information of the host response can uncover important contact points of *S. aureus* with infected cells to further increase knowledge of this pathogen. Therefore, this thesis aims to provide new techniques and strategies which are appropriate to investigate host-pathogen interactions. Understanding of intracellular processes is indispensable for future development of efficient treatments against severe infections. With this thesis, to my knowledge, for the first time a comprehensive picture of both, host's and pathogen's reaction during *S. aureus*-cell culture infection is presented. By identifying proteins that are regulated during internalization with the newly developed approaches, the way is paved for follow-up studies with detailed analyses in order to find targets for therapy.

To accomplish this goal, an internalization assay allowing sorting of GFP-expressing bacteria and subsequent nanoLC-MS/MS analysis of bacterial proteins had to be optimized. The aim was to increase the number of detected and quantified bacterial proteins by improvement of data analysis and interpretation. With that the proteomic adaptation of the pathogen after internalization by different host cells should be compared. Since the host cell seems to influence the pathogen's behavior, the established internalization method had to be altered to simultaneously analyze also host cell proteins. In particular it should be distinguished between the proteome of infected and non-infected host cells. To enhance information on host side, secretion of cytokines upon infection as well as apoptosis induction were studied in additional experiments. Because it is not always possible to apply GFP-expressing bacteria, a subtask was to develop a new technique enabling enrichment of non-fluorescent bacteria by preceding labeling with fluorescent or paramagnetic nanoparticles (NP). Important virulence factors of the pathogen which were secreted into the host after internalization should be made accessible by establishment of a new protocol. Low abundant secreted bacterial proteins had to be enriched by isolation of phagosomes and detected with a more sensitive MS method, the MRM. Taken together, new insights into the host-pathogen interactions should be gained by establishment of sampling and analysis techniques and investigation of time-dependent proteomic changes for infected host cells and internalized *S. aureus*.

MATERIAL & METHODS

Cultivation of bacteria

Bacterial strains and cultivation conditions

The *S. aureus* strain HG001 (Herbert et al., 2010) was used throughout the whole study. For experiments involving fluorescence microscopy or fluorescence activated cell sorting, bacteria carrying plasmids for constitutive expression of green fluorescence protein (GFP) or cyan fluorescent protein (CFP) were applied. Among the plasmids were pMV158GFP [(Nieto and Espinosa, 2003), *HG001 pMV158GFP obtained from Susanne Engelmann*] with a tetracycline resistance, pJL74 (GFP) and pJL76 (CFP) [*pJL plasmids obtained from Jan Liese*] each with resistance to erythromycin.

For long time storage, bacteria were cultivated in tryptic soy broth (TSB) with the appropriate antibiotic (erythromycin 10 *µg*/mL, tetracycline 20 *µg*/mL) until exponential phase and frozen with 20% (v/v end concentration) glycerol in 100 *µ*L aliquots at -80°C. The bacteria were grown in prokaryotic minimal essential medium [pMEM; 1x MEM without sodium bicarbonate (Invitrogen, Karlsruhe, Germany), supplemented with 1% non-essential amino acids (PAA Laboratories GmbH, Pasching, Austria), 4 mmol/L L-glutamine (PAA), 10 mmol/L HEPES (4-(2-hydroxyethyl)-1-piperazineethanesulfonic acid, PAA), and 2 mmol/L of each L-alanine, L-leucine, L-isoleucine, L-valine, L-aspartate, L-glutamate, L-serine, L-threonine, L-cysteine, L-proline, L-histidine, L-phenylalanine, and L-tryptophan (Sigma-Aldrich, St. Louis, USA); pH 7.4; sterile filtered]. In experiments for SILAC quantification of the staphylococcal proteome, bacteria were cultivated in so-called SILAC pMEM with 0.597 mmol/L $^{13}C_6$ L-arginine and 0.397 mmol/L $^{13}C_6$ L-lysine instead of the light isotope-containing amino acids L-arginine and L-lysine.

Prior to infection experiments, bacteria were cultivated in serial dilutions overnight at 37°C and 220 rpm in medium containing the appropriate antibiotic and additionally 0.01% (m/v) yeast extract to enhance growth. Before infection of the host cells, a main culture with fresh medium without antibiotic and yeast extract was inoculated with an exponentially overnight culture to an optical density at 600 nm (OD_{600}) 0.05 and cultivated until OD_{600} of 0.4. The OD was determined on a V-1200 Spectrophotometer (VWR) with pMEM as standard for OD_{600} <0.3 and TSB for OD_{600} >0.3 together with a 1:10 dilution of the bacterial culture in TSB. The main culture was incubated in a water bath (OLS 200 Grant Instruments, Cambridge, UK) at 37°C and linear shaking (stroke length 28 cm) depending on the size of the flask (100 mL flask: 150 strokes per min, 300 mL flask: 130 strokes per min, 500 mL flask: 120 strokes per min).

Cultivation of *S. aureus* HG001 in presence of fluorescence-labeled nanoparticles (NP)

[Protocol development together with Maren Depke, cell sorting performed by Petra Hildebrandt; NP obtained from Sarmiza Stanca and Wolfgang Fritzsche]

S. aureus HG001 cells were labeled with gold (Au) core or ferric oxide (FeOx) core, poly(vinyl alcohol)-(PVA) shell, fluorescence-labeled [fluorescein isothiocyanate (FITC) and rhodamine B isothiocyanate (RBITC)] nanoparticles (NP) as a new method for enrichment of bacteria from infected host cells. *S. aureus* HG001 cells were cultivated in pMEM with the appropriate antibiotic overnight at 37°C with 220 rpm in a shaking incubator (Innova 4200, New Brunswick Scientific, Edison, NJ, USA). With a culture in exponential growth phase, 0.5 mL of fresh pMEM containing additional 6.25 µL of NP-stock solution with either Au-core or FeOx-core NP were inoculated to an OD_{600} of 0.05. Bacterial culture was incubated at 37°C and 220 rpm in 15 mL tubes in a shaking incubator (New Brunswick Scientific). Incorporation of NP was determined after 15 min, 1 h, 2 h, 3 h, 4 h, 6 h, and 24 h by fluorescence microscopy and flow cytometry in a FACSAria high-speed cell sorter (Becton Dickinson Biosciences, San Jose, CA, USA). For fluorescence microscopy 2 µL bacterial cultures were mixed with 10 µL Mowiol embedding solution [33% (m/v) glycerol, 13% (m/v) Mowiol, and 0.1% (m/v) p-phenylendiamine in 0.133 mol/L Tris pH 8.5]. From each culture-Mowiol suspension, droplets of about 6 µL were placed onto microscope slides, covered with high-precision cover slips (Roth, Karlsruhe, Germany) and dried for 24 h. Microscope pictures were taken as described below.

For flow cytometry analysis 10 µL of bacterial culture were diluted in 100 µL phosphate buffered saline (PBS, PAA Laboratories GmbH, Pasching, Austria). Before analysis of bacterial samples, proper functioning of the instrument was checked using the cytometer setup and tracking module with appropriate beads (Becton Dickinson Biosciences, San Jose, CA, USA). First, side scatter (SSC) and forward scatter (FSC) data were used to gate the bacterial cell population, then thresholds and photomultiplier tube (PMT) voltages for RBITC-negative bacteria (*S. aureus* HG001) were adjusted. A blue coherent sapphire solid state laser with 488 nm excitation at 18 mW and a 50 mW yellow-green laser with 561 nm excitation were used. Optical filters were set up to detect the emitted RBITC fluorescence at 582/15 nm [phycoerythrin (PE) channel]. For each sample the RBITC fluorescence of 10,000 events in the scatter gate was analyzed. Data were recorded with the FACSDiva v6.1.3 software (Becton Dickinson Biosciences, San Jose, CA, USA) at logarithmic scale. Proteomic changes of the bacteria caused by NP were investigated after 24.5 h of cultivation with a SILAC approach by mixing NP labeled bacteria on a membrane filter with the same amount of bacteria without NP but heavily labeled with $^{13}C_6$ L-arginine and $^{13}C_6$ L-lysine. For internalization experiments with NP-labeled bacteria, *S. aureus* cells were labeled for 24.5 h with Au-NP or FeOx-NP prior to infection (Depke et al., 2014).

Counting of colony forming units (CFU) and numbers of bacteria

Serial dilutions of bacterial culture in PBS were plated in triplicates on TSB agar plates. After incubation for 24 to 48 h at 37°C colonies were counted and the CFU was determined. After purchase of the Guava easyCyte™ flow cytometer (Merck-Millipore, Billerica, MA, USA) the number of bacteria was determined by flow cytometry using the green filter (530 nm for FITC/GFP) by usage of GFP expressing bacteria or fluorescent staining with the dye SYTO® 9 nucleic acid stain (SYTO 9, Invitrogen, Karlsruhe, Germany). Syto9 was added directly before measurement to a final concentration of 0.5 μmol/L. When using SYTO 9, bacterial suspensions were diluted in 0.9% (m/v) NaCl instead of PBS, due to possible interactions of Syto9 with phosphor groups. The number of bacteria was determined in the Guava easyCyte™ flow cytometer by measuring the number of bacteria (concentration of 100-700 bacteria/mL required for accurate measurement) and the according volume which contained the counted bacteria. An average value of results from several experiments of CFU determination or bacterial counting at an OD_{600} of 0.4 was used to calculate the multiplicity of infection (MOI) prior to preparation of an infection mix (see below). Numbers or CFU from intracellular bacteria after infection were determined after host cell lysis with 0.1% Triton X-100 (7 min, 37°C) and adequate dilution series in PBS or 0.9% (m/v) NaCl. For optimal performance the Guava easyCyte™ flow cytometer had to be rinsed and its performance checked with fluorescent beads regularly according to manufacturer's instructions (Merck-Millipore, Billerica, MA, USA).

Cultivation of human cell lines

Human cell lines and cultivation conditions

S9 cells [ATCC® number CRL-2778 (Egan et al., 1992, Zeitlin et al., 1991)] and A549 cells [ATCC® number CCL-185 (Lieber et al., 1976)] were cultivated in eukaryotic minimal essential medium [eMEM; 1xMEM (Biochrom AG, Berlin, Germany), supplemented with additional 4% (v/v) fetal bovine serum (FBS, Biochrom AG), 2% (v/v) L-glutamine (PAA), and 1% (v/v) non-essential amino acids (NEAA, PAA)]. HEK 293 cells (Graham et al., 1977) were cultivated in modified eMEM for HEK 293 cells [HEK-eMEM; 1xMEM (Biochrom AG), supplemented with additional 10% (v/v) dialyzed FBS (Invitrogen, Karlsruhe, Germany), 2% (v/v) L-glutamine (PAA), 1% (v/v) sodium pyruvate (PAA), and 1% (v/v) non-essential amino acids (PAA)].

All types of cell lines, when not stated otherwise, were cultured for 3-4 days in 10 cm diameter tissue culture plates at 37°C, 5% CO_2 in a humid atmosphere. When confluent, medium was aspirated from the cells. After careful washing with PBS, 1 mL trypsin-ethylenediaminetetraacetic acid (trypsin-EDTA, PAA) was added to the cells for 7 min at 37°C to detach the cells from the culture plate. Cell suspensions were diluted in 3 mL fresh medium, resuspended by pipetting and, subsequently, 1 mL was transferred into a fresh culture plate containing 9 mL appropriate medium (referred to as new "passage" of cells). For long term storage of cell lines, confluent cells were detached with trypsin-EDTA as described above and resuspended in 1 mL eMEM or HEK-eMEM

containing 10% dimethylsulfoxide (DMSO) for each 10 cm diameter plate. The cells were cooled consistently in a container with isopropanol at -80°C for 24 h before long-term storage in liquid nitrogen. In order to adapt stored cells to culture, frozen aliquots of human cells were defrosted quickly and transferred into a tissue culture plate with 20 mL medium to dilute the DMSO. After 24 h of incubation (37°C, 5% CO_2, humid atmosphere) the medium was removed and replaced with 10 mL fresh medium, and cultivation was executed as described above.

A549 cells designated for host proteome analysis were cultivated in medium consisting of 1x MEM without L-arginine and L-lysine (Customer formulation, PromoCell) which was supplemented with 4% FBS, 2% L-glutamine, 1% NEAA and 30 μg/mL $^{12}C_6$ L-arginine, and 70 μg/mL $^{12}C_6$ L-lysine (Sigma-Aldrich, St. Louis, USA) for at least 14 days under the same conditions as described above. In parallel, cells were cultivated as a standard for relative SILAC quantification where $^{12}C_6$ L-arginine and L-lysine were replaced with $^{13}C_6$ L-arginine and $^{13}C_6$ L-lysine (Cambridge Isotope Laboratories, Inc., Andover, MA, USA) in equal concentrations.

S9 cells which express lysosomal-associated membrane protein 1 (LAMP-1) labeled with yellow fluorescent protein (LAMP-1-YFP) were obtained from Martin Fraunholz, Würzburg (Giese et al., 2009) and used to visualize phagosomes by fluorescence microscopy. YFP positive S9 cells were enriched by cell sorting with a FACSAria high-speed cell sorter (Becton Dickinson Biosciences, San Jose, CA, USA) using a 85 μm nozzle and 85 psi sheath pressure. The emission of the YFP was detected in the FITC-channel (Ex 488 nm/Em 530/30 nm). YFP positive cells were cultured further on as described above in eMEM supplemented with 3 μg/mL blasticidin (Blasticidin S-Hydrochlorid BioChemica, AppliChem, Darmstadt, Germany) for selection of YFP positive cells.

Preparation of cell lines for infection experiments

Three days before infection, human host cells were seeded into tissue culture plates whereby the size of plates differed depending on the experiment (Table 2). All cell culture plates were cell+ types containing charged surfaces which support attachment of adhesive cell lines (Sarstedt). Different sizes were chosen depending on the amount of cells needed. 12-well plates were chosen for the microscopy experiments because cover-slips fitted best in these wells. For 10 cm diameter and 15 cm diameter plates, cultivation was performed as described above by preparing fresh culture plates with one fourth of the previous confluent plate. For seeding cells into all other types of tissue plates including wells containing 18 mm high precision cover slips (Roth, Karlsruhe, Germany) for fluorescence microscopy (washed once with PBS before seeding of cells), confluent cells from the previous passage were detached with trypsin-EDTA, resuspended in fresh medium and counted in a Neubauer counting chamber for subsequent dilution with medium to a start concentration of $8*10^4$ human cells/mL prior to seeding.

Table 2. Overview of usage of different types of cell culture plates depending on the experiment. *Type/size of the plate, culture volume, and the corresponding experiments are listed.*

type of tissue culture plate	culture volume per unit/well [mL]	infection experiment/purpose
15 cm diameter	25	metabolome analysis after treatment with sterile infection medium
10 cm diameter	10	anti-caspase Western Blots, NP-internalization, isolation of phagosomes, transmission electron microscopy (TEM) for cell- and bacteria-counting
6-well plate	4	qRT-PCR for analysis of the immunoproteasome
12-well plate	2	fluorescence microscopy analyses on cover slips
24-well plate	1	proteome analyses of bacteria and host cells, cytokine profiling from cell culture supernatant

Internalization experiment

Infection assay

The internalization assay which was developed in our group is already published (Pförtner et al., 2013) and depicted in Figure 8. The approach described below was used in principle throughout the whole study but was also optimized and adapted in parts depending on the question of the experiment. The changes are described as method optimization in the results part.

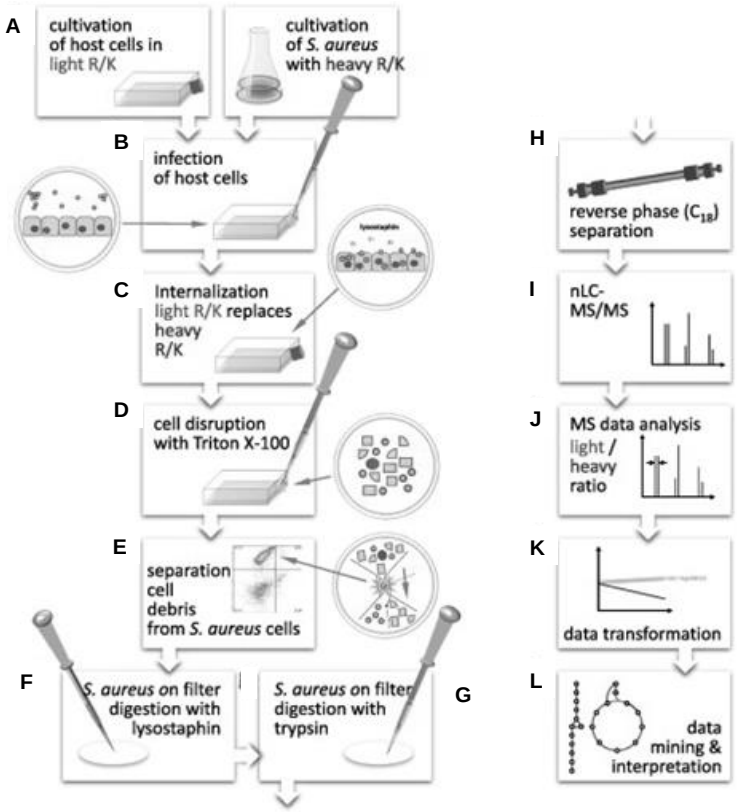

Figure 8. General workflow to identify and quantify proteins from internalized *S. aureus* HG001 cells in a time-resolved manner. *(A) S9 human bronchial epithelial cells were grown to confluence in eMEM containing light arginine and lysine. In parallel S. aureus was cultivated to exponential growth in pMEM, containing the $^{13}C_6$ heavy isotopes of arginine and lysine. (B) The S. aureus culture was diluted with eMEM to a MOI of 25 and transferred to the host cells. (C) After 1 h of internalization remaining non-internalized bacteria were killed with lysostaphin. After internalization, bacteria can only incorporate light counterparts of the heavy amino acids into their proteins. (D) Hourly, host cells were disrupted by Triton X-100 and internalized S. aureus were released. (E) At each point in time, GFP-positive bacteria were separated from cell debris and sorted on a low protein binding filter device, (F) and subjected to proteolytic digestion first by lysostaphin, (G) followed by trypsin. (H) Tryptic peptides were purified by ZipTip and (I) measured via nanoLC–LTQ-Orbitrap XL MS. (J) Identification and determination of peptide ratios were performed with the Rosetta Elucidator® software. (K) Protein light vs. heavy ratios with a more than twofold change relative to the median over time were defined up- or down-regulated. Proteins with a smaller deviation of their ratio from the average ratio of all proteins were defined non-regulated. (L) Regulated proteins were interpreted in on their role in cellular physiology (Pförtner et al., 2013).*

On the day of experiment, the number of confluent host cells was determined in an automatic cell counter (Countess®, Invitrogen, Karlsruhe, Germany) after detachment with trypsin-EDTA (compare "Human cell lines and cultivation conditions") and mixing equal volumes of cell suspension and Trypan blue dye solution (Invitrogen, Karlsruhe, Germany). Taking into account the CFU or number of bacteria at OD_{600} of 0.4 (compare "Counting of CFU and number of bacteria") an exponentially growing *S. aureus* culture (or NP-labeled bacterial culture after 24.5 h incubation) was diluted in eMEM or HEK-eMEM buffered with 2.2 g/L sodium bicarbonate. Dilution was chosen to yield a suspension which infected the host cells at a MOI of 25 when the normal cell culture plate filling volume was added. Supernatant from confluent cells was replaced by equal volumes of the infection mix. Bacteria were allowed to sediment, to attach to the host cells and to be internalized for 1 h at 37°C, 5% CO_2 in humid atmosphere. Afterwards, the infection mix was replaced with fresh medium containing 10 µg/mL lysostaphin (Ambi Products, LLC, Lawrence, NY, USA) which killed non-internalized bacteria. The volume of the infection mix was adapted to the type of cell culture plate used for the respective experiment (Table 2). For non-infected control host samples, bacteria-containing infection mix was replaced by sterile pMEM with a pH of about 7 which correlated to the pH of a bacterial culture at OD_{600} of 0.4 (Figure 9), while all other treatment procedures remained the same. These control samples served as baseline to which the data of internalization samples was compared afterwards.

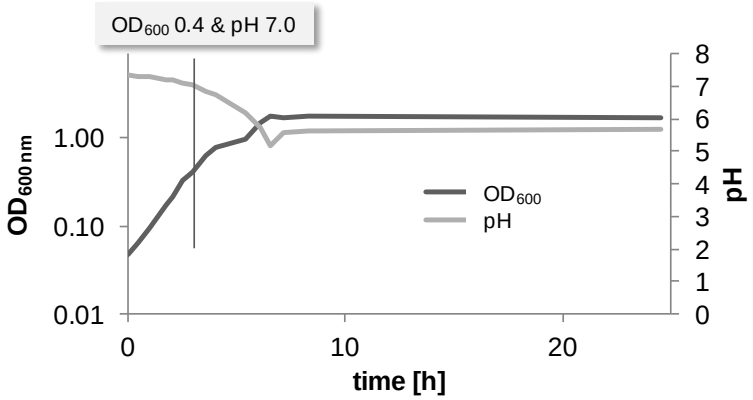

Figure 9. Correlation of optical density and pH during growth of *S. aureus* HG001 pMV158GFP in pMEM. *Measurement of pH was performed with a pH-meter (SCHOTT Instruments GmbH, Mainz, Germany).*

Sampling of bacteria or intact host cells after infection for proteome analysis

Cell culture supernatant was aspirated hourly between 1.5 h and 6.5 h *p.i.*, and cell monolayers were washed twice with PBS containing Ca^{2+} and Mg^{2+} (PAA).

For proteome analysis of *S. aureus* cells 150 µL 0.1% (v/v) Triton X-100 were added to each well of a 24-well-tissue culture plate. After incubation at 37°C for 7 min host cells were lysed and remaining bacteria and host cell debris were resuspended using a pipette and transferred into a reaction tube. All wells were rinsed with each 50 µL PBS, and the rinsing solution was added to the tube with the lysed cells. 100 µL of this solution were diluted for counting of CFU after plating on TBS agar or for counting bacteria with the Guava easyCyte™ flow cytometer (Merck-Millipore, Billerica, MA, USA). GFP-expressing bacteria were sorted from host cell debris using flow cytometry (see below).

As a control, bacteria which were not internalized after 1 h exposure to the host cells (referred to as non-adherent control), were harvested and analyzed by nanoLC-MS/MS. Therefore, in the A549 project, each 1 mL of supernatant 1 h after incubation of host cells with infections mix was centrifuged (16,000x*g*, 4°C, 10 min) and washed once with PBS. The cell pellets were prepared for nanoLC-MS/MS analysis similar to the bacteria on the filter plates as described below. For the comparative analysis of adaptation of *S. aureus* HG001 to different cell lines, non-adherent control samples were prepared with an improved protocol by incubation of 1 mL infection supernatant (1 h) with 0.01% Triton X-100 (37°C, 7 min) and subsequent exposure to the FACSAria by sorting two million bacteria on a membrane filter to improve comparability to the internalized bacteria.

For analysis of the host cell proteome intact A549 cells (after exposure to bacteria or treatment with sterile pMEM) were detached from the culture plate with 150 µL trypsin-EDTA (PAA) in each well for 7 min at 37°C and subsequent inactivation of trypsin with 50 µL eMEM in each well. After centrifugation (500x*g*, 4°C, 5 min) cell pellets were resuspended in PBS. Infected host cells

containing GFP expressing bacteria were separated from cells without bacteria by flow cytometry. Additionally, host cells of one well were lysed using 1% Triton X-100 at each point in time after infection as described above and used for determination of CFU by plating or counting of bacteria with the Guava easyCyte™ flow cytometer (Merck-Millipore, Billerica, MA, USA).

Methods to enrich bacteria, host cells and their proteins

Fluorescence assisted cell sorting of bacteria from host cell lysates and collection on filter membranes

[Cell sorting performed by Petra Hildebrandt]

Prior to sorting, the Accudrop routine was used to adjust the drop delay to ensure proper sorting. GFP expressing bacteria were sorted in a FACSAria high-speed cell sorter (Becton Dickinson Biosciences, San Jose, CA, USA) in the FITC-channel (Ex 488 nm/Em 530/30 nm) applying appropriate SSC-A gates out of host cell debris onto a low protein binding filter membrane (0.22 µm pore size, hydrophilic low protein binding, Durapore membrane) of a 96-well microtiter plate (Merck-Millipore, Billerica, MA, USA). The liquid was removed constantly using vacuum (450-550 mbar). After sorting the filter membrane was rinsed with 200 µL PBS and cut into four pieces with a scalpel. The pieces were placed into a reaction tube and stored at -20°C until preparation for MS (see below).

When bacteria were labeled with Au-NP, they were analyzed with the 488 nm laser and the 561 nm laser at 70 psi sheath pressure with the 70 µm nozzle in place. Signal discrimination was set on FSC. Bacteria were sorted onto the 96-well filter plates (0.22 µm, Merck-Millipore, Billerica, MA, USA) using the SSC and RBITC fluorescence properties of the NP.

Fluorescence assisted cell sorting of intact A549 cells

[Cell sorting performed by Petra Hildebrandt]

Trypsinated single cells in PBS were separated with the FACSAria (Becton Dickinson Biosciences, San Jose, CA, USA) for host cell proteome analyses. Here, the GFP fluorescence of the internalized bacteria was used to discriminate between infected and non-infected cells. Infected GFP-positive and GFP-negative non-infected host cells were sorted into 15 mL reaction tubes, centrifuged at 500x*g*, 4°C for 5 min and resuspended in a reduced volume of PBS (about 500 µL). The concentration and number of cells was determined by microscopic counting using a Neubauer chamber. Non-infected control cells were also sorted in the FACSAria with the same settings as the GFP-negative A549 cells to provide comparable stress conditions for infected sample and control cells without contact to bacteria.

Magnetic separation of bacteria from lysed host cells

[Performed together with Maren Depke]

S. aureus HG001 cells carrying plasmid pJL74 (GFP) and FeOx-NP were isolated from lysed host cells with a two Tesla magnet (HOKIMag) which was applied to the suspension after lysis with 0.1% Triton X-100 (4°C, 40 min). Afterwards, the magnetic NP-labeled fraction of bacteria was captured, washed and then eluted in PBS. Cell counts were determined for all fractions (lysate before exposure to magnet, non-magnetic flow-through, wash solution, and magnetic fraction) in the Guava easyCyte™ flow cytometer (Merck-Millipore, Billerica, MA, USA) using GFP.

Isolation of phagosomes from infected host cells

Medium was aspirated at 2.5 h and 6.5 h *p.i.*, and cell layers were washed twice with PBS. To each plate 1 mL homogenization buffer [8.55% (m/v) sucrose in 20 mmol/L HEPES (PAA) diluted in HPLC grade water (J. T. Baker, Center Valley, PA, USA), with protease inhibitor 1:20 (Complete EDTA-free Protease Inhibitor Cocktail Tablets, one tablet dissolved in 50 mL extraction solution according to instructions, aliquots were frozen at -20°C until usage, Roche, Germany); pH 6.5] was added, and cells were removed from culture plate using a cell scraper and resuspended by pipetting. All further steps of isolation of phagosomes were conducted on ice with cooled solutions. All cells of one point in time were pooled and centrifuged (2,000x*g*, 4°, 10 min). Cells were resuspended in 500 µL homogenization buffer and lysed using a 21 gauge syringe needle (10 times up and down). After centrifugation (500x*g*, 4°C, 7 min) of the lysed cells the supernatant was transferred into a clean vial, and the remaining pellet was resuspended again in 500 µL homogenization buffer. Lysis was repeated with a syringe needle of size 20 gauge. After repeated centrifugation (500x*g*, 4°C, 7 min) both supernatants were combined with the pellet and centrifuged twice with the same settings in order to rinse all phagosomes out of the insoluble pellet. In between the centrifugation steps, the sample was mixed thoroughly to increase extraction and homogenization. One mL homogenized sample was placed carefully on top of a sucrose gradient consisting of 1 mL 50% (m/v) sucrose in 20 mmol/L HEPES solution, pH 6.5, at the bottom and 1 mL 12% (m/v) sucrose in 20 mmol/L HEPES solution, pH 6.5, as the second layer in a 15 mL reaction tube. Samples were centrifuged in a swing-out rotor without breaks engaged (4°C, 800x*g*, 45 min). Afterwards, different cellular compartments were distributed between the three phases which were carefully separated from each other by pipetting in fresh vials. For each gradient phase CFU were determined. Distribution of bacteria to the different sucrose phases was calculated by comparing numbers of bacteria in the single phases to the whole amount of bacteria at one point in time considering the exact volume of each phase. Remaining suspensions were centrifuged (2,000x*g*, 4°C, 15 min), supernatant was removed, and pellets of the 12% (m/v) phase were stored at -80°C until preparation of samples for MS as described below.

Sample preparation for mass spectrometry

Preparation of proteins

Sorted whole human A549 cells (GFP-positive, GFP-negative, non-infected control cells) were counted in a Neubauer chamber. They were mixed with equal numbers of untreated, heavy isotopically labeled A549 cells grown in medium with $^{13}C_6$ L-arginine and $^{13}C_6$ L-lysine (see above) as internal standard for relative quantification. The standard cells grown in heavy medium were detached from the tissue culture plates with trypsin-EDTA as described above. Cells were centrifuged (16,000x*g*, 4°C, 10 min). Pellets were resuspended in buffer containing 8 mmol/L urea and 2 mmol/L thiourea (UT-buffer) and immediately frozen in liquid nitrogen. Human proteins were extracted by five cycles of freezing (in liquid nitrogen) and subsequent thawing (30°C, 1,400 rpm, 10 min) in a shaking incubator (Eppendorf) combined with ultrasonication (on ice, 3x3 s, 50% power, SonoPuls, Bandelin electronic, Berlin, Germany). Amounts of proteins which were dissolved in the supernatant after centrifugation (45 min, 16,000x*g*) were quantified using a Bradford assay (Biorad, München, Germany).

Pellets of isolated phagosomes were resuspended in 50 µL UT-buffer. Proteins were extracted by five cycles of freezing in liquid nitrogen and thawing at 30°C, at vigorous shaking for 10 min and subsequent ultrasonication three times for 3 s and 50% power (SonoPuls, Bandelin electronic). After centrifugation (16,000x*g*, 20°C, 45 min) supernatant was transferred into fresh vials and stored at -80°C until protein estimation. Protein amount was determined using a Bradford assay (Biorad, München, Germany) and the VarioSkan Flash photometer (Thermo Fisher Scientific, Waltham, MA, USA).

Determination of protein concentration using a Bradford assay

The concentration of protein solutions was determined using the VarioSkan Flash photometer (Thermo Fisher Scientific, Waltham, MA, USA) in 96-well-flatbottom-plates. Each sample, blank or standard was assembled to a final volume of 200 µL including 40 µL Bradford solution (Biorad) containing the dye Coomassie-Brillant-Blue G-250 at room temperature. Standard curves were prepared in triplicates using different concentrations of bovine serum albumin (BSA) between 0 and 0.03 µg/µL. If necessary, samples were pre-diluted with HPLC-grade water (Baker) and the blank, which was always the solvent of the sample (*e.g.* UT-buffer), was diluted with water to the same extend as the sample. All samples were incubated with the Bradford reagent for the same time as the corresponding standard curve, but not longer than 20 min and subsequently measured at 595 nm. Data were acquired and analyzed with the SkanIt v2.4.3 software (Thermo Fisher Scientific, Waltham, MA, USA).

On-membrane digestion

Filter membranes containing *S. aureus* cells after fluorescence assisted cell sorting were incubated in 12.33 µL 20 mmol/L ammonium bicarbonate (ABC) and 1 µL 0.05 µg/µL lysostaphin (Ambi Products LLC, Lawrence, NY, USA) for 30 min at 37°C. Afterwards, 6.66 µL 0.01 ng/µL trypsin (Promega, Madison, WI, USA) were added, and protease digestion occurred for 16-18 h at 37°C. Reaction was stopped by adding trifluoroacetic acid [TFA, final concentration 0.1% (v/v)] and incubation for 5 min at 37°C. After centrifugation (16,000x*g*, 10 min) peptide solutions were desalted and purified using C_{18} ZipTip columns (Merck-Millipore, Billerica, MA, USA) as described below.

For proteome analysis of bacterial cells labeled with NP after isolation by cell sorting or by capture using a two Tesla magnet (HOKIMag), the samples were applied to a filter plate, and liquid was aspirated using vacuum and washed. First, 1 µL 0.05 µg/µL lysostaphin and 20 µL 20 mmol/L ABC were added and incubated at 37°C for 30 min. Then, disruption was supported using an ultrasonic bath (45 kHz, 60 W, 3 min). Proteins were reduced with 5 mmol/L tris-2-carboxyethyl-phosphine (TCEP) at 37°C and 500 rpm shaking for 30 min and alkylated with 10 mmol/L iodoacetamide (IAA), 25°C, 500 rpm, 30 min). Afterwards, remaining TCEP/IAA was removed with 15 mmol/L N-acetyl-cysteine (25°C, 500 rpm, 10 min), and proteins were digested with 1 µg trypsin per sample in the presence of 0.1% RapiGest (Waters Corp., Milford, MA, USA) at 37°C for 16 h. Digestion was stopped by acidification, and tryptic peptides were purified using C_{18} ZipTip columns (Merck-Millipore, Billerica, MA, USA) as described below.

Liquid digestion after reduction and alkylation of proteins

Trypsins enzymatic activity tolerates only a maximum concentration of 2 mol/L urea. Thus, samples of 2 µg protein in UT buffer (8 mol/L urea, 2 mol/L thiourea) were diluted with 20 mmol/L ABC in order to achieve urea concentrations compatible with tryptic digestion. Proteins were reduced with 2.5 mmol/L dithiothreitol (DTT) at 60°C for 1 h, alkylated with 10 mmol/L IAA at 37°C for 30 min in the dark, and digested overnight at 37°C using trypsin (Promega, Madison, WI, USA) in a protease to protein (m/m) ratio of 1:25. Digestion was stopped with a final concentration of 1% (v/v) acetic acid (HAc). Insoluble components were removed by centrifugation for 10 min at 16,000x*g*. The peptide-containing supernatant was purified and desalted with C_{18} material. For some approaches the digestion protocol had to be adapted, differing protocols are described below.

After phagosomal preparation required volumes for 10 µg sample protein were filled with 20 mmol/L ABC to 20 µL sample volume, reduced (2.5 mmol/L DTT, 60°C, 1 h), alkylated (10 mmol/L IAA, 37°C, 30 min), and digested with trypsin (protease to sample (m/m) ratio 1:25, 37°C, 16-18 h). Trypsin reaction was stopped adding HAc to a final concentration of 1% (v/v). Acidified peptides were purified using C_{18} ZipTip columns (Merck-Millipore, Billerica, MA, USA) with the protocol described below. This step was repeated and thus, two samples of purified tryptic peptides were finally produced from each tryptic digestion reaction mix. Peptides were dried by high speed vacuum

centrifugation (Eppendorf, Hamburg, Germany) and reconstituted in 20 µL buffer A and stored at -20°C until analysis by shotgun MS and MRM.

Peptide purification with C_{18} material

ZipTip (Merck-Millipore, Billerica, MA, USA) columns were equilibrated by pipetting three times in 100% acetonitrile (ACN), five times in 80% (v/v) ACN in 1% (v/v) HAc, five times with 50% ACN in 1% (v/v) HAc, five times in 30% (v/v) ACN in 1% (v/v) HAc and twice in 1% (v/v) HAc. Subsequently, the sample was loaded by 20 times pipetting for C_{18} columns, ten times for µC_{18} columns, respectively. The column was rinsed five times in 1% (v/v) HAc. C_{18} bound peptides were eluted into HPLC vials (VWR, Darmstadt, Germany) first by ten times pipetting in 5 µL 50% (v/v) ACN in 1% (v/v) HAc and second by ten times pipetting in 5 µL 80% ACN in 1% HAc. When µC_{18}-columns were used, only five pipetting steps were applied for each elution step. Peptides were dried in a vacuum centrifuge (Eppendorf, Hamburg, Germany), reconstituted in 10-20 µL (depending on sample concentration) buffer A (2% (v/v) ACN in 0.1% (v/v) HAc) and stored for few days at -20°C until nanoLC-MS/MS analysis.

Acquisition of proteome data by mass spectrometry

Data acquisition by high precision shotgun nanoLC-MS/MS

[Shotgun mass spectrometers were operated by Vishnu M. Dhople and Manuela Gesell Salazar]

The nanoLC-MS/MS measurements for A549 cell proteome, phagosomal proteome analysis and time-resolved response of *S. aureus* HG001 to internalization by A549 cells were carried out on an LTQ Orbitrap Velos mass spectrometer (Thermo Fisher Scientific, Waltham, MA, USA) coupled with a Proxeon Easy nanoLC (Proxeon Biosystems A/S, Denmark).

For analysis of A549 host cell proteome and bacterial proteome after internalization by A549 cells the peptides were separated using an analytical column, Acclaim PepMap 100 (C_{18}, particle size 3 µm, 100 Å; manufactured by LC-Packings, Dionex, USA) of 15 cm bed length and two solvents: buffer A (2% acetonitrile in water with 0.1% HAc) and buffer B (acetonitrile with 0.1% HAc). The peptides were enriched on a pre-column, Biosphere C (ID 100 µM, particle size 5 µm, length 20 mm, pore size 120 Å manufactured by NanoSeparations, Netherlands). Peptides were eluted at a flow rate of 300 nL/min with formation of a solvent gradient of Buffer A and B (2-5% buffer B in 1 min, 5-25% B in 59 min, 25-40% B in 10 min, 40-100% B in 8 min) and were ionized using a nano source. The mass spectrometer was operated in data-dependent analysis (DDA) mode to automatically switch between Orbitrap-MS and LTQ-MS/MS acquisition. Survey full scan MS spectra (from *m*/*z* 300 to 1700) were acquired in the Orbitrap with a resolution *R*=30,000. The method allowed sequential isolation of up to 20 most intense ions, and, depending on signal intensity, they were subjected to fragmentation in the linear ion trap using collision-induced dissociation. Target ions already selected with an isolation width of 2 Da for MS/MS were dynamically excluded for 60 s. The general MS

conditions were electrospray voltage, 1.6-1.75 kV; no sheath and auxiliary gas flow. Ion selection threshold was 2,000 counts for MS/MS, an activation Q-value of 0.25 and activation time of 10 ms were also applied for MS/MS with normalized collision energy (CE) of 35%. The charge state screening and monoisotopic selection was enabled with the rejection of +1, +4 and higher along with unassigned charge states.

Peptide separation for phagosomal proteins was performed on a NanoAcquity BEH130 C_{18} column (10 cm length, 100 μM inner diameter and 1.7 μm particle size from Waters Corporation) using a nanoAcquity UPLC with a flow rate of 400 nL/min and applying a nonlinear gradient ranging from 1% to 100% ACN with 0.1% HAc in 100 min.

Peptide separation of samples from internalized *B. pertussis* cells [*cultivation of B. pertussis Tohama I and sample preparation performed by Yanina Lamberti*] was performed on a Proxeon nanoLC system (Proxeon, Odense, Denmark) with the help of am Acclaim PepMap 100 column (C_{18}, 3 mm, 100A, Dionex, Sunnyvale CA, USA) capillary of 15 cm length. The solvent gradient used started from 100% buffer A/0% buffer B (15 min) to 60% B (290 min) with a flow rate of 300 nL/min. Afterwards, peptides of phagosomal proteins and from internalized *B. pertussis* were ionized using electro spray and analyzed in a LTQ-Orbitrap-Velos mass spectrometer (Thermo Electron, Bremen, Germany) in DDA mode to switch automatically between Orbitrap-MS and LTQ MS/MS acquisition. Survey full scan MS (from m/z 300 to 1700) was acquired in the Orbitrap with resolution R=30,000 at m/z 400. Up to 20 most intense ions were sequentially isolated for collision induced dissociation (CID) in the linear ion trap. Selected target ions were dynamically excluded for the next 60 s.

NanoLC-MS/MS analysis of peptides from iron-starved *B. pertussis* pellets [*cultivation of B. pertussis Tohama I and sample preparation performed by Yanina Lamberti*] were performed on a Proxeon nanoLC system (Proxeon, Odense, Denmark) connected to a LTQ-Orbitrap-MS (ThermoElectron, Bremen, Germany) equipped with a nanoESI source. For LC separation, an Acclaim PepMap 100 column (C_{18}, 3 mm, 100 A, Dionex, Sunnyvale CA, USA) capillary of 15 cm length was used. The solvent gradient used started from 100% buffer A/0% buffer B (15 min) to 60% B (290 min) with a flow rate of 300 nL/min. The MS was operated in DDA mode to automatically switch between Orbitrap-MS and LTQ-MS/MS acquisition. Survey full scan MS spectra (from m/z 300 to 2,000) were acquired in the Orbitrap with resolution R 60,000 at m/z 400 (after accumulation to a target of 1,000,000 ions in the LTQ). The method used allowed sequential isolation of up to five of the most intense ions, depending on signal intensity, for fragmentation on the linear ion trap using collision-induced dissociation at a target value of 100,000 ions. Target ions already selected for MS/MS were dynamically excluded for 60 s. General MS conditions were: electrospray voltage, 1.5 kV; no sheath and auxiliary gas flow. Ion selection threshold was set to 500 counts for MS/MS, and an activation Q-value of 0.25 and activation time of 30 ms were also applied for MS/MS.

Peptides of *S. aureus* HG001 separated from three infected cell lines after 2.5 h and 6.5 h post-infection as well as samples derived from experiments with NP-labeled bacteria were analyzed on a

Q Exactive mass spectrometer (Thermo Fisher Scientific, Waltham, MA, USA) coupled to a Dionex UltiMate 3000 nanoLC system (Dionex/Thermo Fisher Scientific, Idstein, Germany) *via* a TriVersa NanoMate source (Advion, Ltd., Harlow, UK). In both cases peptides were separated using a trap column (75 μm inner diameter, packed with 3 μm C_{18} particles, Acclaim PepMap 100, Thermo Fisher Scientific, Waltham, MA, USA). For the comparative cell line infection experiment a 25 cm analytical column packed with 2 μm C_{18} particles (Acclaim PepMap RSLC, Thermo Fisher Scientific, Waltham, MA, USA) was applied, for NP experiments this column was 15 cm long. Peptides were separated by a linear gradient of buffer B at a flow rate of 300 nL/min from 2% to 25% in 120 min for the cell line infection experiment (Surmann et al., 2014b). In the NP approach, gradient lasted for 90 min for SILAC experiments and 30 min for bacteria enriched form cell debris using NP (Depke et al., 2014). For MS analysis the Q Exactive was operated for both projects in DDA mode with a full scan resolution of 70,000 in a range from 300 to 1,650 m/z. the ten most abundant isotope patterns (centroid data) with charge ≥2 from the survey scan were selected for MS/MS analysis and fragmented by higher energy collisional dissociation (HCD). More details for both projects are provided as Supplementary_Material_01_Details of LC-MS-analysis.docx (Depke et al., 2014, Surmann et al., 2014b).

Multiple reaction monitoring (MRM)

For MRM analysis of *S. aureus* proteins, peptides were separated with a nanoHPLC (EASY-nanoLC, Proxeon Biosystems A/S, Odense, Denmark) using an Acclaim PepMap 100 reverse phase column (3 μm, 75 μm inner diameter x 150 mm, LC Packings, Dionex, Idstein, Germany) at a flow rate of 300 nL/min and a gradient ranging from 5-90% ACN in 0.1% HAc in 33 min and allowing subsequent column equilibration (Table 3). Separated peptides were ionized applying electrospray and analyzed with a TSQ Vantage triple quadrupole mass spectrometer in scheduled MRM mode (Thermo Electron, Bremen, Germany) with an 8 min RT window for each transition. Precursors were fragmented by CID after analysis in the first quadrupole. CE was optimized starting from factory defaults by applying different eV in steps of + or -2 eV. Settings were adjusted to a resolution of 0.7 full width at half maximum (FWHM) for both quadrupoles. The final cycle time was set to 3 s. For each peptide the double charged precursor and the four most abundant product ions were chosen for MRM acquisition.

Table 3. LC-gradient used prior to MRM analysis. *ACN (acetonitrile).*

time [min]	0	3	26	32	33	38	39	42
ACN [%]	5	10	35	60	90	90	0	0

Identification, quantification, and visualization of proteome data

Data analysis from shotgun nanoLC-MS/MS measurements

Identification of human A549 and staphylococcal proteins was achieved with the Rosetta Elucidator® software (Rosetta Biosoftware, Ceiba Solution Inc., Boston MA, USA) with an automated database search against a UniProt-Prot database from 2012 limited to human proteins (UniProt_12_08) or a *S. aureus ssp. aureus* NCTC8325 sequence from NCBI updated with annotations from genome and protein sequence comparisons (Sau_8325_BLAST_HGW) together with the SEQUEST algorithm rel. 3.5 (Sorcerer built 4.04, Sage-N Research Inc., Milpitas, CA, USA). An alignment search was performed in a search distance of 4 min retention time and 10 ppm instrument mass accuracy. Carbamidomethylation of cysteine (57.02 Da) was a fixed modification only in the human search. Oxidation of methionine (15.98 Da) and SILAC labeling of arginine and lysine (6.02 Da) were variable modifications. A maximum of three SILAC labels per peptide was allowed in a tolerance of 20 ppm and 0.5 min RT location tolerance. Peptides were annotated based on Peptide Teller allowing a predicted error of maximum 0.01. *S. aureus* proteins which were identified with at least two peptides or one peptide and at least 10% sequence coverage were considered for quantification to cover also small bacterial proteins. Host proteins were only considered when they were identified with more than one peptide. For data analysis of the bacterial proteome the raw protein intensities were median normalized based on the intersection of all samples and only proteins, which were found in at least two biological replicates (BR), were considered for further analysis. The mean of the BR was used for linear fit modeling. Obtained fitted bacterial protein values were used for ratio calculation (ratio= t_6/t_1). Voronoi-like treemaps (Bernhardt et al., 2013) for *S. aureus* proteins were generated using the Paver software (DECODON GmbH, Greifswald, Germany) and the latest functional categorization of the SEED database (Overbeek et al., 2005) of *S. aureus* NCTC8325 (SEED DB version 2.0).

For SILAC quantification of host proteins, only labeled pairs reaching a labeled pair status of "good" were considered. Host proteins could only be analyzed between 2.5 h and 6.5 h *p.i.* as the 1.5 h value gave unstable results for the GFP-positive A549 cells due to the low number of internalized bacteria at this sampling point. Only proteins that were analyzed in all the three types of A549 cells were considered for further analysis. Ratios of the host proteins were calculated between each between the sample (control, GFP-positive or GFP-negative) and the heavy labeled standard. Principal component analysis (PCA) of host proteins was performed for medians of three BR for each point in time per treatment group with the normalized values using the Genedata Analyst v7.6 software (Genedata AG, Basel, Switzerland). Pathway analysis of host proteins was performed using IPA (Ingenuity® Systems, www.ingenuity.com).

For the cell line comparison project resulting raw data files were converted to mzML format using msconvert (ProteoWizard, http://proteowizard.sourceforge.net). Then, the mzML files were searched using COMET (Eng et al., 2013) and SpectraST (Lam et al., 2007) and processed using Trans-

Proteomic Pipeline (TPP) (Keller and Shteynberg, 2011). The database contained 84,911 human protein entries [complete proteome and VARSPLIC (Kersey et al., 2000)] and 2891 sequences for *S. aureus*. Common contaminants (115 cRAP) and a sequence-shuffled decoy counterpart were added to the database. For COMET the parent mass error was set to ±50 ppm. N-terminal protein acetylation and methionine oxidation were set as variable modifications. The maximum number of missed cleavage sites was set to 2, and number of enzyme termini was set to 1. For SpectraST, the parent mass error was set to ±1.0 Daltons. The spectra library was constructed from previous Q Exactive runs which were searched using COMET with the same parameters using a *S. aureus* protein database only (Michalik et al., unpublished data). Peptides identified with iProphet probability ≥ 0.9 were used to construct the spectral library (Shteynberg et al., 2011). The PeptideProphet outputs from both search engines were combined using iProphet.

The reSpect (Positive Probability, Ltd., Isleham, United Kingdom) algorithm was applied to identify and attenuate the peaks in the MS/MS spectra that were excluded by the first pass search. A second search round was performed on the reSpect processed spectra, with a mass tolerance matching the selection window of the mass spectrometer and using possible charge states of 1 through 5, which allowed the identification of novel distinct peptide sequences not seen in the single pass analysis. The reSpect searches were analyzed separately from the first pass searches, and also using PeptideProphet and iProphet to establish accurate error rates.

Only peptides with a probability greater than 0.8 (~TPP error rate <0.01) and without missed cleavages were considered for further relative quantification on protein level. The quantification was performed using the “MSstats R package for statistical relative quantification of proteins and peptides” implemented in Skyline package v2.5 freely available in the internet (https://skyline.gs.washington.edu) (Choi et al., 2014, Schilling et al., 2012). The areas under the curve (AUC) of peptides were summed to obtain single protein intensities. Mean values from three BR were used which were median normalized to the values of non-adherent bacteria control.

The MS proteomics data have been deposited to the ProteomeXchange Consortium (Vizcaíno et al., 2014) *via* the PRIDE partner repository with the dataset identifier PXD001003.

PCA was performed using the Genedata Analyst v7.6 software (Genedata AG, Basel, Switzerland). Median normalized $\log_{10}$ transformed intensity values for all proteins quantified in all cell lines were used for calculation of the variances of the cell lines and sampling points. For each time point data from three independent biological samples were used to calculate average values. Box blots of functional groups were generated using the SEED database of *S. aureus* NCTC8325 [SEED DB version 2.0 (Overbeek et al., 2005)] and Voronoi-like treemaps were created using the Paver software (DECODON GmbH) (Surmann et al., 2014b, Bernhardt et al., 2013).

Phagosomal proteins and staphylococcal proteins were analyzed *via* the Rosetta Elucidator® software (Rosetta Biosoftware, Ceiba Solution Inc., Boston, MA, USA) with an automated database search against a UniProt-database from 2012 limited to human proteins or *S. aureus* strain

NCTC8325 in combination with a SEQUEST algorithm rel. 3.5 (Sorcerer built 4.04, Sage-N Research Inc., Milpitas, CA, USA). Data from two points in time and five BR were processed in an alignment search with a search distance of 4 min and 10 ppm instrument mass accuracy. Carbamidomethylation of cysteine (57.02) was included as fixed modification. Peptides were annotated based on Peptide Teller allowing a maximal predicted error of 0.01. Only proteins identified with at least two peptides or sequence coverage of more than 10% were considered for further analysis using the Genedata Analyst software v7.6 (Genedata, Basel, Switzerland). Data were log-2 transformed and median normalized. For the human and staphylococcal dataset each the ratios between the two sampling points (ratio = $t_{6.5h}/t_{2.5h}$) were calculated per biological replicate using the control point normalization tool and values transformed back to linear space. Average values from the single replicates were created for all ratios. Proteins showing a p-value <0.05 in the one-group t-test from Genedata together with a FDR of <5% were regarded as significantly different over time. Staphylococcal proteins were defined regulated when at least four of five BR showed an absolute fold change of 1.5.

As human cells replicate much slower than bacteria (generation time of human cells about 24 h, generation time of internalized bacteria about 2 h), human proteins were already considered regulated when the protein intensities varied between 6.5 h and 2.5 h with an absolute fold change of 1.2. For bacterial proteins an absolute fold change of 1.5 was defined as limit for significant regulation over time. Furthermore, for shotgun data, trends (ratio >1 or <1) were considered when they were observed in at least four of five BR. Proteins showing a trend of regulation did not have to comply with the significance cutoff.

MassSpec raw data files of samples from NP-experiments were imported into the Refiner MS software package (Genedata, Basel, Switzerland). The analysis workflow included a MASCOT database search and is already published and provided as Supplementary_Material_02_Genedata_Refiner_Workflow_identification_NP.pdf and Supplementary_Material_03_Genedata_Refiner_Workflow_quantification_NP.pdf http://onlinelibrary.wiley.com/doi/10.1002/cyto.a.22425/suppinfo (Depke et al., 2014).

Proteome data of iron-starved or internalized *B. pertussis* Tohama I were analyzed by spectral counting. For protein identification, raw data were post-processed with the Sorcerer™ software package v3.5 (Sage-N Research Inc. Milpitas, CA, USA). Afterwards, all Tandem-MS spectra were searched using the SEQUEST® search engine (ThermoFinnigan, San Jose, CA, USA, version v.27, rev.11) against the *B. pertussis* Tohama I FASTA database assuming the digestion with trypsin, precursor ion tolerance of 20 ppm and a fragment ion mass tolerance of 1 Da. Oxidation of methionine was specified as variable modification. Scaffold software v3.0 (Proteome Software, Portland, OR, USA) was used to validate protein identifications derived from MS/MS sequencing results. Peptide identifications were accepted if they could establish >95% probability respectively, as specified by the Peptide Prophet algorithm (Keller et al., 2002). Protein identifications were accepted

if they reached >99% probability according to the Protein Prophet algorithm (Nesvizhskii et al., 2003) and were identified with at least two unique peptides. These identification criteria typically established <0.01% false discovery rate based on a decoy database search strategy at the protein level. Identified peptides/proteins were further quantified using unweighted spectral counting. To this end, total spectra identified in a dataset were normalized with spectra identified in dataset that was to be compared. This normalization, which is achieved by using a display option called "Quantitative value" in Scaffold v3.0 (Proteome Software, Portland, OR, USA), was used to determine relative abundance of proteins within datasets and the statistical significance was assessed by using a Student's t test ($p < 0.05$). In the iron project, ratios between iron-limited and iron-containing conditions were calculated. Proteins exceeding an absolute fold change >1.5 and a p-value <0.05 were regarded regulated in that project. Data of internalized bacteria were related on the non-internalized control. Voronoi-like treemap for the ratio 48 h/2 h *p.i.* was created using the Paver software [DECODON GmbH (Bernhardt et al., 2013)] on the basis of the *B. pertussis* Tohama I database from SEED version 2.0 (Overbeek et al., 2005). For p-value determination and ratio calculation for preparation of Voronoi-like treemaps, values with zero spectral counts were replaced by “0.1” as described previously (Lee et al., 2012). PCA plots were created using the Genedata Analyst software v8.2 (Genedata, Basel, Switzerland) analyzing median normalized data for each sampling point (control, 2 h, 48 h) and biological replicate (3 BR).

Analysis of MRM data

Standard peptides for MRM

For reliable identification of secreted staphylococcal proteins in a complex mixture, recombinant standard proteins of *S. aureus* including virulence associated proteins were obtained from Protagen (Protagen, Dortmund, Germany). Purified proteins were digested in mixtures of each 1 pmol per protein with trypsin after reduction and alkylation as described above. The digested peptides were diluted in buffer containing 2% (v/v) ACN and 0.1% (v/v) HAc in order to acquire a calibration curve (0.01, 0.05, 0.1, 0.5, 1, 5, 10, and 50 fmol/injection) by MRM.

Analysis and quantification of MRM data

The program Skyline was used for method development and optimization of CE as well as data analysis and quantification (Maclean et al., 2010a, Maclean et al., 2010b). Appropriate transitions originated from previous shotgun analyses. Therefore, .raw files were subjected to database analysis using the Sorcerer platform and TPP. Resulting .xml data were implemented as library into the program Skyline. If shotgun analysis did not yield enough peptides, theoretical tryptic digestion of the amino acid sequence for each protein was performed. Identification of secreted staphylococcal proteins was achieved with an external standard sample consisting of digested purified standard proteins obtained from Protagen (Protagen, Dortmund, Germany). The final transition list is provided

as Supplementary_Material_Table_01_MRM_transitions_S_aureus_HG001.xlsx. Relative quantification between 2.5 h and 6.5 h *p.i.* was executed comparing the ratios between each two samples. Prior to quantification external standard curves were recorded for each digested purified standard protein in known concentrations (0.01, 0.05, 0.1, 0.5, 1, 5, 10, and 50 fmol per injection). After manual evaluation of each of four injections average area values were used to create the standard curves for each protein. Only peaks of the final samples whose areas were not smaller than those in the linear range of the standard curve were considered for relative quantification.

For analysis of internalized *B. pertussis* Tohama I, setup and validation of transitions and collision energy as well as area calculation were again established using Skyline v3.5 (Maclean et al., 2010b). The final transition list is provided as:
Supplementary_Material_Table_02_MRM_transitions_B_pertussis_Tohama_I.xlsx.
Identification of peptides in the different samples was validated by retention time and transition pattern of the peak without standard proteins. As many peptides as possible were acquired for each protein, but only those which gave distinct peak patterns in all replicates were used for ratio calculation for relative quantification, they are highlighted in:
Supplementary_Material_Table_02_MRM_transitions_B_pertussis_Tohama_I.xlsx.
Average values were calculated from multiple injections for each peptide. Final relative quantification between the two points in time and the control was carried out on protein level. Therefore, average values were built from the area values for the proteotypic peptides of each protein. The average areas of the two housekeeping proteins MaeB and GdhA were used for normalization. Results were given as ratios related to the control sample.

Microscopy

Transmission electron microscopy (TEM)

[Acquisition of TEM pictures was done by Rabea Schlüter]

At 2.5 h, 4.5 h, and 6.5 h after infection cells were trypsinated, centrifuged, washed with PBS, and then fixed with 2% glutaraldehyde and 5% paraformaldehyde in cacodylate buffer (Table 4) for 1 h at room temperature and then at 4°C overnight. Subsequent to embedding in low gelling agarose cells were post-fixed in 1% osmium tetroxide in cacodylate buffer. After dehydration in graded series of ethanol the material was embedded in LR White resin. Sections were cut on an ultramicrotome (Reichert Ultracut, Leica UK Ltd, Milton Keynes, UK), stained with 4% aqueous uranyl acetate followed by lead citrate and analyzed with a transmission electron microscope LEO 906 (Zeiss, Oberkochen, Germany).

For each point in time for each sample more than 100 clips from two slices (each about 260 host cells per slice were counted) were analyzed (one biological replicate). The total number of human cells, the number of infected cells and the number of intracellular bacteria were counted, and average values for infection rate and number of bacteria in infected cells were determined.

Table 4. Overview on solutions for chemical fixation of samples for TEM analysis. *GA (glutaraldehyde), PFA (paraformaldehyde), CCB (cacodylate buffer).*

fixative			wash buffer		
stock solution	**end concentration**	**volume [µL] for 1 mL**	**stock solution**	**end concentration**	**volume [µL] for 1 mL**
2x wash buffer		500	1 mol/L CCB (pH 7)	100 mmol/L	100
2.5 M NaN_3	25 mmol/L	10	1 mol/L sucrose	0.09 mol/L	90
25% GA	2%	80	1 mol/L $CaCl_2$	10 mmol/L	10
16% PFA	5%	312.5	1 mol/L $MgCl_2$	10 mmol/L	10
A. bidest.		97.5	*A. bidest.*		790

Fluorescence staining on coverslips

Cells grown and/or infected on 18 mm diameter precision coverslips (Roth, Karlsruhe, Germany) in a 12-well tissue culture plate were fixed with 2% formaldehyde in PBS with Ca^{2+}/Mg^{2+} (PAA) at 4°C for at least 20 min. Afterwards, cell layers were rinsed once with PBS with Ca^{2+}/Mg^{2+} and stored in PBS with Ca^{2+}/Mg^{2+} at 4°C until staining.

Unspecific binding sites of the cells on the cover slips were blocked with 10% FBS in PBS for 20 min at room temperature. Afterwards, host cell membranes were permeabilized with 0.1% Triton X-100 in HPLC-grade water (J. T. Baker, Center Valley, PA, USA) at 37°C for 5 min. Cells were washed again with PBS. Further on, the F-actin was stained with Phalloidin conjugated to Alexa Fluor 568 staining solution (1 U/mL in PBS) at 37°C for 20 min. After two further washes with PBS, DNA was stained by incubation with HOECHST 33258 (10 ng/mL) at room temperature for 10 min in the dark. The cover slips were removed from the tissue culture plates and rinsed carefully three times with *Aqua dest*., dried and placed upside down on a droplet of 5 µL Mowiol mounting medium (33% (m/v) glycerol, 13% (m/v) Mowiol, and 0.1% (m/v) p-phenylendiamine in 0.133 mol/L Tris pH 8.5) on a microscope slide, which was finally dried overnight at 4°C before microscopy analysis.

Fluorescence microscopy analysis

Preparations were visualized on a Deltavision RT Image Restoration Workstation with an Olympus IX71 w/ Nomarski Differential Interference Contrast microscope with a 40x or 60x objective using immersion oil. Depending on the preparations and staining agents applied, several filters were available for visualization. The filter with Excitation (Ex) 360/40 nm/Emission (Em) 457/50 nm was applied for visualization of nuclei after staining with Hoechst 33258. The filter with Ex 490/20 nm/Em 528/38 nm was applied for GFP expressing bacteria, FITC-fluorescence of NP or visualization of S9 cells containing LAMP-1-YFP. The filter with Ex 555/28 nm/Em 617/73 nm was used for phalloidin-labeled F-actin stained with Alexa Fluor 568 and RBITC-fluorescence of NP. Finally, the filter with Ex 436/19 nm/Em 470/30 nm served for visualization of CFP expressing bacteria.

The pictures obtained were processed with ZIK-ImageJ (www.functional-genomics.de/Group_Bioinformatics_Toponomics_DE/data.html) for adding scale bars and optimization of brightness and contrast in the final pictures.

For investigation of formation of bacteria-containing phagosomes, preparations with S9 cells expressing LAMP-1-YFP infected with GPF expressing bacteria were additionally visualized on a Zeiss LSM 510 Meta Confocal Microscope (Carl Zeiss AG, Oberkochen, Germany) with a 60x objective using water instead of inversion oil.

[Confocal microscope operated by Jan Pané-Farré]

Detection of human cytokines from cell culture supernatant

Cell culture supernatants of infected A549 cells and non-infected control A549 cells (treated with sterile pMEM) were collected to analyze eleven secreted cytokines (IFN-γ, IL-1β, IL-2, IL-4, IL-5, IL-6, IL-8, IL-10, IL-12 p70, TNF-α, and TNF-β) by flow cytometry using a fluorescence based bead assay (Flow Cytomix Multiple Analyte Detection, eBioscience, Frankfurt am Main, Germany). After labeling according to the manufacturer's instructions samples were analyzed according to the protocol provided by eBioscience using a FACSAria high-speed cell sorter (Becton Dickinson Biosciences, San Jose, CA, USA). Data of five BR were analyzed with FlowCytomics Pro (eBioscience).

RNA isolation and analysis of the immunoproteasome by quantitative RT-PCR (qRT-PCR)

At selected points in time (t0, 1.5 h, 2.5 h, 4.5 h, 6.5 h, and 24.5 h) after infection with *S. aureus* HG001 pMV158GFP (infection) or sterile infection medium at pH 7 (mock-infection), supernatant was aspirated and cells were washed with PBS (PAA). One mL TRIzol® (Life technologies™, NY, USA) was added to each well of the 6-well plate, cells were lysed and removed from culture plate by pipetting and immediately frozen in liquid nitrogen. Samples were defrosted and incubated 5 min at room temperature. Separation of RNA, DNA, and proteins followed by adding 20% (v/v) chloroform. After vigorous shaking, short incubation and subsequent centrifugation (12,000x*g*, 4°C, 15 min) the upper aqueous phase containing RNA was transferred to a new vial. RNA precipitation occurred in 50% (v/v) isopropanol overnight at -20°C. Following a further centrifugation (12,000x*g*, 4°C, 10 min) supernatant was removed and pellet was washed in 75% (v/v) ethanol (7,500x*g*, 4°C, 10 min). The pellet was dried, reconstituted in RNAse-free water and incubated on ice for 3 h and further 30 min at room temperature before the pellet was incubated again on ice. Concentration of RNA was determined with a NanoDrop (NanoDrop 8000, Thermo Fisher Scientific, Waltham, MA, USA), and quality was investigated with an Agilent 2100 Bioanalyzer (Agilent Technologies, Santa Clara, CA, USA). Synthesis of cDNA from RNA was accomplished with a High Capacity cDNA Reverse Transcription Kit and TaqMan® pre-developed assay reagents (Life Technologies, Carlsbad, California, USA) according to manufacturer's instructions.

The cDNA master mix containing 2 μg sample RNA was incubated for 10 min at 25°C, 120 min at 37°C, and 5 min at 85°C. According to manufacturer's instructions, Gene Expression Mastermix (Life Technologies), sample cDNA, one of the provided Assays (Human GAPDH - Hs02758991_g1 (reference), PSMB8 - Hs00544760_g1, PSMB9 - Hs00160610_m1, PSMB10 - Hs00988194_g1, Life Technologies), and water were mixed and the PCR was accomplished with a real time cycler (Cycle: 95°C 10 min, 95°C 15 s, 60°C 1 min; 7900HT Fast Real-Time PCR System, Applied Biosystems, CA, USA). Data were relatively analyzed comparing compounds of the immunoproteasome and the reference GAPDH according to the $2^{-\Delta\Delta CT}$ method (Livak and Schmittgen, 2001). The sample from the mock-infection of each point in time served as control. In brief, fold changes were calculated using the following formulas: $\Delta CT = CT_{\text{target genes}} - CT_{GAPDH}$, $\Delta\Delta CT = \Delta CT_{\text{target genes (infection)}} - \Delta CT_{\text{control (mock infection)}}$, fold change = $2^{-\Delta\Delta CT}$.

Characterization of selected caspases by Western Blot analysis

[Western Blotting performed together with Sebastian Stentzel and Kirsten Bartels]

Infected host cells and non-infected control cells were harvested after 2.5 h and 6.5 h *p.i*. using trypsin and separated by cell sorting. Proteins were extracted, and the concentration was determined using the Bradford assay as described above. Samples were prepared for 1D-Gels (NuPAGE4-12% acrylamide Bis-Tris Midi Gel, Novex Life Technologies, Darmstadt, Germany) by adding 1 μL reducing agent and 2.5 μL sample buffer to 6.5 μL sample (10 μg). The mixtures were denatured at 70°C for 10 min. Gels were run for 10 min at 200 mA and further 30 min at 150 mA. Afterwards, gels were transferred into buffer consisting of 1x transfer buffer (Novex Life Technologies), 20% (v/v) methanol and 0.25% sodium dodecyl sulfate (SDS) in *A. dest*. Coomassie brilliant blue staining of gels allowed control of separation of the samples prior to antibody binding on the membranes. Therefore, gels were fixed for 1-2 h in 40% EtOH and 10% HAc in *A. dest*. Gels were washed twice for 10 min in *A. dest*. OneD-gels were stained one day with colloidal Coomassie solution (CCS, Table 5).

Table 5. Composition of solutions for Coomassie staining.

Coomassie Brilliant Blue (CBB) stock	colloidal Coomassie stock (CCD)	colloidal Coomassie solution (CCS)
5 g CBB G-250	50 g $(NH_4)_2SO_4$	200 mL CCD
ad. 100 mL *A. dest.*	6 mL 85% phosphoric acid	50 mL methanol
	ad. 490 mL *A. dest*	
	10 mL CBB-stock	

When 1D-gels were processed for further Western Blotting, gels were not stained using Coomassie brilliant blue but blotted on membranes in a Western Blot device (Milliblot Graphit Electroblotter II). Appropriate values for current in mA were calculated using the values of length (cm) X width (cm) X number of gels X 1.5 mA/cm^2. Blotted membranes were stained with ink [200 mL PBS-Tween (1x), 2.5 mL HAc (100%) and 0.25 mL ink (Pelikan, Hannover, Germany)]. Ink-stained membranes were scanned, destained again for 15-20 min shaking in PBS with 0.1% (v/v) Tween until ink was not visible anymore. Membranes were shrink-wrapped and stored at -20°C until further use.

Membranes were then treated with blocking buffer consisting of 5% milk powder in Tris-buffered saline-Tween (TSB-T) buffer (20 mmol/L Tris-HCl, 137 mmol/L NaCl, and 0.1% (v/v) Tween 20 [pH 7.6]) shaking for 1 h at room temperature. Afterwards, the membranes were incubated overnight shaking at 4°C in blocking buffer containing the first antibody in the appropriate concentration (Table 6). After five washes and shaking for 5 min at room temperature in TSB-T buffer, the second antibody (Table 6) was applied in blocking buffer by shaking for 1 h at room temperature. Prior to image detection, membranes were treated with ECL substrate (5 mL/Blot, SuperSignal West Femto Maximum Sensitivity Substrate, Pierce, Rockford, IL, USA). Pictures were acquired with a Western Blot Imager and edited with ImageQuant TL Software (GE Healthcare Life Science, Freiburg, Germany).

Table 6. Antibodies used for Western Blotting. *Primary and secondary antibodies are listed with organism, source and used dilution or concentration when available. POD (peroxidase), IgG (immunoglobulin G).*

antibody	organism	source	dilution of stock or concentration
primary antibodies			
anti-caspase 3	mouse	BioLegend	1 µg/mL
anti-caspase 9	mouse	BioLegend	0.5 µg/mL
anti-caspase 8	rat	BioLegend	0.5 µg/mL
anti-caspase 10	rat	BioLegend	1 µg/mL
secondary antibodies			
anti-mouse IgG-POD (for caspases)	goat	BioRad	1:3000
anti-rat IgG-POD (for caspases)	goat	BioLegend	1:1000
anti-mouse IgG-POD (for hybridome)	goat	Dianova	0.18 µg/mL
anti-human IgG-POD (for serum pool)	goat	Jackson Laboratories	0.008 µg/mL

Metabolome analysis of human cell lines

[Extraction, data acquisition, and analysis of metabolites performed by Philipp Gierok]

Sampling and extraction of host cell metabolites

Confluent cells in 15 cm diameter tissue culture plates were treated for 1 h at 37°C and 5% CO_2 in humid atmosphere with a sterile “infection mix” (as described above; pH about 7, corresponding to pH at OD_{600} of 0.4 (Figure 9); imitating a MOI 25 but leaving out bacteria). Samples of cellular extracts were generated and extracted as described previously (Gierok et al., 2014). In brief, the supernatant was collected separately and the adherent cells were washed four times with ice cold NaCl solution (135 mmol/L). After that, 10 mL ice cold methanol were added to the plate, and cells were immediately scraped from the plate and transferred into a reaction tube. Next, the plate was washed with 10 mL ice cold doubly distilled water, which was also transferred into the same tube. The sample was immediately frozen in liquid nitrogen. For extraction of intracellular metabolites samples were thawed on ice, and 2 mL ice cold chloroform were added to each sample to gain a methanol/water/chloroform extraction with a ratio of 5:5:1. Next, the internal standards [40 nmol ribitol, 40 nmol norvaline and 5 nmol camphorsulfonic acid (Sigma-Aldrich, St. Louis, USA)] were added, and the extraction solution was mixed and incubated for 10 min on ice. After centrifugation (10 min 3,000x*g*, 4°C) both, the separated aqueous and organic phases were separated from the insoluble pellet and transferred into a new tube and mixed again and split into two samples which were lyophilized for GC/MS analysis and for LC/MS analysis.

Acquisition and analysis of metabolome data

Lyophilized samples were derivatized as described elsewhere (Strelkov et al., 2004), using a two step derivatization method with o-methylhydroxylamin-hydrochlorid (MeOx, Sigma-Aldrich, St. Louis, USA) and N-methyl-N-tri-methylsilyltrifluoracetamid (MSTFA, Chromatographie Service GmbH, Langerwehe, Germany). For identification and quantification of metabolites a GC/MS method was used as described (Gierok et al., 2014). Qualitative and quantitative analyses were performed using ChromaTOF software (LECO Corporation, St. Joseph, Michigan, USA). Identification of peaks was carried out by comparison of mass-spectra and retention time of signals with an in-house database. Quantification of integrated signals was performed by using a calibration from 0.5 nmol to 1,000 nmol for each metabolite. A polynomial equation type and weighting were applied for fitting a calibration curve to the data of standard dilutions. The computed metabolite concentrations were related to the respective cell number.

In addition, for identification and quantification of metabolites also an LC/MS method with an ion-pairing reagent and a SymmetryShield RP_{18} column (reversed phase, Waters) was used with a setup as described (Gierok et al., 2014). Metabolite quantification was executed using QuantAnalysis® (Bruker Daltonik, Bremen, Germany). Peak areas of extracted ions were normalized to the internal standard area of camphorsulfonic acid. A calibration with pure standards in concentrations between

0.25 nmol to 100 nmol was measured for absolute quantification. Again, calibration equation was determined *via* a polynomial of degree two and a 1/x weighting. The computed metabolite concentrations were related to the respective cell number.

Extracellular metabolites were analyzed by ^{1}H-NMR. Two mL of the medium were filtered through a 0.22 μmol/L syringe sterile filter (Sarstedt AG&Co) and directly frozen. Qualitative and quantitative data analysis was carried as described previously (Dörries and Lalk, 2013). According to this, each 400 μL supernatant were buffered to a pH of 7.0 with 0.2 mol/L sodium hydrogen phosphate buffer in 50% D_2O (Euriso-Top, St-Aubin Cedex, France). The buffer contained further 1 mmol/L 3-trimethylsilyl-[2,2,3,3-D4]-1-propionic acid (TSP, Sigma-Aldrich, St. Louis, USA) as internal standard. Samples were analyzed by ^{1}H-NMR in 5 mm glass tubes (7 inch length; NORELL ST-500, NORELL, Inc., USA). All spectra were collected at 600.27 MHz and 310 K using a Bruker AVANCE-II 600 NMR spectrometer, operated by TOPSPIN 2.1 software (Bruker Biospin GmbH, Rheinstetten, Germany). A 1D-NOESY pulse sequence was detected with pre-saturation on the residual HDO signal during the relaxation delay and the mixing time. In the end 64 free induction decays were acquired, applying a spectral width of 30 ppm for a one-dimensional spectrum. For data analysis the using AMIX®-Viewer v3.9.11 (Bruker Biospin), identification was based on spectra alignment of pure standard compounds (Sigma-Aldrich, St. Louis, USA). For quantification designated peaks were integrated and compared to the TSP signal, considering the number of protons for each signal and checked manually (Dörries and Lalk, 2013).

RESULTS

Adaptation of S. aureus HG001 to internalization by human cell lines

Method optimization for improved detection of staphylococcal proteins

During her PhD studies, Dr. Sandra Ernst successfully developed an internalization protocol which allowed analysis of the proteome of GFP-expressing *S. aureus* HG001 from human bronchial epithelial cells. Applying this protocol she investigated the intracellular adaptation of the bacteria by identifying 591 and quantifying 367 staphylococcal proteins during the first 6.5 h *p.i.* (Schmidt et al., 2010b). Since the applied protein database of *S. aureus* HG001 contains 2,892 distinct proteins, it is obvious that not all *S. aureus* proteins affected during internalization were covered in her analysis. The knowledge about the behavior of *S. aureus* HG001 upon internalization should be extended within this thesis. Thus, several steps of the initial standard protocol (Schmidt et al., 2010b) were further optimized. First, the number of bacteria has to be precisely known prior to internalization in order to facilitate precise adjustment of the multiplicity of infection (MOI), which is required for good reproducibility of the data. The second goal was to enable proteome analysis of bacteria, which do not express GFP and to cover secreted proteins, which have not been covered so far. The biological interpretation of the proteome data was further enhanced by introducing non-internalized control bacteria, by increasing the number of functional annotations within the database, and by raising the number of identified and quantified proteins by combining new data acquisition methods and sophisticated search strategies.

Improved cell counting of bacteria using flow cytometry

For reproducible results of internalization assays, the number of bacteria which are utilized for infection of host cells referred to as MOI must be constant. Therefore, the numbers of human host cells in a cell culture plate as well as the number of bacterial cells in culture have to be known prior to infection. The number of bacteria also had to be determined during intracellular growth of internalized bacteria.

Human cells were seeded three days in advance from mixtures of the same concentration of cells and grown until confluence in several plates or wells of a tissue culture plate. Thus, it is possible to directly count the number of host cells immediately before infection as described before [“Material & Methods” and (Pförtner et al., 2013)]. In brief, the number of eukaryotic cells can be determined easily, reproducibly, and fast using the Countess® device in a semi-automatic manner. In contrast to determination of bacterial counts, this counting of host cells did not require further optimization. Counting of bacteria can be performed with a Neubauer counting chamber, which allows determination of total counts but does not discriminate living and dead bacteria without additional staining. However, *S. aureus* forms clusters which complicate discrimination of single bacterial cells.

Thus, this method was not applied. A widely employed method to determine amounts of living bacteria is the counting of colony forming units (CFU), which had been the standard protocol in our laboratory, too. This determination is based on the assumption that each bacterium will form a colony. However, this method is time-consuming (pouring agar, cooling time of agar, preparation of PBS dilution series, placement of glass beads, waiting time for agar cooling and incubation of bacteria, counting of colonies) and material-intensive (agar, petri dishes). From each culture at least three different dilutions were plated each in three technical replicates to allow a statistical evaluation. Thus, for each sample at least nine agar plates had to be poured, bacteria were spread on them with glass beads and counted after incubation. For improving reproducibility colonies were only counted when between 30 and maximum 1,000 colonies were grown per plate according to the protocol used in our group. This dilution could not be controlled before incubation. Besides the labor-intensiveness of the method, standard deviations were high, resulting also from long durations between sampling, preparation of all dilutions, and plating. Formation of clusters by *S. aureus* is also a problem of this method, as colonies created by two bacterial cells in a cluster are hard to distinguish.

For improvement of bacterial counting a Guava easyCyte™ flow cytometer (Merck-Millipore, Billerica, MA, USA) was employed. By counting of fluorescent particles by flow cytometry and the corresponding volume, fast determination of the absolute (living and dead) amount of cells is possible. As limitation, only fluorescent particles can be counted clearly. Mostly, *S. aureus* strains that express GFP were used in this study. The number of GFP-expressing bacteria was directly determined by flow cytometry using a green filter (530 nm for FITC/GFP). Non-fluorescent bacteria had to be stained with the dye SYTO® 9 nucleic acid stain (SYTO 9, Invitrogen, Karlsruhe, Germany) which is visible in the same channel as GFP. Before the Guava easyCyte™ flow cytometer could be generally applied in our group, its functionality and reproducibility had to be tested in several approaches with the aim to develop a standard operation procedure with the best settings. The standard operating procedure was established together with student assistant Nicole Normann under supervision and support of Petra Hildebrandt and me. A summary of the optimization and testing of the developed protocol is presented in the following section.

Counting of bacteria using this flow cytometer was performed by counting a constant number of fluorescent events (5,000) which are defined with a certain fluorescence threshold and side scatter by the user. The device measures the volume that is needed for 5,000 events and applies the value for concentration calculation. Other than during CFU plating, for cell counting by flow cytometry only one dilution is necessary. For more reliable results, technical replicate of this dilution in PBS should be prepared. According to the manufacturer's instructions the optimal concentration of cells measures 250 cells/μL. This statement was controlled by measuring different concentrations between 100 and 2,600 bacteria/μL. As illustrated in Figure 10 a linear range of the instrument is achieved in a concentration range of 100 to 700 bacteria/μL. A more accurate and therefore time-consuming

dilution is not necessary. However, less diluted (>900 bacteria/µl) samples resulted in lower bacterial counts.

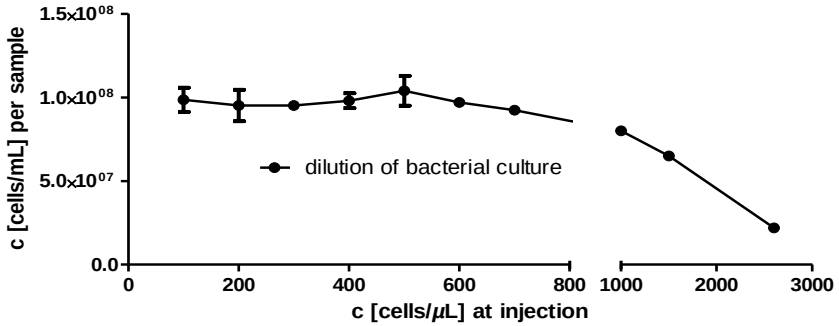

Figure 10. Dilution of *S. aureus* HG001 pMV158GFP bacterial culture prior to cell counting by flow cytometry. *The linear range of the Guava easyCyte™ flow cytometer was determined using a bacterial culture in different dilutions in PBS. Resulting bacterial counts were similar in a range between 100 and 700 cells/µL. Average and standard deviations of each five injections are depicted. The coefficient of variation always amounted to less than 10%.*

Compared to CFU determination, incubation steps are omitted and appropriate dilution can be adjusted immediately. Each technical replicate of dilution was measured at least twice in the cytometer. When only one technical replicate of dilution was available, the concentration value was acquired three times. The reproducibility of bacterial counting was tested for multiple injections as well as multiple independent dilutions of the same sample (Table 7). Inter-measurement coefficient of variance (CV) of the same diluted sample accounted for 1% to 5%, while the CV of samples with independent dilutions averaged to 9%. Nevertheless, even a CV of 9% is rather low. The bacterial counts of one sample can now be analyzed with three to six technical replicates in less than 10 min.

Table 7. Variation of bacterial counting for multiple injections and independent dilutions at the Guava easyCyte™ flow cytometer. *CV (coefficient of variation).*

sample	concentration [bacteria/mL]	average of injections per independent dilution [bacteria/mL]	CV [%] of injections per independent dilution	average of values from five dilutions [bacteria/mL]	CV [%] from five dilutions
dilution 1	1.05E+08 1.12E+08 1.02E+08	1.06E+08	4.7		
dilution 2	1.09E+08 1.05E+08 1.07E+08	1.07E+08	1.9		
dilution 3	1.14E+08 1.15E+08 1.13E+08	1.14E+08	0.9	1.15E+08	8.8
dilution 4	1.16E+08 1.17E+08 1.21E+08	1.18E+08	2.3		
dilution 5	1.33E+08 1.30E+08 1.29E+08	1.31E+08	1.6		

When comparing the results from CFU plating and Guava easyCyte™ flow cytometer counting, about twice as many bacteria were counted by flow cytometry compared to the colonies counted after plating (Figure 11). One reason might be on the one hand that not all bacteria, which can be counted by flow cytometry actually form colonies, on the other hand, the thin capillary of the flowcell (GUAVA® Flowcell II, Millipore, Hayward, CA, USA) might provide a better separation of clusters of bacteria.

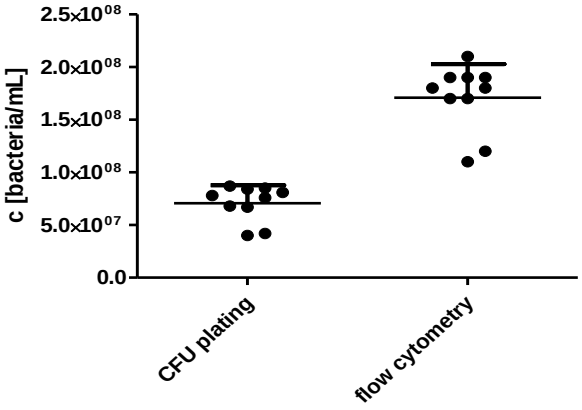

Figure 11. Determination of CFU by plating and bacterial counts measured by flow cytometry. *Values from ten measurements of each bacterial culture at OD_{600} 0.4 are depicted. Standard deviations are similar between both types of counting but average values differ by factor two.*

After testing the Guava easyCyte™ flow cytometer for pure bacterial culture, also internalized GFP-expressing bacteria were counted from host cell lysate. The population of free fluorescent bacteria was clearly separated from non-fluorescent host debris. A further small population of high fluorescent particles was observed consisting of bacteria stuck to host cell nuclei (Figure 12).

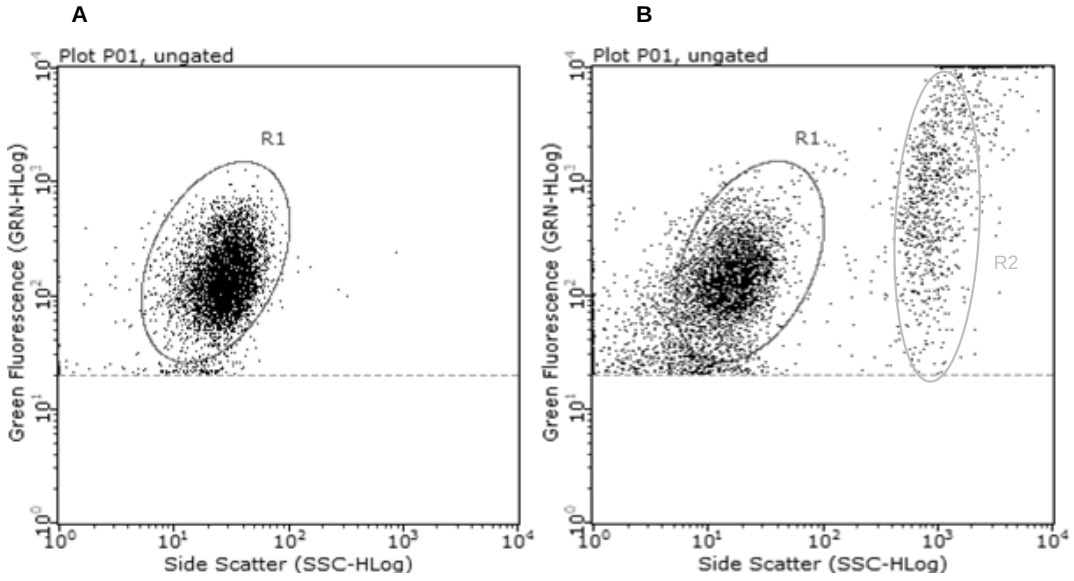

Figure 12. Analysis of GFP-expressing *S. aureus* HG001 before (A) and after (B) internalization by A549 cells. *Intensity of green fluorescence and the side scatter are depicted. The circles labeled R1 mark the region where only bacteria should be acquired. The region R2 in B) highlights bacterial cells, which are bound to host cell structures such as nuclei.*

In a second step after establishing the protocol for fluorescent bacteria, the method was adapted for non-fluorescent bacteria by combining the flow cytometry approach with a staining protocol. *S. aureus* cells without the plasmid encoding *gfp* were stained with the fluorescent dye SYTO 9. This dye stains RNA and DNA, thus, the compatibility of staining internalized bacteria in host cell debris was a critical point. First, different concentrations and duration of staining were tested with pure bacterial culture. An optimal concentration of 0.5 *µ*mol/L SYTO 9 was identified. This concentration is reached by mixing equal volumes of 1 *µ*mol/L SYTO 9 solution in PBS or water and the pre-diluted bacterial solution for 10 s with regard to the optimal concentration range of cells. As seen in Figure 13A, staining of pure bacterial culture with SYTO 9 leads to distinct fluorescent bacterial populations which can clearly be counted.

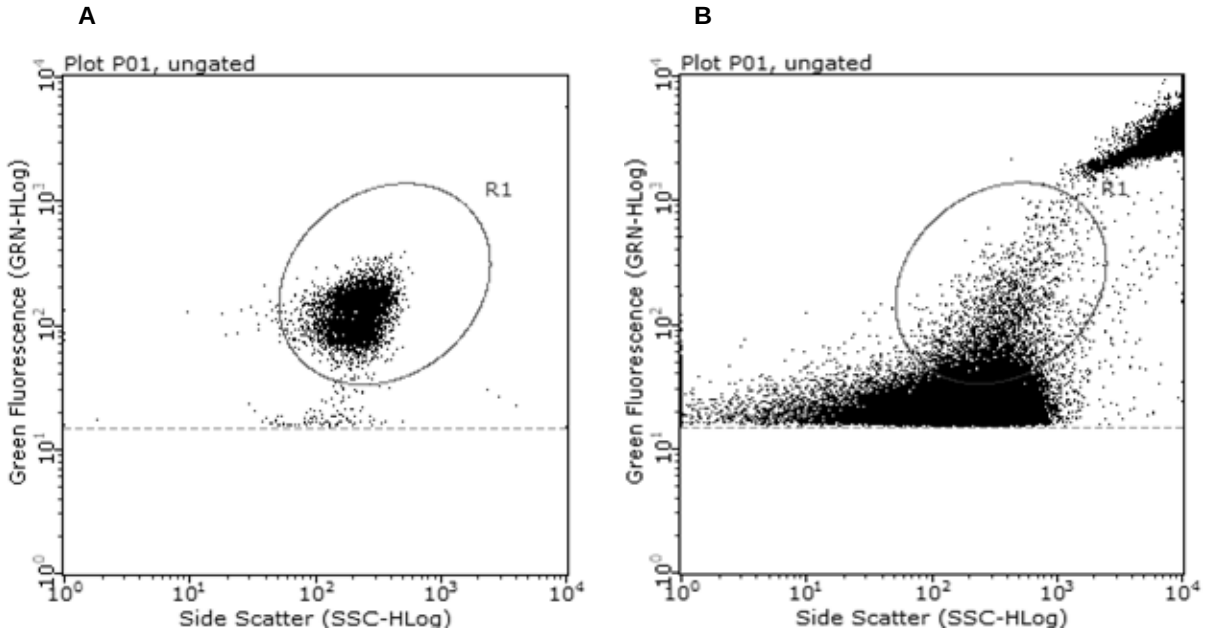

Figure 13. Bacterial and human cell culture stained with SYTO9. Intensity of green fluorescence and the side scatter are depicted. *(A) S. aureus HG001 was stained with SYTO9. (B) A549 cells were stained with SYTO9 after cell lysis. The circles labeled R1 mark the region where only bacteria should be acquired. Data obtained from Nicole Normann.*

As expected, counting of internalized cells in debris of host cells lysed by 0.1% Triton X-100 was a major challenge. Also host debris was stained with this dye (Figure 13B). Although non-infected SYTO-9 stained host cells showed a relatively low number of events in the “bacteria gate” this number is still a source of inexactness. Furthermore, the number of false positive events increased over time when host cell lysis proceeded. Thus, it is not yet possible to count non-fluorescent bacteria from an internalization assay. However, for GFP-expressing *S. aureus* employed in infection approaches and for non-fluorescent *S. aureus* grown in pure-culture medium, cell counting by flow cytometry was established as the new standard in our working group.

In this thesis internalized bacteria were additionally counted by transmission electron microscopy (TEM). Many (about 100 per sample) pictures of several host and bacterial cells were acquired after internalization. The advantage in this approach lies in the discrimination between infected and non-infected host cells which is not possible by CFU counting or flow cytometry without previous separation with the help of GFP. In addition, the number of internalized bacteria and the distribution between host cells can be seen. A drawback of this method is the long preparation time of more than 14 days between sampling of cells and acquisition of pictures in combination with the high costs. Since spherically shaped cells are cut two-dimensionally, not all internalized bacteria are monitored because a fraction of them is located above or below the cutting layer, a further disadvantage of the TEM analysis which argues against its use as standard technique. However, in this thesis this method provided valuable additional information on the infection rate and the actual range of bacterial numbers inside infected host cells (for values see chapter “Intracellular persistence and replication of bacteria after internalization”).

Separation of *S. aureus* from infected human host cells using nanoparticles

The protocol which was already standardized in our group for separating internalized bacteria from lysed host cells required bacteria which expressed fluorescent proteins such as GFP. These GFP-producing bacteria were employed for subsequent flow cytometry based cell sorting of fluorescent bacteria from non-fluorescent host debris (Pförtner et al., 2013) as illustrated in Figure 8. This protocol was applied to investigate the time-resolved proteome response of *S. aureus* to A549 cells. The comparative analysis of *S. aureus* adaption to three different host cell lines was performed with the same protocol only leaving out the SILAC labeling but employing improved label-free quantification techniques.

As the standard workflow requires the use of a plasmid coding for a fluorescent protein which is not always practicable for example when using clinical isolates, the aim was to develop an alternative protocol which would allow efficient enrichment of internalized bacteria even in the absence of constitutive expression of fluorescence proteins. Therefore, together with Maren Depke, fluorescent and/or para-magnetic nanoparticles (NP) were used to label the bacteria prior to infection. Enrichment of bacteria after infection was performed by cell sorting or with the help of a two Tesla magnetic field. The final protocol (Figure 14) as well as results from method optimization and two proof-of-principle infection experiments which showed the applicability of the approach are already published with a shared first-authorship with Maren Depke (Depke et al., 2014). The results of this publication are presented in the next section.

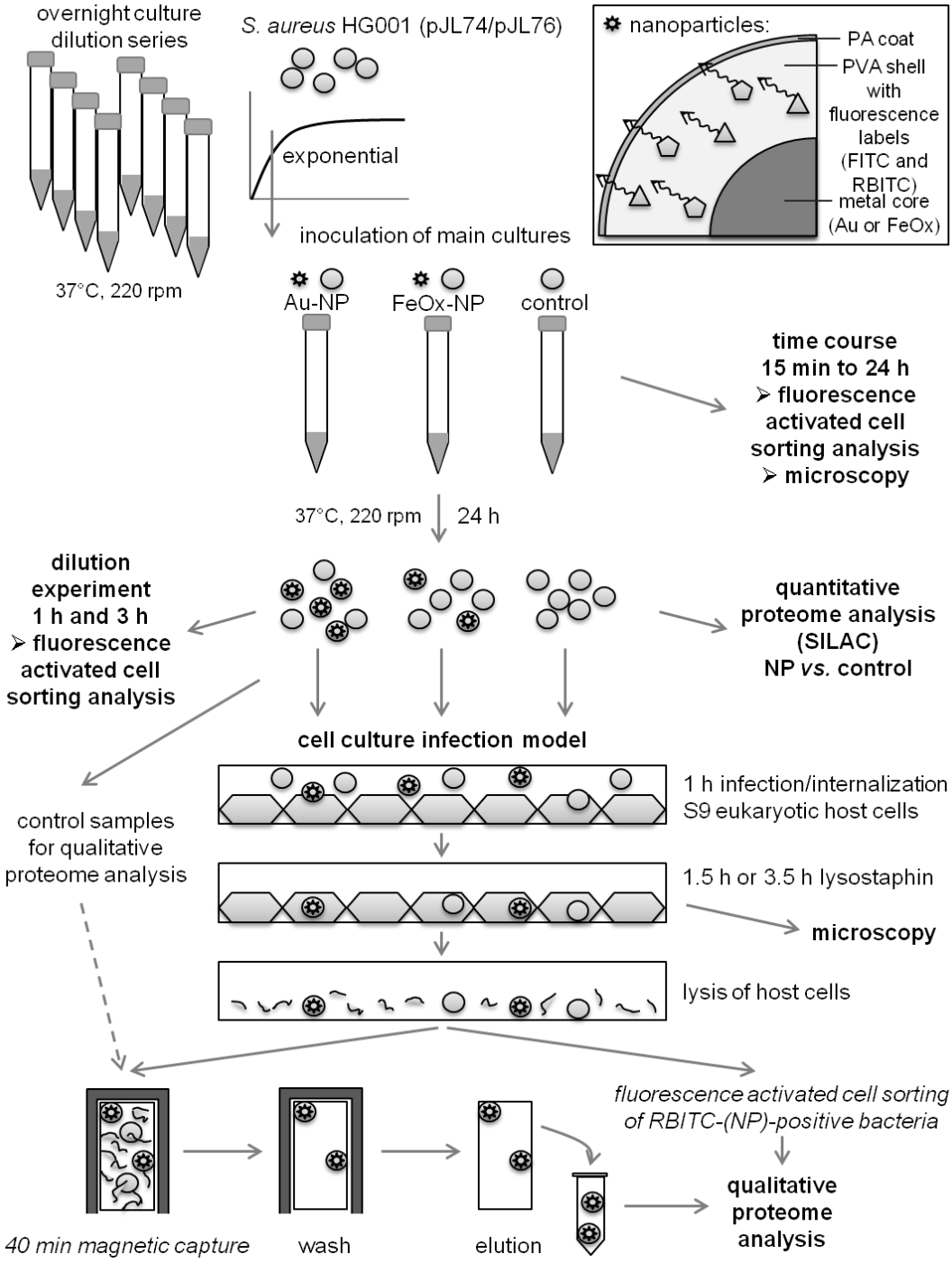

Figure 14. Schematic overview of the experimental workflow of labeling bacteria with NP, the cell culture infection experiment, magnetic capture, fluorescence-activated cell sorting, and qualitative and quantitative proteome analysis. *S. aureus HG001 pJL74 (GFP-expressing strain), S. aureus HG001 pJL76 (CFP-expressing strain), PVA [poly(vinyl alcohol)], FITC (fluorescein-isothiocyanate), RBITC (rhodamine B isothiocyanate), Au (gold), FeOx (ferric oxide), NP (nanoparticles) (Depke et al., 2014).*

Labeling efficiency of S. aureus during growth in presence of NP

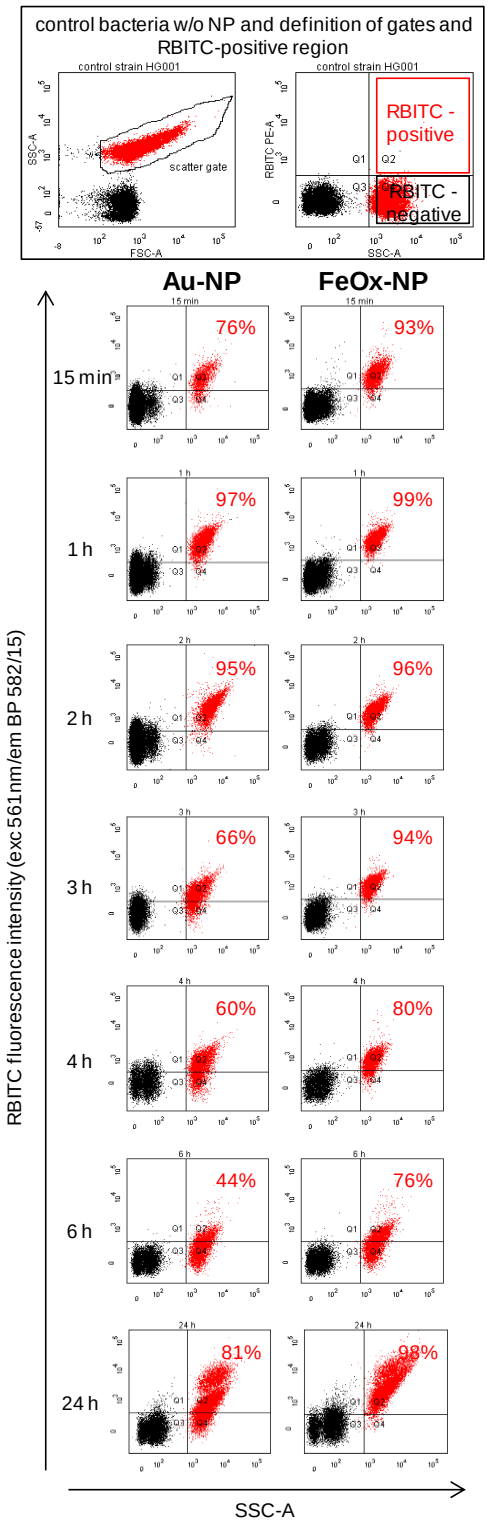

Figure 16. Labeling efficiency of *S. aureus* HG001 by NP. *Data of one representative biological replicate are displayed.*

As first step in protocol development, it was necessary to verify whether *S. aureus* HG001 is able to grow in medium containing fluorescence dye-labeled Au-NP or FeOx-NP and that the bacteria can indeed be efficiently labeled.

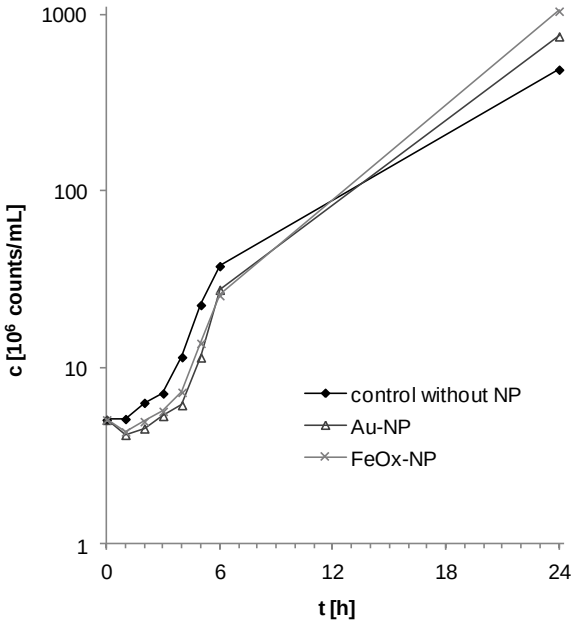

Figure 15. *S. aureus* HG001 growth in presence or absence of NP. *Mean values of three independent biological replicates are depicted.*

Bacterial growth was determined by counting bacteria during cultivation in medium with and without NP for 24 h (Figure 15). Growth of bacteria for the three cultivation conditions (without NP, with Au-NP, with FeOx-NP) was comparable. However, for both NP-containing media a lag phase was observed leading to the conclusion that bacteria might have to adapt to the NP. The growth rates of bacteria after the adaptational lag phase were similar between the three cultivation conditions. After 24 h little higher values were measured for bacterial growth in medium with FeOx-NP or Au-NP. Labeling efficiency was determined by flow

cytometry (Figure 16). At several points in time between 15 min and 24 h after inoculation of the bacteria in NP-containing medium, the percentage of RBITC-positive events was measured. Already after 15 min incubation time a high percentage of bacteria was labeled with NP (about 80% for Au-NP, about 90% for FeOx-NP). The highest labeling efficiency was recorded after 1 h of incubation. Until 6 h of incubation, meaning during exponential growth phase of *S. aureus*, decreasing numbers of NP-labeled bacteria were observed. Cultivation of bacteria for 24 h yielded again about 80% RBITC-positive events for Au-NP and almost 100% RBITC-positive events for FeOx-NP. In order to avoid loss of NP-labeled bacteria due to bacterial replication, *S. aureus* was pre-labeled for 24 h in NP-containing media prior to subsequent internalization experiments. Fluorescence microscopy pictures proved that NP-labeled bacteria were equally stained with FITC and RBITC (Figure 17).

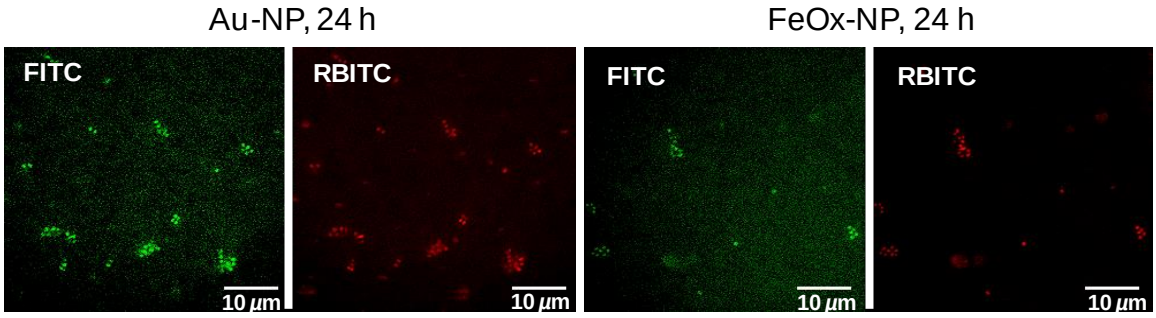

Figure 17. *S. aureus* HG001 labeled for 24 h in presence of Au-NP or FeOx-NP. *NP were equally stained green/FITC or red/RBITC (Depke et al., 2014).*

Influence of incubation with NP on the proteome of S. aureus

In order to determine if the *S. aureus* proteome was altered after incubation in presence of NP, possible changes in the protein pattern were investigated using the SILAC method (Ong et al., 2002). A control culture was grown in medium containing $^{13}C_6$-arginine and $^{13}C_6$-lysine (heavy amino acids) whereas the bacteria incubated with NP were cultured with $^{12}C_6$-arginine and $^{12}C_6$-lysine (light amino acids). After mixing equal amounts of each NP-labeled and control bacteria subsequent MS analysis revealed only small changes in the protein pattern. A complete list of all proteins identified including statistical testing is provided online as Supporting Material from Depke et al., 2014 (http://onlinelibrary.wiley.com/doi/10.1002/cyto.a.22425/suppinfo supptab1.pdf). From more than 600 proteins which were quantified using the H/L ratios of peak areas, only 24 proteins for Au-NP and 30 proteins for FeOx-NP incubation were found to be significantly changed due to influence of NP (Figure 18). Nine of them changed in level after incubation with Au-NP as well as FeOx-NP. The physiological impact of the proteins displaying altered levels in NP-treated bacteria compared to the non-labeled control was explored using Voronoi-like treemaps, which visualize proteome changes in the physiological context of biological pathways (Bernhardt et al., 2013). The differentially expressed

proteins were spread to different pathways and could not be assigned to a defined physiological response (Figure 18).

MetI and MetQ belong to the group of proteins that were affected by changed protein abundance especially for FeOx-NP. These proteins are involved in methionine biosynthesis/degradation pathways. Further, the methionine sulfoxide reductase MsrA2 was slightly reduced in abundance while the main methionine sulfoxide reductase MsrA1 of *S. aureus* exhibited a trend of increased abundance. These results could probably be caused by mild oxidative stress; however, proteins which also function in anti-oxidative stress defense like superoxide dismutase (SodM) and catalase (KatA) were not significantly increased in level. Even if single proteins were affected by NP, *S. aureus* was able to adapt and grow normally or even a little better in the presence of NP. As no further pathways were significantly changed probably only minor physiological effects of NP occurred during NP-labeling.

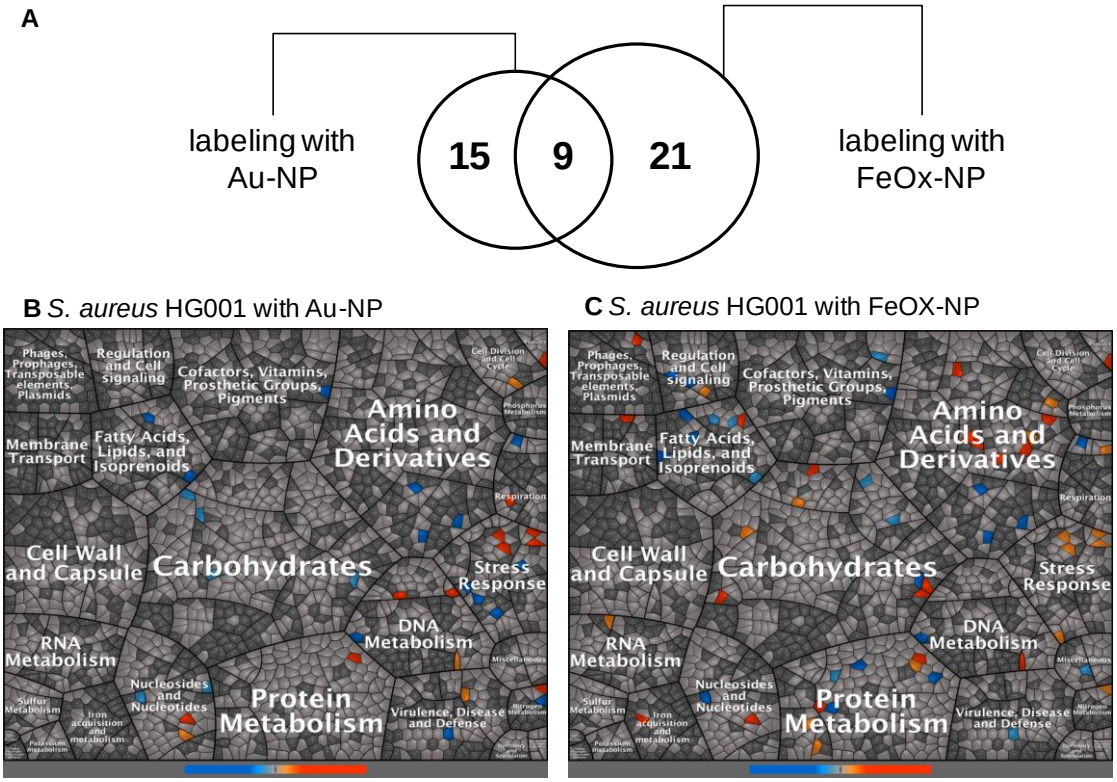

Figure 18. Proteins with different abundance after incubation with NP in comparison to non-treated controls. *The Venn diagram (A) displays proteins exhibiting different abundance after Au-NP incubation (24 proteins) or FeOx-NP incubation (30 proteins). Proteins were regarded as regulated when the H/L ratio was significantly different from 1 with $p \leq 0.01$ in a one-sample t-test and when the absolute fold change exceeded the threshold of two. All L/H log_2-ratio values of proteins with different abundance after incubation with Au-NP (B) or FeOx-NP (C) are presented in a Voronoi-like treemap. Here, proteins with higher abundance after NP-treatment are colored orange to red, while proteins with lower abundance in the NP-treated bacteria are colored in shades of blue. Proteins identified and quantified in the analyses are colored light gray, and dark gray marks proteins not quantified in the analyses. In cases when a protein can be linked to more than one function this protein will appear more than once in such functionally grouped Voronoi-like treemaps (Depke et al., 2014).*

Application of fluorescent NP labeled S. aureus in infection experiments

Human epithelial S9 cells were infected with pre-labeled *S. aureus* HG001 for two reasons. The first goal was to check if the fluorescent NP could be utilized for intracellular tracing of internalized bacteria. Second, it should be investigated if enrichment of bacteria with NP was sufficient for proteome analysis of internalized bacteria. If observation of intracellular bacteria using the fluorescent dyes has been successful, this method could later on be transferred to settings were bacteria cannot be easily modified for expression of CFP or GFP. This would be especially advantageous for investigation of clinical isolates. In this study CFP-expressing bacteria were employed to confirm detection of bacteria by green fluorescence from FITC-conjugated NP with an independent cyan-fluorescence signal specific for the bacteria. *S. aureus* HG001 pJL76 was incubated with NP prior infection experiments. Fluorescence microscopy pictures were exemplarily analyzed at 4.5 h after infection of S9 cells with *S. aureus* HG001 pJL76. Figure 19 shows S9 cells (F-actin in red, nucleus in blue) infected with CFP-expressing bacteria (cyan). Signals from FITC-positive and CFP-expressing (cyan) bacteria were always located at the same position for bacteria labeled with either Au-NP or FeOx-NP. When bacteria without preceding NP-incubation were internalized, distinct FITC-positive structures were not detected. Only a green background of overlapping emission spectra appeared in this channel. Thus, these pictures confirm on the one hand the results from flow cytometry that almost all bacteria were labeled and on the other hand that the NP were a useful tool of observing bacteria. Furthermore, as green spots were only observed at positions, where also cyan fluorescence was detected it was obvious that free NP were not incorporated into the human cells in our approach. This could lead to the conclusion that intact bacteria did not lose NP and possible remaining free NP from pre-cultivation did not cause distinct spots in the microscopy pictures.

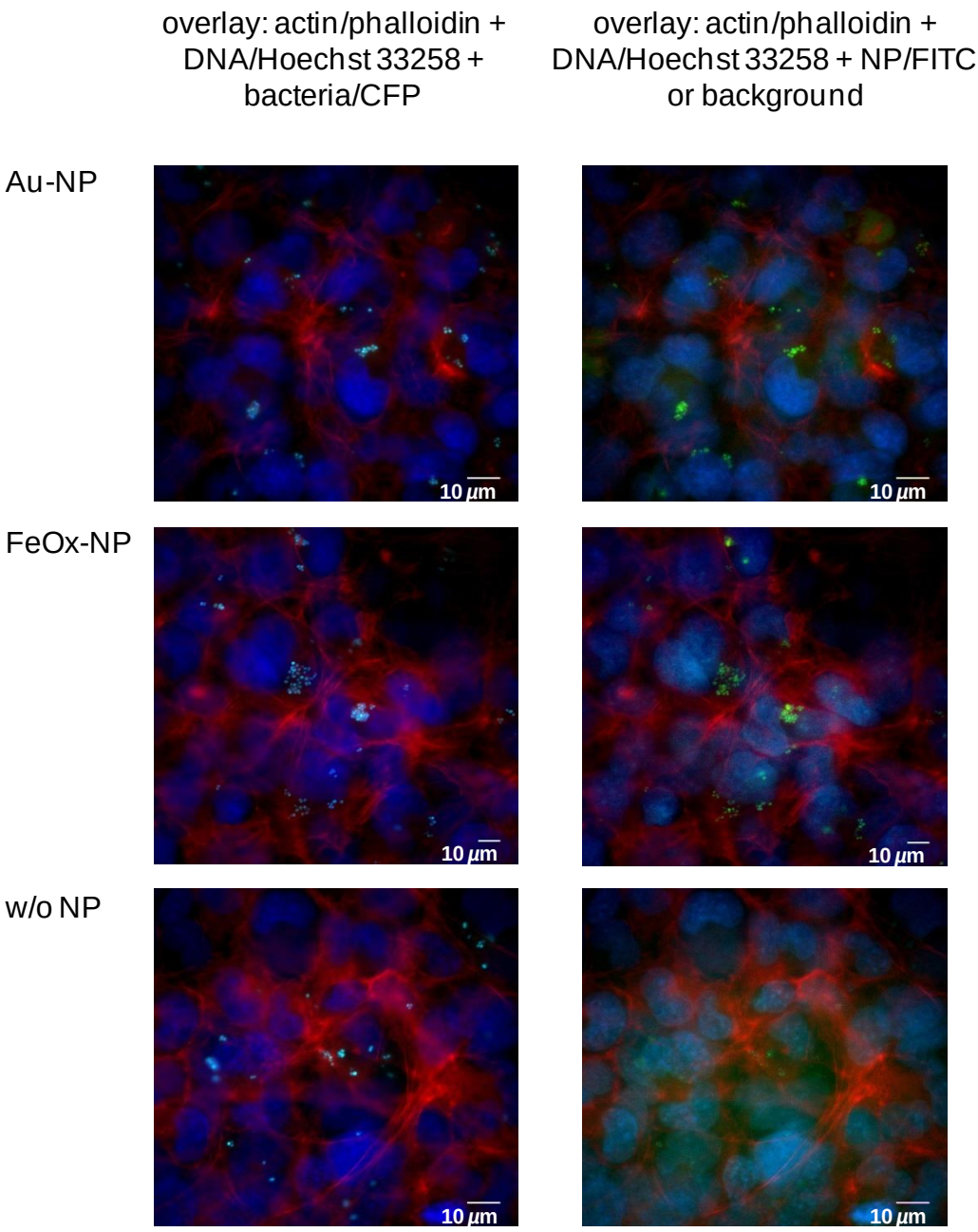

Figure 19. Fluorescence microscopy of S9 cells after 4.5 h of infection with CFP-expressing *S. aureus* HG001 pJL76 which had been incubated for 24 h with Au-NP, FeOx-NP or without NP prior to cell culture infection. *Host cell F-actin cytoskeleton was stained with Phalloidin Alexa Fluor 568 (red); the presence of NP was visualized by FITC (green), which was linked to the NP; DNA was stained by Hoechst 33258 dye (blue); and bacteria were detected by CFP (cyan), which was overexpressed by strain S. aureus HG001 pJL76. Images on the left show bacteria, but no NP; the images on the right show only NP. Images reveal co-localization of bacteria and NP but no FITC-positive particles in control cells (Depke et al., 2014).*

Having proven that internalized bacteria, which were co-cultivated with NP, were still labeled, two enrichment strategies for bacteria were tested. Samples of enriched bacteria were investigated by proteome analysis. First, Au-NP pre-incubated *S. aureus* HG001 were sorted from host cell debris after internalization *via* the red fluorescent dye (RBITC) of the NP using flow cytometry. In one experiment 289 proteins from internalized *S. aureus* HG001 2.5 h and 4.5 h *p.i.* were detected. In the case of bacteria which were pre-incubated with FeOx-NP, the paramagnetic property of the FeOx was taken advantage of. Thus, bacteria could be separated from host cell debris by magnetic capture using a two Tesla magnetic field with a specially designed chamber (Figure 20). Subsequent proteome analysis yielded 379 proteins from internalized *S. aureus* HG001 2.5 h and 4.5 h *p.i.* in a first approach. In both independent experiments with NP-labeled bacteria, 191 proteins were identified in common (66% of all identified protein for Au-NP, 50% of all identified proteins for FeOx-NP, Figure 21). All identified proteins from these two experiments are available online as Supporting Material from Depke et al (http://onlinelibrary.wiley.com/doi/10.1002/cyto.a.22425/suppinfo, supptab2 and 3.pdf).

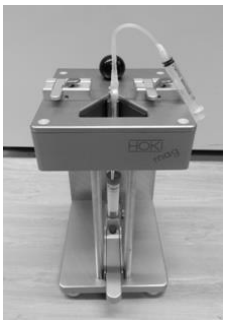

Figure 20. Two Tesla magnet (HOKI mag) for separation of FeOx-pre-labeled bacteria.

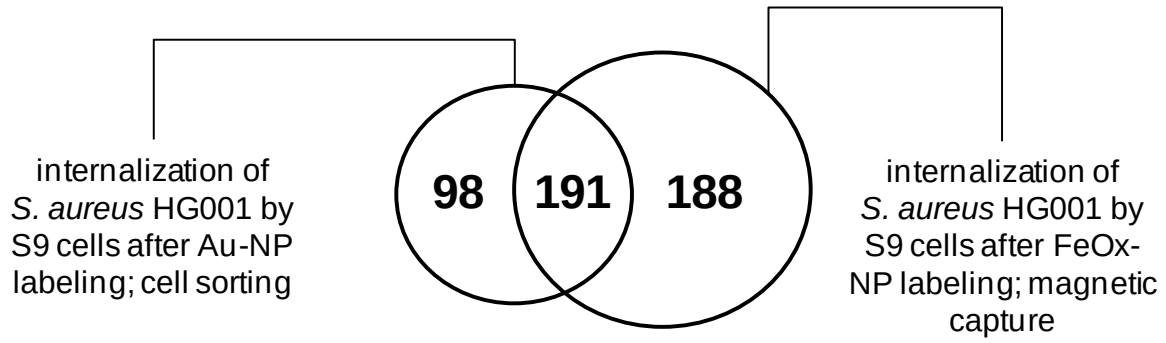

Figure 21. Bacterial proteins identified after internalization of *S. aureus* HG001 into S9 cells and comparison of identifications between both methods applied to retrieve internalized bacteria following infection. *289 bacterial proteins were identified when NP-labeled bacteria were recovered from the lysate of host cells by cell sorting after Au-NP labeling. When FeOx-NP were used and captured using a strong magnetic field, 379 bacterial proteins were identified from the recovered NP-labeled bacteria. One hundred and ninety-one proteins were detected in both approaches (Depke et al., 2014).*

Protocol for enrichment of bacteria and secreted proteins by isolation of phagosomes

When sorting *S. aureus* from host debris as illustrated in Figure 8, non-fluorescent particles, meaning host cell debris and bacterial proteins which were secreted into the host cell environment are washed away and thus are not available for analysis. However, especially those secreted proteins are important factors of the virulence and pathogenicity of *S. aureus* as they are in direct contact to the host cells and contribute to host cell lysis, spreading of bacteria or survival by acquisition of nutrients from the host. Thus, a new protocol had to be developed. Alternatively to lysis of all host cell membrane types, only the outer plasma-membrane should be destroyed enabling enrichment of whole, intracellular, membrane-surrounded compartments which contain bacteria, namely the phagosomes. First, the appearance of bacteria inside the phagosomes was proven by confocal fluorescence microscopy. *S. aureus* HG001 cells were found to be engulfed by lysosomal-associated membrane protein 1 (LAMP-1) positive membranes 2.5 h and 6.5 h post-infection (Figure 22).

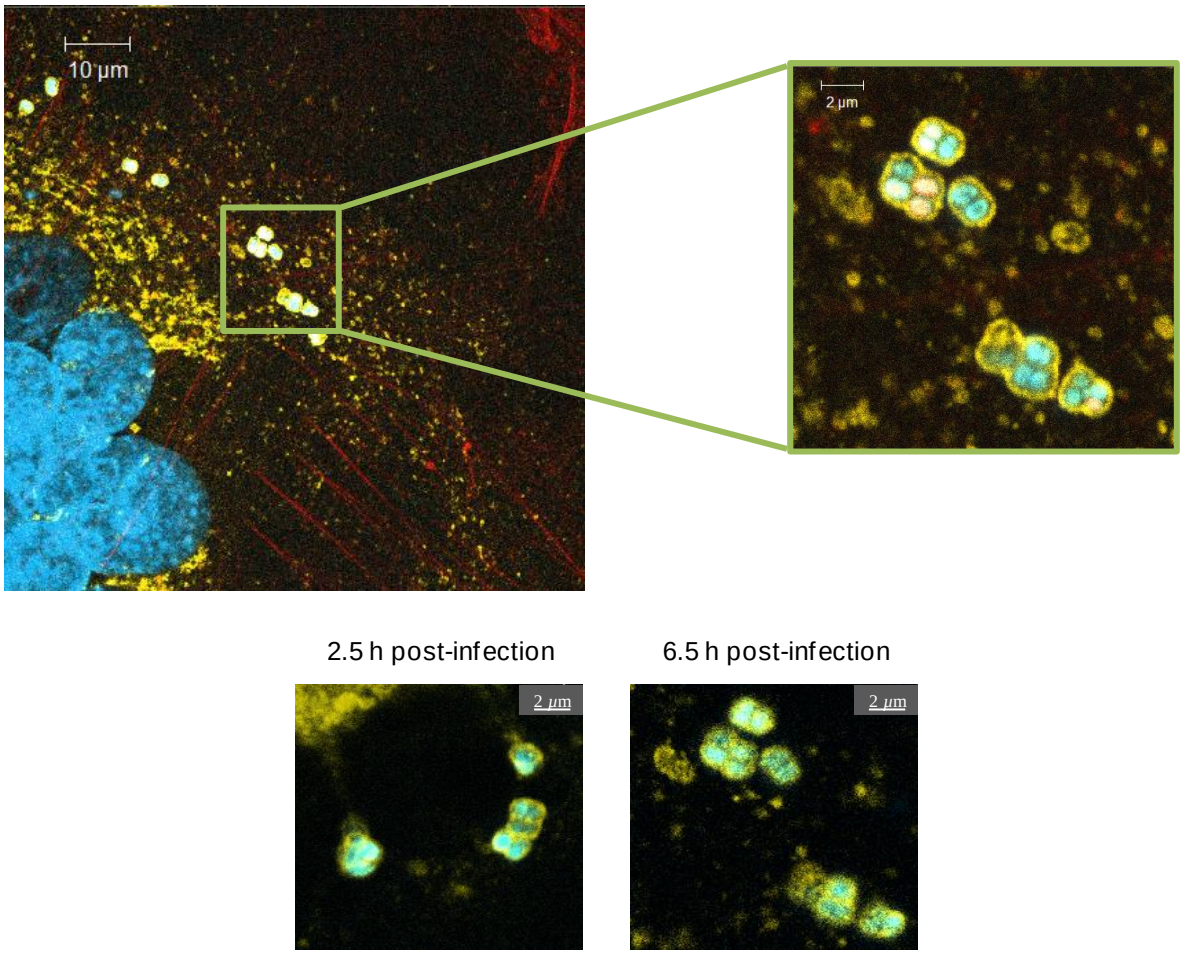

Figure 22. Fluorescence microscopy of bacteria engulfed by LAMP-1 positive membranes. *Nuclei were stained in blue with HOECHST 33258, F-actin was stained in red with phalloidin-Texas Red. S. aureus HG001 pJL76 is visible in cyan. S9 cells expressed LAMP-1 which was fused to YFP and apparent in yellow.*

The protocol for enrichment of phagosomes was adapted from a protocol originally established by Ulrich Schaible, FZ Borstel. The adapted workflow which could be applied for the infection setting of *S. aureus* and human cell lines is depicted in Figure 23. After infection, host cells were detached from the plate and homogenized using a syringe (Figure 23A-C). After density gradient centrifugation the distribution of bacteria into the three layers of different sucrose concentrations was determined by CFU plating. Subsequently, the phagosomes with enclosed bacteria were separated from the 12% sucrose layer by centrifugation and prepared for MS by cell disruption and trypsinization (Figure 23D-G). Phagosomal and staphylococcal proteins were investigated by shotgun MS and MRM (Figure 23H).

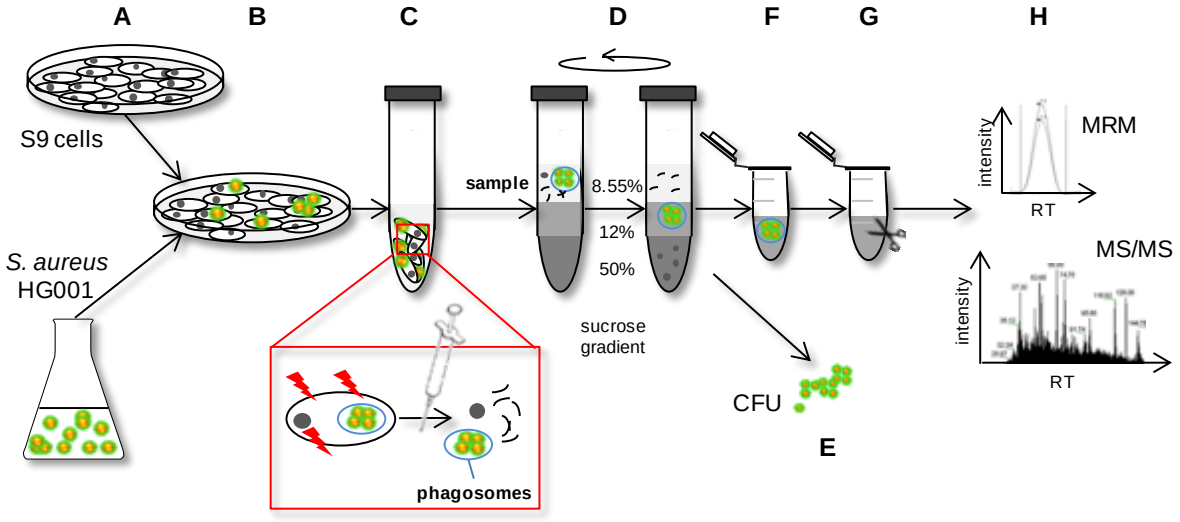

Figure 23. Isolation of phagosomes from infected S9 cells. *(A) Cultivation of S9 cells in eMEM and S. aureus HG001 pMV158GFP in pMEM, (B) standard internalization setup, (C) sampling of whole cells in 8.55% sucrose, resuspension of pelleted cells in 8.55% sucrose and subsequent lysis of cell membrane with a syringe, (D) application of homogenized sample onto a sucrose grandient (12% and 50% sucrose) and density gradient centrifugation, (E) CFU determination of S. aureus in the three phases, (F) isolation of the 12% phase, (G) sample preparation by protein extraction and tryptic digestion, (H) MS analysis by MS/MS and MRM.*

After lysis of the cells, the nuclei and F-actin skeleton were destroyed. Bacteria were still engulfed by intact phagosomes (Figure 24A). However, due to lysis with the help of a needle destruction of few phagosomes could, as expected, not be completely be avoided. Therefore, a small proportion of *S. aureus* which was not enclosed by a membrane was observed as well. After density gradient centrifugation of the lysed cells, almost 80% of the bacteria were found in the 12% phase of the sucrose gradient (Figure 24B). Almost no bacteria were detected in the 8.55% interphase. The 50% sucrose layer contained about 20% of the bacteria in the lysed sample. Likely they were bound to human proteins or cellular sub-compounds of higher density. Thus, the 12% sucrose layer was used for investigations of the phagosomal and bacterial proteome further on.

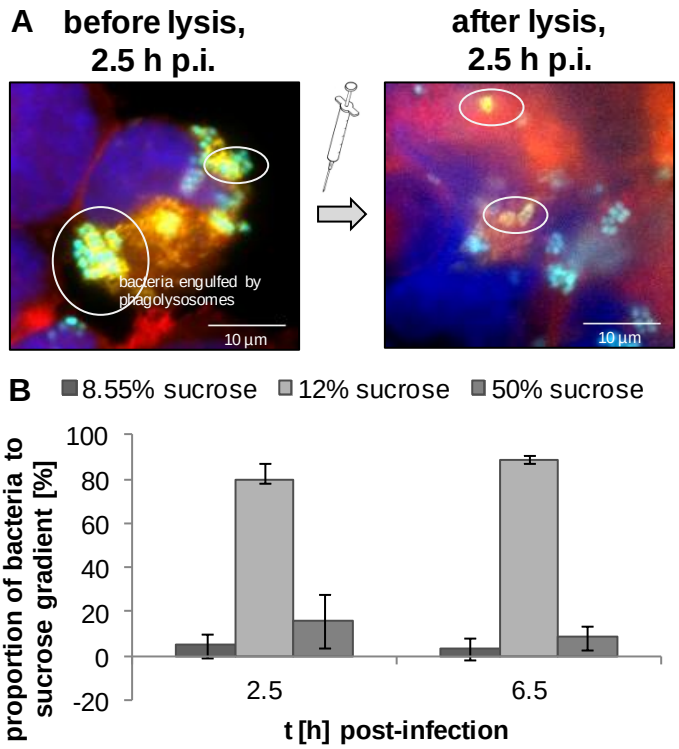

Figure 24. Investigation of the functionality of the phagosome enrichment protocol. *(A) After cell lysis, phagosome (encircled in white, yellow due to LAMP-1-YFP) containing bacteria (cyan, CFP) are still intact, but nuclei (blue, HOECHST 33258) and cytoskeleton (red, phalloidin-Texas Red) are disrupted. (B) CFU determination revealed clear separation of the bacteria into the 12% phase of the sucrose gradient after centrifugation. Mean and standard deviation of three BR are displayed.*

Sampling of non-adherent bacteria as a control for proteome analysis upon infection

Our standard internalization protocol (Pförtner et al., 2013) describes the sampling of internalized bacteria out of host cell lysate. The impact of internalization was observed in a time-dependent manner between 1.5 h and 6.5 h *p.i.* (Pförtner et al., 2013, Schmidt et al., 2010b). It would additionally be very interesting to observe the early effect of internalization. Bacteria of the infection medium which had contact to the host cell culture but were not internalized should serve as a control for the internalization step. These so-called “non-adherent control bacteria” were first harvested by centrifugation and proteome analysis was performed after tryptic digestion of resulting pellets. In the framework of this thesis and the herein supervised diploma thesis of Marjolaine Simon, non-adherent *S. aureus* HG001 cells were harvested from the supernatant of A549 cells by centrifugation. Sometimes protein abundance of non-adherent control bacteria was much higher compared to an early sampling point of internalized bacteria (2.5 h *p.i.*) which took place only 1.5 h later than the control sampling. As such enormous decreases are hardly explainable by protein degradation, the non-adherent bacteria control was excluded from the A549 project (compare “Time-resolved analysis

of *S. aureus* HG001 internalized by A549 cells"). There, the proteome adaptation of internalized bacteria was analyzed in a time-dependent manner using the 1.5 h point in time as baseline.

In order to improve the quality of the non-adherent control in the follow-up project (cell line comparison), the non-adherent bacteria from the cell culture supernatant were treated with Triton X-100 at 37°C and were subjected to cell sorting and thus, experienced the same treatment as the internalized bacteria. As a consequence, in the two experimental approaches, non-adherent bacteria were harvested each in a different way. However, the sampling process of internalized bacteria was accomplished using the same protocol for both approaches. When comparing data of non-adherent and internalized samples for both experiments it became obvious that ratios between the internalized sample and the non-adherent control differed drastically (Figure 25). However, when calculating the ratios between 2.5 h and 6.5 h *p.i.* for both experiments from the ratios to the control given in Figure 25, they were similar within each of the two independent projects.

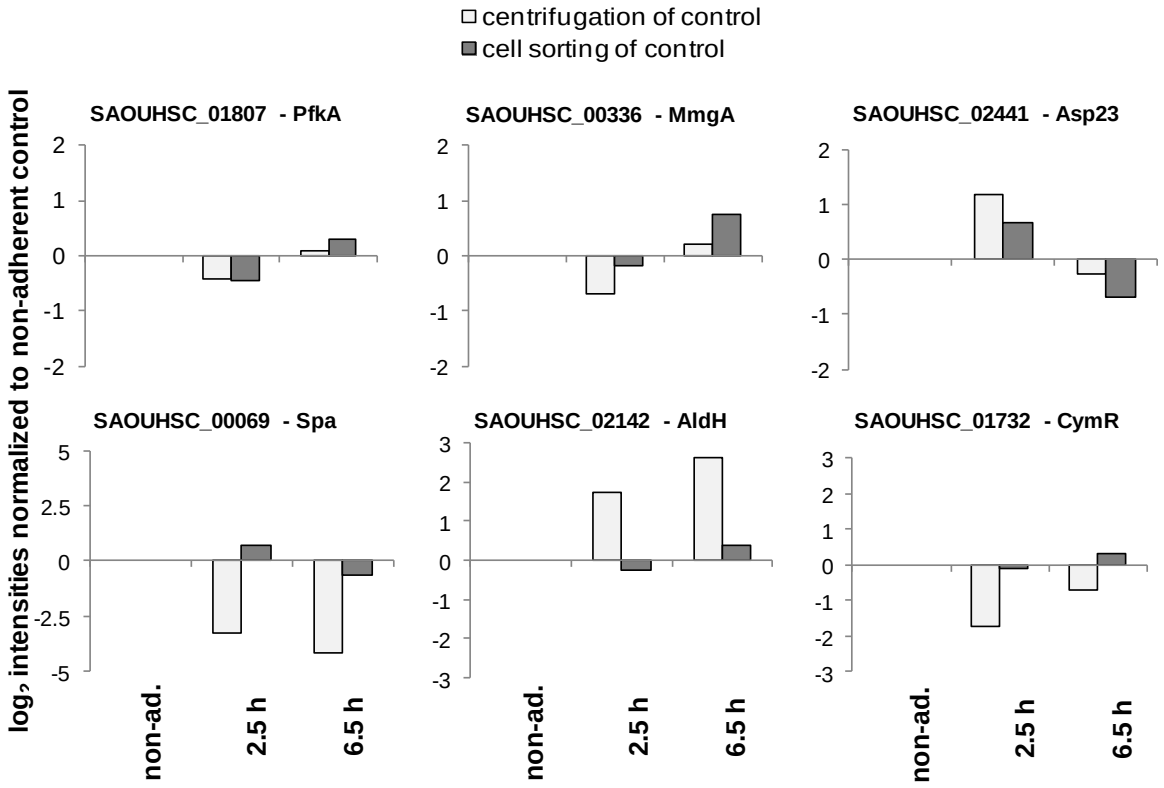

Figure 25. Relative protein abundance of non-adherent bacteria (non-ad.) and internalized bacteria 2.5 h and 6.5 h after internalization. *Internalized data are depicted in reference to the non-adherent control. This control was either sampled by centrifugation (light gray) or treated with Triton X-100 and subjected to cell sorting (dark gray). Sampling of internalized samples was in both cases performed by Triton X-100-treatment and cell sorting. Average values of each three BR are depicted.*

Update of annotations for *S. aureus* HG001

Since the genome of strain NCTC8325 was completely sequenced in 2006 (Gillaspy et al., 2006), proteome analysis of this strain was possible. Annotations of protein names and functions assigned to the corresponding gene facilitate biological analysis of the examined strains. Such annotations can be found in several public online databases such as NCBI (http://www.ncbi.nlm.nih.gov/) or UniProt (http://www.UniProt.org/). Those annotations are continuously updated according to latest research. Meanwhile a large number of *S. aureus* strains had been sequenced but quality of annotation greatly varies. According to the NCBI database for strain NCTC8325 (release 2011) out of total 2,892 proteins, 1,177 proteins were already assigned protein names and function. For 1,715 proteins no annotation was available, they were called “hypothetical protein”. Since the value of OMICs analyses increases with the quality of annotation, the improvement of the annotation of *S. aureus* HG001 was a subtask of this thesis to improve analysis of proteome adaptation by identifying more gene functions for this strain. Although physiological and genetic differences between different *S. aureus* strains exist, many protein sequences are homologous between them and it is expected that their functions are conserved. NCBI and others provide tools allowing comparison of whole genomes for selected strains and also basic local alignment search tools (BLAST, http://blast.ncbi.nlm.nih.gov/Blast.cgi) finding same amino acid sequences in different strains.

First, already sequenced *S. aureus* strains were compared. A tool from NCBI (http://www.ncbi.nlm.nih.gov/sutils/geneplot.cgi) extracted sequence comparisons for all listed *S. aureus* strains, *S. epidermidis*, *Bacillus subtilis*, and *B. licheniformis* (06-08/2011). If a functional annotation was available in any strain, it was used, and the source of the function was added to our in-house database. However, about 1,000 genes had to be searched manually with the BLAST tool from NCBI. The entry with the highest identification rate and query coverage (but at least 90%) was used as new annotation of a function in strain NCTC8325. Here again, the source of annotation was documented. After strain and protein sequence comparison, additional 1,188 proteins of *S. aureus* HG001 were associated with functions. Annotations remained still unknown for only 527 proteins. Finally, a newly annotated database with functions assigned for 2,365 proteins of *S. aureus* HG001 was developed (Supplementary_Material_Table_03_S_aureus_DB_NCTC8325_BLAST_HGW.xlsx). These new annotations were also utilized for numerous studies in our groups. Within this thesis it played an important role for selection of secreted virulence factors for further analyses. In addition, general pathway analyses could be improved as all newly found functions were implemented in our data analysis pipeline for proteome analysis of *S. aureus*. The improved pathway analyses were applied in this thesis and other projects (Pförtner et al., 2014). To also facilitate functional analysis for a broad scientific community, this extensive annotation list was implemented into the newly developed AureoWiki-platform (http://www.protecs.uni-greifswald.de/aureowiki/Main_Page). At the moment three commonly used *S. aureus* strains (COL, NCTC8325, and N315) are described in AureoWiki. Moreover a pan-genome was created, with the aim to elucidate as many gene functions

and names as possible by comparison of several *S. aureus* strains. The results from this database comparison were embedded in this section.

Improved analysis of proteome data from internalized bacteria

Analyses of complex biological samples such as those from infection settings containing proteins from two organisms always pose a challenge. Classical database comparisons match acquired spectra with those stored in public databases for example for human or staphylococcal proteins. For the cell line comparison project, where only small differences in the proteome response of *S. aureus* to internalization in the different cell lines were expected, the highly sensitive Q Exactive mass analyzer was employed and an extended data analysis pipeline was developed (Surmann et al., 2014b). First, a COMET (Eng et al., 2013) search was applied using a decoy database of *S. aureus* HG001 combined with human UniProt/Swissprot protein records. Thereby, 1,393 staphylococcal proteins were identified in total with a peptide probability greater than 0.8 (false discovery rate (FDR) <0.01). Using SpectraST (Lam et al., 2007), a spectral library comparison using a *S. aureus* HG001 specific database (Depke et al., manuscript submitted) was accomplished. Finally, protein identification was complemented with a reSpect search (Positive Probability, Ltd., Isleham, United Kingdom). Using the reSpect algorithm, peaks that were not assigned to peptides in the first search were checked again. Tolerating increased mass and charge state (one to five) windows, further peptide sequences were analyzed and also verified with PeptideProphet and iProphet. Finally, 1,484 proteins were identified with an FDR less than 0.01 combining all identification steps. Out of them, 1,443 staphylococcal proteins could be quantified over time for all three cell line models (Supplementary_Material_Table_04_S_aureus_proteins_quantified_from_infected_celllines.xlsx).

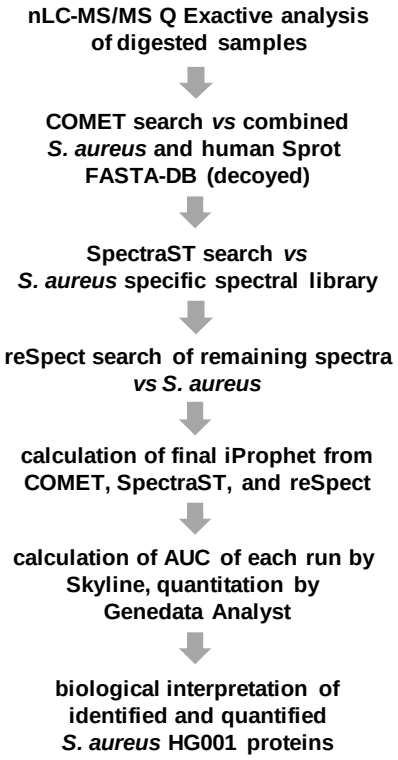

Figure 26. Pipeline for proteome analysis using databases and spectral library search. *Modified from Surmann et al., 2014b.*

With the improved settings in both MS and data analysis (Figure 26) it was now possible to quantify about 50% of the whole proteome (2,891 sequences for *S. aureus* NCTC8325 in the database*)* from as few as two million *S. aureus* HG001 cells after internalization and therefore provide a comprehensive description of the behavior of this important pathogen during internalization.

Intracellular persistence and replication of bacteria after internalization

In order to characterize internalization, especially intracellular replication of the bacteria occurring after exposure of *S. aureus* HG001 to human cell lines, microscopy techniques were applied and internalized bacteria were counted.

Fluorescence microscopy visualized the distribution and replication of GFP-expressing bacteria in human host cells after staining of F-actin and DNA. Within the diploma thesis of Marjolaine Simon pictures were acquired after internalization of bacteria by A549 cells (Figure 27). Comparing the point in time 1 h after infection but before treatment with lysostaphin and the point in time 1.5 h after infection which included 30 min treatment with lysostaphin, it was obvious that extracellular bacteria were efficiently killed as their number was clearly reduced. Until 6.5 h post-infection the intracellular number of bacteria increased, after 24.5 h again less bacteria were present. In addition, formation of bacteria clusters was observed after 4.5 h, 5.5 h, and 6.5 h (Figure 27).

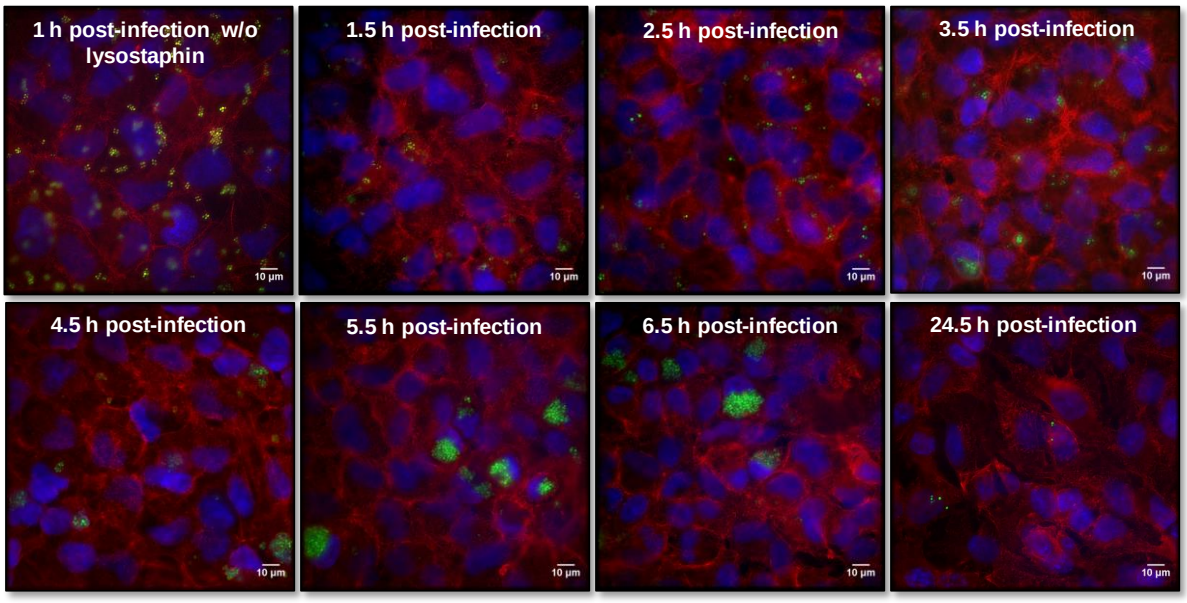

Figure 27. Nuclei and F-actin staining of A549 cells and GFP expressing bacteria with a 40x magnification. *The size bars indicate 10 µm. The phalloidin-Texas Red stain is shown in red, coloring the F-actin. It permits to visualize the contours of eukaryotic cell nuclei. Bacteria expressing GFP were detected in green. The Hoechst 33258 stain visualizes the DNA of the A549 nuclei in blue. Besides an increase of bacteria, also a trend of forming bacterial clusters was detected.*

To determine the extent of intracellular replication the number of internalized bacteria was counted from TEM slides for internalization into A549 cells after 2.5 h, 4.5 h, and 6.5 h. Numbers of host cells, the number of infected host cells, and the number of bacteria inside infected A549 cells were determined. Over all points in time only 12-20% of host cells carried bacteria (Table 8). The intracellular number of bacteria doubled between all sampling points (Figure 28) but varied strongly between infected host cells:

Table 8 Supplementary_Material_Table_05_TEM_slides_A549_S_aureus_cell_counting.xlsx.

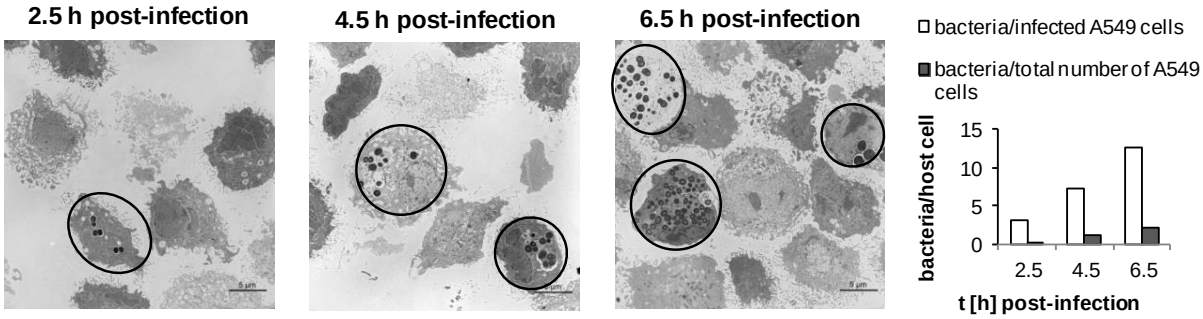

Figure 28. TEM analysis of A549 cells infected with *S. aureus* HG001. *Infected and non-infected A549 cells as well as bacteria were counted in more than 100 pictures (about 260 cells per slice) for each point in time (2.5 h, 4.5 h, and 6.5 h p.i.). In the bar chart, the proportion of bacteria per infected and per total number of A549 cells are displayed.*

Table 8. Overview of host cell and bacteria counting from TEM analysis. *For each time point 100 sections were counted each of two slices.*

sampling point	sum infected host cells	sum non-infected host cells	percentage infected host cells [%]	average bacteria/ infected host cells	average bacteria/total number of host cells
2.5 h *p.i.*	61	511	12	3.1	0.3
4.5 h *p.i.*	96	485	20	7.3	1.1
6.5 h *p.i.*	132	603	22	12.6	2.1

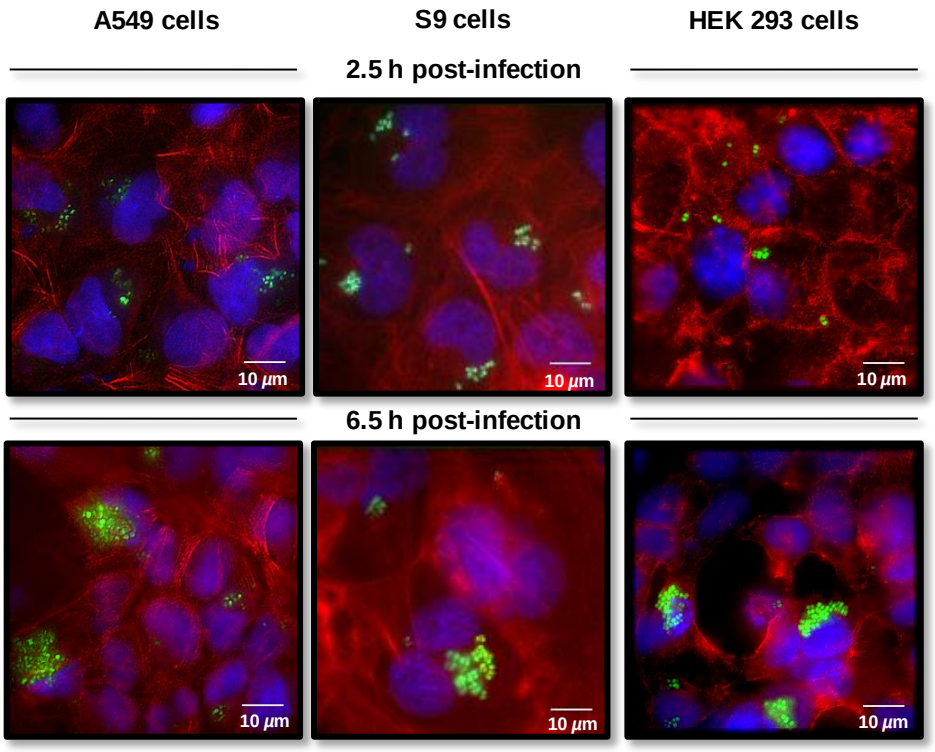

Figure 29. Fluorescence microscopy of *S. aureus* HG001 pMV158GFP internalized by A549, S9, and HEK 293 cells. *Pictures were acquired with 60x magnification. The size bars indicate 10 µm. The phalloidin-Texas Read stain is shown in red, coloring the F-actin. GFP expressing bacteria are detected in green. Hoechst 33258 stains DNA for visualization of the host cell nuclei in blue (Surmann et al., 2014b).*

A comparative internalization study revealed that *S. aureus* HG001 pMV158GFP was internalized by A549, S9 or the HEK 293 cells (Surmann et al., 2014b). Fluorescence microscopy at 2.5 h and 6.5 h *p.i.* supported this observation, and further established that these bacteria tend to build clusters at later points in time after internalization (Figure 29) not only inside A549 cells which was described above (Figure 27) but also inside the two other cell lines employed.

The intracellular replication of *S. aureus* HG001 inside A549, S9, and HEK 293 cells was also supported by counting intracellular bacteria hourly by flow cytometry (Figure 30). Host cells carrying bacteria and those which did not carry bacteria were not discriminated and, therefore, were both included during counting host cell numbers. Thus, the number of bacteria can only be related to the total number of human cells, infected and non-infected cells were not distinguished as in TEM analysis. However, the average values for A549 resulting from flow cytometry can be compared to TEM analysis when taking the value of bacteria/total number of host cells into account (Table 8, last column, Figure 30, A549 data). Similar numbers were detected 2.5 h, 4.5 h, and 6.5 h *p.i.* with both methods which again indicates the usefulness of the newly employed flow cytometry-based cell counting method described above. When comparing the different growth behavior, the lowest number

of bacteria was counted in A549 cells with about one bacterium per host cell after 2.5 h. The highest number of intracellular bacteria after 2.5 h was observed inside S9 cells with almost three bacteria per host cell. The number of bacteria inside A549 and S9 cells doubled between 2.5 h and 6.5 h post-infection. The amount of intracellular *S. aureus* HG001 inside HEK 293 cells remained very low during the first hours after internalization but increased strongly 6.5 h *p.i.* to more than four bacteria per HEK 293 cell.

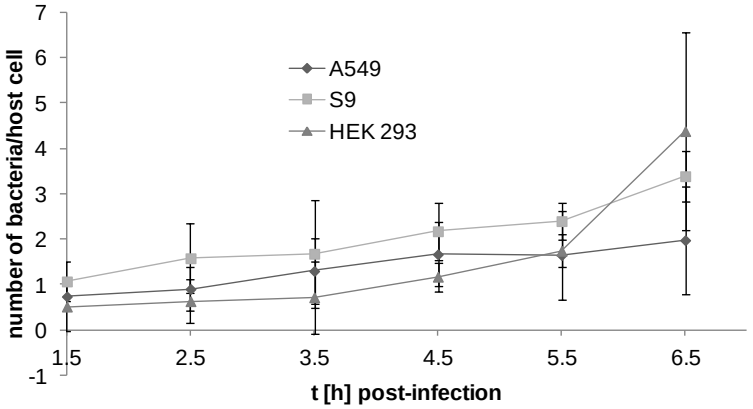

Figure 30. Intracellular replication of *S. aureus* HG001 pMV158GFP. *GFP-expressing bacteria were counted by flow cytometry from lysed host cells. For all three cell lines time-resolved bacterial counts are provided. Results represent the mean and standard deviation of three BR (Surmann et al., 2014b).*

Between the first 6.5 h after infection, the doubling time of *S. aureus* HG001 pMV158GFP measured inside A549 cells about 3.5 h, inside S9 cells 3 h, and inside HEK 293 cells less than 2 h. In contrast to that, the same strain doubled once every 55 min when cultivated in pMEM in a flask during exponential growth phase (Figure 31).

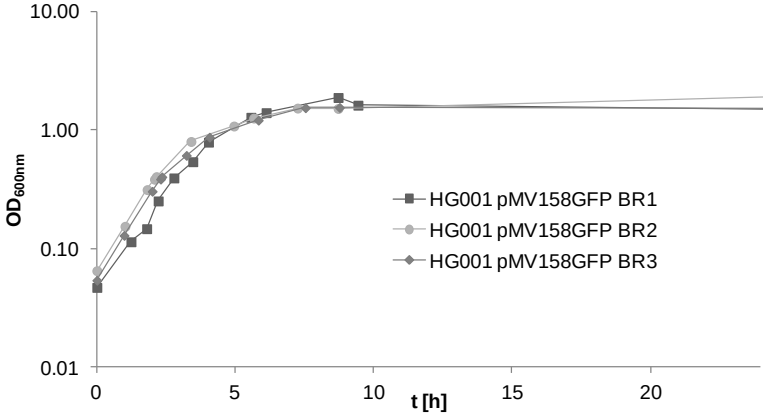

Figure 31. Growth curve of *S. aureus* HG001 pMV158GFP grown in pMEM in flasks. *Three independent growth curves are depicted. Generation time in the exponential phase amounts about 55 min. Bacteria at OD_{600} 0.4 were used for infection of host cells.*

Host cell metabolome as nutrient reservoir for invading bacteria

The intra- and extracellular host cell metabolome of non-infected host cells treated with sterile infection medium was determined in collaboration with Philipp Gierok and Michael Lalk from the Institute of Biochemistry in Greifswald. Metabolite levels might change in infected host cells, but since only few host cells indeed carried *S. aureus* it was not possible to measure metabolite levels specifically in this sub-proportion. Extracellular metabolites were measured by ^{1}H-NMR, intracellular metabolites by LC-MS and GC-MS: These data represent the starting conditions of intracellular nutrients available for internalized *S. aureus* cells. On the other hand, extracellular metabolite concentrations were determined to compare the conditions for *S. aureus* prior to internalization even if different media were used for different host cells. Those extracellular metabolites are available for the so-called "non-adherent control bacteria". These metabolome data were collected to complement and discuss proteome analyses of internalized bacteria and are already published (Surmann et al., 2014b). While intracellular metabolite amounts were quantified in relation to the number of host cells, the extracellular metabolite concentrations were calculated in relation to the volume of the supernatant. Morphological data for A549 cells are available in literature (Jiang et al., 2010). With the estimated cell volume of 1,670 μm^3 according to Jiang et al. the molar concentrations of intracellular metabolites were determined and directly compared to the extracellular concentrations. Almost all amino acids could be measured intracellularly in the host cells. Only arginine could not be detected with the applied methods due to technical limitations. The required derivatization for GC-MS would destroy the molecule, only few amino acids were acquired by LC-MS, and other peaks were interfering with the arginine signal in ^{1}H-NMR analysis making an explicit detection impossible. At the start of infection, glucose was present inside and outside the host cells in similar amounts of about

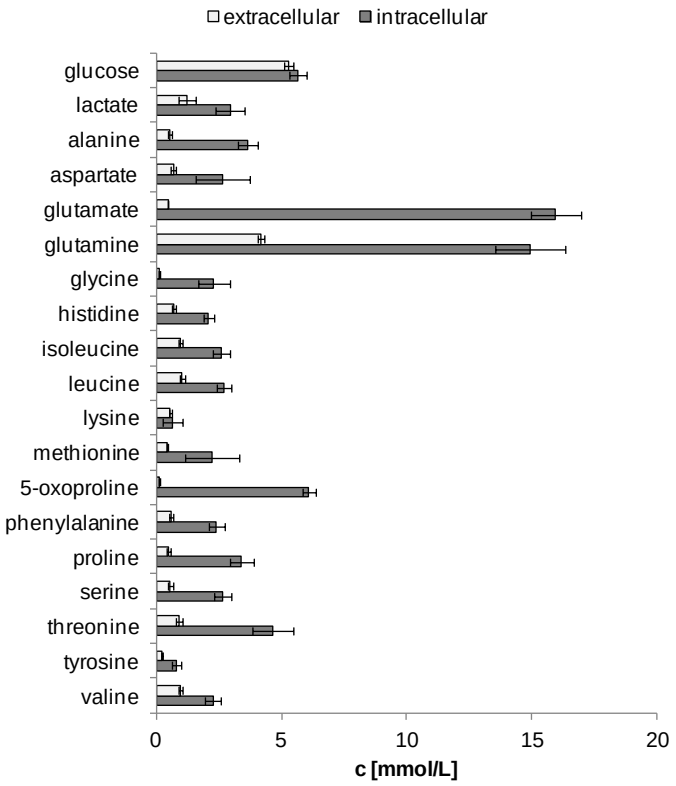

Figure 32. Metabolome analysis of non-infected A549 cells treated with sterile infection mix. *The extracellular metabolome was measured by 1H-NMR from supernatant. The intracellular metabolome was extracted from the cells and analyzed by GC-MS and LC-MS. Average values and standard deviations from four biological replicates are depicted.*

5 mmol/L. The most abundant intracellular compounds were glutamate and glutamine. Extracellular glucose and glutamine were present in highest amounts. The other amino acids were detected mostly with 2-4 mmol/L intracellularly with the exceptions of lysine (0.7 mmol/L), 5-oxo-proline (6.1 mmol/L), and threonine (4.7 mmol/L, Figure 32). The host cell metabolome was additionally determined for S9 and HEK 293 cells. Here, intracellular values are given in nmol/10^6 host cells due to missing information on host cell volume. In order to allow comparison of intracellular metabolite concentrations between the cell lines, data for A549 cells are provided in mmol/L and nmol/10^6 host cells in Table 9. In the following sections the metabolic pools of the three cell lines are compared for extra- and intracellular metabolites with special regard on certain pathways.

Table 9. Intracellular metabolite concentrations of A549 cells. *Average values from four BR are given in mmol/L or nmol/10^6 host cells.*

intracellular metabolite	aspartate	glutamate	glutamine	glycine	histidine	isoleucine	leucine	lysine
c [mmol/L]	2.7	16.0	14.9	2.3	2.1	2.6	2.7	0.7
c [nmol/10^6 host cells]	4.4	26.7	24.9	3.9	3.5	4.3	4.5	1.1

intracellular metabolite	5-oxoproline	proline	phenylalanine	serine	threonine	tyrosine	valine	glucose
c [mmol/L]	6.1	3.4	2.4	2.6	4.7	0.8	2.3	5.7
c [nmol/10^6 host cells]	10.2	5.7	4.0	4.4	7.8	1.3	3.8	9.5

Extracellular metabolome of three different host cell lines

Although HEK 293 cell culture medium is composed differently than the medium of the other cell lines A549 and S9, the supernatant of all three cell lines shows similar metabolite concentrations after 1 h treatment with sterile infection medium. Highest abundant metabolites in the sterile infection medium are glucose (about 5 mmol/L) and glutamine (about 4 mmol/L). Tyrosine, glycine, and 5-oxoproline were measured in amounts below 0.5 mmol/L (Figure 33, Supplementary_Material_Table_06_extracellular_metabolome_host.xlsx).

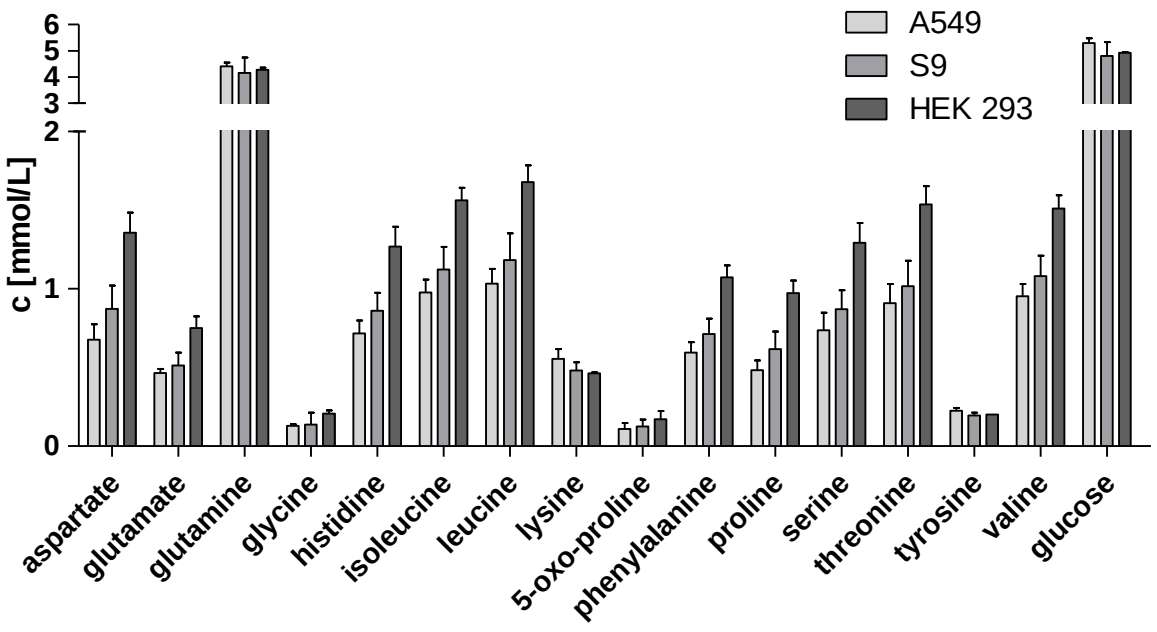

Figure 33. Extracellular metabolome of A549, S9, and HEK 293 cells. *Average values and standard deviations from four BR for A549 and HEK 293 cells, and three BR for S9 cells are depicted.*

Intracellular metabolome of three different host cell lines

After treating A549, S9, and HEK 293 cells for 1 h with sterile infection medium, 51 intracellular metabolites were quantified (for values of all replicates compare Supplementary_Material_Table_07_intracellular_metabolome_host.xlsx). Among them were 23 amino acids, eleven metabolites which can be generally assigned to central carbon metabolism and 17 molecules involved in energy metabolism. Most metabolites of energy metabolism (Figure 34) were detected in low amounts clearly below 1 nmol/10^6 host cells. Highest amounts were measured for myo-inositol (5-30 nmol/10^6 host cells), ATP (4.5-6.5 nmol/10^6 host cells), and glutathione (GSSG, 2-6 nmol/10^6 host cells). Differences between the cell lines were detected for myo-inositol (in S9 cells six times more compared to HEK 293 cells and almost three times more compared to A549 cells), GSSG (three times more in A549 cells compared to S9 cells) and cytidine-triphosphate (half amount in S9 cells compared to both other cell lines). An important control of metabolite sampling is the calculation of the energy charge. It describes the relation between the amounts of ATP, ADP, and AMP as follows:

$$energy\ charge = \frac{[ATP] + ½\,[ADP]}{[ATP] + [ADP] + [AMP]}$$

This value amounted to 0.96 for A549 cells, 0.95 for S9 cells, and 0.94 for HEK 293 cells. According to Atkinson, the value for living cells is estimated between 0.80 and 0.95 (Atkinson, 1968). Thus, the high energy charges calculated from the nucleotide concentrations of A549, S9, and HEK 293 cells indicate successful sampling of living cells and fast and reproducible inactivation of enzymes whose activity would have changed the energy level.

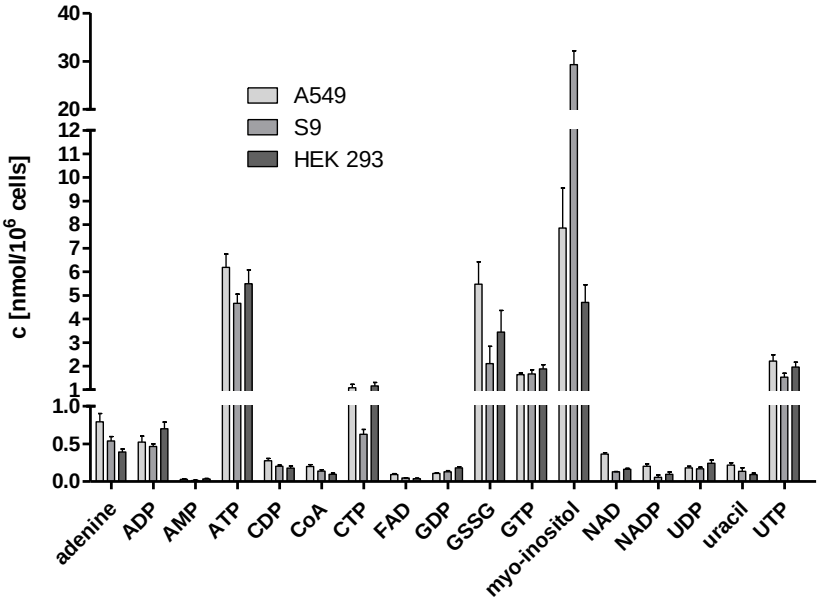

Figure 34. Intracellular metabolites involved in energy metabolism. *Average values and standard deviations from four BR for A549, S9 and HEK 293 cells are depicted.*

Furthermore, concentrations of intracellular metabolites involved in central carbon metabolism were similar for the three host cell lines (Figure 35). For all three cell lines, glucose was the most abundant intracellular metabolite with concentrations of more than 7 nmol/10^6 host cells. Two molecules of the tricarboxylic acid cycle (TCA), 2-oxoglutarate and citrate, were detected more than twice as much inside HEK 293 cells compared to the two lung epithelial cell lines. The concentration of malate was otherwise detected in similar amounts for S9 and HEK 293 cells (2.2 nmol/10^6 host cells in S9 cells, 2.0 nmol/10^6 host cells in HEK 293 cells) and lower for A549 cells (1.3 nmol/10^6 host cells). Lactate was only slightly higher inside the A549 cancer cells compared to the two other cell lines (A549 5.2 nmol/10^6 host cells, S9 4.2 nmol/10^6 host cells, HEK 293 3.1 nmol/10^6 host cells). Sugar fructose was measured with 1.4 nmol/10^6 host cells about four times more in A549 cells compared to S9 (0.3 nmol/10^6 host cells) and HEK 293 cells (0.4 nmol/10^6 host cells).

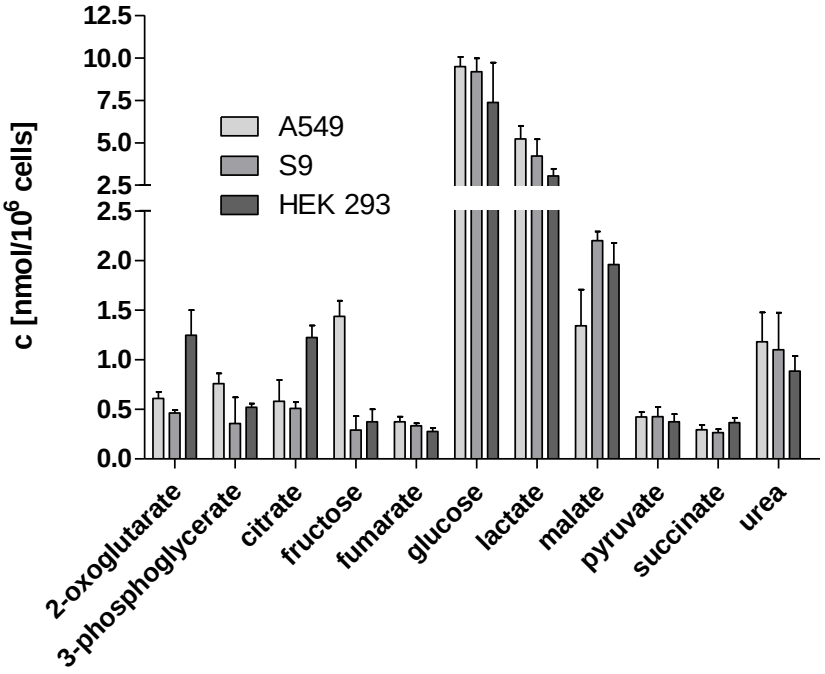

Figure 35. Intracellular metabolites involved in central carbon metabolism. *Average values and standard deviations from four BR for A549, S9 and HEK 293 cells are depicted.*

Due to technical limitations (see above) only arginine was not detected of the 20 proteinogenic amino acids. In total, 23 amino acids were quantified when including amino acid derivatives (Figure 36). For all three cell lines glutamate (>27 nmol/10^6 host cells) and glutamine (>19 nmol/10^6 host cells) were the most abundant intracellular amino acids. The lowest abundant amino acids were ornithine (<0.2 nmol/10^6 host cell), 4-hydroxyproline (<0.3 nmol/10^6 host cells), lysine (<1.2 nmol/10^6 host cells), and tyrosine (<1.4 nmol/10^6 host cells). Between the cell lines some differences were noted. For example, alanine, asparagine, glycine, and serine were detected about twice as much in HEK 293 cells compared to A549 cells. *Vice versa*, cysteine, methionine, tyrosine, and tryptophan were more abundant (about factor two) in A549 cells compared to HEK 293 cells. Levels of S9 metabolites were mostly in between those of the two other cell lines (Figure 36).

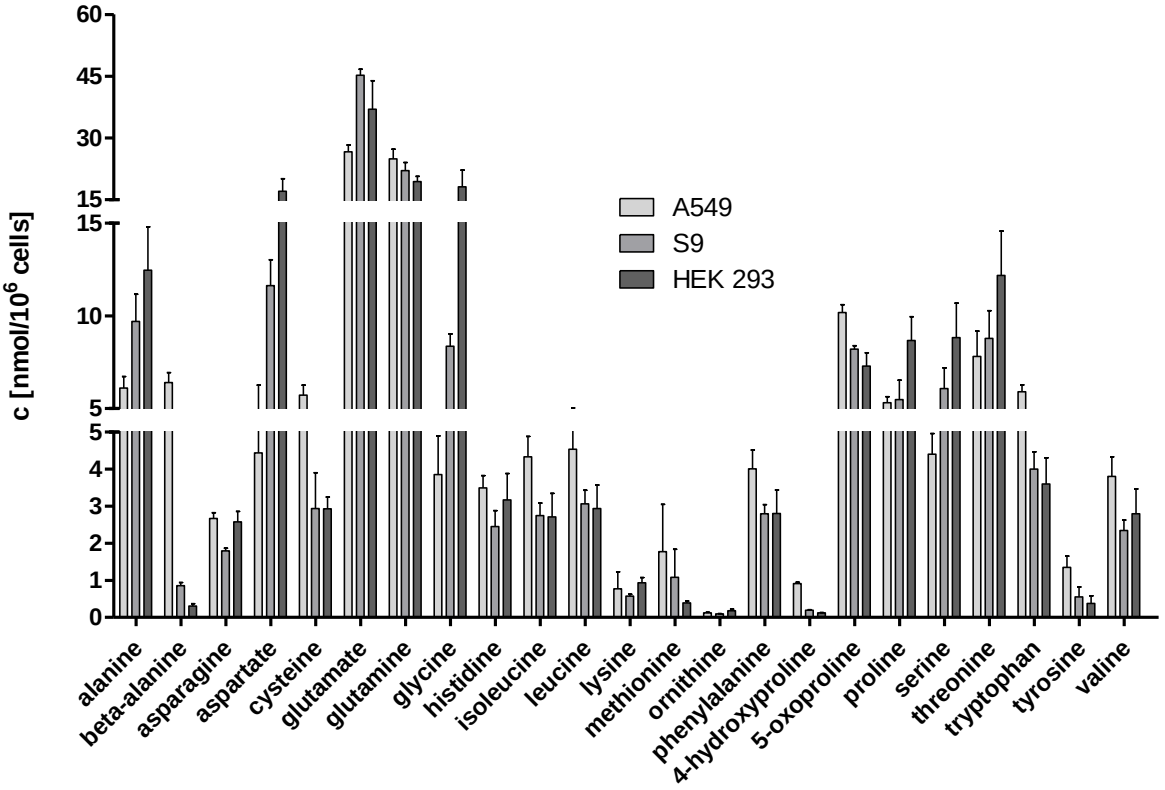

Figure 36. Intracellular amino acid concentrations. *Average values and standard deviations from four BR for A549, S9 and HEK 293 cells are depicted.*

Besides the few differences mentioned before, the nutrient pool available for the bacteria at the starting time of internalization was equal for all three cell lines. Thus, reflecting the comparable nutrient supplies, the bacteria internalized by S9, A549, and HEK 293 cells were not expected to show major variations in their proteome patterns. However, having the metabolome data at hand, it was possible to compare proteomic adaptations of single metabolic sub-pathways resulting from the different availability of few metabolites within the different host models and to suggest explanations for differential protein levels by different metabolite concentrations.

Proteome analysis of internalized *S. aureus* HG001

Time-resolved analysis of *S. aureus* HG001 internalized by A549 cells

As described above, *S. aureus* HG001 is able to replicate inside A549 cells during the first 6.5 h after internalization. However, the intracellular doubling time is about four times longer compared to growth in pure bacterial culture in flasks. In order to observe the molecular background of this adaptation to intracellular lifestyle the staphylococcal proteome was analyzed hourly between 1.5 h and 6.5 h after infection. Data in Table 10 show that some proteins were regulated upon infection. The number of proteins with different abundance compared to the first sampling point (1.5 h *p.i.*) was highest after 6.5 h. The number of proteins with increased or decreased levels compared to the first point in time after infection was almost similar.

Table 10. Numbers of differentially regulated bacterial proteins after internalization by A549 cells at different points in time after infection. *Increased (ratio >2) and decreased (ratio <0.5) trend in levels between the later sampling points and the first, 1.5 h p.i., are displayed. Totally, 824 proteins were identified and quantified. Data derive from three BR.*

	2.5 h/1.5 h	3.5 h/1.5 h	4.5 h/1.5 h	5.5 h/1.5 h	6.5 h/1.5 h
number of proteins with ratio to 1.5 h > 2	20	65	32	58	63
number of proteins with 0.5 <ratio to 1.5 h <2	783	719	749	704	674
number of proteins with ratio to 1.5 h <0.5	21	40	43	62	87

The Voronoi-like treemap in Figure 37 gives a first overview of the proteomic adaptation pattern of *S. aureus* HG001 when internalized by A549 cells. It is obvious that proteins constituting the large and small ribosomal subunits decreased in levels as well as some pathways of the carbon and amino acid metabolism (Figure 37). Other pathways of the central carbon metabolism such as pentose phosphate pathway or fermentation slightly increased during ongoing time of internalization. However, a more detailed picture on the complex regulation of *S. aureus* proteome was observed by detailed time-resolved analysis as described in the following paragraphs.

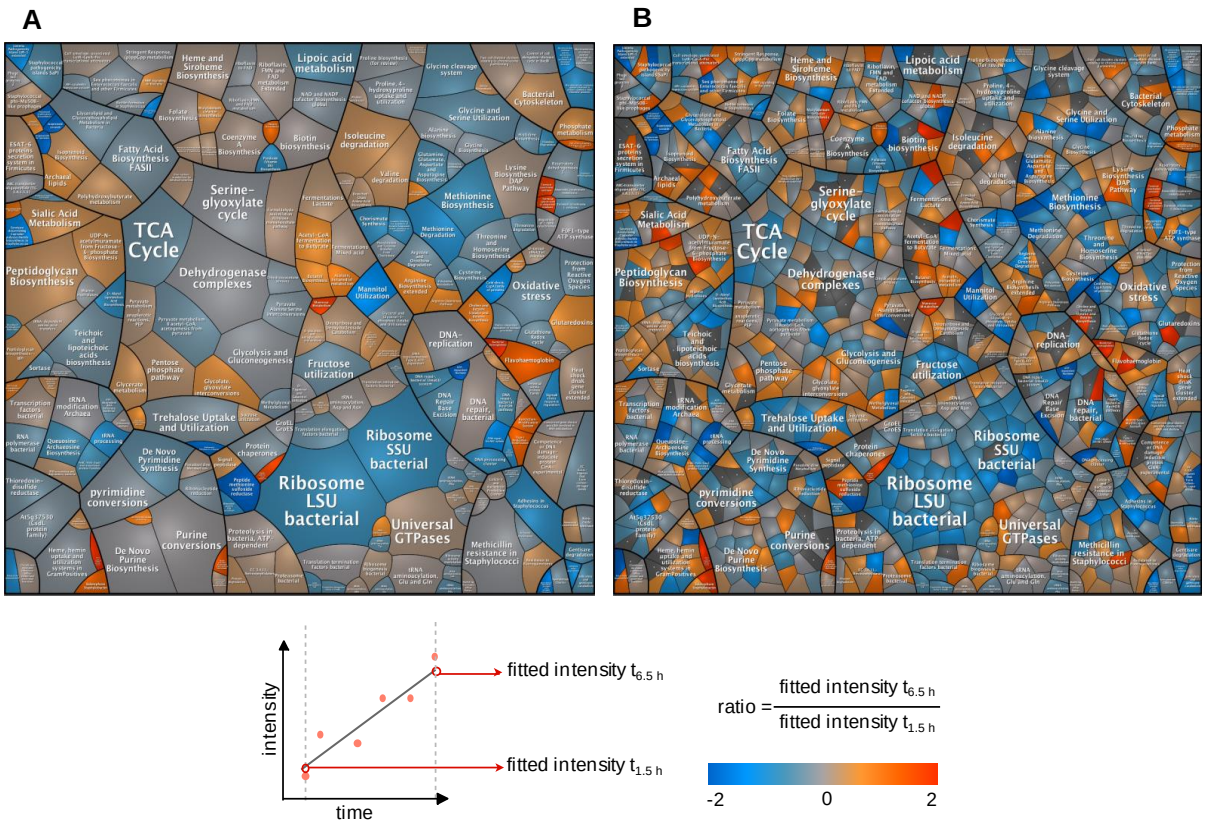

Figure 37. Voronoi-like treemap of functional categories of *S. aureus* HG001. *Ratios (log_2) of trend fitted protein intensities (6.5 h vs. 1.5 h p.i.) are illustrated: (A) mean ratios of the proteins of a pathway cluster; (B) single protein ratios of a pathway cluster. Bluish colors indicate levels which decrease; reddish colors indicate increased amounts of proteins due to internalization effects. Light gray cells indicate proteins, which were not regulated during infection, and cells in dark gray illustrate proteins, which were not detected in this approach. Treemaps are also provided as Supplementary_Material_04_Voronoi-like_treemaps.pdf to allow zooming.*

Adaptation of enzymes involved in growth and metabolism of S. aureus HG001 upon internalization

Different regulation patterns were observed in the initial phase after internalization between 1.5 h and 6.5 h. Time-resolved data of ribosomal proteins, both of the large ribosomal subunit (LSU) and the small ribosomal subunit (SSU), showed a clear reduction in level during infection (Figure 38), which is in agreement with the reduced growth rate inside the host cells.

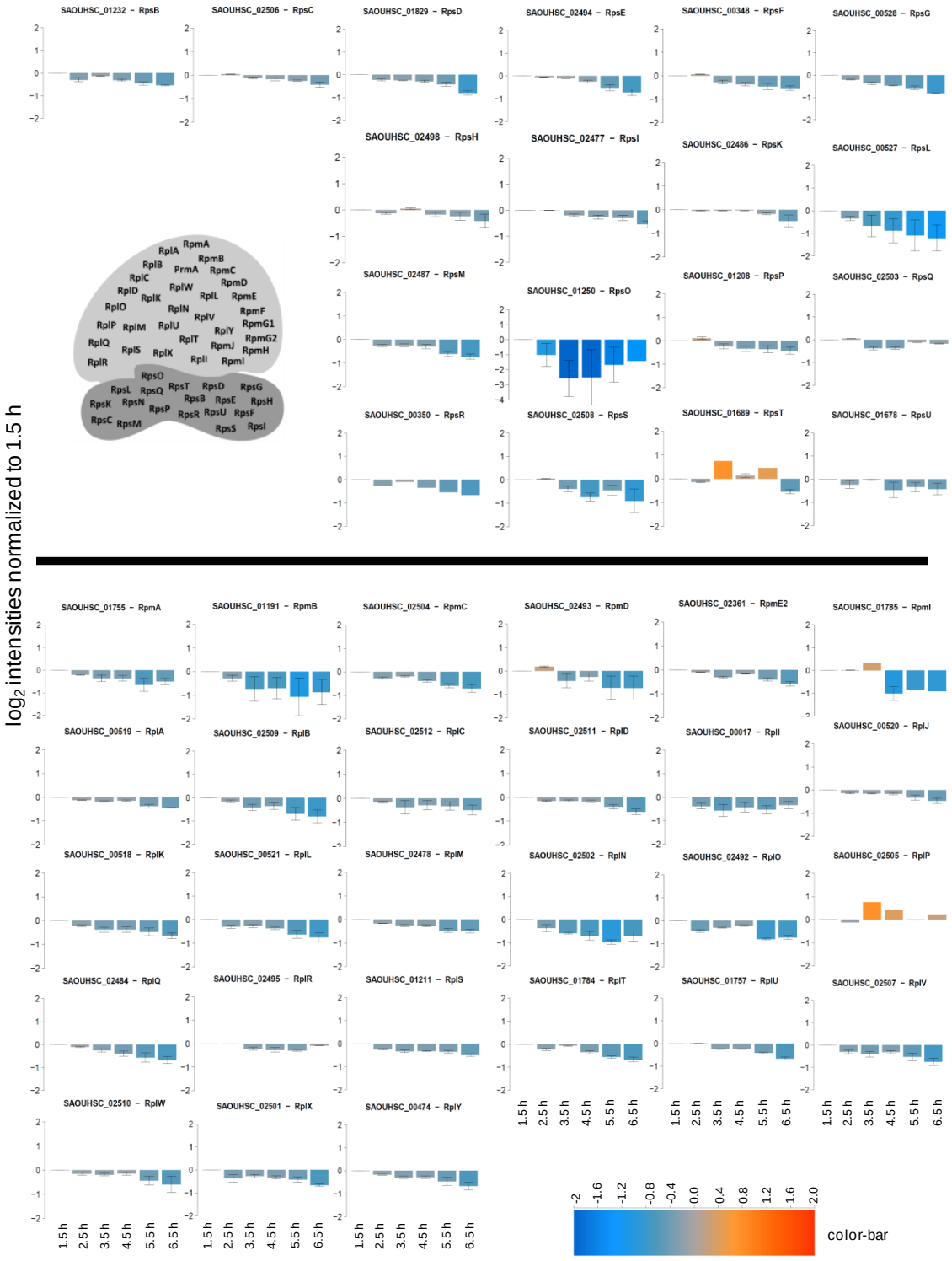

Figure 38. Ribosomal proteins. *Time-course data (median normalized log_2 intensities) of all monitored ribosomal proteins are depicted in the bar charts. Mean results and standard deviations from three BR are displayed. Localization of the ribosomal proteins in the large and small ribosomal subunits is indicated in the gray schematic image.*

Many proteins involved in peptidoglycan synthesis were increased in level with intracellular life time [among others UDP-N-acetylglucosamine 1-carboxyvinyltransferase (MurAB), glycosyltransferase (SgtB), penicillin binding protein 2 (Pbp2)] (Figure 39). The cell wall enzymes MurAB, SgtB and Pbp2 are under VraR control and their induction therefore indicates cell wall stress while internalized.

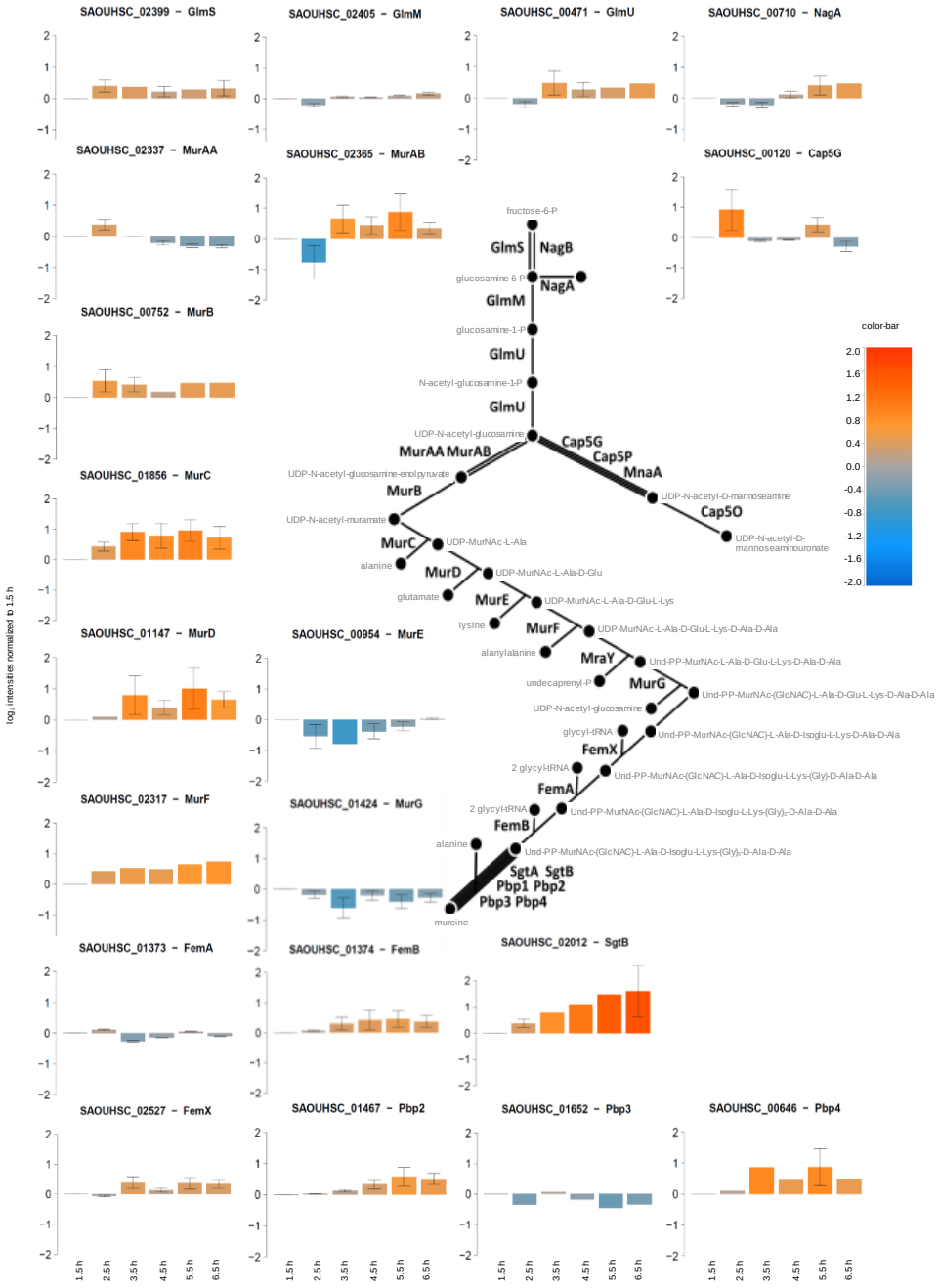

Figure 39. Proteins involved in peptidoglycan synthesis. *Time-course (median normalized log_2 intensities) data for all monitored proteins of this pathway are displayed in the bar charts. Mean results and standard deviations from three BR are depicted. Interactions of the proteins are indicated with the pathway scheme.*

The stringent response is an emergency reaction to nutrient limitation. It is triggered by the intracellular signaling molecule (p)ppGpp and in *S. aureus* by the products of the three genes SAOUHSC_01742, SAOUHSC_00942, and SAOUHSC_02811 which are homologues of genes found in *Bacillus subtilis.* They encode the GTP pyrophosphokinases RSH, RelQ, and RelP, and can thus catalyze (p)ppGpp production. The homologue to RSH was found in decreased amounts after internalization whereas levels of RelP and RelQ increased during later hours of infection (Figure 40A).

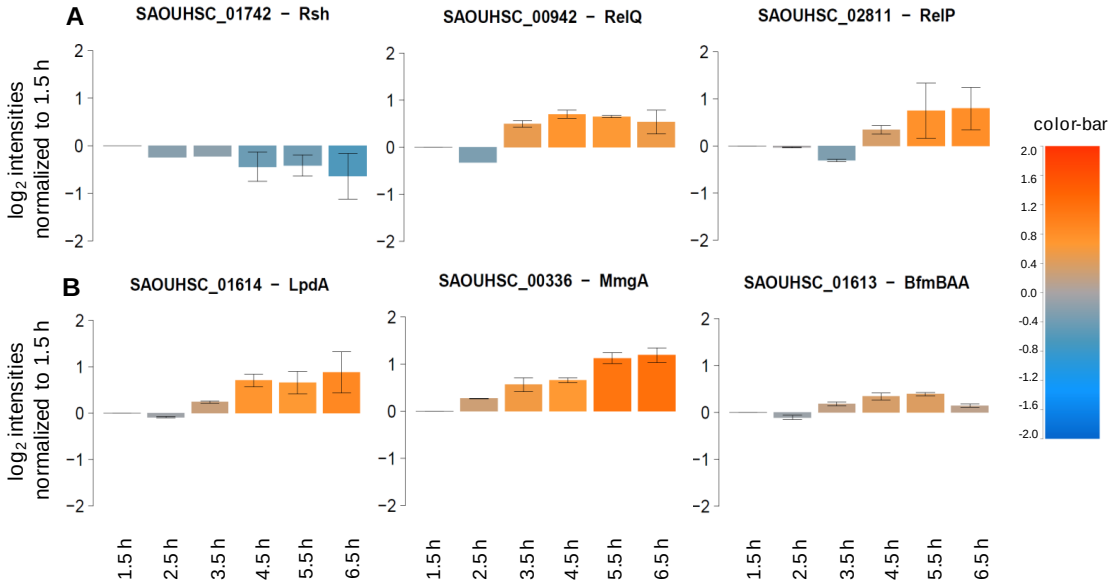

Figure 40. Proteins of the stringent response (A) and those involved in branched-chain amino acid degradation (B). *Time-course data (median normalized log_2 intensities) for selected enzymes are depicted in the bar charts. Mean results and standard deviations from three BR are depicted.*

In addition enzymes involved in the degradation of branched-chain amino acids were detected in increased levels over time (Figure 40B). Intracellular metabolome analysis of A549 cells revealed a concentration of branched-chain amino acids of approximately 3-4 mmol/L at the start of internalization (Figure 36).

Glucose was present inside the human host cell at the time of infection with a concentration of more than 5 mmol/L (Figure 35). Many glycolysis proteins showed increased levels during ongoing internalization [glucokinase (GlcK), phosphoglucomutase (PgcA), glucose-6-phosphate isomerase (Pgi), 6-phosphofructokinase (PfkA), fructose-1,6-bisphosphate aldolase (FdaB)]. Levels of fructose-1,6-bisphosphate aldolase class II (FbaA) and phosphoglyceromutase (Pgm) were hardly altered during internalization. Trends of decreased protein intensities were observed for triose-phosphate isomerase (TpiA) and phosphopyruvate hydratase (Eno). Phosphoglycerate kinase (Pgk) and glyceraldehyde 3-phosphate dehydrogenase (GapA) were induced 2.5 h *p.i.* and subsequently decreased in level (Figure 41).

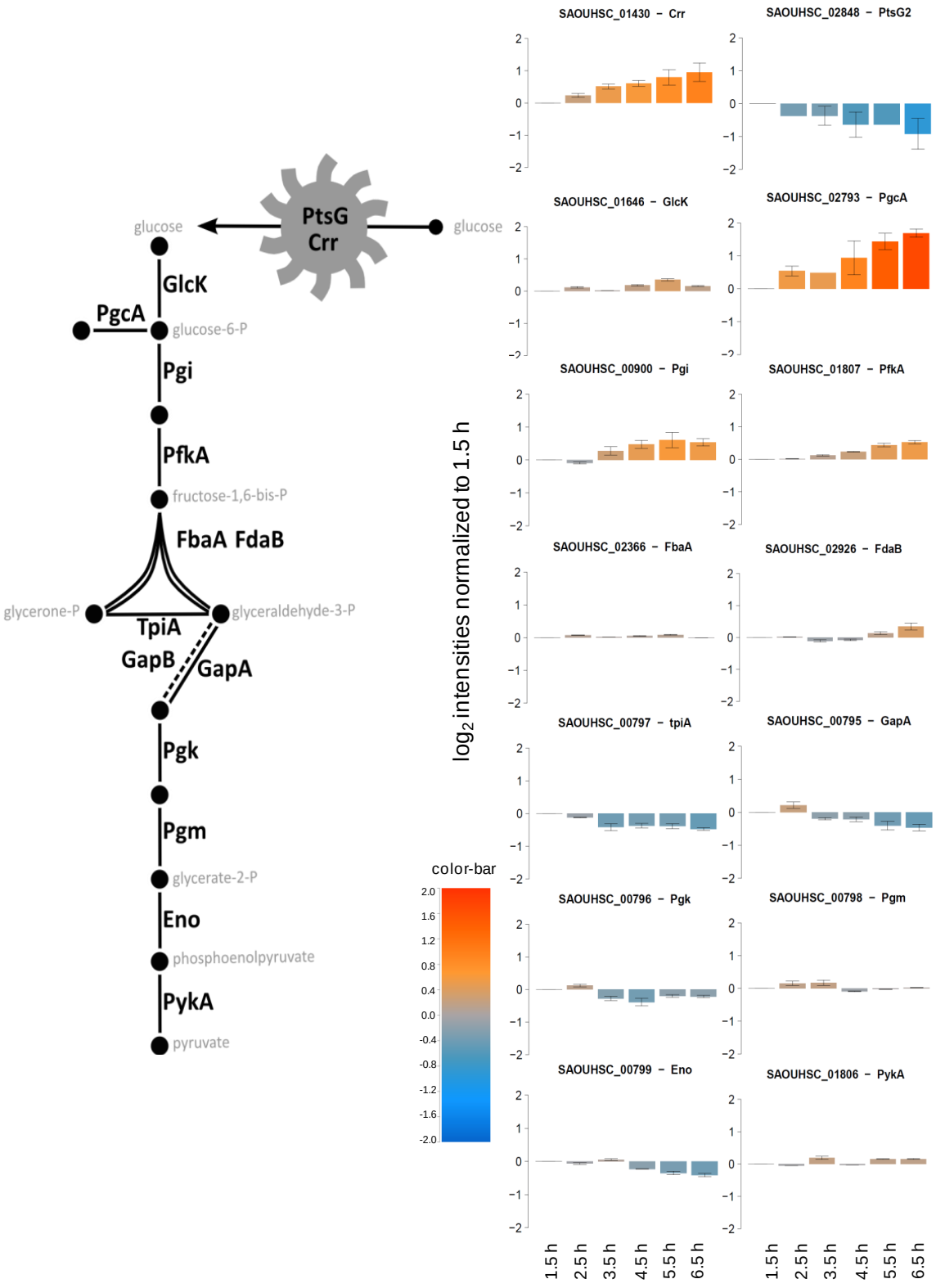

Figure 41. Proteins of the glycolysis. *Time-course data (median normalized log_2 intensities) for the glycolysis enzymes are depicted in the bar charts. Mean results and standard deviations from three BR are displayed. Interactions of the proteins are indicated with the pathway scheme.*

Some proteins of the TCA cycle displayed increased levels during infection [pyruvate carboxylase (PycA), fumarase FumC] but other proteins such as aconitate hydratase (CitB), isocitrate dehydrogenase CitC, succinate dehydrogenase (SdhB), dihydrolipoamide succinyltransferase (SucB and D) or branched-chain alpha-keto acid dehydrogenase (PdhC and D) showed reduced amounts after 6.5 h compared to early points in time (Figure 42).

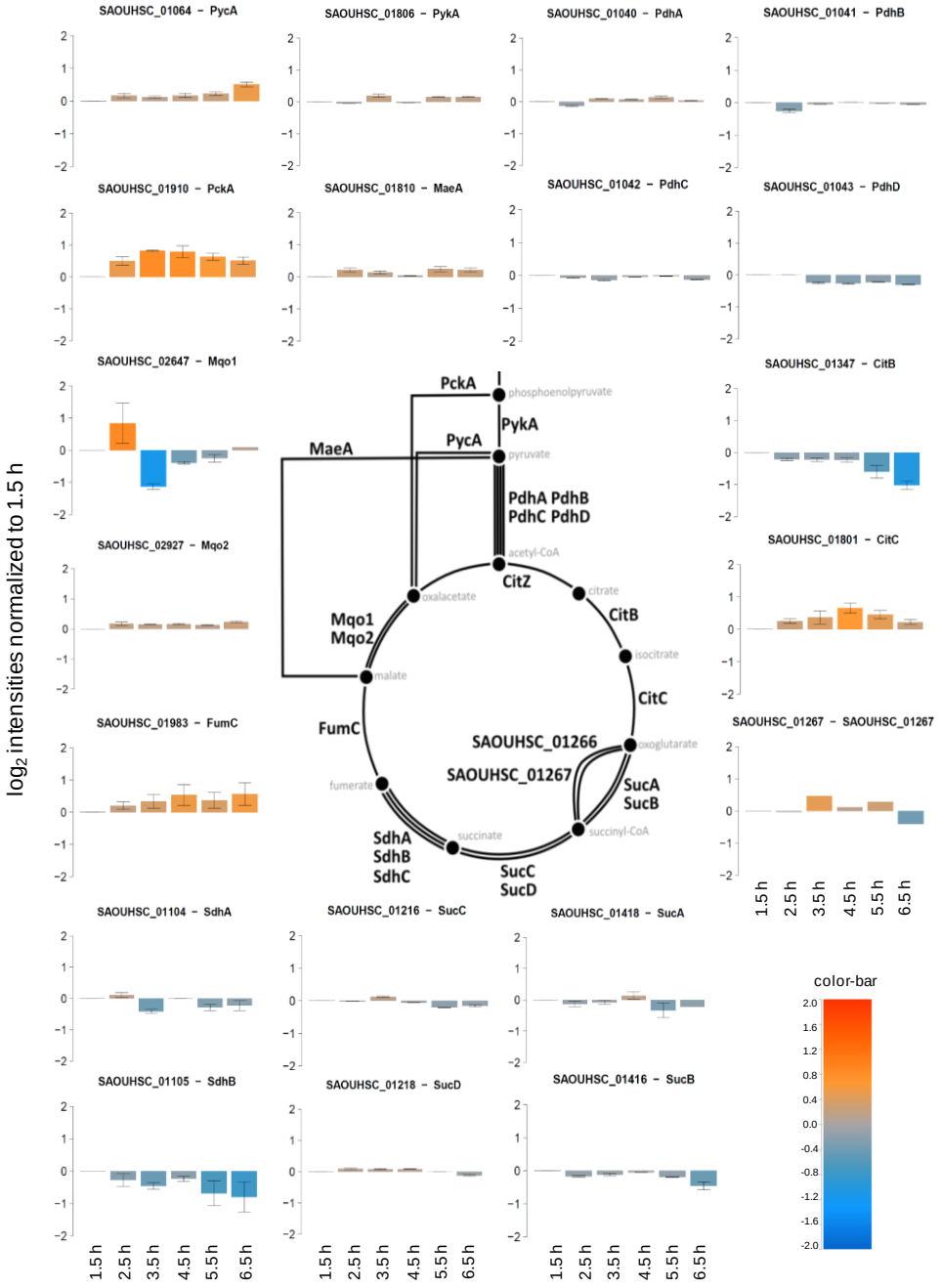

Figure 42. Proteins of the TCA cycle. *Time-course data (median normalized log_2 intensities) for the TCA enzymes are depicted in the bar charts. Mean results and standard deviations from three BR are displayed. Interactions of the proteins are indicated with the pathway scheme.*

In contrast, proteins of the pentose phosphate pathway such as glucose-6-phosphate 1-dehydrogenase (Zwf), putative transaldolase (Tal), transketolase (Tkt) or phosphoglucomutase (PgcA) were found with higher amounts during time course of internalization (Figure 43).

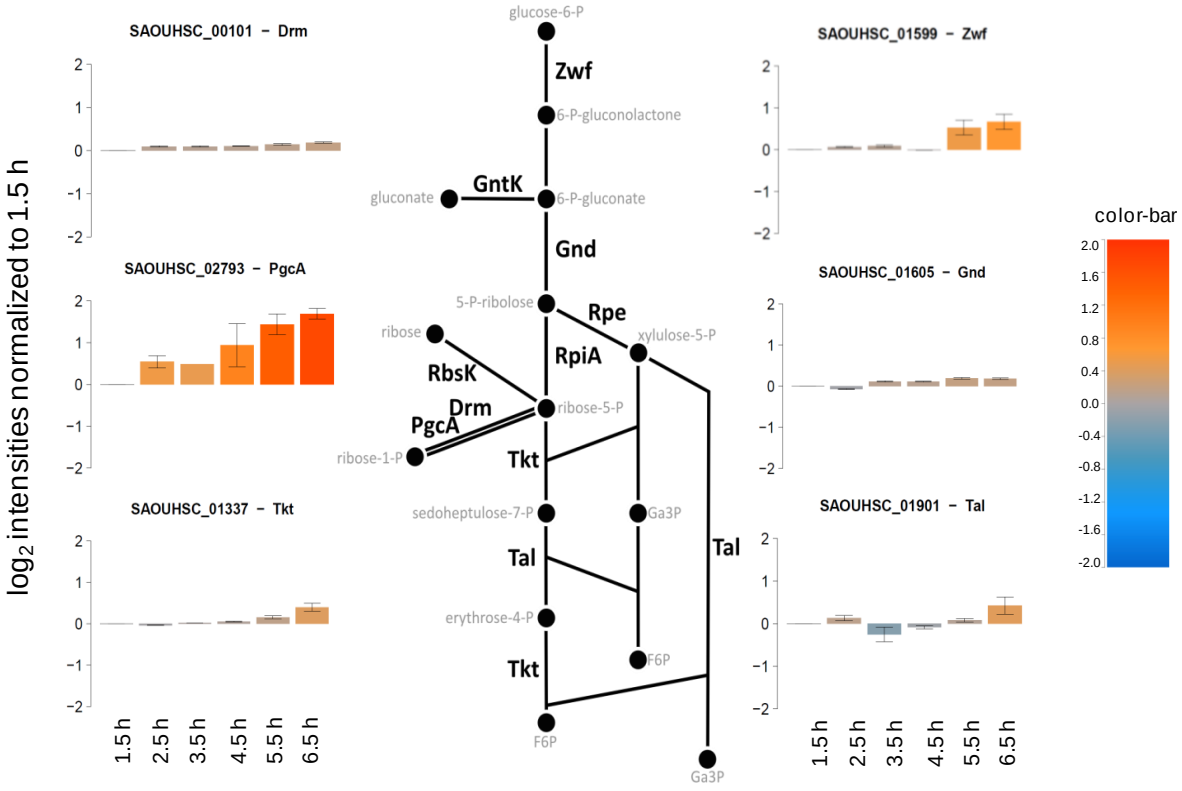

Figure 43. Proteins of the pentose phosphate pathway. *Time-course data (median normalized log_2 intensities) for the monitored enzymes are depicted in the bar charts. Mean results and standard deviations from three BR are displayed. Interactions of the proteins are indicated with the pathway scheme.*

Similar to glycolysis the fermentation proteins such as L-lactate dehydrogenase (LctE), acetoin reductase (ButA) or aldehyde dehydrogenase (AldH) were found to slightly increase in level during internalization (Figure 44), an indication of oxygen-limited microaerobic conditions.

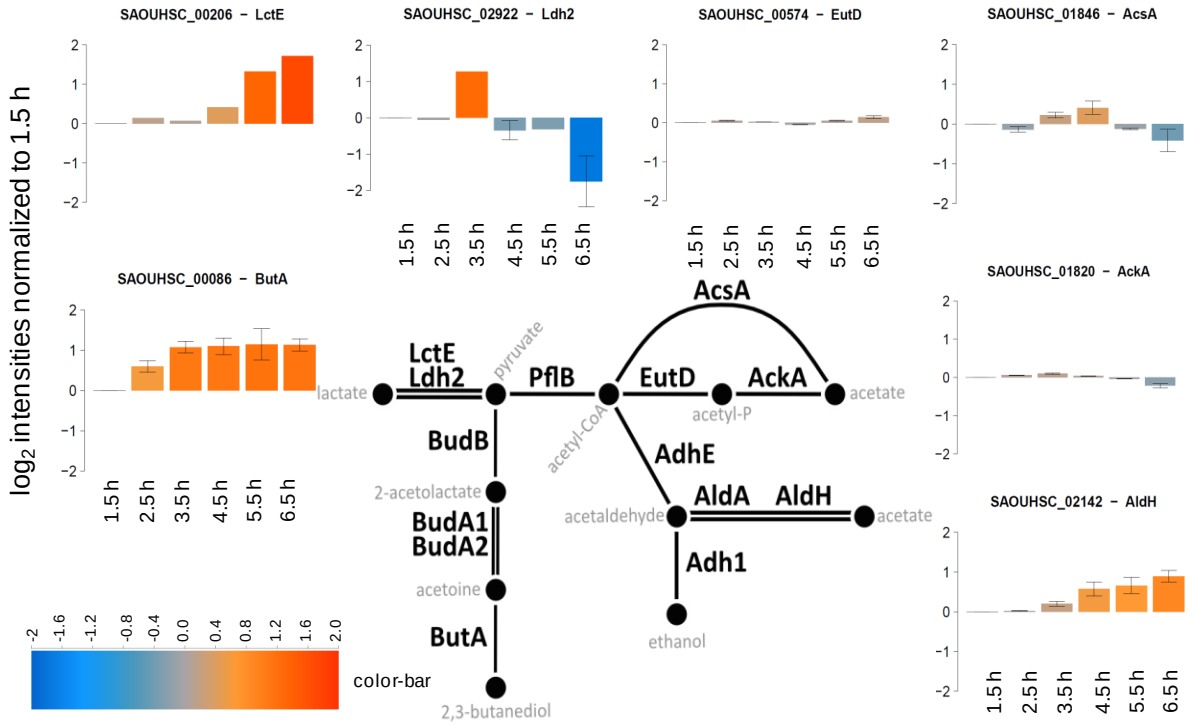

Figure 44. Fermentation proteins. *Time-course data (median normalized log_2 intensities) for the monitored enzymes are depicted in the bar charts. Mean results and standard deviations from three BR are displayed. Interactions of the proteins are indicated with the pathway scheme.*

A further hint of this limited oxygen supply is the increased level of the cytochrome d ubiquinol oxidase CydA, while the main oxidase QoxAB was decreased in amount over time (Figure 45).

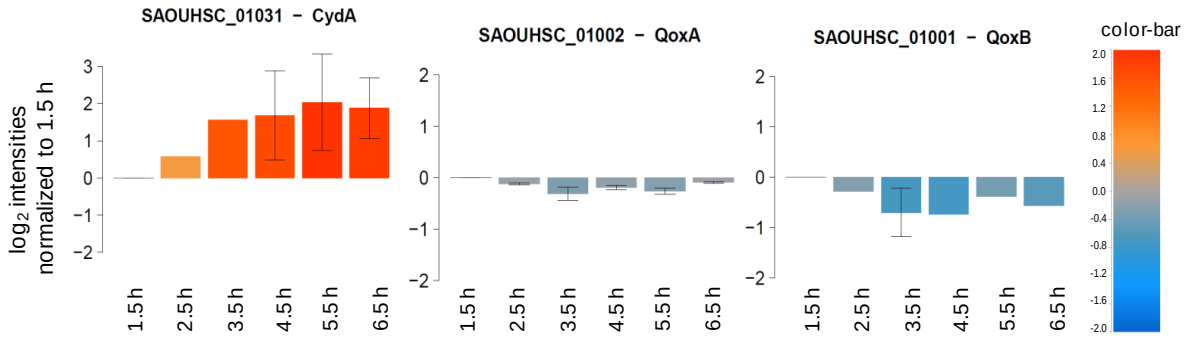

Figure 45. *S. aureus* oxidases. *Time-course data (median normalized log_2 intensities) for the monitored enzymes are depicted in the bar charts. Mean results and standard deviations from three BR are displayed. Interactions of the proteins are indicated with the pathway scheme.*

Regulation of selected virulence proteins during internalization

Besides altered levels of metabolic enzymes many proteins with a direct role in virulence were likewise differentially abundant during adaptation to the intracellular environment. Proteins involved in the adhesion of *S. aureus* to host cells such as protein A (spa), clumping factor A (ClfA), and the SdrD protein decreased in level during the time course (Figure 46), probably since adhesion was no longer needed.

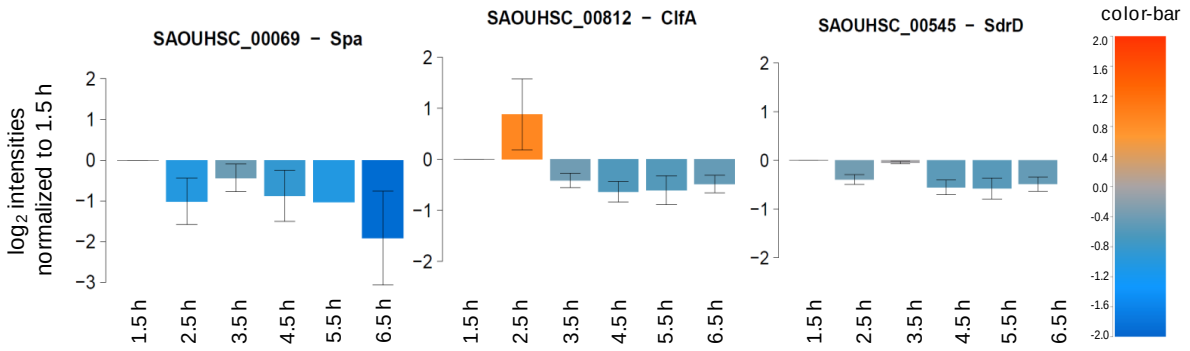

Figure 46. *S. aureus* proteins involved in adhesion. *Time-course data (median normalized log_2 intensities) for the monitored enzymes are depicted in the bar charts. Mean results and standard deviations from three BR are displayed. Interactions of the proteins are indicated with the pathway scheme.*

In addition, enzymes involved in nitric oxide stress adaption (flavohaemoglobins) were increased in level over the time-course. The heme-binding flavohaemoglobin SAOUHSC_02430, Rrf2 family protein SAOUHSC_01732, and the nitric oxide reductase activation protein SAOUHSC_01413 were slightly increased over time. The nitric oxide dioxygenase Hmp (SAOUHSC_00204) was considerably increased in level. After 6.5 h the level of this protein was about five times higher compared to the first sampling time after 1.5 h of internalization (Figure 47).

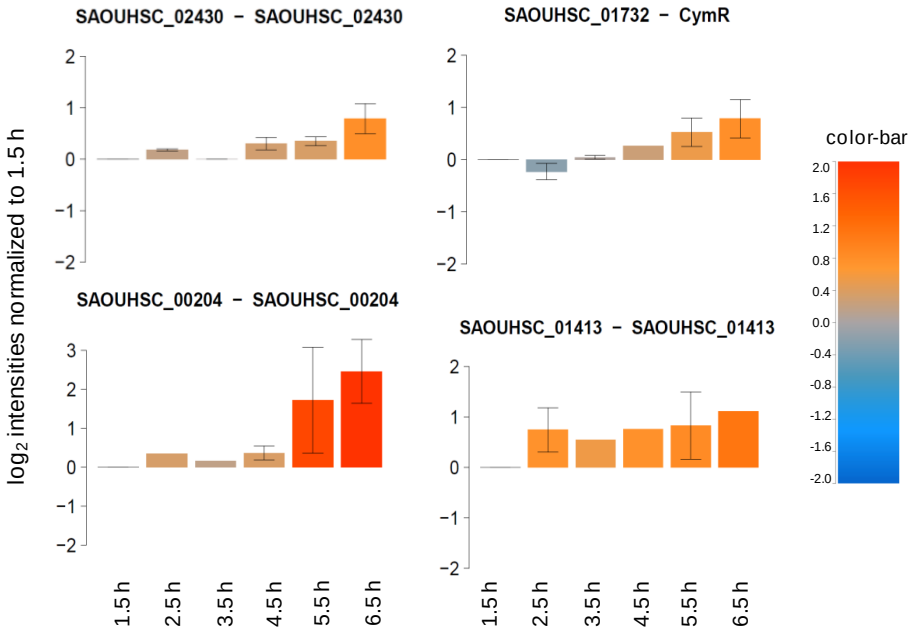

Figure 47. Flavohaemoglobins. *Time-course data (median normalized log_2 intensities) for the monitored enzymes are depicted in the bar charts. Results from three BR are presented.*

Further, *S. aureus* needs to acquire iron from the host. Enzymes contributing to iron acquisition and metabolism showed a general increase in abundance during ongoing time course, due to a limited amount of intracellular iron in the host. In detail, heme degrading monooxygenase (IsdI), SAOUHSC_02430 involved in iron binding, iron uptake transporter SAOUHSC_00749, and iron transporter EfeM were increased over time (Figure 48).

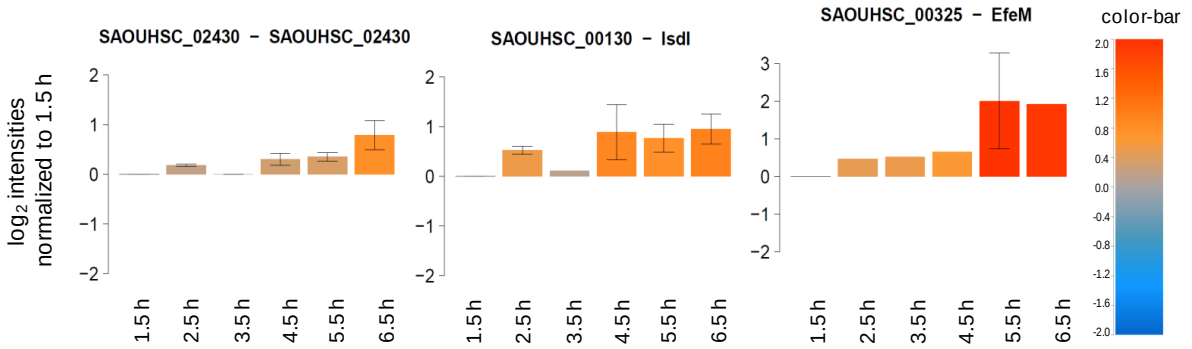

Figure 48. Proteins involved in iron acquisition. *Time-course data (median normalized log_2 intensities) for the monitored enzymes are depicted in the bar charts. Mean results and standard deviations from three BR are displayed. Interactions of the proteins are indicated with the pathway scheme.*

Quantitative information on further detected staphylococcal proteins is provided as Supplementary_Material_Table_08_S_aureus_internalized_by_A549.xlsx.

Comparative proteome analysis of *S. aureus* HG001 internalized by different cell lines

Experimental setup and data analysis

After comprehensive investigation of time-resolved adaptation of *S. aureus* HG001 to internalization by A549 cells, the impact of the host cell line on the proteome changes of internalized bacteria was analyzed. Three different non-professional phagocytic cell lines were infected with *S. aureus* HG001 pMV158GFP in order to find protein groups which are regulated commonly after internalization and those which are specifically abundant depending on the host cell line. The results of this project have already been published (Surmann et al., 2014b) and are summarized in the following section. In this study, the human alveolar epithelial A549 cell line, the human bronchial epithelial S9 cell line, and, additionally, the human embryonic kidney HEK 293 cell line were infected with *S. aureus* HG001 pMV158GFP. After 2.5 h and 6.5 h the *S. aureus* cells were enriched from host cell debris prior to proteome analysis. These two points in time were chosen as representative sampling points according to the intracellular growth (Figure 30). As early sampling point 2.5 h *p.i.* was chosen when intracellular growth inside A549 and S9 cells already started. The 1.5 h time point is not as reproducible during cell sorting as the 2.5 h time point because the internalization was already stabilized at the later point in time. At the late point in time (6.5 h *p.i.*) bacteria were replicating inside HEK 293 cells as well. Data of internalized bacteria were compared to the proteome of non-adherent control bacteria (compare section “Sampling of non-adherent bacteria as a control for proteome analysis upon infection”). These findings of regulated protein abundance were again supported by data of the metabolite pool present inside all three host cell line prior to infection (Figure 49).

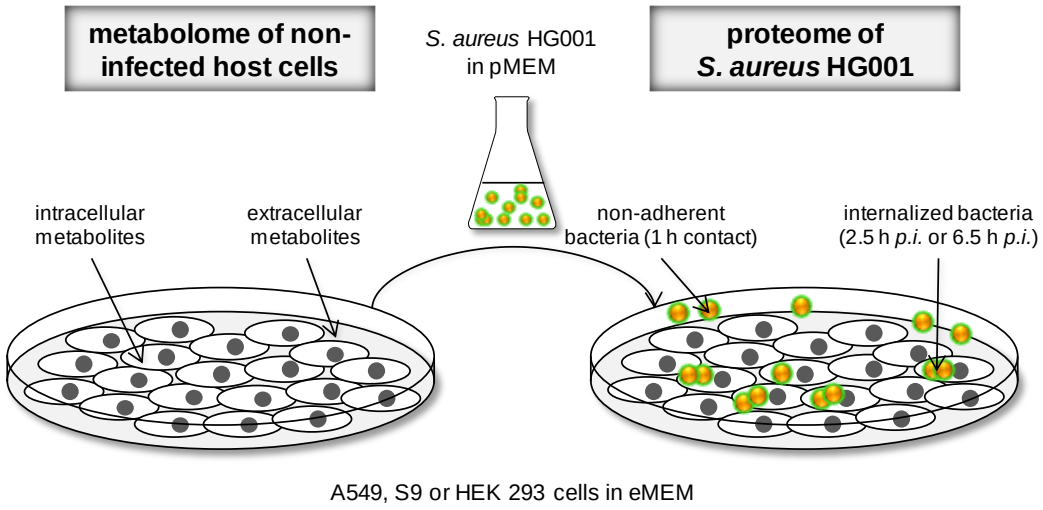

Figure 49. Experimental setup comparing internalization of *S. aureus* HG001 pMV158GFP by different host cell lines. *The metabolome of non-infected human cells and the cell culture supernatant prior to infection was recorded. GFP-expressing bacteria were cultivated in pMEM until OD_{600} 0.4 (exponential growth). Human cell lines (S9, A549, and HEK 293) were cultivated in eMEM and infected with S. aureus HG001 pMV158GFP cells. The proteome of the non-adherent and the internalized bacteria was investigated after cell sorting via flow cytometry.*

Two million bacteria per replicate were sorted by flow cytometry and subjected to nanoLC-MS/MS analysis. Applying the optimized data analysis pipeline combining database search and spectral library matching (compare section “Improved analysis of proteome data from internalized bacteria”) almost 50% of the proteins listed in the database (2,892) were identified and quantified. More precisely, first a classical COMET (Eng et al., 2013) search using a decoy database of *S. aureus HG001* combined with a human UniProt database identified 1,393 staphylococcal proteins in total. An additional search against a spectral library and the reSpect algorithm resulted in 1,484 proteins finally identified with an FDR less than 0.01. Out of them, 1,450 proteins could be quantified with unique peptides in at least two of three replicates within one cell line for final consideration. 1,263 proteins were found and quantified in all datasets. Very few proteins were detected only in samples of one or two cell lines. In total, 1,443 proteins were detected and quantified over all cell lines in at least two of three replicates per cell line (Figure 50).

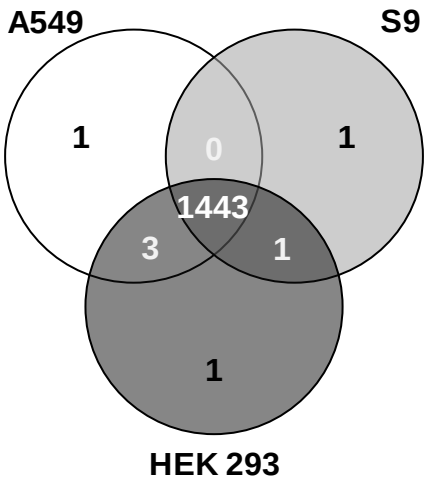

Figure 50. Venn diagram of numbers of quantified proteins in all three cell lines and selected subgroups.

Global proteome response of S. aureus HG001 after internalization by different host cells

PCA of median-normalized data of all quantified proteins was performed to obtain a first overview on general proteomic differences due to different host cell types (Figure 51). A clear separation of the non-adherent control and the two internalized sampling points was detected. The non-adherent control was very similar for all cell lines. After 2.5 h the samples of all three host models showed more variations. After 6.5 h of internalization the proteome pattern of *S. aureus* HG001 internalized by HEK 293 cells differed most distinctly from S9 and A549 cells. Thus, this gives a hint of different behavior of *S. aureus* inside the embryonic kidney cells compared to the two lung epithelial cells.

A general view on regulation is provided in Table 11. The numbers of regulated proteins after internalization compared to the non-adherent control are displayed. Most proteins were not regulated after internalization. Furthermore, it is obvious that more proteins were found in increased levels than in decreased levels after internalization. Most proteins with increased levels were found 2.5 h *p.i.* in bacteria internalized by HEK 293 cells. In general the total numbers of regulated proteins did not differ much between the used host models used (Table 11).

Table 11. Numbers of differentially regulated bacterial proteins after internalization by A549, S9 or HEK 293 cells 2.5 h and 6.5 h after infection. *Increased (ratio >2) and decreased (ratio <0.5) trend in levels between the internalized samples and non-adherent control (non-ad) are displayed. In total, 1,450 proteins were identified and quantified over any of the cell lines in three BR.*

	A549 2.5 h /non-ad	**A549 6.5 h /non-ad**	**S9 2.5 h /non-ad**	**S9 6.5 h /non-ad**	**HEK 293 2.5 h /non-ad**	**HEK 293 6.5 h /non-ad**
number of proteins with ratio to non-ad >2	348	284	326	341	419	318
number of proteins with 0.5 <ratio to non-ad <2	1,020	1,058	1,058	987	978	1,008
number of proteins with ratio to non-ad <0.5	82	108	66	122	53	124

A first glance which pathways might be affected differently is displayed in Voronoi-like treemaps (Bernhardt et al., 2013, Surmann et al., 2014b). Ratios between 2.5 h *p.i. vs.* non-adherent control (Figure 52) as well as 6.5 h *p.i. vs.* non-adherent control (Figure 53) per host model are represented in a color code for each protein (red-increased levels upon internalization, blue-decreased levels upon internalization). Single proteins are assembled to pathways. Once more, protein patterns of internalized *S. aureus* HG001 are more similar inside A549 and S9 cells compared to the HEK 293 cells. For example, protein biosynthesis is more reduced 2.5 h *p.i.* in *S. aureus* enriched from the lung epithelial host cells compared to control bacteria than from the from HEK 293 cells (Figure 52). *Vice versa* after 6.5 h proteins of the bacterial central carbon metabolism were found to be more increased compared to the non-adherent control inside A549 and S9 cells than in the host model HEK 293 cells (Figure 53). In the following sections, specific physiological adaptions are described on pathway level. Therefore, $\log_2$ intensities of the proteins belonging to these pathways were plotted in box-plots.

Mostly, the third level of the functional categories from SEED (Supplementary_Material_Table_09_the_SEED_functional_categories_S_aureus_HG001.xlsx) was used for physiological interpretation of proteome data. This third level combines several proteins that participate in the same functional pathways and is, thus, more robust than analysis at the level of individual proteins. In addition to the pathway name, also the number of related proteins which were identified in this study (x) and the total number of protein assigned to the pathway (y) was given in the form (x of y).

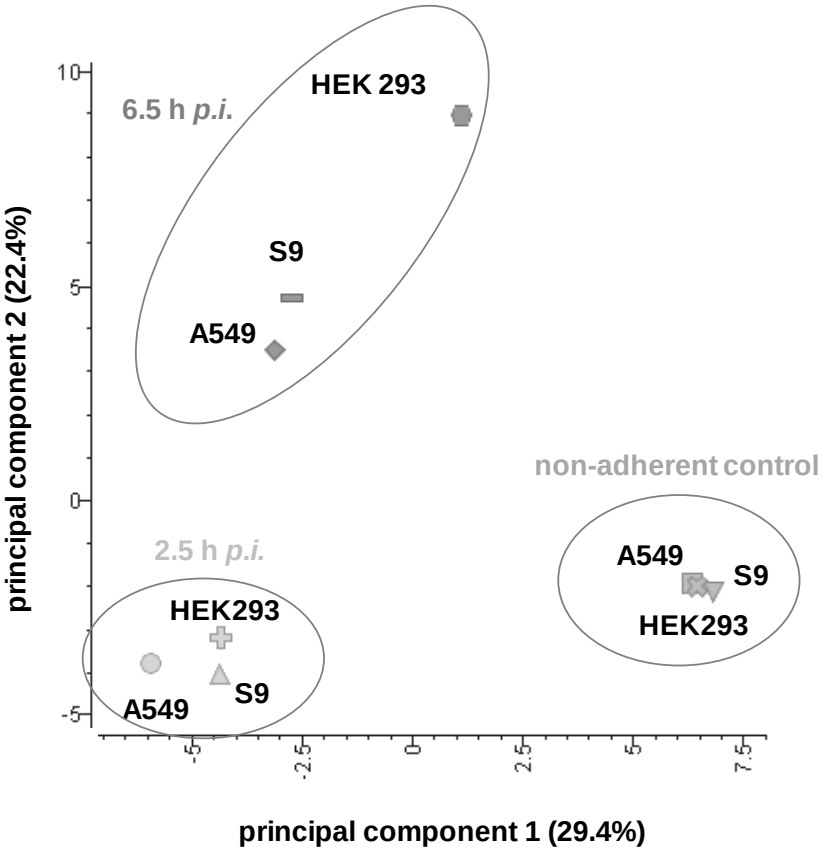

Figure 51. Principal component analysis of *S. aureus* HG001 pMV158GFP proteins. *The variance of the data was influenced by the cell lines (component 1, 29.4% variance) as well as the different treatment groups (component 2, 22.4% variance). Only proteins with quantitative data for all samples, (median normalized AUC data, probability >0.8) were considered for the analysis. Average values from three BR were calculated to perform the PCA (Surmann et al., 2014b).*

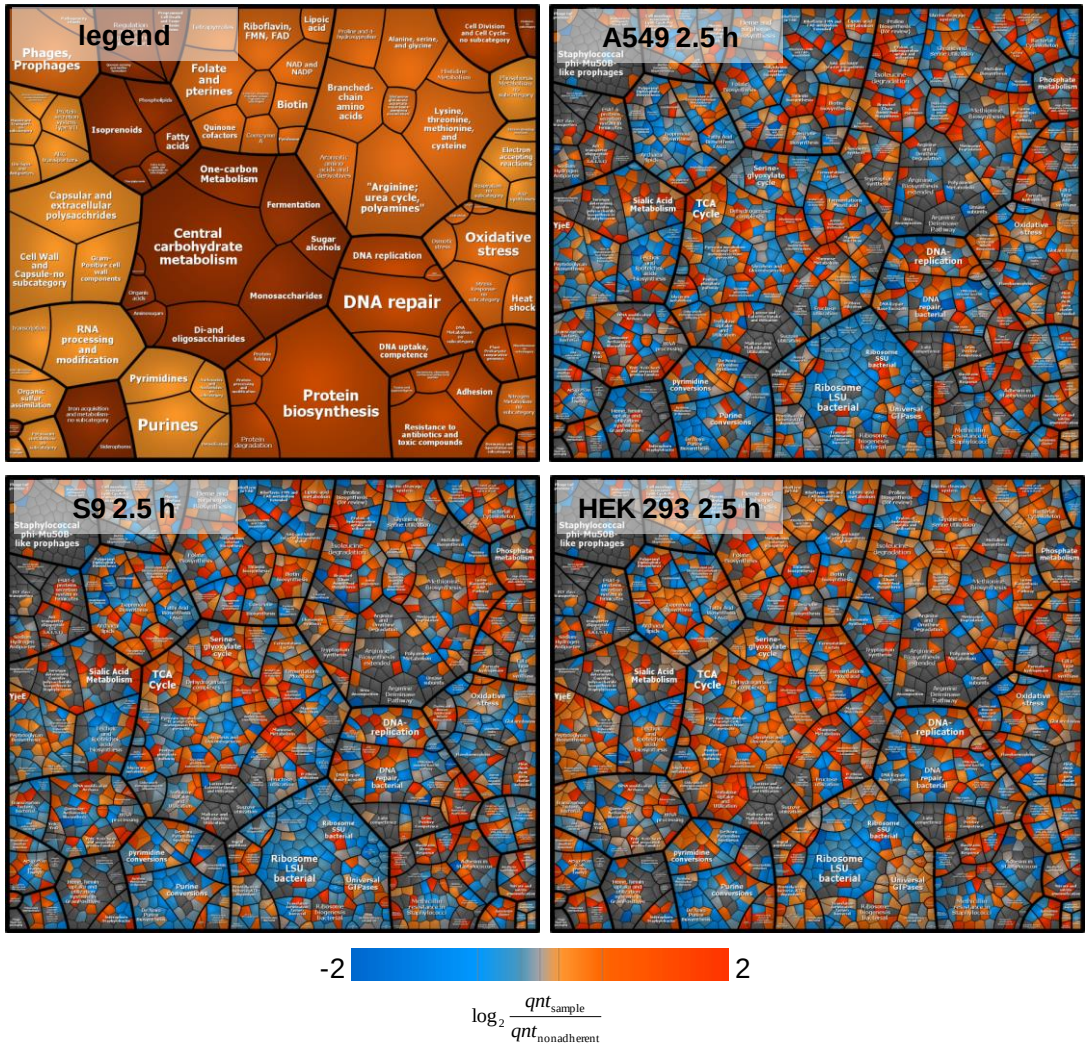

Figure 52. Voronoi-like treemap analysis of *S. aureus* HG001 proteins 2.5 h after internalization. *Ratios from intensity values 2.5 h p.i. compared to the non-adherent control are depicted. All pictures represent data on protein level clustered by pathways. Blue spots indicate lower levels in the internalized bacteria compared to the non-adherent control; red colors represent higher levels of proteins in response to internalization compared to the non-adherent control. Average values from three independent biological samples are displayed (Surmann et al., 2014b). Treemaps are also provided as Supplementary_Material_04_Voronoi-like_treemaps.pdf to allow zooming.*

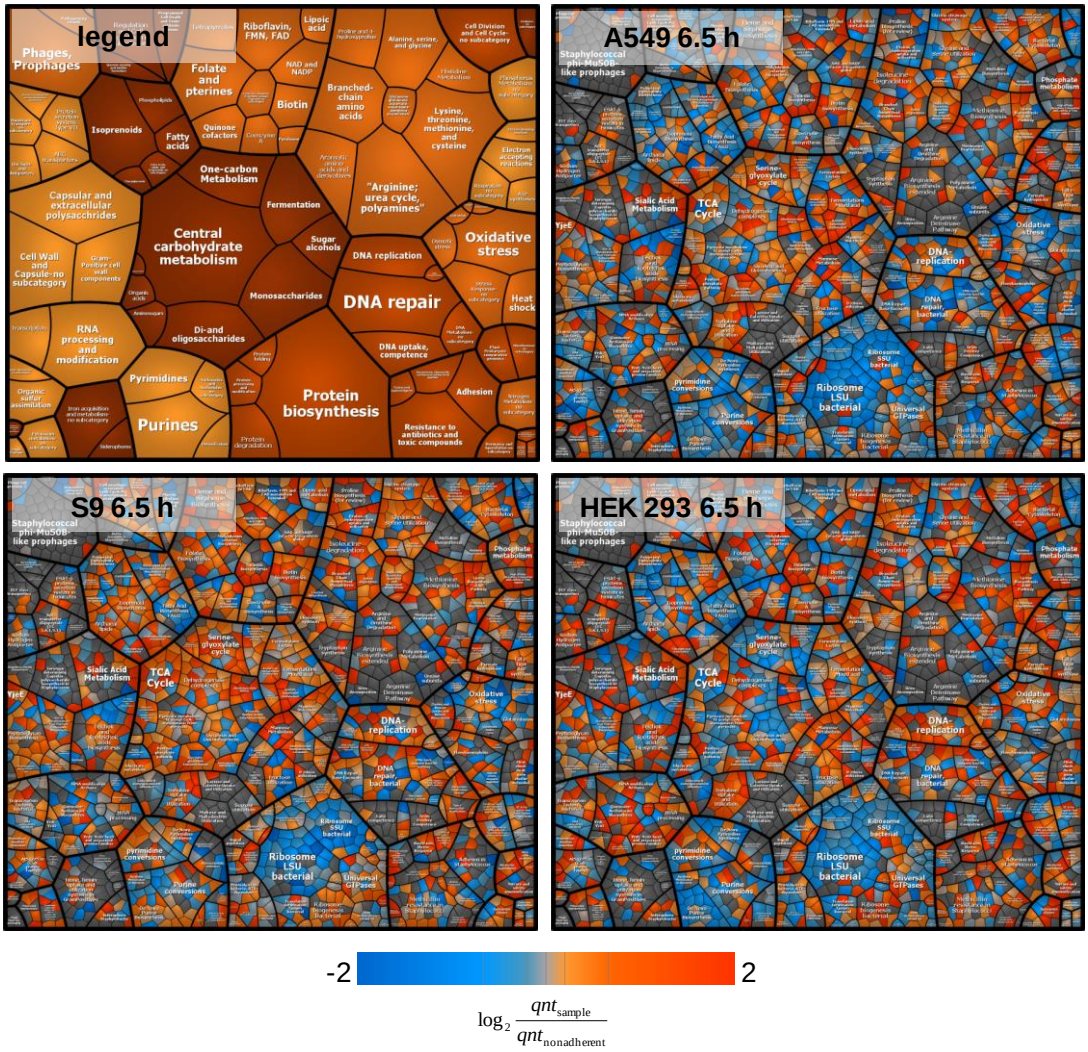

Figure 53. Voronoi-like treemap analysis of *S. aureus* HG001 proteins 6.5 h after internalization. *Ratios from intensity values 6.5 h p.i. compared to the non-adherent control are depicted. All pictures represent data on protein level clustered by pathways. Blue spots indicate lower levels in the internalized bacteria compared to the non-adherent control; red colors represent higher levels of proteins in response to internalization compared to the non-adherent control. Average values from three independent biological samples are displayed (Surmann et al., 2014b). Treemaps are also provided as Supplementary_Material_04_Voronoi-like_treemaps.pdf to allow zooming.*

Commonly regulated proteins of S. aureus HG001 after internalization by three different host cell lines

Staphylococcal proteins of many pathways were similarly regulated upon internalization by three different cell lines. Three general regulation patterns were distinguished: pathways with decreasing protein abundance levels directly after internalization, pathways with increased protein amount after internalization compared to the non-adherent control, and specific regulation patterns between 2.5 h and 6.5 h after internalization.

In agreement with the probably decreased intracellular growth rate of *S. aureus* HG001 pMV158GFP after internalization compared to growth in medium alone, decreased levels of proteins composing the large (ribosome LSU bacterial, 29 of 35) and small (ribosome SSU bacterial, 20 of 21) subunit of the ribosome were observed during the first 6.5 h of internalization into all three cell lines (Figure 54). Furthermore, proteins involved in *de novo* purine biosynthesis (15 of 15) and ribonucleotide reduction (4 of 7) were also decreased in level (Figure 54). The level of cold shock proteins was also commonly reduced after internalization compared to that in non-adherent control cells. Interestingly, the level of components of the cytochrome C oxidase Qox (3 of 5) was also reduced in internalized bacteria *versus* the non-adherent control (Figure 54). In contrary, the level of terminal cytochrome d ubiquinol oxidases (3 of 5) was increased (Figure 55). Also other staphylococcal pathways were induced inside all three host cell models as *S. aureus* needed to adapt to the new environment (Figure 55). Commonly increased levels were monitored for example in biosynthesis of some amino acids, such as lysine (9 of 11) and arginine (5 of 14). However, intra- and extracellular lysine concentrations were similar at the starting point of infection (Figure 33, Figure 36). Commonly increased protein levels for all three internalization models were further measured for flavohaemoglobins (8 of 13), peptide methionine sulfoxide reductases (3 of 4), and bacitracin stress response (5 of 8). The same was true for proteins involved in the colicin V and bacteriocin production clusters (4 of 5) and choline and betaine uptake and betaine biosynthesis (7 of 11). Additionally, proteins of the functional group “ESAT-6 protein secretion system in Firmicutes” (6 of 17) were increased in level upon internalization (Figure 55). These selected pathways show clearest similarities within the three host model. Also other staphylococcal proteins and pathways were regulated commonly (Supplementary_Material_Table_04_S_aureus_proteins_quantified_from_infected_celllines.xlsx).

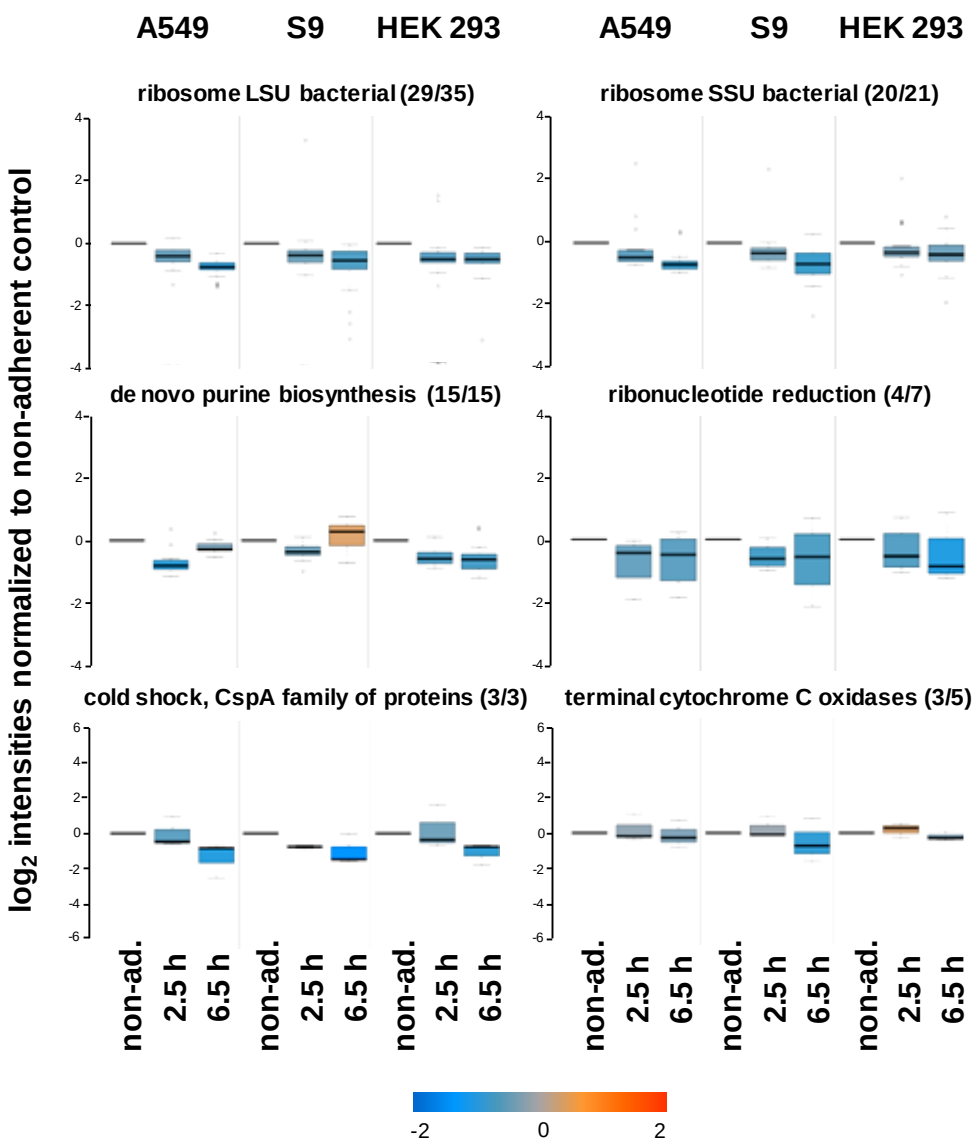

Figure 54. Protein groups displaying reduced levels after internalization by all three cell lines. *Mean values and standard deviations of median-normalized log_2 intensities from three BR each for non-adherent bacteria as well as 2.5 h and 6.5 h p.i. are represented by the black line and the whiskers, the colored boxes represent quartiles. Blue spots indicate lower levels in the internalized bacteria compared to the non-adherent control, red colors represent higher levels of proteins in response to internalization compared to the non-adherent control (Surmann et al., 2014b).*

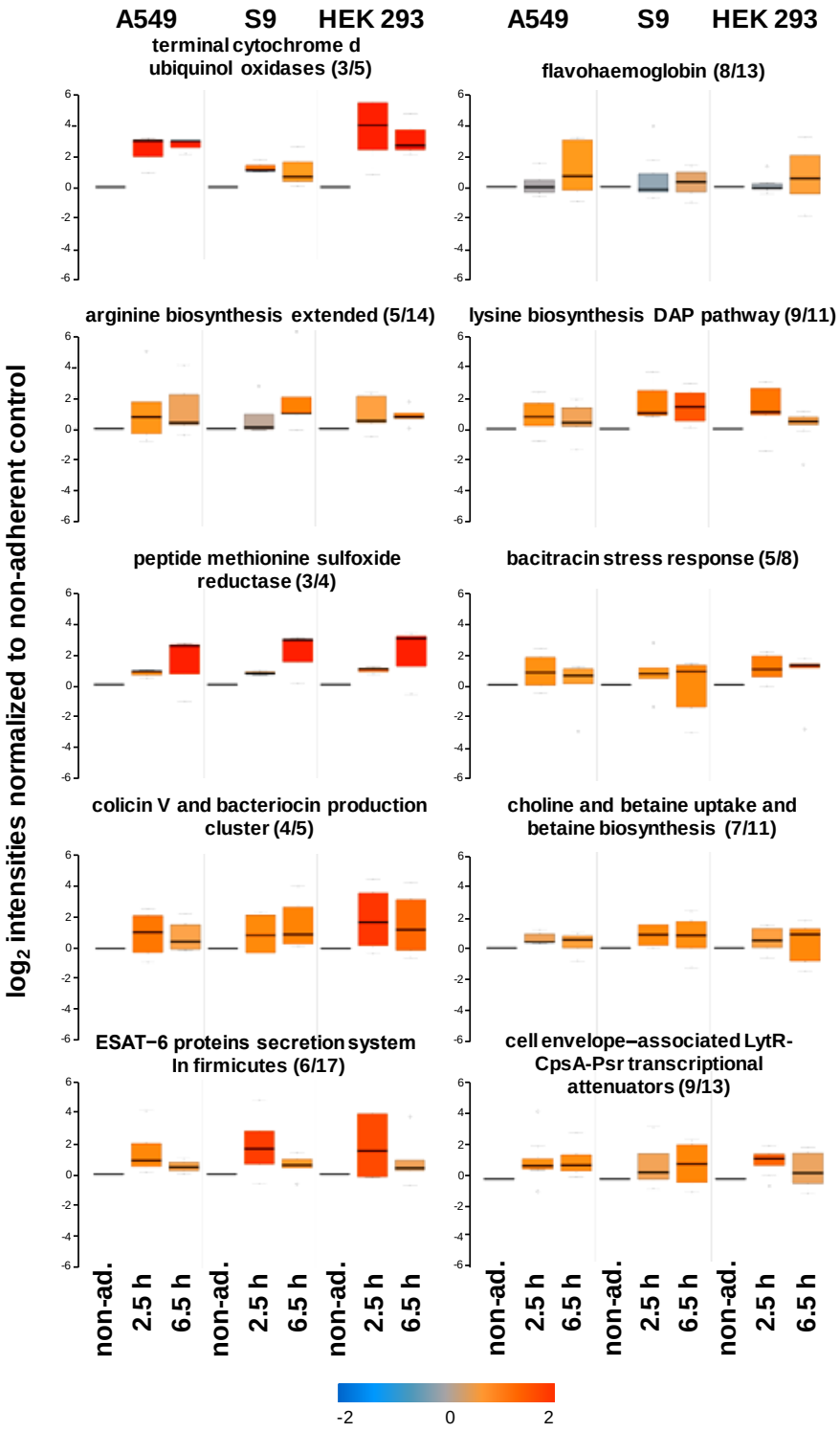

Figure 55. Protein groups displaying increased levels after internalization by all three cell lines. *Mean values and standard deviations of median-normalized log_2 intensities from three BR each for non-adherent bacteria as well as 2.5 h and 6.5 h p.i. are represented by the black line and the whiskers, the colored boxes represent quartiles. Blue spots indicate lower levels in the internalized bacteria compared to the non-adherent control; red colors represent higher levels of proteins in response to internalization compared to the non-adherent control (Surmann et al., 2014b)*

SigB is an important regulator of many *S. aureus* genes with impact on virulence and known to be activated upon internalization by S9 cells (Pförtner et al., 2014). In addition levels of six proteins which were clearly shown to be regulated by SigB were observed on protein level. Besides slight differences in particular protein patterns, most of these proteins [alkaline shock protein 23 (Asp23), putative septation protein (SpoVG), clumping factor A (ClfA), ATP-dependent Clp protease ATP-binding subunit (ClpL), and general stress protein SAOUHSC_02665] were found increased in level 2.5 h *p.i.* compared to the non-adherent control but decreased 6.5 h after infection. The increased level of ClpL was even maintained after 6.5 h. Only protein YfkM was found in decreased levels in internalized samples at both points in time after internalization (Figure 56).

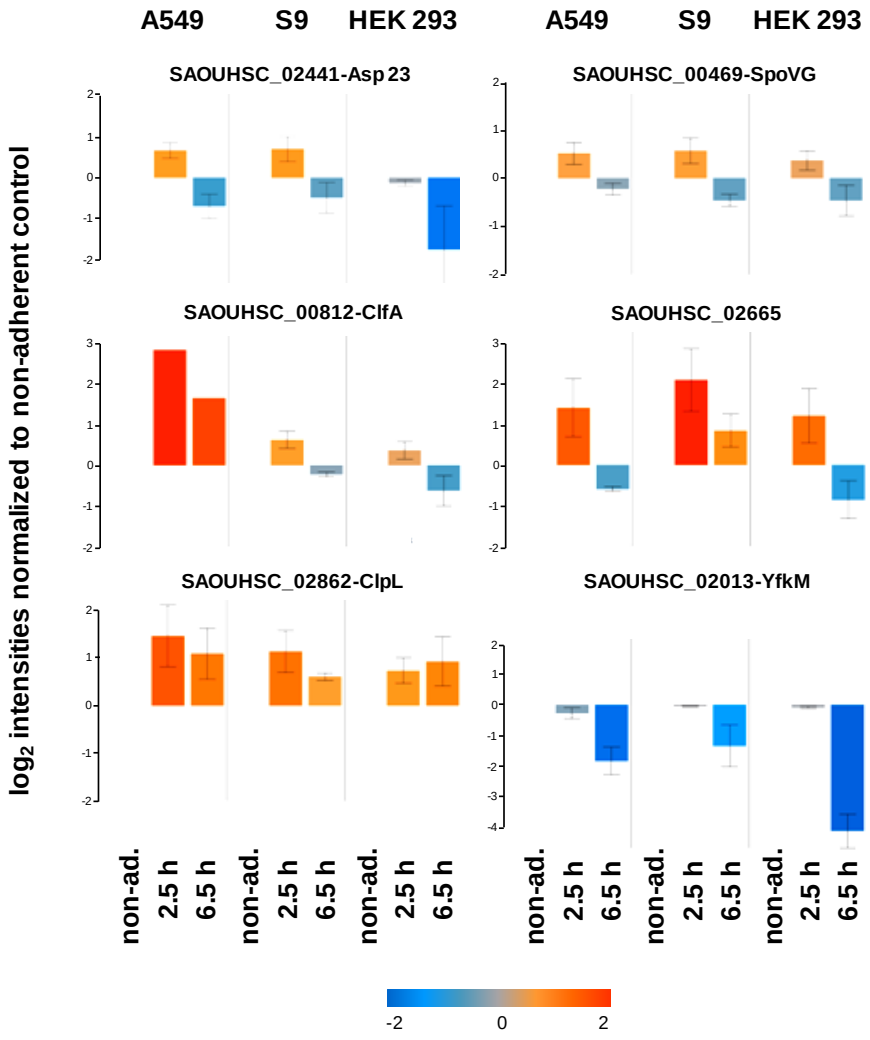

Figure 56. Activation of SigB following internalization. *Mean values and standard deviations of median-normalized log_2 intensities from three BR each for non-adherent bacteria as well as 2.5 h and 6.5 h p.i. are represented by the black line and the whiskers, the colored boxes represent quartiles for six proteins encoded by members of the SigB regulon. Blue spots indicate lower levels in the internalized bacteria compared to the non-adherent control; red colors represent higher levels of proteins in response to internalization compared to the non-adherent control (Surmann et al., 2014b).*

Differential adaptation of S. aureus HG001 proteome to internalization by three different host cell lines

Besides many common adaptation reactions of *S. aureus* caused by internalization also differences depending on the host model were observed. The PCA plot already indicated strongest variation for bacteria internalized by HEK 293 cells. But altered adaptation patterns of *S. aureus* HG001 proteome were also detected in between the two epithelial cell lines. Selected differentially regulated pathways are displayed in Figure 57. Among others, different patterns were observed for proteins involved in threonine degradation (5 of 5) in HEK 293 cells compared to the two epithelial cell lines. Levels of these enzymes were higher inside HEK 293 cells. In agreement with that, the intracellular level of host cell threonine was higher in these cells (Figure 36). Another exemplary protein group contains fermentation enzymes (9 of 9), whose levels were lower in bacteria isolated from in S9 cells compared to *S. aureus* HG001 internalized by either A549 or HEK 293 cells. On single protein level enzymes such as alcohol dehydrogenase (Adh1), L-lactate dehydrogenase (LctE), L-lactate dehydrogenase 2 (Ldh2) and D-lactate dehydrogenase (Ddh) increased in level after internalization by A549 and HEK 293 within 6.5 h up to 2-3 fold (Ldh2 and Ddh) or 8-10 fold (Adh1 and LctE) (Figure 58A). Furthermore, few proteins of the TCA cycle (16 of 16) were differentially regulated in *S. aureus* depending of the host. While many of the detected enzymes increased in level following internalization by all three cell lines a number of TCA cycle enzymes including citrate synthase (CitZ), isocitrate dehydrogenase (CitC), succinyl-CoA synthetase subunit beta (SucC) and succinate dehydrogenase flavoprotein subunit (SdhA) increased in level upon internalization by epithelial cells but not in *S. aureus* internalized by HEK 293 cells (Figure 58B). Enzymes utilized in response to oxidative stress (9 of 10) were found to be slightly increased 2.5 h *p.i.* compared to the non-adherent control for all three cell lines, and the levels decreased afterwards during ongoing internalization. The levels after 6.5 h were even lower for bacteria internalized from epithelial cells than in control bacteria. *S. aureus* HG001 obtained from HEK 293 cells showed higher amounts of oxidative stress enzymes 6.5 h *p.i.* compared to the non-adherent control.

Additionally bacterial enzymes involved in biosynthesis and metabolism of few amino acids displayed different patterns depending on the host (Figure 57). Proteins involved in the biosynthesis of “phenylalanine- and tyrosine-branches from chorismate” (3 of 4) were increased in level compared to non-adherent control bacteria 2.5 h *p.i.* inside all cell lines but decreased 6.5 h *p.i.* only inside HEK 293 cells. L-cysteine uptake and metabolism (3 of 5) was increased after internalization in bacteria internalized by all three host cells, but decreased further on inside HEK 293 and even more strongly inside A549 cells but not inside S9 cells. When comparing intracellular metabolite concentrations of cysteine, phenylalanine, and tryptophan, these amino acids were present in slightly higher concentrations inside A549 cells at the starting point of infection compared to starting levels in the other two cell lines. But with maximum concentrations of about 5 nmol/10^6 cells, these three compounds belong to the lower abundant intracellular amino acids (Figure 36).

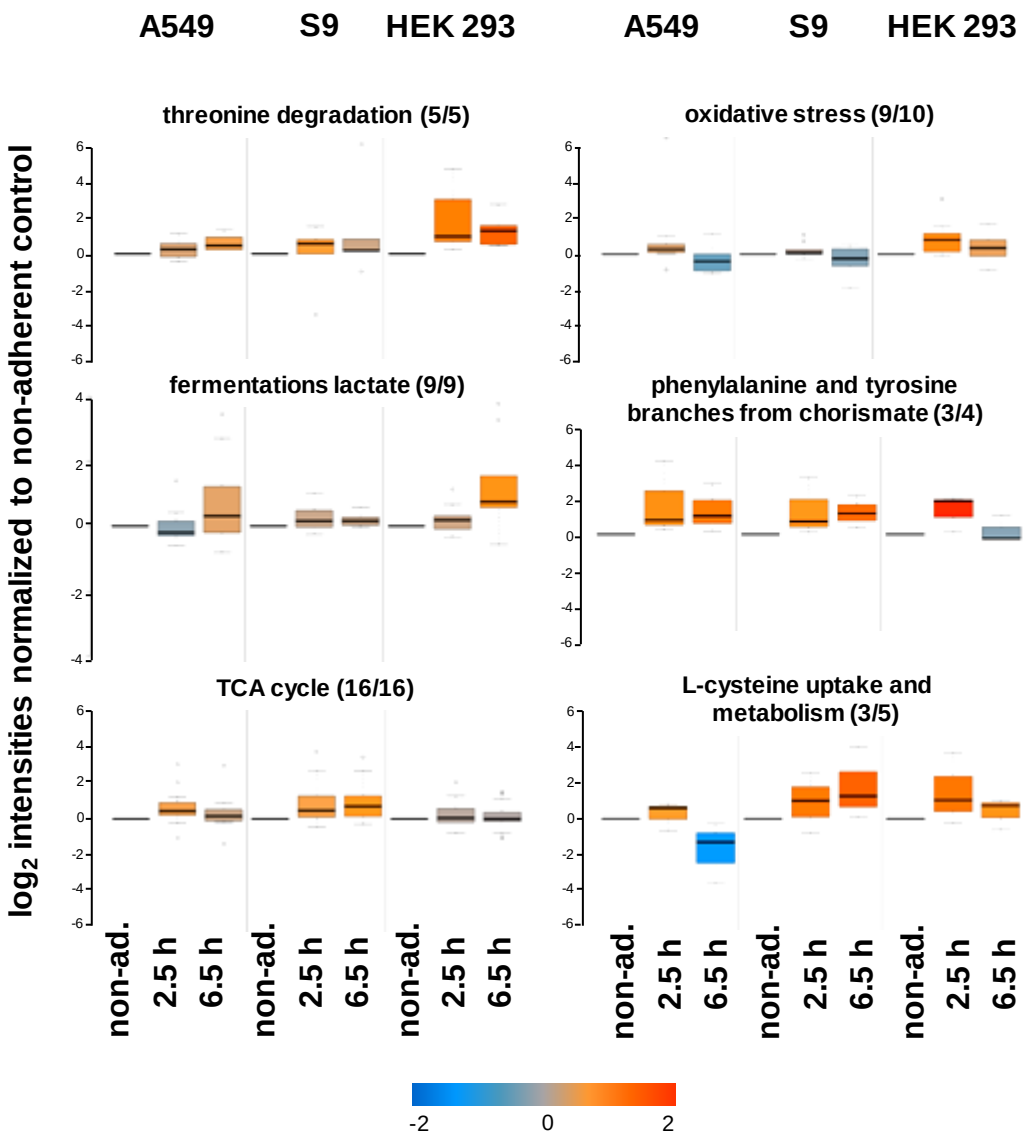

Figure 57. Protein groups displaying differentially abundant level after internalization depending on the host cell line. *Mean values and standard deviations of median-normalized log_2 intensities from three BR each for non-adherent bacteria as well as 2.5 h and 6.5 h p.i. are represented by the black line and the whiskers, the colored boxes represent quartiles.. Blue spots indicate lower levels in the internalized bacteria compared to the non-adherent control, red colors represent higher levels of proteins in response to internalization compared to the non-adherent control (Surmann et al., 2014b).*

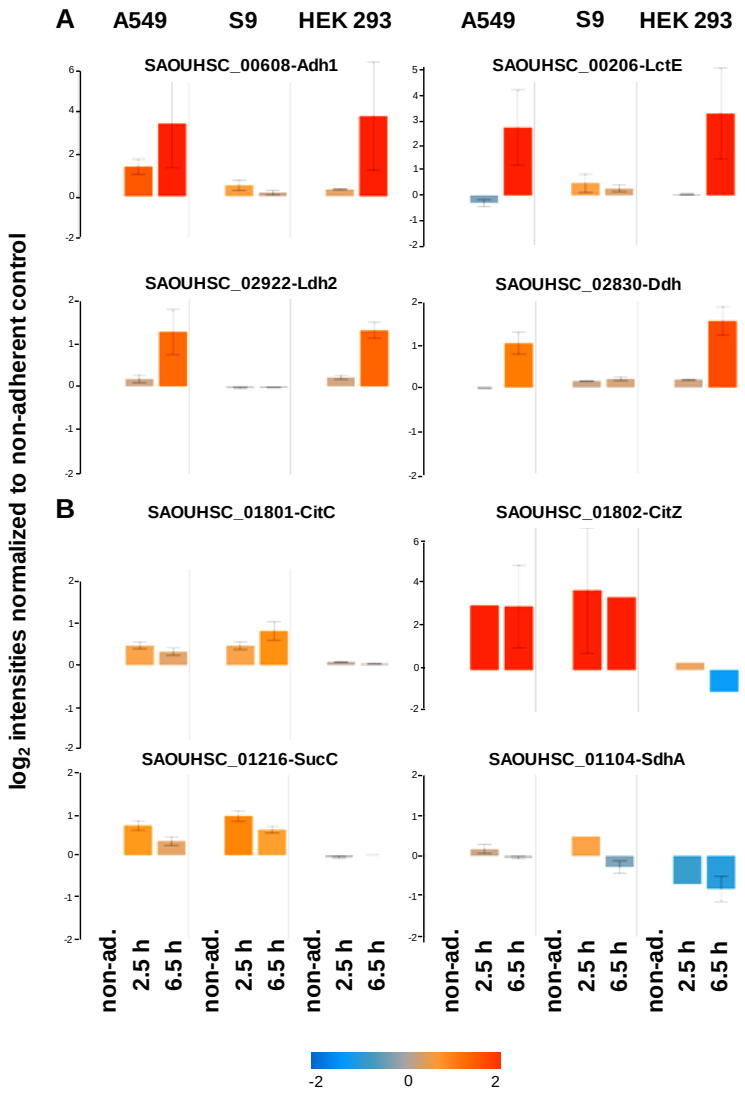

Figure 58. Differential regulation of proteins involved in fermentation and TCA cycle after internalization by different cell lines. (*A) Proteins involved in fermentation are found in lowest amounts inside S9 cells and are induced 6.5 h p.i. inside A549 and HEK 293 cells. (B) Proteins of the TCA cycle were found in lower amounts after internalization by HEK 293 cells compared to A549 and S9 cells. Protein groups displaying increased levels after internalization by all three cell lines. Blue spots indicate lower levels in the internalized bacteria compared to the non-adherent control, red colors represent higher levels of proteins in response to internalization compared to the non-adherent control (Surmann et al., 2014b).*

These selected examples suggest that *S. aureus* adapted its physiology to the intracellular life style by conserved reactions. On the other hand the data indicated that *S. aureus* additionally had the capacity to respond to subtle differences encountered in the different host cell niches. Quantitative information about further proteins analyzed in this approach as well as their classification to functional groups is provided as:
Supplementary_Material_Table_04_S_aureus_proteins_quantified_from_infected_celllines.xlsx and Supplementary_Material_Table_09_the_SEED_functional_categories_S_aureus_HG001.xlsx.

Quantification of secreted staphylococcal proteins

S. aureus secretes several virulence factors which contribute to its pathogenicity, but to my knowledge most of these proteins were only detected in culture supernatants from shake flask cultivation until now. When GFP-expressing bacteria are enriched from host cell lysate by fluorescence assisted cell sorting, secreted bacterial proteins are washed away. In order to cover also some important secreted virulence factors of *S. aureus* HG001 pMV158GFP another protocol analyzing proteins from isolated phagosomes was employed (compare "Protocol for enrichment of bacteria and secreted proteins by isolation of phagosomes"). First, staphylococcal proteins were analyzed from those phagosomes in a shotgun approach. Afterwards, as still many human proteins were detected in the phagosome preparation, identification and quantification of secreted proteins should be enhanced using the more sensitive MRM method. Selected *S. aureus* proteins were identified and relatively quantified between 2.5 h and 6.5 h after internalization.

Shotgun analysis of staphylococcal proteins from enriched phagosomes after infection of S9 cells

Isolated phagosomes with the enclosed bacteria were analyzed in a discovery approach. To elucidate time-dependent changes, the total proteome of the phagosomes was monitored 2.5 h and 6.5 h after internalization. From five independent replicates 547 staphylococcal proteins were quantified between 2.5 h and 6.5 h inside the phagosomes at both sampling points (Supplementary_Material_Table_10_S_aureus_HG001_proteins_in_isolated_phagosomes_shotgun.xlsx).

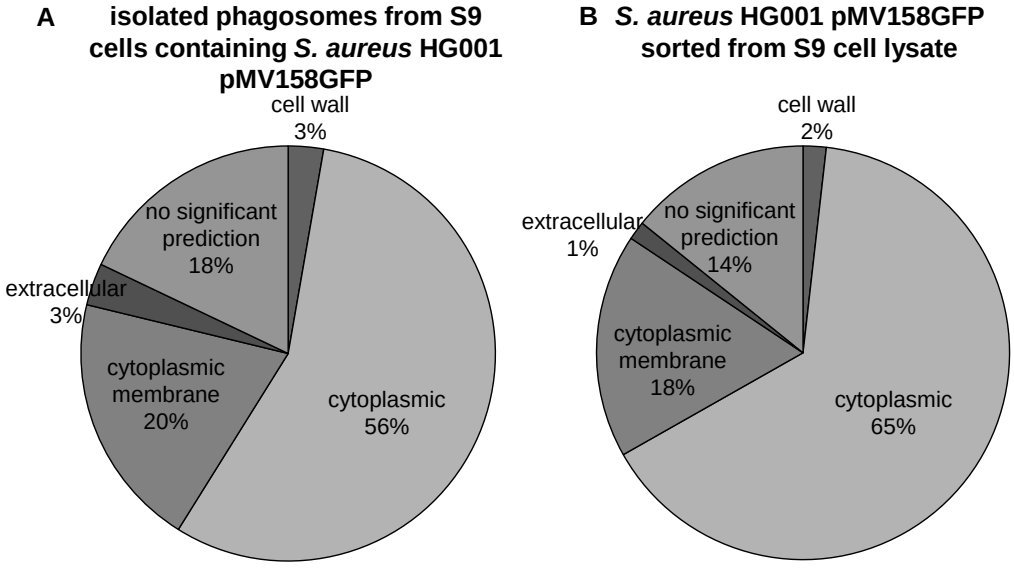

Figure 59. Localization prediction of *S. aureus* HG001 proteins. *Percentage distribution of number of detected proteins is depicted for (A) isolated phagosomes from S9 cells infected with HG001 pMV158GFP and for (B) S. aureus HG001 pMV158GFP sorted by flow cytometry from host cell debris. Localization prediction was performed with PSORT (Nakai and Horton, 1999).*

Out of the 547 quantified bacterial proteins 3% could be assigned to extracellular localization and 3% to the cell wall (cell wall 15 proteins, extracellular 18 proteins) predicted by the PSORT algorithm (Nakai and Horton, 1999) The complete PSORT list for *S. aureus* HG001 is available as Supplementary_Material_Table_11_PSORT_NCTC_8325_protein_localization.xlsx. Still 56% cytosolic bacterial proteins were detected which indicates cell lysis during internalization or sample preparation (Figure 59). These results were compared to quantitative data obtained from internalization of *S. aureus* HG001 pMV158GFP internalized by S9 cells within the cell line comparison project ("Comparative proteome analysis of *S. aureus* HG001 internalized by different cell lines"). From two million bacteria which were sorted out of S9 host cell lysate 1,445 staphylococcal proteins were quantified (Surmann et al., 2014b). As expected the percentage of extracellular bacterial proteins was slightly less in sorted bacteria compared to the enriched phagosomes. Only about 1% (26 of 1,445 proteins) of all detected proteins was predicted as extracellularly located and 2% (21 proteins) were assigned to cell wall proteins. The percentage of staphylococcal cytoplasmic proteins was clearly increased to 65% for bacteria sorted from S9 cell debris compared to 58% found inside isolated phagosomes (Figure 59, Supplementary_Material_Table_12_PSORT_S_aureus_isolated_from_phagosomes_or_sorted_from_S9_cell_debris.xlsx). The percentage of extracellular proteins was twice as high in enriched phagosomes compared to sorted bacteria. Although the total amount of identified and quantified staphylococcal proteins from isolated phagosomes comprised only one third of those monitored from sorted bacteria, eleven secreted proteins were exclusively found in enriched phagosomes. Among them were virulence factors such as lipase (Lip), α-hemolysin precursor (Hly), fibrinogen-binding protein-related protein SAOUHSC_01110, and truncated secreted von Willebrand factor-binding protein SAOUHSC_00814 as well as several hypothetical proteins. This proves the efficiency of the protocol and indicates that isolation of phagosomes indeed helps to capture secreted proteins which are located in the phagosomal lumen. However, the absolute number of quantified secreted proteins was not increased. More than 110 proteins in the database of the strain applied in this study were predicted to be extracellular localized (Supplementary_Material_Table_11_PSORT_NCTC_8325_protein_localization.xlsx). Proteins with an FDR <5% were defined as regulated between the sampling points in the discovery approach when additionally ratio values from at least four out of five BR exceeded a fold change value of 1.5 in the same direction for these four or five replicates. Further, no replicate should be regulated in the opposite direction. Finally, 31 proteins fulfilled these strict criteria (Supplementary_Material_Table_10_S_aureus_HG001_proteins_in_isolated_phagosomes_shotgun.xlsx). Out of them, 13 proteins with mostly cytoplasmic localization showed decreased levels 6.5 h after infection compared to 2.5 h after infection. Among 18 proteins with increased levels 6.5 h *p.i.* were the extracellular protein secretory antigen precursor (SsaA2) and malate:quinone-oxidoreductase which was assigned to cell wall by PSORT. When relaxing the regulation restrictions,

in a way that four of five replicates should show a fold change of more than 1.2 in the same direction and one replicate could be regulated in the opposite direction, seven more proteins were found with increasing trends 6.5 h *p.i.* compared to the earlier time point (Supplementary_Material_Table_10_S_aureus_HG001_proteins_in_isolated_phagosomes_shotgun.xlsx). However, extracellular localization or cell wall association was not predicted for these additional proteins.

In order to validate the results and to increase the number of detectable virulence-associated and especially extracellular proteins, which are probably secreted by the bacteria only in small amounts, the highly sensitive and selective MRM method was applied. It additionally helped to avoid false-positive values from database analysis of shotgun data which are likely to occur due to the prevailing number of human proteins in isolated phagosomes.

Preparation of standard curves of selected S. aureus proteins

MRM analysis allows sensitive quantification of targeted proteins of interest. For this study 61 *S. aureus* proteins with impact on metabolism and virulence were chosen. Among them were proteins which either interact directly with host molecules or help the pathogen to defend itself against host cell response. Also high abundant cytosolic proteins (*e.g.* Eno, Tuf) were ordered as positive controls and references. Their abundances were expected to increase with the number of bacteria according to earlier studies (Schmidt et al., 2010b) were added to the list. Cell wall bound and membrane proteins were also included in the protein set because not only secreted proteins act as virulence factors. The program PSORT served again as tool for localization prediction (Table 12).

Table 12. Standard proteins for MRM. *Proteins and the acquired proteotypic peptides are listed together with the minimum quantifiable concentration (conc.) and the R^2 value of the linear concentration range. Localization was predicted using PSORT (Nakai and Horton, 1999). Proteins that were detected by shotgun analysis are highlighted in bold letters.*

locus	gene name	peptide	R^2	minimum detectable conc. [fmol]	predicted localization by PSORT
SAOUHSC_00390	*set10*	NGTVFSYGGVTK NQDAYYDYINAPR	0.999 0.987	0.5 0.5	extracellular
SAOUHSC_01949	*epiP*	TSNESLFSR VEYDALQK	0.998 0.998	0.1 0.1	extracellular
SAOUHSC_00248	*lytM*	DASWLTSR	1	0.1	extracellular
SAOUHSC_02333	*sceD*	YQFLQSTWDSVAPAK LYNTGGAGHWVTA	0.977 0.991	5 1	extracellular
SAOUHSC_02167	*scn*	IYNEIDEALK	0.997	0.01	no significant prediction
SAOUHSC_00545	*sdrD*	SGDYFTIK QTIYVNPSENSLTNAK ELTDVTNQYLQK	0.999 0.989 0.993	0.01 1 0.05	cell wall
SAOUHSC_02971	*aur*	AGVDANYYAK NNAAWIGDK	0.999 1	0.5 0.5	extracellular
SAOUHSC_00069	*spa*	DDPSQSTNVLGEAK DDPSQSANLLSEAK DDPSQSANLLAEAK	1 0.999 1	0.5 0.5 5	cell wall
SAOUHSC_01121	***hlY***	**SGLAWPSAFK** **QQTNIDVIYER**	**0.996** **0.999**	**0.01** **0.01**	**extracellular**
SAOUHSC_01941	*splB*	SATGFVVGK GFNFNDNVTPFK	0.999 0.993	0.05 0.5	extracellular

locus	gene name	peptide	R^2	minimum detectable conc. [fmol]	predicted localization by PSORT
SAOUHSC_01431	***yppQ***	**ALDDDEIIELVDK** **LEELGYGDLISHFDK**	**0.986** **0.994**	**1** **5**	**cytoplasmic**
SAOUHSC_00257	*SAOUHSC_00257*	QILSDLTR FEEQFQQLSPK	0.999 0.998	0.01 0.1	extracellular
SAOUHSC_03006	***lip***	**EIVNETEIEK** **VDFGLAQWGLK** **TSLNPNIVYK**	**1** **0.989** **0.999**	**0.01** **0.5** **0.01**	**extracellular**
SAOUHSC_01939	*splC*	DTNIFPYNGVVSFK DATGFVIGK VIGYPLPAQNSFK	0.992 0.998 0.997	0.01 0.01 0.01	extracellular
SAOUHSC_01938	*splD*	EDIAVVQVEEK FNIASEAK SFAVYFSPEIK	0.999 0.999 0.994	0.01 0.01 0.01	extracellular
SAOUHSC_01801	*citC*	ITDSIEDTIASK VVTYDFAR	0.999 0.999	0.01 0.01	cytoplasmic
SAOUHSC_01714	*greA*	DEQGFIEQDIQR NALIIEDTGDNNVVK	0.998 0.998	0.01 0.01	cytoplasmic
SAOUHSC_02710	*hlgB*	ISQILTFNFIK ITVTYQR	0.994 0.999	0.01 0.01	extracellular
SAOUHSC_00019	***purA***	**ITDFLAEQSDVIAR** **GIPTSNLR** **VGWFDSVVLR**	**0.994** **0.999** **0.993**	**0.01** **0.01** **0.01**	**cytoplasmic**
SAOUHSC_00814	***SAOUHSC_00814***	**YESVFNTLK** **QTQQQIIYNAPK**	**0.999** **0.999**	**0.5** **0.5**	**extracellular**
SAOUHSC_01110	***SAOUHSC_01110***	**YDQYQTNFK** **QIDLVLK**	**0.997** **0.998**	**0.5** **0.01**	**extracellular**
SAOUHSC_00356	*SAOUHSC_00356*	GISFENSNGEWAYK SGEESEVLVADK	0.996 1	0.01 0.01	no significant prediction
SAOUHSC_01854	*SAOUHSC_01854*	TQLEETVAYTK VEGFLNK	1 0.999	0.01 0.01	cell wall
SAOUHSC_01316	*nuc2*	TLAYVWISK NVFIEAQNK	0.998 1	0.01 0.01	extracellular
SAOUHSC_01942	*splA*	ISVIGYPK NFGVYFTPQLK	0.999 0.995	0.01 0.1	extracellular
SAOUHSC_02709	***hlgC***	**ANSFATESGQK** **GSSDTSEFEITYGR**	**1** **0.985**	**0.05** **0.05**	**extracellular**
SAOUHSC_02972	*isaB*	GNEASQLQFVVK EADSGIFYYQNAK	0.998 0.998	0.1 0.01	extracellular
SAOUHSC_01081	*isdA*	TINVAVEPGYK	0.997	0.01	cell wall
SAOUHSC_01114	*fib*	LIQAQNLVR AVNLVSFEYK	1 0.998	0.05 0.01	extracellular
SAOUHSC_01955	*lukE*	DPNVSLINYLPK YLFVQSPNGPTGSAR GSSDTSEFEISYGR	0.986 0.988 0.989	1 0.01 0.05	extracellular
SAOUHSC_02171	*sak*	VVELDPSAK IEVTYYDK	1 1	0.01 0.05	extracellular
SAOUHSC_01219	*lytN*	GYEQNVFAK SNSNSSTLNYLK AEPGDLVVFSGR	1 0.999 0.993	0.01 0.5 0.5	cytoplasmic membrane
SAOUHSC_02260	*hld*	WIIDTVNK	0.998	0.05	no significant prediction
SAOUHSC_02169	*chp*	NSGLPTTLGK SSYVINGPGK	0.999 0.999	0.01 0.01	no significant prediction
SAOUHSC_01843	***sasI***	**FEVYENNQK** **FPVSDGTQELK** **TLIFPYIPDK**	**1** **1** **0.984**	**0.1** **0.5** **0.5**	**cell wall**
SAOUHSC_01079	*isdB*	EVEAPTSETK TIIFPYVEGK	0.999 0.995	0.1 0.5	cell wall
SAOUHSC_01954	*lukD*	DYNYSQFYWGGK DSYDPTYGNELFLGGR	0.984 0.982	1 0.5	extracellular
SAOUHSC_02463	*hysA*	GGNLVDISK VFTYVQDSATGK IVFLGTGIK	0.997 0.999 0.998	0.5 0.5 0.5	extracellular
SAOUHSC_02019	*SAOUHSC_02019*	VLFGLLLK NGLVNAPLSR	0.992 0.999	5 0.1	extracellular
SAOUHSC_02161	***SAOUHSC_02161***	**SGIYTANLINSSDIK** **SDIFTPNLFSAK**	**0.996** **0.995**	**0.5** **0.01**	**cytoplasmic membrane**
SAOUHSC_00816	*ssp*	FVVPESGINK LGNIVPEYK	0.999 0.999	0.01 0.01	cell wall
SAOUHSC_00530	***tuf***	**NVGVPALVVFLNK** **ALEGDAQYEEK** **TVGSGVVTEIIK**	**0.992** **0.999** **0.997**	**0.01** **0.01** **0.01**	**cytoplasmic**
SAOUHSC_01653	***sodA2***	**LNAAVEGTDLESK** **VDELYNATK**	**0.999** **0.988**	**0.01** **0.1**	**extracellular**
SAOUHSC_02466	*SAOUHSC_02466*	TYFIFPENK NVLYQEIDSK	0.997 0.999	0.01 0.01	cytoplasmic membrane

locus	gene name	peptide	R^2	minimum detectable conc. [fmol]	predicted localization by PSORT
SAOUHSC_00812	***clfa***	**LNYGFSVPNSAVK** **TVLVDYEK**	**0.989** **1**	**0.5** **0.01**	**cell wall**
SAOUHSC_02241	***SAOUHSC_02241***	**ESNYSETISYQQPSYR** **LSALYEVDWK**	**0.983** **0.985**	**0.5** **0.5**	**extracellular**
SAOUHSC_00799	***eno***	**AAADLLGQPLYK** **GIENGIGNSILIK** **IEDELFETAK**	**0.995** **0.993** **0.999**	**0.01** **0.5** **0.5**	**cytoplasmic**
SAOUHSC_00196	*SAOUHSC_00196*	DTDTIIFNTAQR IGFIDLLK	0.998 0.995	0.01 0.01	no significant prediction
SAOUHSC_00300	*geh*	AAPTSTTPPSNDK YSNIDLGLTQWGFK	1 0.992	0.01 1	extracellular
SAOUHSC_02887	***isaA***	**TGVSASTWAAIIAR** **AQGLGAWGF**	**0.991** **0.995**	**0.01** **0.1**	**extracellular**
SAOUHSC_01467	***pbp2***	**IYYSDGVTGIK** **TGGLVAISGGR**	**0.999** **1**	**0.05** **0.01**	**cytoplasmic membrane**
SAOUHSC_02571	***ssaA2***	**SISSGYTSGR** **AGYTVNNTPK** **TISASQAAGYNFIH**	**1** **0.998** **0.997**	**0.01** **0.1** **0.05**	**extracellular**
SAOUHSC_02706	***sbi***	**SQQVWVESVQSSK** **QLDALVAQK**	**0.997** **0.999**	**0.05** **0.1**	**no significant prediction**
SAOUHSC_00994	***atl***	**FYLVQDYNSGNK** **LYTVPWGTSK** **DYNSPTLIGWVK**	**0.998** **0.998** **0.994**	**0.01** **0.05** **0.05**	**extracellular**
SAOUHSC_01972	*prsA*	DQIANASFTEMLNK DGELGYVLK DGEVSEVVK	0.987 0.999 0.997	0.5 0.05 0.5	cytoplasmic membrane
SAOUHSC_02243	*SAOUHSC_02243*	IATVENPELSFASK TQFEVTYTR	0.992 0.995	0.5 0.05	extracellular
SAOUHSC_01432	*msrA2*	TFDPTDDQGQFFDR AFIESHWGNQNA	0.995 0.998	0.05 0.1	no significant prediction
SAOUHSC_02254	***groEL***	**NVTSGANPVGLR** **DNTTVVDGDGDENSIDAR**	**0.996** **0.997**	**0.01** **0.05**	**cytoplasmic**
SAOUHSC_01869	*SAOUHSC_01869*	ATQLGTIANETIK IVTEEDLK	0.998 0.999	0.01 0.01	no significant prediction
SAOUHSC_01779	*tig*	QFNISVEDIK NTLGNTDIIK	0.996 1	0.01 0.01	cytoplasmic
SAOUHSC_02798	*sasG*	SVDEGSFDITR	0.997	0.01	cell wall

First, these standards were analyzed separately from the samples in order to monitor the retention time and transition pattern. Later this information allowed exact identification of the corresponding proteins in bacterial samples. Furthermore, these pure synthetic standards served to optimize collision energy in combination with the software Skyline (Maclean et al., 2010a, Maclean et al., 2010b) for improved measurements. Peptides from digested standard proteins were diluted between 0.01 and 50 fmol/injection and analyzed by MRM. That way the linear concentration range, a requisite for accurate quantification, was determined for each peptide. Linear correlation between peptide concentration and peak area was only accepted with R^2 >0.95.

Only sample data within the pre-determined linear range of the assay were approved for relative quantification. Finally, for each protein in the screening approach one to three peptides could be detected by MRM using the four most intense pairs of precursor and transitions per protein (Table 12, Supplementary_Material_Table_01_MRM_transitions_S_aureus_HG001.xlsx). Many peptides showed a good linearity over the complete range from 0.01 fmol to 50 fmol of the standard curves (R^2 >0.97, Table 12, example in Figure 60). Hence, accurate relative quantification of the selected standard proteins was confirmed for the measurements. Sixteen of the 61 proteins in the set of recombinant standards could already be identified by shotgun MS (highlighted in Table 12). As the MRM method is much more sensitive, it was expected to analyze more proteins using that method.

The additional aim was to take advantage from the large dynamic range of targeted MRM technique for the quantification of proteins.

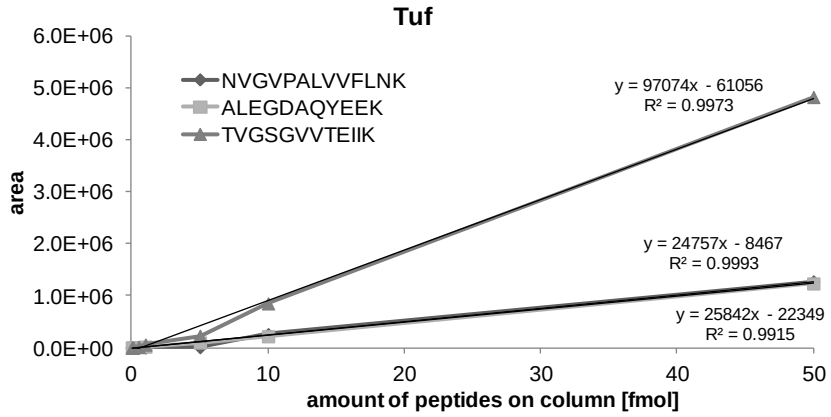

Figure 60. Example of dilution series. *Areas of three peptides from protein Tuf are plotted depending upon the amount of protein digest loaded on column. Resulting equations of standard curves and linearity values are included.*

Quantification of selected S. aureus proteins using MRM

In the final MRM analysis of five independent replicates of phagosomes isolated 2.5 h and 6.5 h *p.i.* 47 of 61 targeted proteins could be identified by one or more peptides in at least one replicate using the previously recorded chromatograms of standard proteins for comparison. Proteins identified in shotgun MS approaches with only one peptide are often rejected from analysis to avoid false positive results. However, for some proteins only a single peptide was eligible for MS analysis (for example IsdA) and could be lost due to such strict filter criteria. Therefore, throughout this thesis proteins which were detected with only one peptide but more than 10% sequence coverage where additionally considered in discovery approaches. Using MRM identity can be confirmed with unambiguous detection based on recombinant standard proteins. Due to these standards, unique peptides can be reliably identified, and the corresponding proteins can be considered in MRM analysis but not in shotgun analysis which lacks reference proteins/peptides as a measure to increase confidence. However, eleven of these 47 identified proteins could still not be quantified (Table 13), as they were only detected at one point in time or peak areas were too close to noise level and below the linear range of the standard curves. Six of them were identified using MRM but not detected by shotgun MS. Among them were the extracellular Sak, cell wall anchored proteins SdrD and IsdB as well as CitC, chemotaxis-inhibiting protein (Chp), and SAOUHSC_00196. However, they could not be quantified, as they were only detected 6.5 h after internalization. The advantage of applying the MRM method compared to shotgun analysis is proven by the fact that only 43% (20 of 47 targeted proteins, among them eight extracellular proteins) of the proteins that were detected by MRM were also found by shotgun MS (Table 13).

None of the 61 targeted proteins was exclusively detected by shotgun analysis. Interestingly, five of the proteins quantified by shotgun MS 2.5 h and 6.5 h *p.i.* [adenylosuccinate synthetase (PurA), truncated secreted von Willebrand factor-binding protein VWbp (SAOUHSC_00814), hemolysin Hly, cell wall surface anchor family protein SasI, and MHC class II analog protein (SAOUHSC_02161)] were only detected 6.5 h *p.i.* using MRM and could therefore not be quantified over time in the targeted approach. Finally, changes of 20 targeted proteins were quantified between 2.5 h and 6.5 h after infection by shotgun MS and 36 by MRM. Chaperonin GroEL was detected among the targeted proteins in decreased levels 6.5 h after infection compared to the 2.5 h time point with the discovery approach. The four proteins elongation factor Tu (Tuf), methionine sulfoxide reductase MsrB, staphylococcal secretory antigen SsaA2, and immunoglobulin G-binding protein Sbi were found to be increased during ongoing time of infection in the shotgun approach. As also low abundant proteins were detected by MRM and no alignment search but strict manual validation was performed, proteins were often not found in all replicates. This is a technical difference compared to the alignment search performed during shotgun analysis. There, when a spectrum could be assigned to one peptide in a single sample data set, this peptide is assigned to similar matching spectra in the aligned samples as well. This bears the risk of false positive identifications. Thus, ratios were only calculated replicate-wise in the MRM analysis when peaks were found 2.5 h *p.i.* and 6.5 h *p.i.* Therefore, a different definition for a regulation trend of proteins had to be defined. Proteins were regarded regulated after MRM measurement, when the majority of the replicates, where the protein could be quantified, showed an absolute fold change of at least 1.5 in the same direction. One opposite regulation was only allowed when five replicates were available (Table 13). Thus, 17 proteins showed a trend of regulation. Solely the secreted leukocidin HlgC was found to be decreased. However, it was only detected inside one replicate. Six extracellular proteins [LytM (3 of 4 BR), Efb (3 of 3 BR), the leukocidins SAOUHSC_02241 (3 of 3 BR) and SAOUHSC_02243 (4 of 4 BR), SsaA2 (4 of 5 BR), and IsaA (3 of 4 BR)] were found to be increased in level over time. The four targeted proteins which were found increased over time by shotgun MS (Tuf, MsrB, SsaA2, and Sbi) could be confirmed to increase 6.5 h *p.i.* compared to 2.5 h *p.i.* by MRM. Interestingly, chaperonin GroEL which was found decreased over time in the shotgun approach, was not found regulated by MRM. The other way round, HlgC which was found decreased by MRM was not regulated in the shotgun experiment. The trend regulation of staphylococcal proteins obtained from MRM data is illustrated in Figure 61 for all proteins that were assigned to localizations by PSORT.

Table 13. Comparison of MRM and shotgun MS data. *The 47 targeted S. aureus proteins which were detected by MRM are listed with fold change 6.5 h p.i/2.5 h p.i. (FC) for each BR when available. FC <-1.5 are highlighted blue, FC >1.5 are marked in red. Additionally, numbers of peptides (# pep) and average values (Av) for 5 BR are given. P-values and false discovery rates (FDR) <0.05 for shotgun data are marked in yellow. Proteins meeting criteria for regulation are highlighted in dark green and labeled "yes". nq (not quantified), na (not available), reg. (regulated).*

protein identification		MRM analysis								shotgun analysis									
locus	gene name	# pep	FC BR1	FC BR2	FC BR3	FC BR4	FC BR5	FC Av 5BR	trend reg. yes/no	# pep	FC BR1	FC BR2	FC BR3	FC BR4	FC BR5	FC Av 5BR	p-value	FDR	trend reg. yes/no
SAOUHSC_00019	*purA*	2	nq	nq	nq	nq	nq	**nq**	**no**	3	-2.0	-1.2	-1.6	1.2	-1.5	**-1.3**	0.00	0.01	**no**
SAOUHSC_00196	*SAOUHSC_00196*	2	nq	nq	nq	nq	nq	**nq**	**no**	na	na	na	na	na	na	**na**	na	na	**no**
SAOUHSC_00248	*lytM*	1	1.7	1.5	2.6	5.1	nq	**2.7**	**yes**	na	na	na	na	na	na	**na**	na	na	**no**
SAOUHSC_00300	*geh*	1	-2.0	2.6	nq	nq	nq	**1.5**	**no**	na	na	na	na	na	na	**na**	na	na	**no**
SAOUHSC_00356	*SAOUHSC_00356*	2	-1.1	-2.0	nq	nq	nq	**-1.4**	**no**	na	na	na	na	na	na	**na**	na	na	**no**
SAOUHSC_00530	*tuf*	3	3.7	2.0	2.7	7.2	3.3	**3.8**	**yes**	8	3.3	1.6	2.4	7.1	1.9	**3.3**	0.03	0.04	**yes**
SAOUHSC_00545	*sdrD*	1	nq	nq	nq	nq	nq	**nq**	**no**	na	na	na	na	na	na	**na**	na	na	**no**
SAOUHSC_00799	*eno*	3	3.1	1.9	nq	3.7	1.6	**2.6**	**yes**	5	3.8	1.6	1.5	7.5	1.6	**3.2**	0.05	0.07	**no**
SAOUHSC_00812	*clfA*	2	7.7	2.1	nq	5.2	3.3	**4.6**	**yes**	2	-1.1	-1.7	-1.8	1.3	-1.1	**-1.2**	0.00	0.01	**no**
SAOUHSC_00814	*SAOUHSC_00814*	1	nq	nq	nq	nq	nq	**nq**	**no**	2	-3.5	2.0	1.1	-1.2	1.1	**1.1**	0.02	0.03	**no**
SAOUHSC_00816	*ssp*	1	1.2	1.4	1.4	-1.1	-1.0	**1.2**	**no**	na	na	na	na	na	na	**na**	na	na	**no**
SAOUHSC_00994	*atl*	2	-1.5	1.2	-1.1	1.4	-2.1	**-1.1**	**no**	5	-1.3	1.0	2.8	-1.0	-2.2	**1.2**	0.04	0.06	**no**
SAOUHSC_01079	*isdB*	1	nq	nq	nq	nq	nq	**nq**	**no**	na	na	na	na	na	na	**na**	na	na	**no**
SAOUHSC_01081	*isdA*	1	1.5	nq	nq	4.4	2.2	**2.7**	**yes**	na	na	na	na	na	na	**na**	na	na	**no**
SAOUHSC_01110	*SAOUHSC_01110*	1	nq	nq	2.7	3.9	nq	**3.3**	**yes**	1	1.9	1.3	5.E+07	6.E+07	-1.7	**2.E+07**	0.18	0.20	**no**
SAOUHSC_01121	*hlY*	2	nq	nq	nq	nq	nq	**nq**	**no**	3	1.1	-1.3	-1.7	1.0	1.6	**1.0**	0.00	0.01	**no**
SAOUHSC_01114	*efb*	1	2.7	1.9	4.2	nq	nq	**2.9**	**yes**	na	na	na	na	na	na	**na**	na	na	**no**
SAOUHSC_01431	*msrB*	1	2.3	nq	nq	nq	nq	**2.3**	**yes**	1	2.3	4.9	3.8	1.4	-2.4	**2.6**	0.03	0.05	**yes**
SAOUHSC_01432	*msrA2*	1	nq	nq	nq	nq	1.7	**1.7**	**yes**	na	na	na	na	na	na	**na**	na	na	**no**
SAOUHSC_01467	*pbp2*	2	1.4	1.6	-1.6	3.0	-1.2	**1.5**	**no**	3	2.0	1.3	1.0	1.7	1.3	**1.5**	0.00	0.01	**no**
SAOUHSC_01653	*sodA2*	2	nq	-2.0	-2.9	12.6	1.4	**3.7**	**no**	2	-1.2	-1.5	2.0	5.2	-1.4	**1.9**	0.10	0.11	**no**
SAOUHSC_01714	*greA*	1	1.8	1.2	nq	nq	nq	**1.5**	**no**	na	na	na	na	na	na	**na**	na	na	**no**
SAOUHSC_01779	*tig*	2	3.0	1.9	-3.5	4.3	-1.2	**2.1**	**no**	na	na	na	na	na	na	**na**	na	na	**no**
SAOUHSC_01801	*citC*	1	nq	nq	nq	nq	nq	**nq**	**no**	na	na	na	na	na	na	**na**	na	na	**no**
SAOUHSC_01843	*sasI*	2	nq	nq	nq	nq	nq	**nq**	**no**	3	-1.3	-2.0	-1.5	-1.3	-1.1	**-1.4**	0.00	0.01	**no**
SAOUHSC_01854	*SAOUHSC_01854*	1	-1.5	nq	nq	nq	nq	**-1.5**	**no**	na	na	na	na	na	na	**na**	na	na	**no**
SAOUHSC_01869	*SAOUHSC_01869*	2	1.1	1.5	1.4	1.9	nq	**1.5**	**no**	na	na	na	na	na	na	**na**	na	na	**no**
SAOUHSC_01941	*splB*	1	-1.1	nq	nq	nq	nq	**-1.1**	**no**	na	na	na	na	na	na	**na**	na	na	**no**
SAOUHSC_01954	*lukD*	1	-1.5	1.1	-2.4	nq	1.4	**-1.1**	**no**	na	na	na	na	na	na	**na**	na	na	**no**
SAOUHSC_01955	*lukE*	1	-2.9	nq	-2.2	nq	3.2	**1.3**	**no**	na	na	na	na	na	na	**na**	na	na	**no**
SAOUHSC_01972	*prsA*	2	4.5	4.5	1.1	2.9	2.5	**3.1**	**yes**	na	na	na	na	na	na	**na**	na	na	**no**
SAOUHSC_02161	*SAOUHSC_02161*	2	nq	nq	nq	nq	nq	**nq**	**no**	2	-1.2	1.3	9.7	2.6	3.0	**3.5**	0.10	0.11	**no**
SAOUHSC_02167	*scn*	1	-2.6	-1.9	-1.8	2.8	2.4	**1.3**	**no**	na	na	na	na	na	na	**na**	na	na	**no**
SAOUHSC_02169	*chp*	1	nq	nq	nq	nq	nq	**nq**	**no**	na	na	na	na	na	na	**na**	na	na	**no**
SAOUHSC_02171	*sak*	1	nq	nq	nq	nq	nq	**nq**	**no**	na	na	na	na	na	na	**na**	na	na	**no**
SAOUHSC_02241	*SAOUHSC_02241*	1	2.8	10.2	nq	nq	14.7	**9.3**	**yes**	2	1.3	2.6	-1.8	-1.0	-1.1	**1.3**	0.02	0.04	**no**
SAOUHSC_02243	*SAOUHSC_02243*	2	10.0	12.2	2.5	nq	4.5	**7.3**	**yes**	na	na	na	na	na	na	**na**	na	na	**no**
SAOUHSC_02254	*groEL*	1	3.8	2.4	-1.2	5.3	1.2	**2.7**	**no**	2	-1.1	-1.1	-2.3	-4.0	-8.2	**-1.9**	0.03	0.05	**no**
SAOUHSC_02466	*SAOUHSC_02466*	1	5.2	2.2	nq	3.0	nq	**3.4**	**yes**	na	na	na	na	na	na	**na**	na	na	**no**
SAOUHSC_02571	*ssaA2*	3	-2.2	1.9	9.6	4.4	4.4	**4.2**	**yes**	5	1.2	1.4	5.2	7.1	2.8	**3.5**	0.04	0.05	**yes**
SAOUHSC_02706	*sbi*	1	1.6	4.1	1.7	2.0	3.4	**2.6**	**yes**	3	1.9	3.1	4.2	8.7	5.7	**4.7**	0.02	0.03	**yes**
SAOUHSC_02709	*hlgC*	1	-2.0	nq	nq	nq	nq	**-2.0**	**yes**	2	1.2	1.2	1.0	-2.6	1.7	**1.1**	0.01	0.02	**no**
SAOUHSC_02710	*hlgB*	2	-2.3	1.3	1.2	-2.1	1.6	**-1.0**	**no**	na	na	na	na	na	na	**na**	na	na	**no**
SAOUHSC_02798	*sasG*	1	-1.4	1.1	nq	1.4	nq	**1.1**	**no**	na	na	na	na	na	na	**na**	na	na	**no**
SAOUHSC_02887	*isaA*	2	1.2	1.8	nq	7.9	5.3	**4.1**	**yes**	4	1.2	1.5	6.6	12.2	6.3	**5.6**	0.05	0.06	**yes**
SAOUHSC_02971	*aur*	1	-1.3	nq	1.8	nq	nq	**1.3**	**no**	na	na	na	na	na	na	**na**	na	na	**no**
SAOUHSC_03006	*lip*	2	-4.8	nq	-2.1	2.0	1.4	**1.0**	**no**	3	-1.0	-1.2	1.5	1.2	1.6	**1.2**	0.00	0.01	**no**

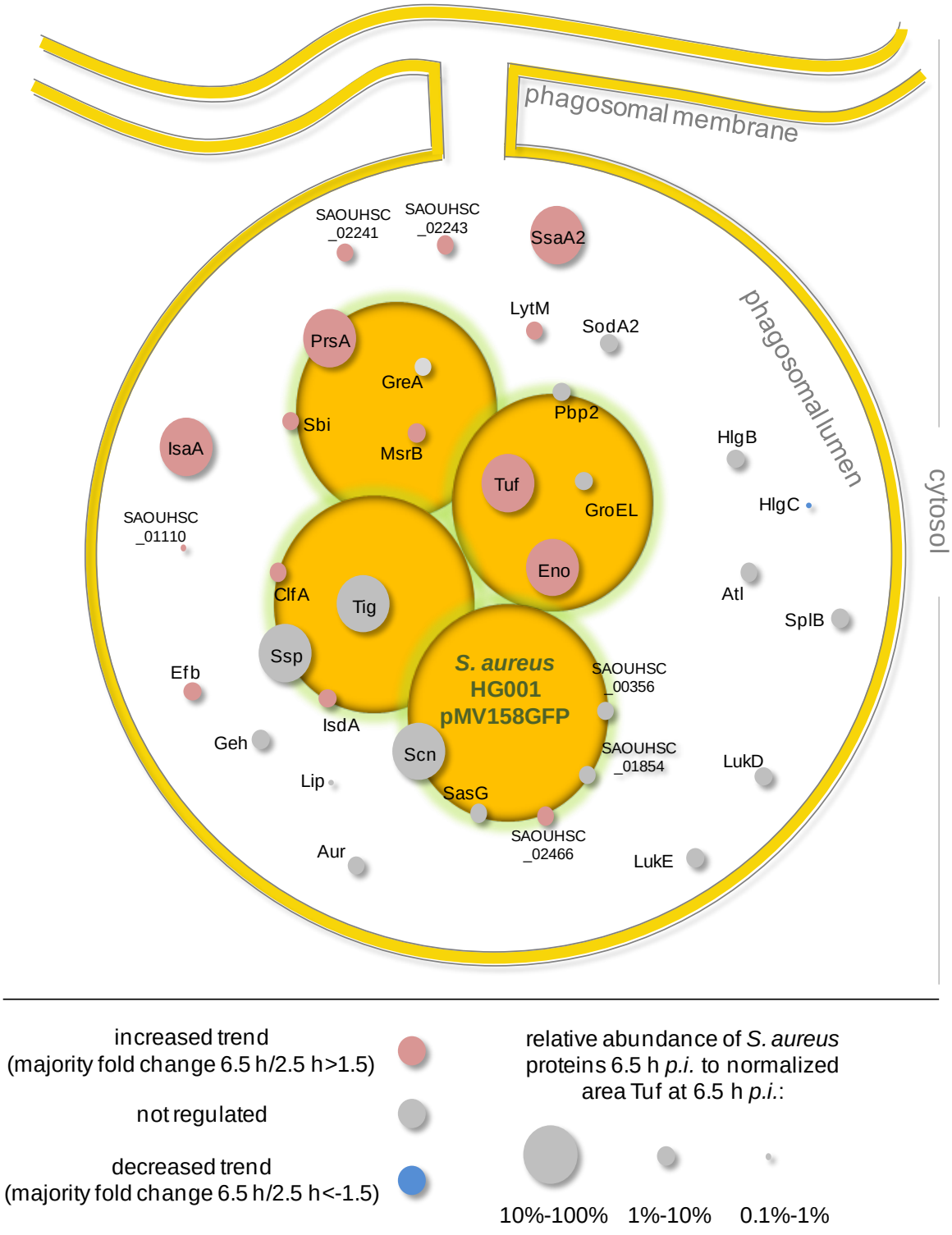

Figure 61. Staphylococcal proteins detected from isolated phagosomes by MRM. *Bacterial phagosomal proteins were arranged according to their localization and principal function assigned by PSORT (Desjardins, 2003, Nakai and Horton, 1999). Proteins colored in red were found in increased levels over time, proteins in blue were decreased over time, proteins in gray were not regulated. Also relative abundance values at time point 6.5 h p.i. related to protein Tuf are illustrated according to Figure 62.*

As some proteins were only detected in few or even one biological replicate, the relative abundance of this protein as a hint of the amount within the sample was of interest. Thus, the average area value for each protein per time point was calculated. The highest value was measured for protein Tuf 6.5 h after infection. When setting this value to 100% the relative abundance among the proteins per time point and also between the two sampling points could be compared (Figure 62).

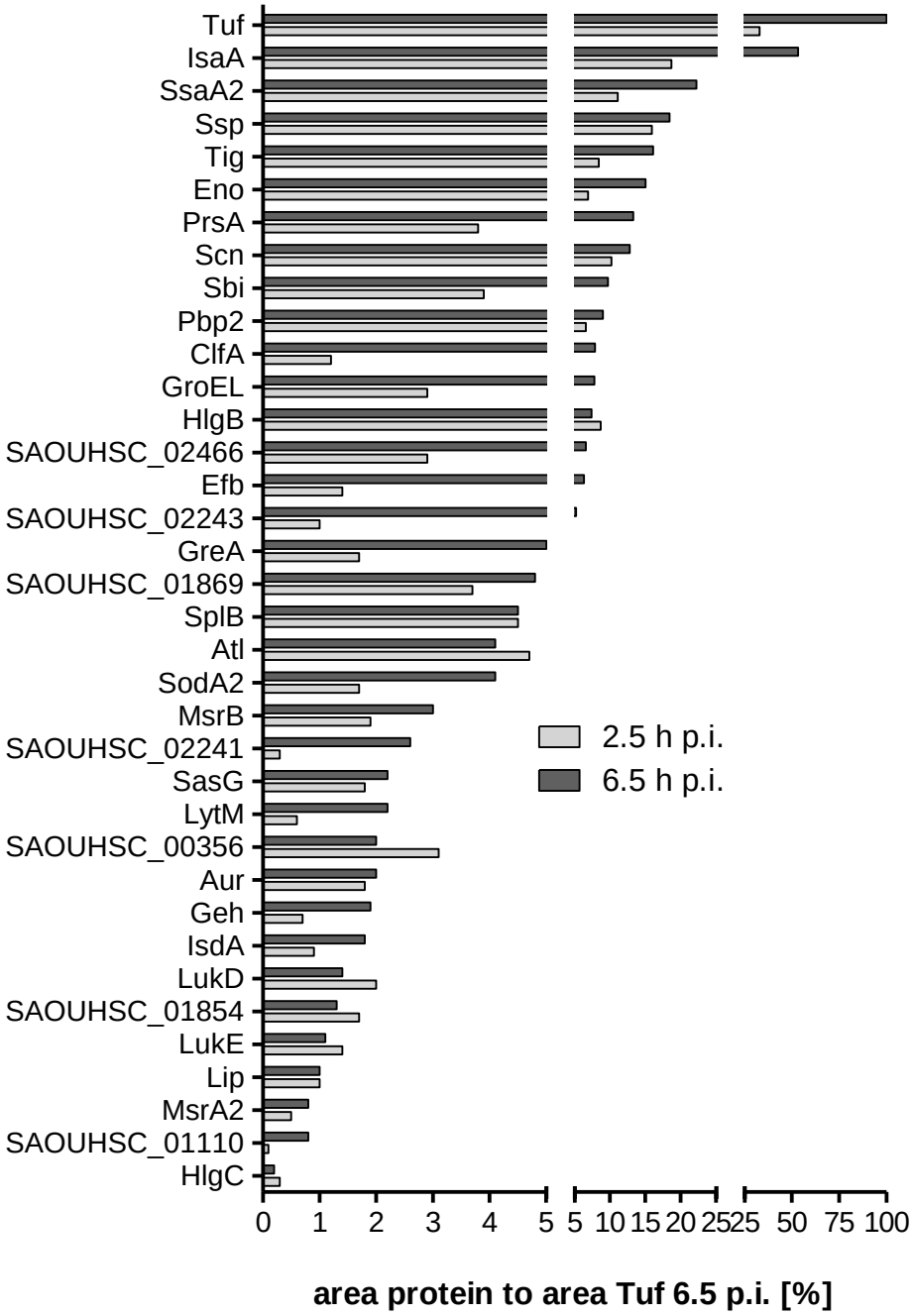

Figure 62. Relative comparison of protein abundance determined by MRM. *Average values of protein abundance (normalized areas) were related to the normalized area of protein Tuf at 6.5 h p.i.*

The lowest abundant proteins were HlgC, fibrinogen-binding protein-like protein SAOUHSC_01110, MsrA2, Lip, and LukE (Figure 62). Accordingly, none of these five proteins was detected in all BR, secreted HlgC even just once. Extracellular Lip and LukE could not be quantified as the results for single replicates differed too much, probably due to peak areas close to detection limit. Two secreted proteins SsaA2 and IsaA belonged to the five most abundant proteins 2.5 h and 6.5 h after infection (Figure 62, for localization see Table 12). Other extracellular proteins were detected with relatively small areas. Furthermore, it is conspicuous that all quantified cytoplasmic proteins Tuf, Tig, Eno, GroEl, GreA, and MsrB not only showed comparatively high abundance (except of GreA and MsrB), but were all found with increased areas 6.5 h *p.i.* probably resulting from increased bacterial numbers caused by intracellular replication. The cell wall anchored protein Ssp was the third most abundant protein 6.5 h *p.i.* and the fourth most abundant protein 2.5 h *p.i.* (Figure 62). The other cell wall proteins ClfA, IsdA, hypothetical protein SAOUHSC_01854, and SasG were detected with relatively small areas and were, thus, not detected in all samples. Membrane associated proteins Pbp2, PrsA, and truncated MHC class II analog protein SAOUHSC_02466 were all detected in the intermediate abundance range, and all of them increased in levels during ongoing infection. Proteins peptidase propeptide SAOUHSC_00356, hypothetical protein SAOUHSC_01869, MsrA2, Scn, and Sbi could not be significantly assigned to certain localization inside *S. aureus* HG001 according to PSORT. As mentioned above, MsrA2 was one of the lowest abundant proteins and was, thus, detected in just one biological replicate, where it showed an increased level between 6.5 h and 2.5 h after infection. Sbi was found increased over time for all five BR. The other three proteins were not significantly regulated during internalization.

Proteome analysis of *Bordetella pertussis,* another intracellular pathogen

The results described above indicate the successful application of proteomics approaches in order to better understand molecular mechanisms of intracellular pathogens. We then used the knowledge acquired to investigate features of the human pathogen *B. pertussis* in a collaboration project with Yanina Lamberti and Maria Eugenia Rodriguez from the University of La Plata, Argentina. This Gram-negative bacterium causes the life-threatening disease pertussis (whooping cough). *B. pertussis* produces various toxins such as pertussis toxin, filamentous haemagglutinin, and tracheal cytotoxin. Lamberti and co-workers showed previously that *B. pertussis* is, similar to *S. aureus,* able to enter, survive, and replicate within human alveolar epithelial A549 cells (Lamberti et al., 2013). Furthermore, it is able to invade and replicate inside human macrophages. Within the project presented here, the effects of iron limitation on the pathogen's proteome and time-dependent proteome adaptations of bacteria that were internalized by THP-I cells (a human leukemic cell line) differentiated into macrophages were investigated. Iron starvation and internalization experiments with *B. pertussis* Tohama I and A549 cells were performed by the group in Argentina, proteome analysis was done in Greifswald. I was especially involved in supporting sample preparation for proteomics, data analysis from discovery approaches by spectral counting for both projects and analyzed selected virulence factors of *B. pertussis* in internalized samples by MRM. Manuscripts are in preparation now.

Proteomic changes caused by iron limitation

Iron limitation is a challenge that pathogens have to face after internalization by the host. During internalization of *S. aureus* HG001 by A549 cells, bacterial proteins enabling iron acquisition from the host such as the monooxygenase (IsdI), SAOUHSC_02430 involved in iron binding, the iron uptake transporter SAOUHSC_00749, and the iron transporter EfeM were increased in level over time (Figure 48). Here, the proteome patterns of *B. pertussis* grown under iron-excess and iron-depleted conditions were compared. Bacteria were cultivated in Stainer-Scholte (SS) liquid medium without iron [depletion with cation exchange resin Chelex 100 (Bio-Rad, Hercules, CA, USA)] or with additional 36 μmol/L iron under iron-replete conditions. Analyzing three biological replicates of each of the two conditions, in total 926 proteins were identified and quantified using spectral counting. Among them 232 proteins were found in different levels between iron-limitation and iron-excess (cut-off for regulation: absolute fold change >1.5 and p-value <0.05). During iron limitation, 113 proteins decreased in level, and 119 proteins increased in amount compared to the control. Iron limitation resulted in modulation of metabolic enzymes. Proteins involved in DNA replication, repair, and transcription as well as ribosomal proteins showed lower levels in bacteria grown under iron-restricted conditions. However, proteins responsible for central intermediary metabolism and carbon utilization were found in higher amounts compared to bacteria, which were provided with iron in the medium. As expected, proteins required for iron acquisition showed higher abundance in the proteome of

B. pertussis cultivated in iron-depleted medium. For example, hemin import ATP-binding proteins BhuT, BhuS, and BhuR as well as alcaligin receptor FauA and putative siderophore receptors BfrB and BfrI showed higher levels during iron starvation. Additionally, two proteins, AfuA and IRP1-3, which are likewise known to be iron-regulated, were increased. A further group of differentially regulated proteins included factors involved in oxidative stress response. The alkyl hydroxyperoxide reductases AhpC and AhpD showed increased levels in iron-starved bacteria. Further, the superoxide dismutases SodA and HslO, a predicted redox regulated chaperonin, were found increased under these conditions. Further, biofilm formation and virulence seemed to depend on iron availability. Some proteins involved in biofilm formation were found in higher abundance for iron-starved *B. pertussis*. In contrast to this, some virulence factors exhibited reduced levels for bacteria grown during iron-limitation. Among them were adhesins such as filamentus hemagglutinin FHA and fimbriae (Fim). In addition the bacterial toxins adenylate cyclase (CyaA) and pertussis toxin (PtxA) were found in reduced levels during iron starvation. Similar results were observed for three members of the type IV secretion system required for secretion of PT (PtlE, PtlF, and PtlH) as well as for other virulence factors such as the autotransporters TcfA, BrkA, and Vag8. Intensities, ratios, and p-values for all quantified proteins and three BR are available as Supplementary_Material_Table_13_B_pertussis_iron_limitation_spectral_counting.xlsx.

Proteome analysis of intracellular B. pertussis

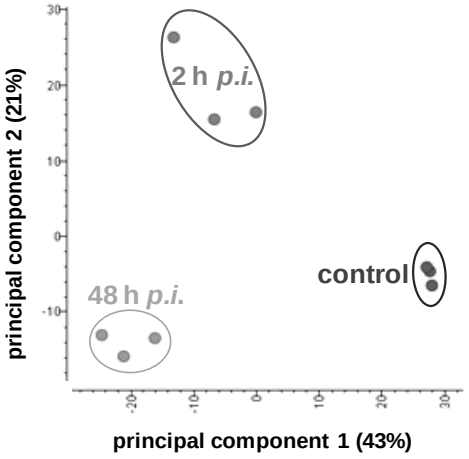

Figure 63. Principal component analysis of internalized *B. pertussis* Tohama I and non-internalized control. *Variances of each three biological replicates for the three conditions are displayed.*

THP-I cells, which were differentiated into macrophages by preincubation with 20 nmol/L of phorbol 12-myristate13-acetate, were infected with *B. pertussis* Tohama I for 2 h and 48 h. Other than for GFP-expressing *S. aureus*, it was not feasible to enrich bacteria from host debris by cell sorting. They were instead isolated using a sucrose gradient. Bacteria grown in Dulbecco's Modified Eagle's Medium (DMEM) medium supplemented with BSA served as control. Thus, the actual number of bacteria per sample was not determined and likely differed between the three sampling points. Normalization occurred by digestion of equal protein amounts and median-normalization of spectral counts after MS analysis. In total 763 bacterial proteins were identified in infected cells and the control. As described by Lee and coworkers, also proteins which revealed no spectral counts in one of the conditions were

included in the analysis and their "0" spectral counts were replaced by "0.1" to allow further calculations and comparison of the samples (Lee et al., 2012). Principal component analysis of three biological replicates revealed a clear separation into control, 2 h, and 48 h after infection (Figure 63). It became obvious that control replicates clustered closer together than the internalized samples which contain contaminations with human proteins. The control bacteria did not have contact to the host cells and therefore, no human proteins were in the control sample different to the internalized samples. Since it was shown for *S. aureus* that the preparation and sampling influences the control, it was not utilized for further functional analysis. In order to analyze general effects during ongoing internalization, Voronoi-like treemaps were created from ratios of normalized spectral counts between internalized bacteria 48 h and 2 h after internalization (Figure 64). Proteins involved in protein biosynthesis such as ribosomal proteins were decreased in level during ongoing infection. Oxidative stress and central carbon metabolism were slightly increased in level 48 h compared to 2 h after infection. Also proteins involved in valine degradation were more abundant at the later point in time after infection (Figure 64, Supplementary_Material_Table_14_B_pertussis_internalized_spectral_counting.xlsx).

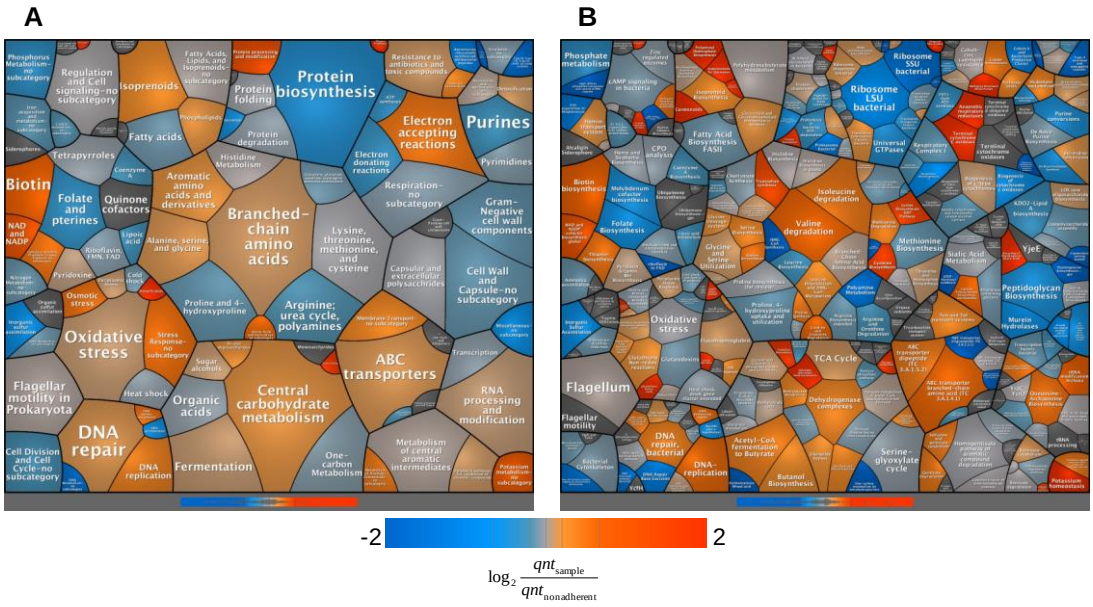

Figure 64. Voronoi-like treemap of *B. pertussis* Tohama I presenting ratios 48 h/2 h after infection by macrophages. *Mean data from three biological replicates for two functional category levels [(A) level 2, (B) level 3] from the SEED (Overbeek et al., 2005) are displayed. Red colored indicate increased protein levels 48 h p.i., blue colors indicate decreased protein levels, and gray colors show pathways whose proteins were not changed in level during ongoing infection. Treemaps are also provided as Supplementary_Material_04_Voronoi-like_treemaps.pdf to allow zooming.*

Since some interesting virulence proteins were present in low amount, the more sensitive MRM method was employed in order to validate the results. Label-free MRM analysis was performed without standard proteins. However, distinct peaks could be detected for the targeted proteins.

Relative abundance values (48 h/2 h *p.i.*) were calculated (Figure 65). Data presented in Figure 65 indicate the need for proper normalization due to the fact that human proteins might prevail in internalized samples and influence the data analysis. Spectral counts from shotgun analysis were median-normalized over the replicates correcting for differences in sample preparation. Since only few proteins were selected for MRM, such median-normalization is not possible during MRM analysis. A further normalization strategy utilizes sample cell counts, but since the exact number of bacteria was not known and may differed between the samples as it was concluded from the PCA plot (Figure 63), it was not possible to normalize on this value. However, the two proteins glutamate dehydrogenase (GdhA) and phosphate acetyltransferase MaeB, which were known to fulfill housekeeping functions, were added to the analysis. As expected, normalized spectral counting values were highly similar at 2 h and 48 h after infection. Thus, the average values of these two proteins were used to normalize MRM data.

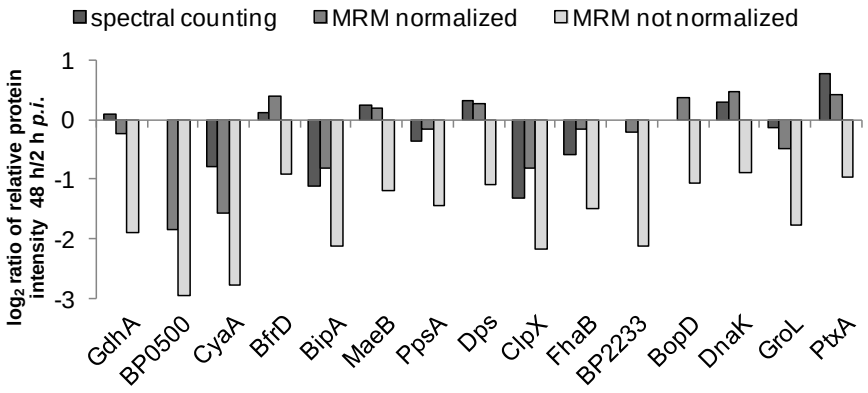

Figure 65 Relative abundance levels of proteins from internalized bacteria as ratio between 48 h and 2 h after infection. *Values were obtained from spectral counting of shotgun MS data or from peak areas of MRM data. MRM data were not normalized (MRM) or normalized on the average area values of the two housekeeping proteins glutamate dehydrogenase (GdhA) and phosphate acetyltransferase MaeB (MRM normalized). Mean values from three biological replicates are displayed.*

As seen in Figure 65 trends in regulation between 2 h and 48 h after internalization were similar for most proteins when comparing spectral counts and normalized MRM data. Non-normalized MRM data differed strongly from the other two analyses. Three proteins were not found in the shotgun approach [uncharacterized proteins BP0500 and BP2233, and putative outer protein (BopD)]. Only values for GdhA showed different direction of regulation between 2 h and 48 h *p.i*. for shotgun and MRM analysis after normalization during ongoing internalization. But the differences in levels were very low and not significant. Interestingly, the toxin PtxA was increased over time which is opposite to the results obtained from iron limitation. It is likely that *B. pertussis* needs to struggle with iron limitation inside the host. But probably other regulatory mechanisms play a role then. Decreased trends during ongoing internalization were observed for example for ATP-dependent Clp protease (ClpX), the toxin CyaA, and putative outer membrane ligand binding protein BipA (Figure 65).

Host response to infection with S. aureus

Method optimization for improved detection of host cell proteins

In order to characterize also the proteome response of host cells to *S. aureus* infection, our standard internalization assay (Pförtner et al., 2013) illustrated in Figure 8 had to be modified (Figure 66). The begin of the infection setup using *S. aureus* HG001 pMV158GFP and A549 cells was performed as illustrated in Figure 8 (Figure 66). As a new modification in the experimental setting, while sampling, host cells were not lysed using a detergent but detached from the plate with trypsin (Figure 66C). As TEM analyses already indicated that not all host cells carry bacteria after exposure, the intact infected host cells were sorted from non-infected host cells in order to elucidate the effect of intracellular bacteria to host cells. This was achieved using the FACSAria to separate hourly between 1.5 h and 6.5 h *p.i.* infected A549 cells (GFP-positive by the use of GFP-expressing *S. aureus*) from those without bacteria (GFP-negative) by the use of GFP hourly between 1.5 h and 6.5 h after internalization Both fractions were sorted in parallel into separate reaction tubes (Figure 66C). To test if pure contact to *S. aureus* already alters the host cell proteome in comparison to pure cell culture medium, another group of control cells was employed (control). These cells were not infected with bacteria but incubated with sterile master mix containing fresh pMEM instead of bacterial culture. Further procedure was identical including same sampling steps and flow cytometry based cell sorting to avoid any bias originating from sample processing.

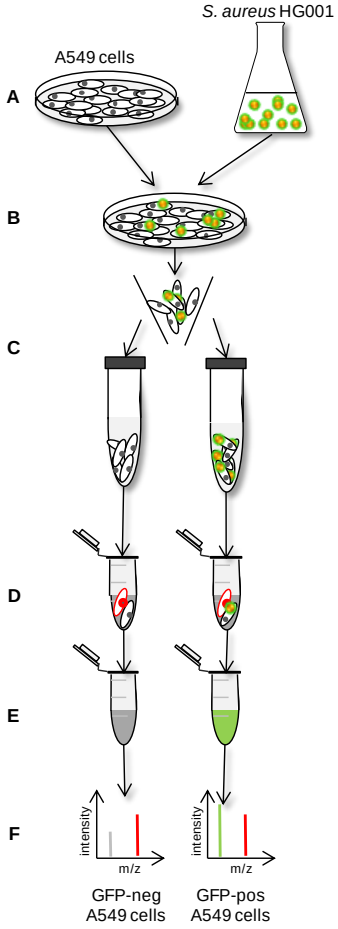

Figure 66. Workflow for proteome analysis of infected A549 cells. *A549 cells were infection with S. aureus HG001 pMV158GFP (A,B). After cell sorting of intact host cells (C), GFP-positive and GFP-negative cells were spiked with heavy labeled control cells (D) prior to cell lysis, tryptic digestion (E), and LC-MS/MS analysis for subsequent SILAC quantification.*

After cell sorting amounts of cells were counted for each replicate and type of cells. A heavy labeled standard of control cells was spiked to each sample in equal amounts (Figure 66D) prior to reduction, alkylation and protease digestion (Figure 66E) to allow relative quantification between the points in time using the SILAC method after nanoLC-MS/MS acquisition (Figure 66F).

Proteomic adaptation of A549 cells during early infection

Overview of proteome response of the host to exposure to *S. aureus* HG001

In order to investigate possible distinct proteome changes due to contact to *S. aureus* or internalization of these bacteria, three groups of A549 cells were analyzed separately. As TEM analyses revealed only a small percentage of infected A549 cells, cells which actually carried *S. aureus* (GFP-positive) were separated from those which just had contact to the bacteria for 1 h in the infection medium but were not invaded (GFP-negative). A549 cells which were not exposed to *S. aureus* but treated like infected cells served as control. From as few as 10^5 A549 cells more than 1,000 human proteins could be identified for each treatment group of A549 cells. Over all samples 737 proteins were quantified using SILAC with heavy labeled non-treated A549 cells between 2.5 h and 6.5 h after internalization. The sampling point 1.5 h *p.i.* was excluded from the analysis because sufficient numbers of GFP-positive cells could not be recovered. PCA of median ratios of three BR of each A549 cell group uncovered a distinct influence of simple contact to *S. aureus* HG001 (Figure 67). Data analysis of SILAC ratios to non-treated heavy labeled cells, illustrated that some host proteins changed in level with an absolute fold change >1.5 fold during the first six hours *p.i.* (Table 14). For example after 2.5 h, 114 proteins changed in level in GFP-negative cells and 199 proteins in GFP-positive cells with an absolute fold change of >1.5. In order to obtain an even more informative picture, proteins with a fold change higher than 1.2 were further taken into account when general trends of increased or decreased levels were investigated.

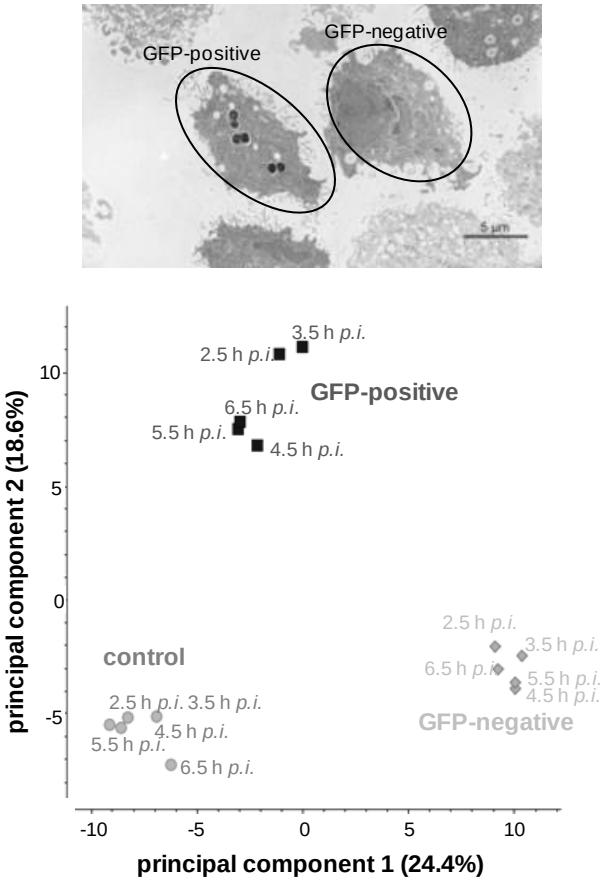

Figure 67. PCA of GFP-positive, GFP-negative, and non-infected A549 control cells. *Median response of A549 cells to infection. In order to obtain a general picture of host response to internalization of S. aureus, the median ratio of all points in time were used to calculate the distance between the different conditions. The TEM picture above the PCA blot illustrates the discrimination of GFP-positive (A549 cells with bacteria) and GFP-negative (A549 cells without bacteria) A549 cells.*

Table 14. Number of proteins detected with different fold changes between GFP-positive (GFP-pos), GFP-negative (GFP-neg) and non-infected A549 control cells (con, control). *Numbers of regulated proteins are given for an absolute fold change (FC) of 1.2 and 1.5.*

	FC > 1.2			FC <-1.2			FC >1.5			FC <-1.5		
sampling time	**GFP-neg/ con**	**GFP-pos/ con**	**GFP-pos/ GFP-neg**	**GFP-neg/ con**	**GFP-pos/ con**	**GFP-pos/ GFP-neg**	**GFP-neg/ con**	**GFP-pos/ con**	**GFP-pos/ GFP-neg**	**GFP-neg/ con**	**GFP-pos/ con**	**GFP-pos GFP-neg**
2.5 h *p.i.*	139	212	217	127	171	199	63	85	100	51	78	99
3.5 h *p.i.*	199	205	131	170	154	130	72	59	50	51	54	54
4.5 h *p.i.*	133	203	159	117	156	145	48	67	61	33	57	53
5.5 h *p.i.*	157	169	127	124	131	139	60	72	45	43	54	55
6.5 h *p.i.*	150	182	150	136	144	142	57	75	60	42	46	56

Taken together, there is a clear separation between GFP-positive, GFP-negative and control A549 cells. Even short contact with *S. aureus* HG001 (1 h) in the infection medium and contact to infected neighbor cells led to clear changes in the proteome pattern of GFP-negative A549 cells compared to the control. Single protein data for all quantified human proteins are provided as Supplementary_Material_Table_15_normalized_SILAC_ratios_of_A549_proteins_infected_with_S_aureus.xlsx.

Pathway analysis of differentially regulated proteins upon infection

In order to elucidate specific adaptation processes in infected or non-infected cells, proteome data of the three differently treated groups of A549 cells were independently compared (GFP-negative *vs.* control, GFP-positive *vs.* control, and GFP-positive *vs.* GFP-negative). Pathway analysis using Ingenuity Pathway Analysis (IPA) highlighted several canonical pathways from the curated Ingenuity literature database that were potentially overrepresented in the dataset (p-value) and further up-, non- or down-regulated in the A459 cells (fold change cut-off 1.2). A few of these pathways revealed slightly different results depending on contact or internalization of *S. aureus* HG001 (Figure 68). As already indicated, most regulated proteins were observed when comparing GFP-positive with control A549 cells. Examples for pathways with strongest up-regulation for GFP-positive against control cells are TCA cycle II, mitochondrial dysfunction, granzyme B signaling, NRF2-mediated oxidative stress response, and apoptosis signaling. The pathways RAN signaling, purine nucleoside *de novo* biosynthesis, and regulation of eIF4 and P70S6K signaling were induced to a greater extend in GFP-negative cells compared to GFP-positive cells. In GFP-positive cells purine nucleoside degradation II (aerobic), apoptosis signaling, clathrin-mediated endocytosis signaling, calcium signaling, and integrin signaling prevailed. Other canonical pathways for which slight changes were observed were tRNA charching, P70S6K signaling, protein ubiquitination pathway, and eIF2 signaling. In the GFP-positive A549 cells the eukaryotic initiation factor 2 (EIF2) was detected in less amounts than in GFP-negative

A549 cells. EIF2 signaling is known to be involved in the response to internalization of bacteria into epithelial cells (Sadighi Akha et al., 2013). Here, eight proteins of this pathway were decreased and four proteins increased in level in the A549 cells containing *S. aureus* compared to A549 cells which were not infected.

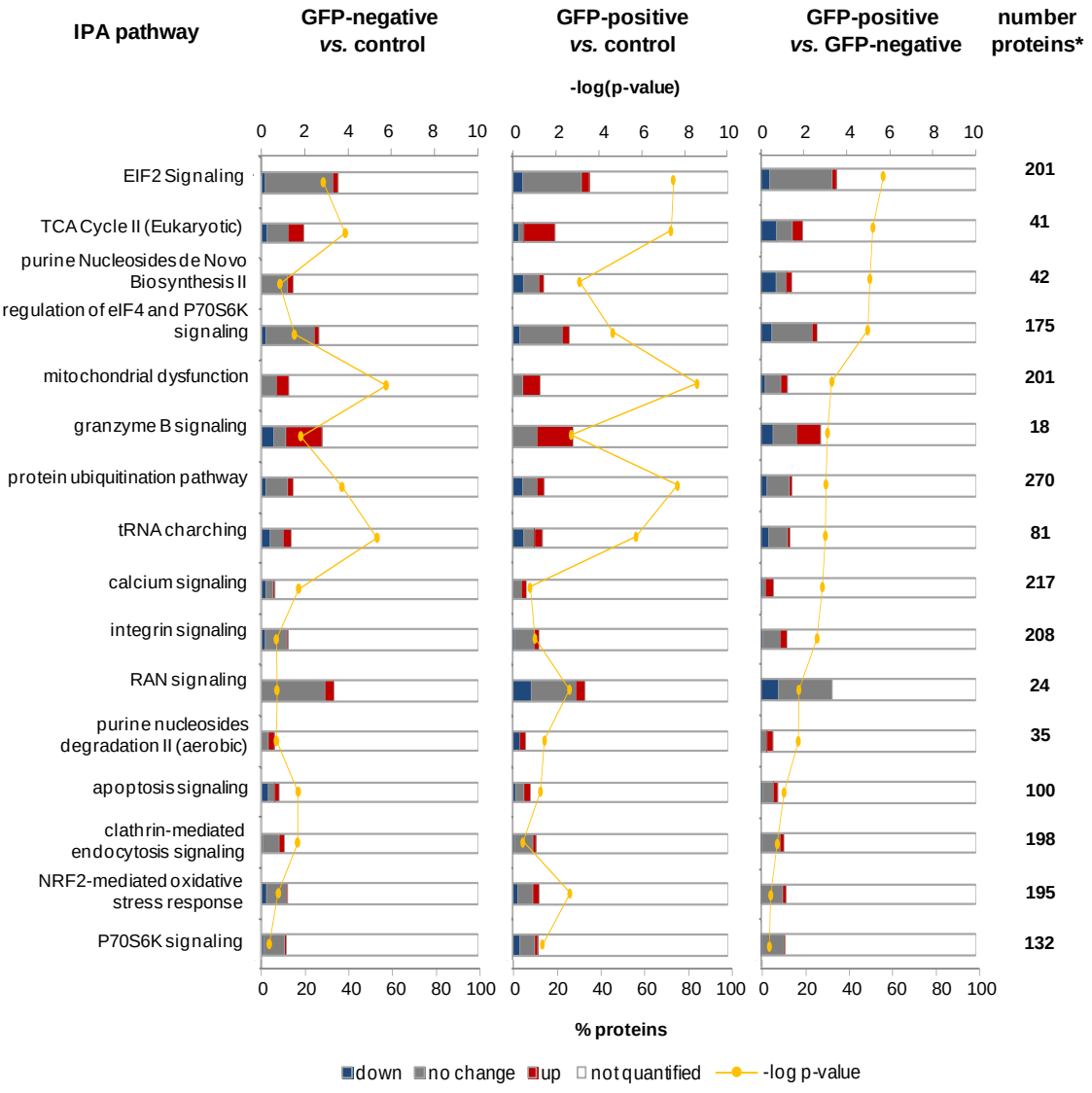

* number of proteins assigned to the pathway by IPA

Figure 68. Changes in selected pathways of three different groups of A549 cells. *Time-resolved comparison of proteomic changes of GFP-positive, GFP-negative, and control-cells. Cut-off for regulation was set to an absolute fold change of 1.2. Assignment of proteins to pathways was accomplished with IPA. P-values calculated by IPA correlate to the numbers of proteins which could be assigned to the pathways in the reference set of IPA.*

Time-resolved analysis of selected pathways in GFP-positive A549 cells

Having analyzed the bacterial adaptation to internalization by A549 cells (compare "Time-resolved analysis of *S. aureus* HG001 internalized by A549 cells"), especially the time-resolved protein regulation of the GFP-positive fraction which carried the bacteria compared to A549 cells without contact to bacteria was investigated. As only relatively few human proteins were detected due to the very low number (about 10^5) of infected host cells available, two additional experiments were performed to support pathway data.

A stronger regulation of mitochondrial proteins was observed in infected A549 cells compared to non-infected control cells after internalization (Figure 68, Figure 69). Glutathione-disulfide reductase (GSR), cytochrome C (CYC S), peroxiredoxin 3 and 5 (PRXD3, PRXD5), and NADH dehydrogenase iron-sulfur protein 8 (NDUFS8) were detected in higher levels in GFP-positive A549 cells. GSR, PRXD3, and PRXD5 are central enzymes of cellular antioxidant defense (Figure 69A). NDUFS8 is involved in the mitochondrial electron transport and the response to oxidative stress. On the other hand, the protein DJ-1 (PARK7), succinate dehydrogenase flavoprotein subunit, mitochondrial (SDHA), and apoptosis-inducing factor (AIFM1) were less abundant in the GFP-positive population (Figure 69A). In order to validate apoptosis activation *via* CYC S and AIFM1 additional Western Blots with antibodies against caspase-3, -8, -9, and -10 for control, GFP-positive and additionally GFP-negative A549 cells were conducted. Distinct band for caspase-3, -8, and -10 were not observed. Only for caspase-9 the presence of the cleaved and therefore activated form (Figure 69B) was detected. At 2.5 h *p.i.* GFP-negative as well as GFP-positive A549 cells showed signals which could be assigned to the cleaved caspase-9 form indicating early apoptosis. The additional band disappeared after 6.5 h.

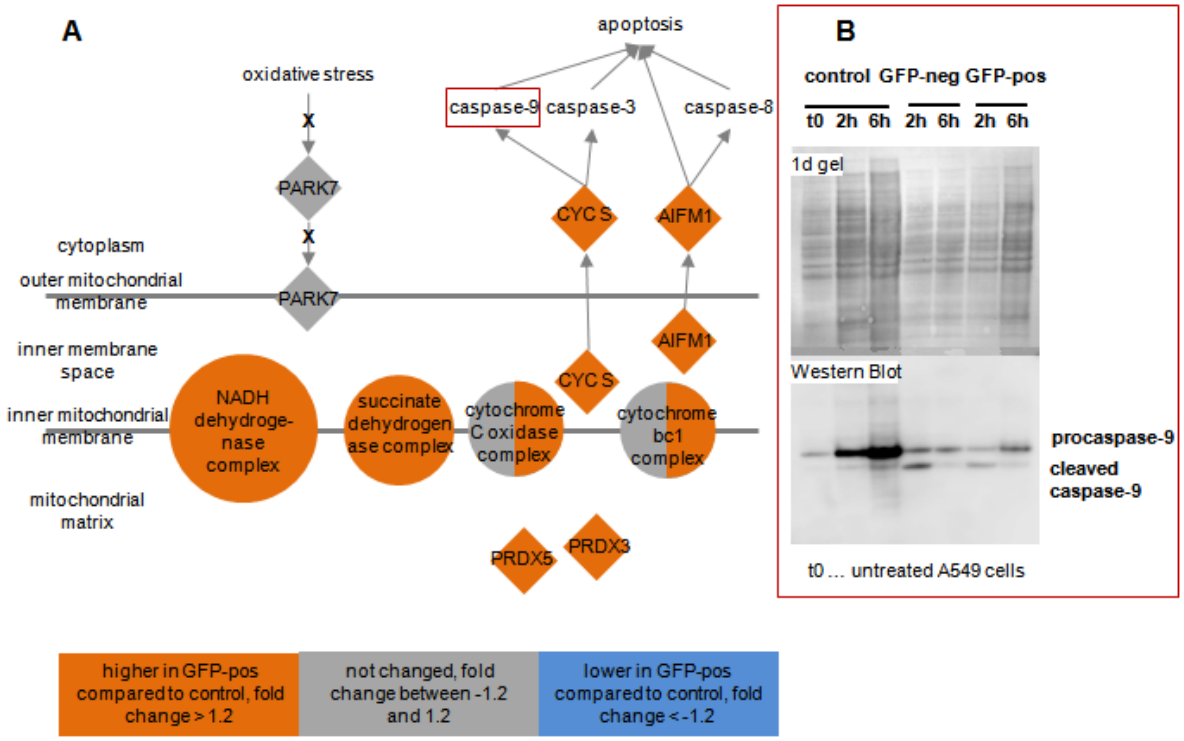

Figure 69. Regulation of mitochondrial proteins. *(A)Simplified scheme of regulated proteins associated to pathways performed by IPA. Red fields show proteins increased in GFP-positive (GFP-pos) cells, blue fields those lower in GFP-positive cells compared to control cells. Protein identifiers derived from UniProt. Median values from three BR are displayed. (B) With an additional 1D gel (upper picture, ink staining) and Western Blot (lower blot) with caspase-9 antibody the cleaved form of this caspase was detected after 2.5 h in A549 cells with contact to S. aureus (GFP-positive and GFP-negative). NADH dehydrogenase complex is represented by NDUFA5 and NDUFS8, succinate dehydrogenase complex by SDHA.*

The IPA pathway of ubiquitination of proteins showed few changes in protein regulation when comparing GFP-positive *vs.* control A549 cells after internalization (Figure 70A). Since some proteins showed changed levels, selected subunits of the proteasome which transform the proteasome into the immunoproteasome were put into focus. Since the proteins of the immunoproteasome were not detected by MS, qRT-PCR of the three missing subunits of the complex namely PSMB8, PSMB9, and PSBM10 was performed. Increased fold changes of about two between infected and non-infected A549 cells after 6.5 h compared to 2.5 h post-infection were observed for all three subunits (Figure 70B). Here, the mixture of GFP-positive and GFP-negative A549 cells was investigated in the infected groups, as cell sorting is not fast enough as required for transcriptome analysis.

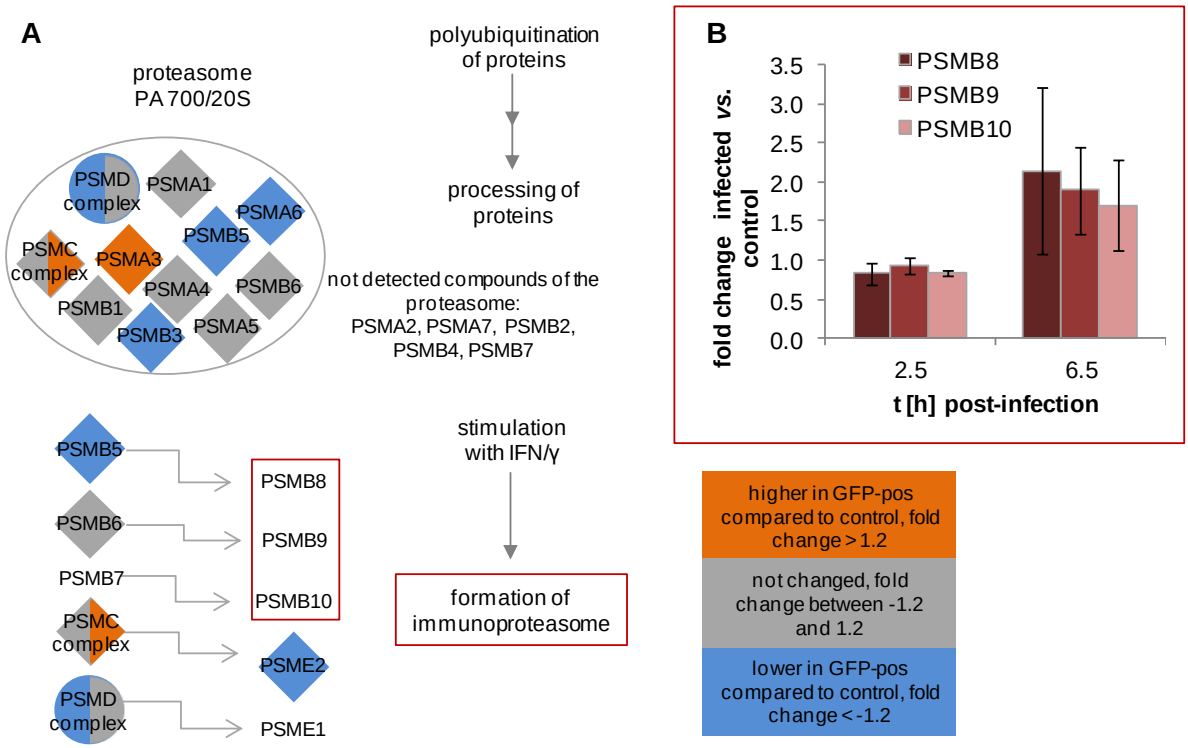

Figure 70. Regulation of the immunoproteasome. *(A) Simplified scheme of regulated proteins associated to pathways done by IPA. Red fields show proteins increased in GFP-positive (GFP-pos) cells, blue fields those lower in GFP-positive cells compared to control cells. Protein identifiers derived from UniProt. Median values from three BR are presented. (B) With additional qRT-PCR an increased fold change of subunits of the immunoproteasome (PSMB8, PSMB9, and PSMB10) after 6.5 h was observed. PSMC complex contains values for proteins PSMC1-PSMC6. PSMD complex contains values for proteins PSMD13, PSDE, PSMD2, and PSMD6.*

The pathway of clathrin-mediated endocytosis signaling was also regulated differentially when comparing differences between GFP-positive and control cells (Figure 71). In general, proteins belonging to this pathway were higher abundant in those cells which had contact to *S. aureus*. Protein substrate cortactin (SRC) and heat shock cognate 71 kDa protein (HSPA8) were present in higher amounts in GFP-positive compared to control cells.

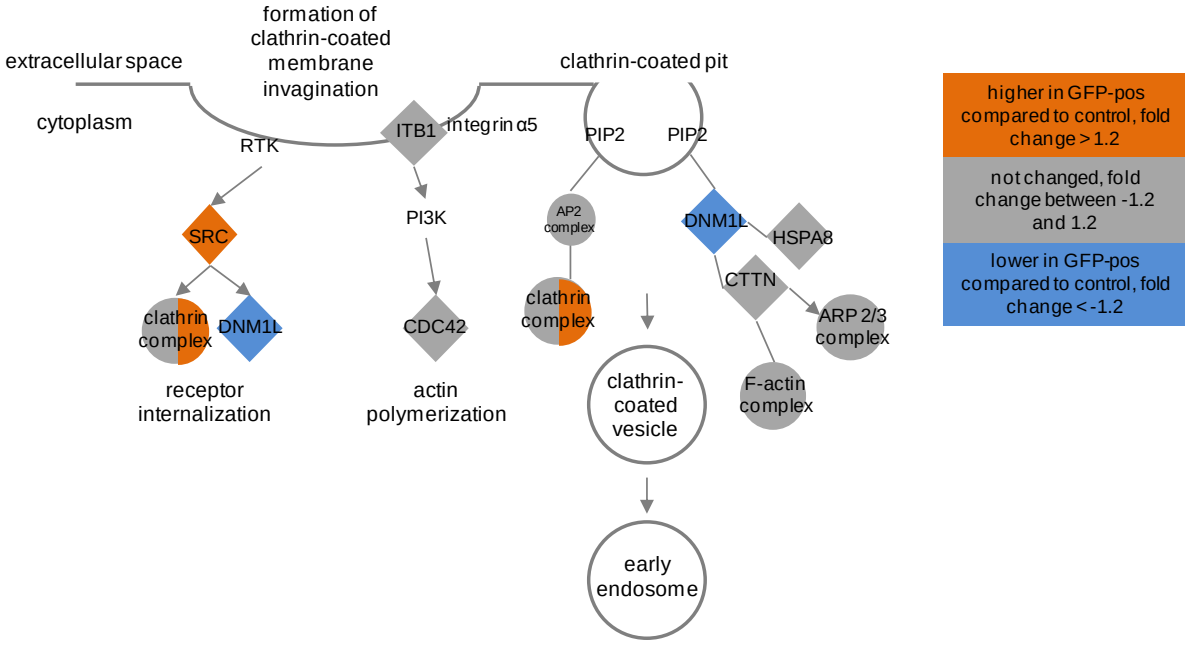

Figure 71. Clathrin-mediated endocytosis signaling. *Simplified scheme of pathway with association of proteins to pathway according to IPA. Red fields show proteins increased in GFP-positive (GFP-pos) cells, blue fields those lower in GFP-positive cells compared to control cells. AP2 complex contains values for proteins AP2A1 and 2. F-actin complex contains values for proteins ACTA1, ACTG1, ACTN1, and 4. ARP2/3 complex contains values for proteins ACTR2 and 3, and ARP3, 4, and 5. Clathrin complex contains values for proteins CLTA and CLTC. Protein identifiers derived from UniProt. Median values from three BR are presented.*

Secretion of cytokines by A549 cells

As the results presented above suggest that simple contact to *S. aureus* leads to proteome changes, the secretion of cytokines into the cell culture supernatant of A549 cells after infection with *S. aureus* (GFP-positive and GFP-negative host cells together) was investigated. The cytokine secretion in the internalization setting was compared to that of non-infected control cells with the help of a fluorescence based bead assay set for eleven cytokines. The cytokine secretion was investigated hourly between 1.5 h *p.i.* and 6.5 h *p.i.* in parallel to the host proteome analysis (2.5 h *p.i.* until 6.5 h *p.i.*). Additionally these mediators could be quantified even 24.5 h *p.i.* and 48.5 h *p.i.* which was not possible on proteome level as the number of GFP-positive cells was not sufficient at these later time point.

Except of IL-6, which was measured close to detection limit (below 10 pg/mL) during the first 6.5 h after internalization, all cytokines were detected in supernatant of infected A549 cells directly 1.5 h post-infection. However, IL-6 was clearly increased after 24.5 h. A slight decrease in abundance was observed for all cytokines starting from 2.5 h *p.i.* except of IFN-γ and IL-8. For IFN-γ the difference between infected and non-infected cells was the highest (about 300 pg/mL) and stayed almost constant over time. During the first 6.5 h *p.i.* a distinct increase of the pro-inflammatory chemokine IL-8 compared to supernatants from non-infected cells was detected. Next most abundant cytokines

were the pro-inflammatory IL-2, IL-1-β, TNF-α and TNF-β, as well as IL-4. The anti-inflammatory cytokine IL-10 was also detected at the early time points with amounts around 100 pg/mL and decreased further on as well. Cytokines detected in lower concentrations were IL-12 p70, and IL-5 (Figure 72). Most cytokines were not detected in cell culture supernatant of non-infected A549 cells. Only the chemokine IL-8 was secreted and accumulated in control cells but in distinctly lower amounts compared to infected cells. All other cytokines were detected in amounts below 100 pg/mL for non-infected A549 cells (Figure 73).

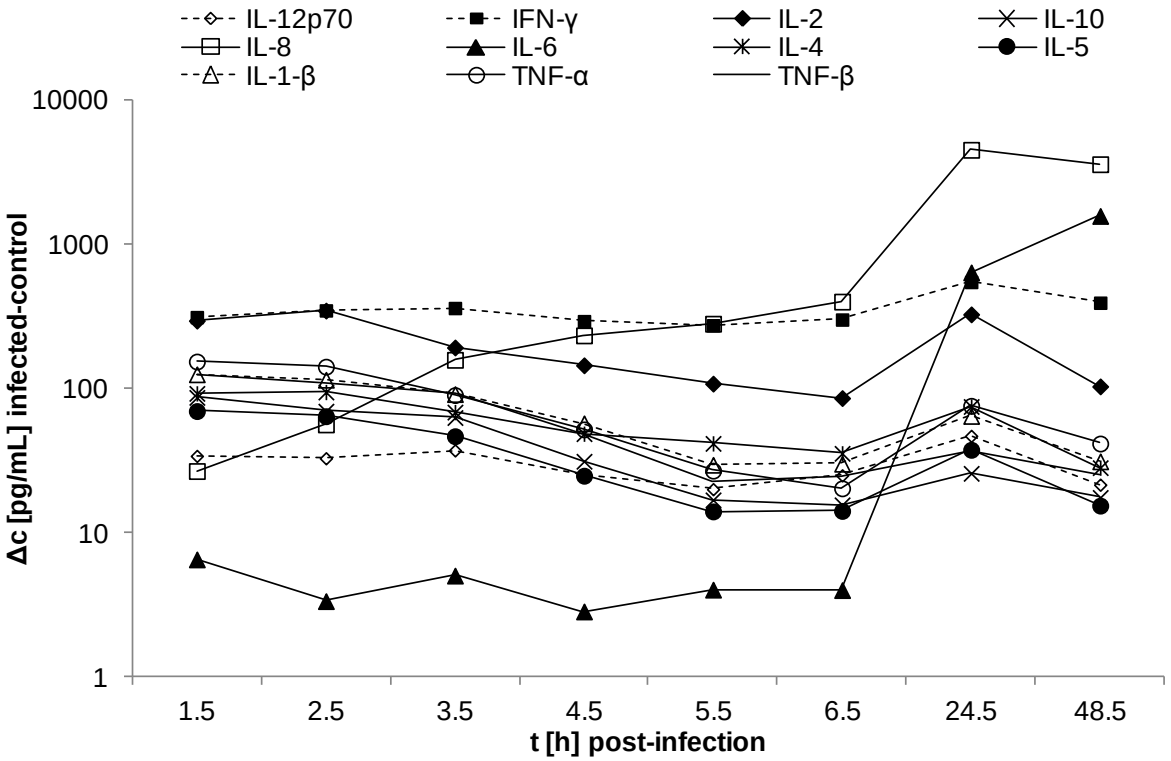

Figure 72. Time courses of eleven secreted cytokines measured in cell culture supernatant until 48.5 h post-infection. *Results are shown as difference between infected and non-infected control groups. Average values from five BR are depicted.*

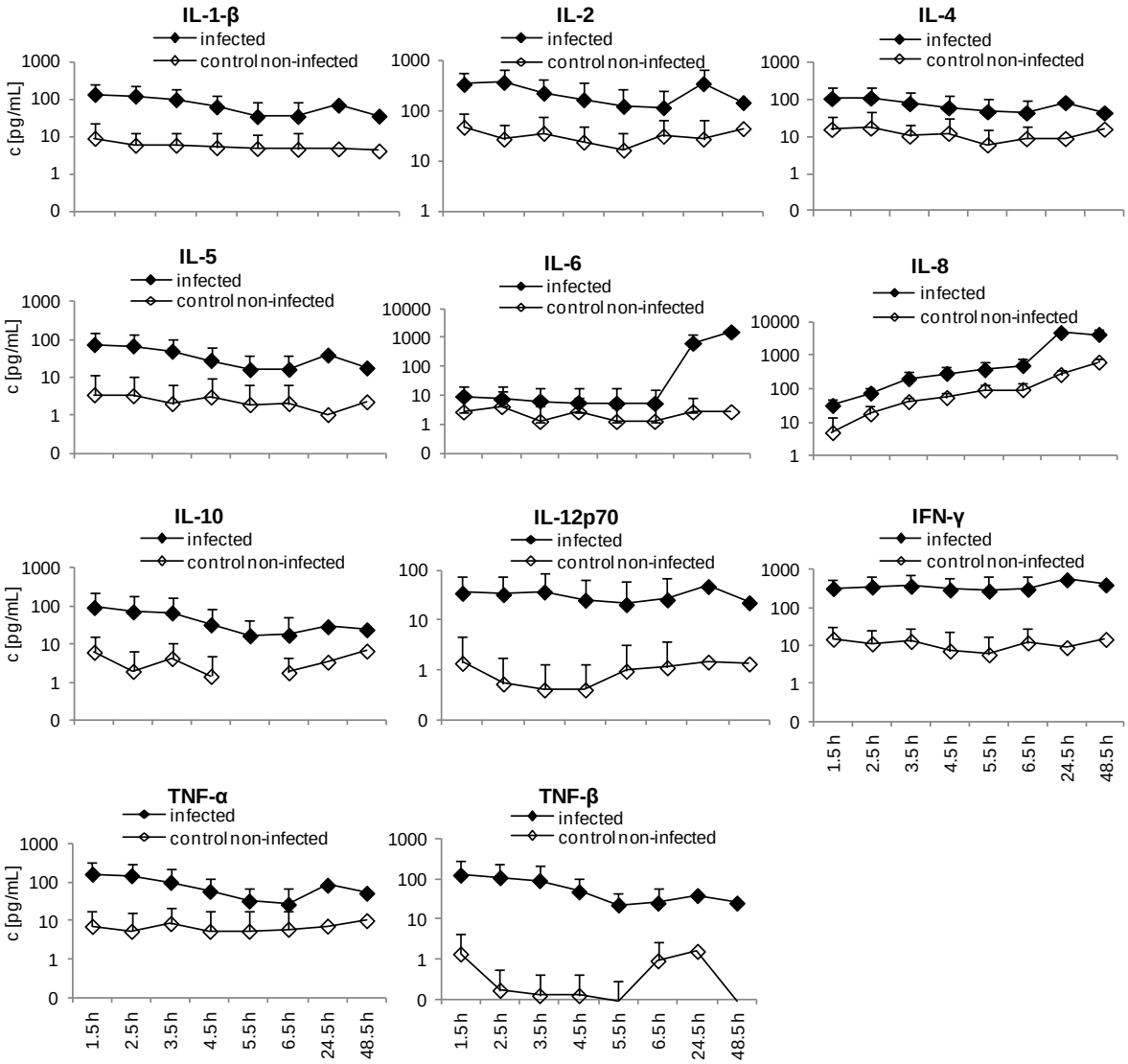

Figure 73. Comparative cytokine quantification from infected and non-infected A549 cells. *Average values and standard deviations (only up-direction) from five BR are displayed.*

These levels of secreted cytokines after infection of A549 cells with *S. aureus* HG001 pMV158GFP wild-type were compared with those measured after infection of A549 cells with the isogenic *ΔmenD* mutant of this strain. This mutant shows the phenotype of small colony variants which are adapted to intracellular long-term persistence. Early cytokine secretion of A549 cells after contact to an isogenic *ΔmenD* SCV mutant of *S. aureus* HG001 pMV158GFP was determined within the framework of Jörn Steinke's bachelor thesis performed in our laboratory (supervised by Henrike Pförtner) with my support in performing the cytokine assay. He performed the infection and cytokine assays similar to the approach presented in this study for the wild-type infection to allow comparisons. The *ΔmenD* mutant triggered almost no cytokine secretion after infection. The levels

were always below those of the wild-type. Again IFNγ and IL-8 were detected in highest levels also after infection with the SCV mutant. IL-4, IL-6, and IL-10 were almost not detected in the *ΔmenD* mutant Figure 74.

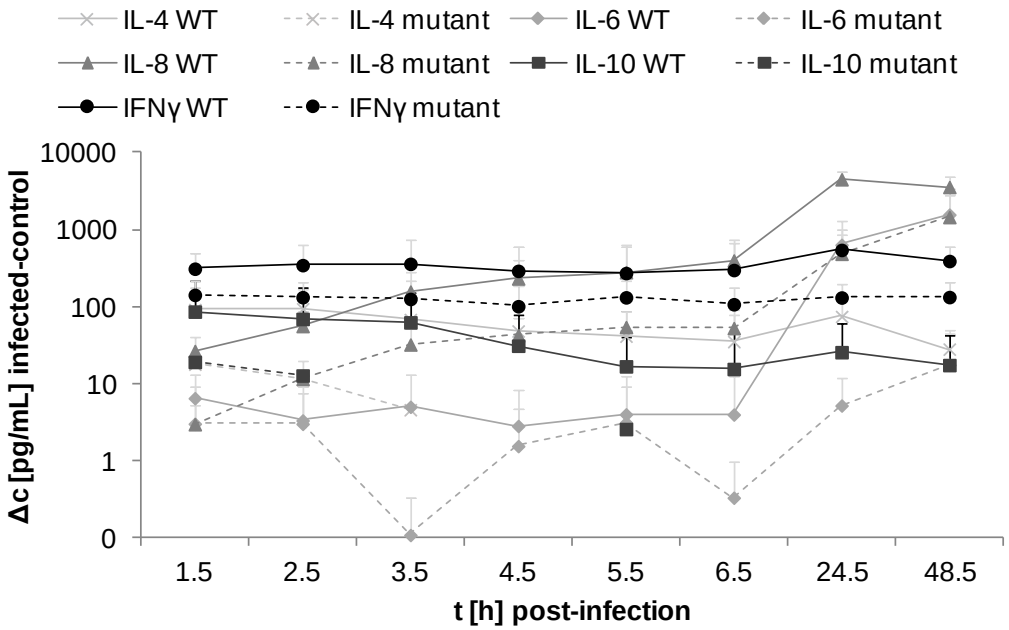

Figure 74. Cytokine secretion by A549 cells after infection with *S. aureus* HG001 pMV158GFP wild-type (WT, drawn through line) or its isogenic *ΔmenD* mutant (mutant, dotted lines). *Average values and standard deviations (WT five BR, mutant four BR) of the differences between levels of the infected A549 cells compared to the corresponding control are displayed over time.*

Analysis of phagosomal proteins after infection of S9 cells by *S. aureus* HG001

As fluorescence microscopy showed that some *S. aureus* HG001 cells were engulfed within phagosomes, it was expected that host proteins of this compartment are affected during early internalization. Further, some virulence associated proteins of *S. aureus* HG001 pMV158GFP which were detected in isolated phagosomes were regulated during ongoing time of infection. Therefore, potential time-dependent changes of phagosomal proteins should be investigated, too. Protein analysis of isolated phagosomes of infected S9 cells 2.5 h and 6.5 h *p.i.* revealed about 2,000 human proteins. A list containing data of all quantified human proteins is provided in Supplementary_Material_Table_16_human_proteins_from_isolated_phagosomes_of_S_aureus_HG001-infected_S9_cells_shotgun.xlsx. As shown in Table 15, 110 proteins could be assigned to phagosomal function according to earlier studies on phagosomes (Buschow et al., 2012, Jutras et al., 2008, Desjardins, 2003) and time-dependent intensity ratios were calculated. Analogous to the staphylococcal results (Figure 61), a detailed overview of function and time-dependent changes between 6.5 h and 2.5 h after infection is presented in Figure 75. Several proteins located inside the phagosomal lumen, phagosomal membrane proteins, and cytosolic proteins controlling phagosomal function were monitored. Almost no changes in protein abundance between these two sampling points were detected. Thus, it seems likely that phagosomes were already established until 2.5 h after infection. After uptake of bacteria, phagosomes mature and finally fuse with lysosomes prior to elimination of the bacteria. There are several markers for different stages. In this study typical markers for early endosomes [ras-related GTPases RAB5B_HUMAN and RAB5C_HUMAN, early endosome antigen 1 (EEA1_HUMAN)], late endosomes (mannose-6-phosphate receptors MPRD_HUMAN and MPRI_HUMAN, ras-related GTPase RAB7A_HUMAN], and phagolysosomes [lysosome-associated membrane glycoprotein 1 and 2 (LAMP1_HUMAN and LAMP2_HUMAN)] were discovered. LAMP-1 was found to be increased 6.5 h *p.i.* compared to 2.5 h *p.i.* together with Niemann-Pick C1 protein (NPC1_HUMAN) which catalyzes vesicular trafficking in late endosomes and lysosomes. Probably fusion with lysosomes to phagolysosomes is increased at later time points. In agreement with this conclusion also two lysosomal enzymes β-galactosidase (BGAL_HUMAN) and an acid protease cathepsin D (CATD_HUMAN) were detected with increased levels 6.5 h *p.i.* compared to the earlier sampling point. Many other lytic enzymes such as other cathepsins, peptidase, phosphatase or hexosaminidases did not change intensity levels during ongoing time of infection. Many of these enzymes function at low pH which is maintained by V-type ATPases of which seven factors were discovered. Fourteen ras-related GTPases which regulated phagosomal membrane trafficking and fusion were also detected in similar amounts in both time points. Only RAB8A_HUMAN was found increased in four of five replicates. Cytoskeleton proteins, more precise proteins associated with microtubules and actin, play a role in phagosome formation. There, actin regulatory protein CAP-G was detected decreased over time. Likewise decreased levels were

measured for protein 1433F_HUMAN, one of several similar adaptor proteins (1433B, E, G, S, T, Z) that regulate several signaling pathways (Table 15).

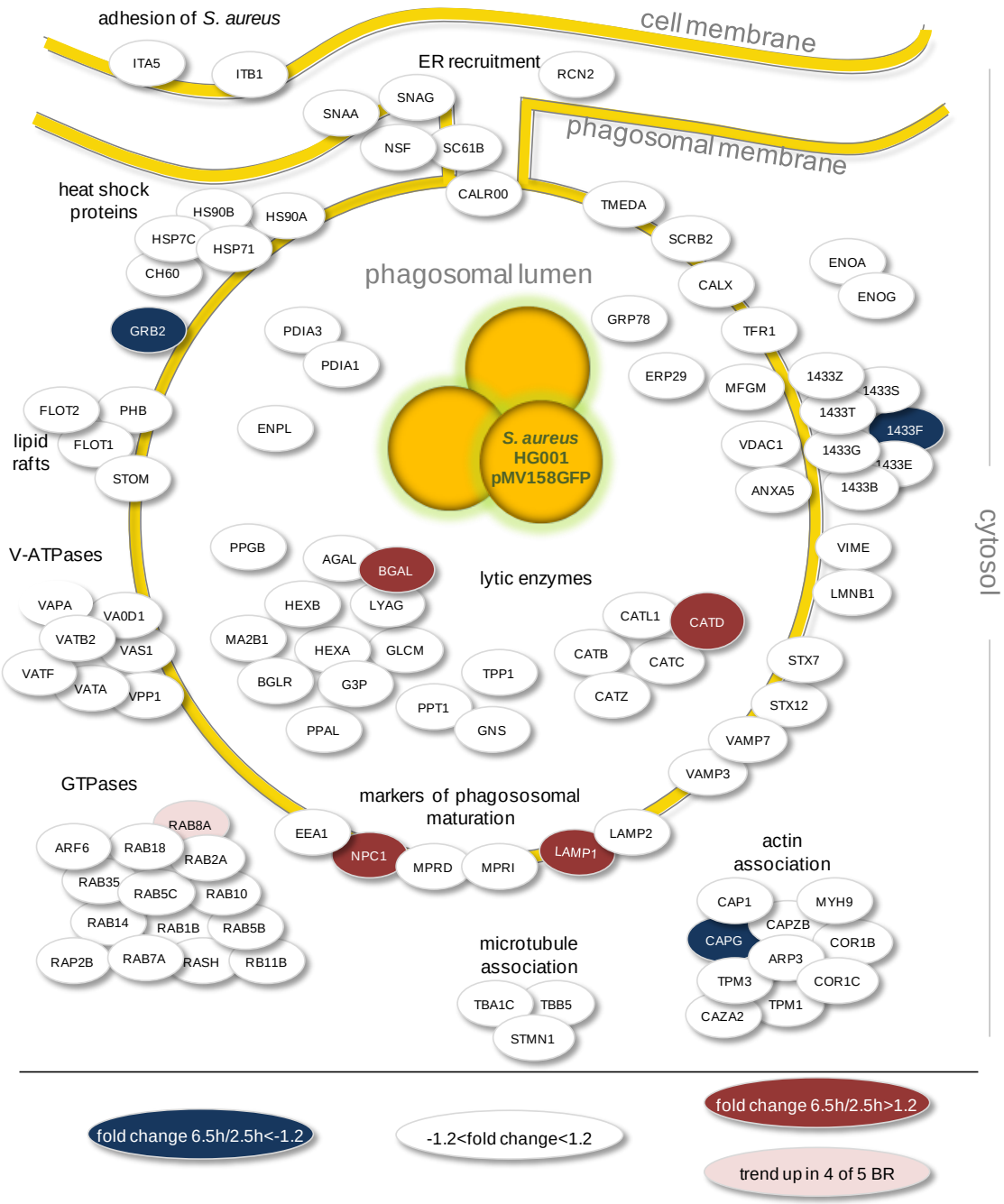

Figure 75. Phagosomal proteins. *Host cell phagosomal proteins were arranged by localization and principal function according to (Desjardins, 2003). Proteins additionally monitored in this study were arranged according to UniProt information (http://www.UniProt.org). Protein identifiers used in this figure derive from UniProt name without "_HUMAN" (Table 15). Fold change calculations of intensity values between 6.5 h and 2.5 h p.i. resulted in almost no significant regulations (white proteins). Proteins colored in red were found increased over time; proteins in blue were decreased over time.*

Table 15. Time-dependent changes in phagosomal proteins after infection by *S. aureus* HG001. *Ratios and fold changes of normalized protein intensities were calculated between 6.5 h and 2.5 h after infection. Proteins which were identified with more than one peptide or at least 10% sequence coverage were considered. Only proteins exceeding an absolute fold change of 1.2 were regarded as significantly different between the sampling points. Protein names derrived from the UniProt name shortened by elimination of "_HUMAN". CV (coefficient of variation), FC (fold change).*

protein name	UniProt ID	annotation	number of peptides	sequence coverage [%]	average ratio 6.5 h/ 2.5 h	FC from average ratio	CV ratio [%]
1433B	P31946	14-3-3 protein beta/alpha	6	34.1	0.92	-1.1	32.5
1433E	P62258	14-3-3 protein epsilon	8	43.5	0.80	-1.2	35.2
1433F	Q04917	14-3-3 protein eta	4	20.7	0.79	-1.3	29.7
1433G	P61981	14-3-3 protein gamma	4	27.9	0.92	-1.1	45.3
1433S	P31947	14-3-3 protein sigma	4	24.6	0.80	-1.2	51.1
1433T	P27348	14-3-3 protein theta	9	40.4	0.89	-1.1	40.5
1433Z	P63104	14-3-3 protein zeta/delta	6	34.3	0.90	-1.1	42.5
AGAL	P06280	alpha-galactosidase a	3	11.0	1.04	1.0	25.5
ANXA5	P08758	annexin a5	16	60.0	0.88	-1.1	48.5
ARF6	P62330	ADP-ribosylation factor 6	3	24.6	1.06	1.1	19.2
ARP3	P61158	actin-related protein 3	12	43.1	0.96	-1.0	21.6
ARSA	P15289	arylsulfatase A	3	8.9	1.09	1.1	51.8
BGAL	P16278	beta-galactosidase	8	15.1	1.26	1.3	17.9
BGLR	P08236	beta-glucuronidase	5	10.9	1.05	1.1	14.7
CALR	P27797	calreticulin	11	49.6	1.03	1.0	15.6
CALX	P27824	calnexin	11	21.6	1.25	1.3	45.9
CAP1	Q01518	adenylyl cyclase-associated protein 1	13	36.0	0.85	-1.2	31.9
CAPG	P40121	macrophage-capping protein	7	26.1	0.75	-1.3	20.3
CAPZB	P47756	F-actin-capping protein subunit beta	6	30.7	0.92	-1.1	32.9
CATB	P07858	cathepsin b	5	22.4	1.21	1.2	17.9
CATC	P53634	dipeptidyl peptidase 1	9	28.9	1.19	1.2	34.0
CATD	P07339	cathepsin d	12	40.3	1.33	1.3	18.0
CATL1	P07711	cathepsin l1	3	18.0	1.11	1.1	30.6
CATZ	Q9UBR2	cathepsin z	7	27.7	1.04	1.0	28.9
CAZA2	P47755	F-actin-capping protein subunit alpha-2	4	26.2	0.98	-1.0	27.6
CH60	P10809	60 kDa heat shock protein, mitochondrial	26	70.2	1.24	1.2	22.4
COR1B	Q9BR76	coronin-1b	3	6.1	0.92	-1.1	30.5
COR1C	Q9ULV4	coronin-1c	8	20.0	0.97	-1.0	33.0
EEA1	Q15075	early endosome antigen 1	3	2.6	1.08	1.1	7.6
ENOA	P06733	alpha-enolase	15	49.1	0.82	-1.2	41.8
ENOG	P09104	gamma-enolase	5	15.4	0.94	-1.1	48.0
ENPL	P14625	endoplasmin	29	46.8	1.07	1.1	13.7
ERP29	P30040	endoplasmic reticulum resident protein 29	7	33.7	1.15	1.2	17.2
FLOT1	O75955	flotillin-1	16	47.5	1.13	1.1	27.4
FLOT2	Q14254	flotillin-2	13	38.3	1.08	1.1	29.6
G3P	P04406	glyceraldehyde-3-phosphate dehydrogenase	12	57.9	0.93	-1.1	20.3
GLCM	P04062	glucosylceramidase	8	20.1	1.29	1.3	34.0
GNS	P15586	n-acetylglucosamine-6-sulfatase	9	24.6	1.13	1.1	21.9

protein name	UniProt ID	annotation	number of peptides	sequence coverage [%]	average ratio 6.5 h/ 2.5 h	FC from average ratio	CV ratio [%]
GRB2	P62993	growth factor receptor-bound protein 2	6	28.6	0.70	-1.4	31.7
GRP78	P11021	78 kDa glucose-regulated protein	17	35.2	1.13	1.1	17.2
HEXA	P06865	beta-hexosaminidase subunit alpha	8	17.6	1.12	1.1	23.1
HEXB	P07686	beta-hexosaminidase subunit beta	10	21.2	1.16	1.2	13.9
HS90A	P07900	heat shock protein hsp 90-alpha	12	23.0	0.81	-1.2	42.7
HS90B	P08238	heat shock protein hsp 90-beta	18	33.0	0.83	-1.2	41.8
HSP71	P08107	heat shock 70 kDa protein 1a/1b	19	47.9	1.01	1.0	41.8
HSP7C	P11142	heat shock cognate 71 kDa protein	22	55.1	1.10	1.1	42.4
ITA5	P08648	integrin alpha-5	7	9.4	1.17	1.2	32.6
ITB1	P05556	integrin beta-1	20	33.2	0.88	-1.1	20.8
LAMP1	P11279	lysosome-associated membrane glycoprotein 1	5	12.2	1.33	1.3	17.3
LAMP2	P13473	lysosome-associated membrane glycoprotein 2	3	7.1	1.13	1.1	20.5
LMNB1	P20700	lamin-b1	20	42.8	1.01	1.0	18.5
LRP1	Q07954	prolow-density lipoprotein receptor-related protein 1	6	1.5	0.94	-1.1	33.3
LYAG	P10253	lysosomal alpha-glucosidase	5	7.6	1.12	1.1	39.8
MA2B1	O00754	lysosomal alpha-mannosidase	9	12.2	1.24	1.2	19.1
MFGM	Q08431	lactadherin	3	13.4	1.10	1.1	45.6
MPRD	P20645	cation-dependent mannose-6-phosphate receptor	2	11.6	1.38	1.4	40.0
MPRI	P11717	cation-independent mannose-6-phosphate receptor	28	14.6	1.24	1.2	32.5
MYH9	P35579	myosin-9	56	36.5	0.97	-1.0	17.0
NDKB	P22392	nucleoside diphosphate kinase b	4	34.9	0.83	-1.2	43.1
NPC1	O15118	Niemann-Pick c1 protein	2	2.0	1.62	1.6	44.5
NSF	P46459	vesicle-fusing ATPase	5	6.9	1.00	1.0	17.7
PDIA1	P07237	protein disulfide-isomerase	17	42.7	1.07	1.1	14.8
PDIA3	P30101	protein disulfide-isomerase a3	19	48.5	1.16	1.2	20.2
PHB	P35232	prohibitin	15	75.4	1.20	1.2	29.1
PPAL	P11117	lysosomal acid phosphatase	2	5.0	1.25	1.3	32.4
PPGB	P10619	lysosomal protective protein	5	15.6	1.13	1.1	23.8
PPT1	P50897	palmitoyl-protein thioesterase 1	5	31.7	1.28	1.3	21.3
RAB10	P61026	ras-related protein Rab-10	3	16.5	1.14	1.1	47.7
RAB14	P61106	ras-related protein Rab-14	4	26.0	1.21	1.2	20.2
RAB18	Q9NP72	ras-related protein Rab-18	4	24.3	1.17	1.2	29.2
RAB1B	Q9H0U4	ras-related protein Rab-1b	6	41.3	1.38	1.4	29.1
RAB2A	P61019	ras-related protein Rab-2a	5	31.1	1.19	1.2	28.1
RAB35	Q15286	ras-related protein Rab-35	5	31.3	0.95	-1.0	27.3
RAB5B	P61020	ras-related protein Rab-5b	6	36.7	1.03	1.0	19.7
RAB5C	P51148	ras-related protein Rab-5c	5	38.4	1.09	1.1	36.4
RAB7A	P51149	ras-related protein Rab-7a	9	53.6	1.18	1.2	26.7
RAB8A	P61006	ras-related protein Rab-8a	5	27.1	1.35	1.4	33.7
RAP2B	P61225	ras-related protein rap-2b	4	35.5	0.90	-1.1	33.2
RASH	P01112	GTPase hras	4	26.5	0.85	-1.2	21.3
RB11B	Q15907	ras-related protein Rab-11b	8	43.1	1.11	1.1	8.3

protein name	UniProt ID	annotation	number of peptides	sequence coverage [%]	average ratio 6.5 h/ 2.5 h	FC from average ratio	CV ratio [%]
RCN2	Q14257	reticulocalbin-2	3	13.6	0.99	-1.0	24.1
SC61B	P60468	protein transport protein sec61 subunit beta	1	10.4	1.29	1.3	62.5
SCRB2	Q14108	lysosome membrane protein 2	3	6.5	1.24	1.2	23.3
SNAA	P54920	alpha-soluble nsf attachment protein	12	56.6	0.95	-1.0	21.3
SNAG	Q99747	gamma-soluble nsf attachment protein	7	29.8	0.99	-1.0	17.9
STMN1	P16949	stathmin	3	22.8	0.83	-1.2	40.2
STOM	P27105	erythrocyte band 7 integral membrane protein	7	36.5	0.98	-1.0	16.9
STX12	Q86Y82	syntaxin-12	4	22.1	1.40	1.4	33.2
STX7	O15400	syntaxin-7	3	14.9	1.18	1.2	39.7
TBA1C	Q9BQE3	tubulin alpha-1c chain	18	61.0	0.79	-1.3	36.9
TBB5	P07437	tubulin beta chain	5	14.6	0.76	-1.3	34.4
TCPA	P17987	t-complex protein 1 subunit alpha	22	55.9	0.87	-1.2	26.9
TCPB	P78371	t-complex protein 1 subunit beta	20	57.8	0.91	-1.1	30.0
TCPE	P48643	t-complex protein 1 subunit epsilon	18	43.8	1.11	1.1	48.7
TFR1	P02786	transferrin receptor protein 1	17	28.7	1.23	1.2	44.0
TMEDA	P49755	transmembrane emp24 domain-containing protein 10	5	31.5	1.21	1.2	40.1
TPM1	P09493	tropomyosin alpha-1 chain	4	17.6	1.06	1.1	40.1
TPM3	P06753	tropomyosin alpha-3 chain	2	8.1	0.95	-1.1	31.8
TPP1	O14773	tripeptidyl-peptidase 1	7	25.9	1.17	1.2	38.7
VA0D1	P61421	V-type proton ATPase subunit d 1	7	22.8	1.26	1.3	33.5
VAMP3	Q15836	vesicle-associated membrane protein 3	1	16.0	1.16	1.2	20.5
VAMP7	P51809	vesicle-associated membrane protein 7	3	13.2	1.17	1.2	55.5
VAPA	Q9P0L0	vesicle-associated membrane protein-associated protein a	4	31.3	1.00	1.0	11.4
VAS1	Q15904	V-type proton ATPase subunit s1	8	22.6	1.20	1.2	27.8
VATA	P38606	V-type proton ATPase catalytic subunit a	9	22.2	1.15	1.2	35.9
VATB2	P21281	V-type proton ATPase subunit b, brain isoform	6	20.2	1.20	1.2	34.6
VATF	Q16864	V-type proton ATPase subunit f	2	34.5	0.91	-1.1	64.6
VDAC1	P21796	voltage-dependent anion-selective channel protein 1	13	71.7	1.16	1.2	25.2
VIME	P08670	vimentin	25	61.8	1.34	1.3	34.1
VPP1	Q93050	V-type proton ATPase 116 kDa subunit a isoform 1	3	4.9	1.28	1.3	36.1

DISCUSSION

The development of effective vaccines and therapeutics for severe *S. aureus* infections requires the knowledge about the molecular background behind the interaction of this pathogen with the human host. Since it was known to even invade non-professional phagocytic cells (Garzoni and Kelley, 2009), this topic was put into focus of this thesis. Persistence inside these types of host cells is important for the bacteria, as they are able to survive and replicate after internalization, and moreover, accomplish protection from the immune system. But also the non-professional phagocytic cells are able to defeat bacteria and to communicate with the immune system. Thus, this interaction model allows investigations of response reactions of both partners upon infection.

Within this thesis, an internalization protocol was applied to analyze proteomic adaptation of the *rsbU* repaired strain *S. aureus* HG001 (Herbert et al., 2010) with restored SigB activity containing the plasmid pMV158GFP (Nieto and Espinosa, 2003) to human host cells during the early stage of internalization. The power of this protocol lies in the enrichment of GFP-expressing bacterial cells from host cell lysate and thereby reduction of human host cells' contaminations and enhanced capture of staphylococcal proteins (Pförtner et al., 2013). In order to apply this protocol also to bacteria, which were not genetically modified and thus do not express GFP, a method employing fluorescent and para-magnetic nanoparticles (NP) was successfully developed in a first proof-of-principle experiment (Depke et al., 2014). Data from this experimental setup were later used to test a newly developed data analysis pipeline (Depke et al., manuscript submitted). The established protocol using GFP-expressing bacteria was applied to compare the proteome response of *S. aureus* HG001 pMV158GFP to two human lung epithelial cell lines (A549 and S9) and human embryonic kidney HEK 293 cells (Surmann et al., 2014b). Additionally, a protocol which allows detection of secreted *S. aureus* virulence factors by isolation of phagosomes in combination with the highly sensitive MRM method was developed and employed to infected epithelial cells (unpublished data). Apart from this thesis, the MRM method was further successfully applied to determine the absolute amounts of components of the KdpFABC potassium transporter and its regulatory two component system KdpDE in *Escherichia coli* K12 depending on the potassium supply (Surmann et al., 2014a). After analysis of proteome adaptation of internalized *S. aureus* HG001, the employed proteomics techniques were adapted to investigate the behavior of another intracellular pathogen, *B. pertussis*, during iron starvation and internalization by epithelial cells (manuscript in preparation). Since the host strongly influences the adaptation of the bacteria to intracellular life-style, the reactions of the internalized *S. aureus* HG001 and the infected A549 cells were investigated hourly during early infection in a time-dependent manner (Surmann et al., manuscript in preparation).

Impact of method optimization on internalization experiments

Achievements of improved experimental design

The outcome of infections depends among others strongly on the infection rate, meaning the number of bacteria which attack host cells. For example intracellular viability and apoptosis induction differ with changing MOIs (Mohammed et al., 2007). Therefore, it is of importance to know the exact concentration of bacterial culture before infection and number of intracellular bacteria during internalization. Previously, quantification of eukaryotic cells within saliva was successfully accomplished by flow cytometry (Aps et al., 2002). Within this thesis a method allowing fast and reproducible bacterial cell counting by fluorescence based flow cytometry was introduced. By application of GFP-expressing bacteria or staining bacteria with the fluorescent dye SYTO9 similar multiplicities of infections and comparable results were always obtained. This method replaced the standard method of plating bacterial suspension on agar plates and counting colonies after incubation which is more time-consuming and allows less control of the researcher, since the results are just visible after about 24 h. In contrast, the concentration is known immediately during counting by flow cytometry, and dilutions for exact counting can be prepared in time. GFP-expressing bacteria can additionally be counted after internalization. However, this is not yet possible for non-fluorescent bacteria from an internalization assay since SYTO9 staining led to interfering events of host and pathogen appearing in the same gate. In future this point has to be further optimized by applying a bacteria-specific dye, for example a labeled antibiotic which binds specifically to cell wall components (van Oosten et al., 2013). Another sophisticated method of cell counting is the use of transmission electron microscopy. Within this thesis it allowed discrimination between infected and non-infected host cells and determination of the infection rate. Little drawbacks were the two-dimensional properties of the employed technique which could hide bacteria outside the cutting layer of the cells and the comparably high costs and duration of the experiment.

Usage of GFP-expressing bacteria facilitated bacterial counting obviously. In addition, GFP was required for enrichment of bacteria from infected host cells which took place *via* fluorescence activated cell sorting. Since only 20% host cells were infected with *S. aureus* HG001, it was necessary to enrich bacteria from infected host cells, as the prevailing number of host proteins would complicate analysis of bacterial proteins. Next to fluorescence activated cell sorting (Becker et al., 2006, Schmidt et al., 2010b) bacteria were separated from host cells in other studies by centrifugation (Xia et al., 2007, Abu Kwaik et al., 1993, Fernández-Arenas et al., 2007) or immunomagnetic separation (Twine et al., 2006). Centrifugation of pathogens from host cells which were destroyed by detergents such as Triton (Fernández-Arenas et al., 2007) or lysed osmotically with water (Abu Kwaik et al., 1993, Xia et al., 2007) is a widely employed and easy enrichment method prior to proteome analysis which does not require genetic alteration of the pathogen like introducing plasmid for GFP-expression. In an early approach, internalized *Legionella pneumophila* cells were separated from lysed macrophages by centrifugation. Radiolabeling and 2D gel analysis allowed comparing proteins

of intracellular bacteria and non-internalized bacteria. As result, 67 proteins were found in different abundance between those two conditions by N-terminal sequencing (Abu Kwaik et al., 1993). In another approach, *Candida albicans* cells were recovered from infected macrophages by centrifugation and subjected to combined 2D PAGE-MS analysis (Fernández-Arenas et al., 2007). Also in that study proteins of the internalized pathogen were compared with those obtained from non-internalized control cells. About 300 protein spots were detected. About 100 of the spots, which were found to differ in the 2D gel, were further analyzed by MS (MALDI-TOF/TOF). Finally, 67 pathogen proteins, which were detected in different abundances upon internalization, were identified (Fernández-Arenas et al., 2007). More recently, the impact of internalization by human gingival epithelial cells was investigated for intra- and extracellular *Porphyromonas gingivalis* (Xia et al., 2007). Bacteria were isolated from the lysed host cells by centrifugation and subjected to HPLC-MS/MS after protease digestion and pre-fractionation. From as many as 10^9 bacterial cells, about 1,200 proteins were identified which comprises about 60% of the applied database of *P. gingivalis.* Thus, this study allowed a comprehensive overview of protein abundance changes for several pathways after internalization. However, in this thesis a similar outcome (coverage of about 50% of possible *S. aureus* HG001 proteins) was achieved with 500 times less bacteria after GFP-sorting (Surmann et al., 2014b). Human proteins are probably not efficiently removed during centrifugation and therefore, a higher number of bacterial cells are required. In another study even 500 host proteins were still sticking to the bacteria after centrifugation and could thus be investigated (Ventura et al., 2008b). Extraction of 10^9 bacteria from an infection assay is not always possible, since internalization and infection rates might differ among the intracellular pathogens. Another option to isolate bacteria from host cells is the immunomagnetic separation technique. Twine and colleagues separated *Francisella tularensis* from infected mouse spleen by application of Dynabeads™ M280 (Dynal, Oslo, Norway) supplied with covalently attached antisera against the pathogen (Twine et al., 2006). After incubation with the beads and subsequent isolation purification, almost no contaminating host proteins were detected and could not disturb the following proteome analysis. This investigation employed 2D gels which resulted in analysis of about 400 identified proteins and detection of 78 proteins in different abundance after internalization (Twine et al., 2006). This is clearly an advantage of this technique. However, the costs and required materials were presumably higher compared to sampling by centrifugation.

For the standard internalization approach employed in our group, GFP-expressing *S. aureus* strains are required to infect host cells. By fluorescence-based cell sorting, bacteria were isolated from host cells, which were previously disrupted using a detergent, in order to reduce the usually prevailing number of human proteins in the subsequent proteome analysis (Pförtner et al., 2013). Other groups already utilized fluorescent protein-producing pathogens to isolate them. As one of the first, Becker and coworkers investigated GFP-expressing *Salmonella enterica* proteins after isolation from infected mouse tissue. They were able to investigate 700 bacterial proteins by subsequent

LC-MS/MS analysis (Becker et al., 2006). In an attempt to apply this protocol to staphylococcal infection, it was already possible to identify about 500 staphylococcal proteins from only few million bacteria (Schmidt et al., 2010b). Also most experiments from this thesis were performed using the GFP-expressing *S. aureus* HG001 strain. A time-resolved internalization study of *S. aureus* HG001 pMV158GFP inside A549 cells (Surmann et al., manuscript in preparation) became possible as well as the comparison of bacterial proteome responses to internalization by different host cell lines (Surmann et al., 2014b). GFP-expressing *S. aureus* HG001 pMV158GFP cells were, in addition, successfully employed for separation of host cells which actually carried bacteria after exposure to the pathogen from those which did not. As the percentage of the bacteria-containing GFP-positive host cells was rather low with about 20%, they needed to be enriched as well by cell sorting prior to host cell proteome analysis. The obtained number of about 10^5 host cells was still rather low and should further be increased by longer sorting times, which would though require restriction of sampling points in time.

However, it is not always possible to introduce a plasmid carrying a gene encoding GFP or another fluorescent protein. Further, it cannot be excluded that introduction of such a plasmid also has an impact on the expression of other genes than the *gfp* gene because the production of GFP might represent a metabolic burden to the bacterial cell. Moreover, another method is required when properties of clinical isolates should be investigated because such isolates are normally not or only under difficulties amendable to genetic manipulation. In the frame of this thesis, a new isolation method was developed which does not depend on the use of GFP-expressing bacteria and is, thus, applicable for a broader type of samples including clinical isolates (Depke et al., 2014). Bacteria pre-labeled with Au- or FeOx-core could be used to infect host cells and be later on extracted with a magnet or by flow cytometry. It would be interesting to discover the mechanism how the NP interacted with *S. aureus* HG001 in a follow-up study. NP could bind to the bacterial cell wall, could be anchored within the cell wall or membrane or might even be taken up. Scanning electron microscopy and TEM could be the methods of choice to answer this question. Steinhäuser and colleagues applied these techniques successfully to elucidate cell surface bound localization of para-magnetic particles which were anchored by lipobiotin within the bacterial membrane (Steinhäuser et al., 2013). However, since our NP are probably smaller – the actual size has yet to be determined – and no lipid anchor supports attachment, the interaction of *S. aureus* HG001 and the NP employed here might differ. Importantly, the impact of NP-labeling on molecular level was tested prior to application in infection experiments. Proteome analysis of NP-labeled bacteria revealed only few unspecific differences to non-labeled bacteria and might thus not be caused by the labeling but due to normal heterogeneities occurring in the stationary phase (Bridson and Gould, 2000, Blom et al., 2011). However, a slight reaction to oxidative-stress was proposed since the methionine sulfoxide reductase (MsrA1) which is able to revert methionine oxidation (Singh and Moskovitz, 2003) was found increased after labeling with NP. Also superoxide dismutase (SodM) and catalase (KatA) which

also act against oxidative stress (Karavolos et al., 2003) showed trends of increased abundance. These findings were not surprising, as it was already reported that iron oxide NP induce concentration dependent oxidative stress in macrophages (Naqvi et al., 2010). However, the increased abundance trends of the proteins mentioned were not strong enough to result in significant regulation (Depke et al., 2014). In a follow-up study these data could be complemented with transcriptome data which would complement information on molecular reactions to NP on RNA level. Nevertheless, bacteria which were labeled for 24 h with NP were successfully employed in first proof-of-principle internalization experiments. NP-labeled bacteria could on the one hand be used for tracing intracellular bacteria by fluorescence microscopy since the NP did not label the host cells. Such intracellular tracing could give important information on replication of bacteria and during spreading of infection inside animals. Such an experiment was already reported with *S. aureus* labeled with vancomycin coupled to a fluorescent dye (van Oosten et al., 2013). Due to its linkage to the bacterial cell wall, vancomycin-labeling could be limited to Gram-positive bacteria whereas the application of fluorescent NP should be possible for diverse organism. The pilot experiments for analysis of NP-labeled *S. aureus* HG001 proteome after isolation from S9 cells allowed identifying almost 400 bacterial proteins. Two enrichment methods, para-magnetic capture of FeOx-NP as well as flow cytometry based cell sorting of fluorescent Au-NP were likewise successfully. These first two approaches indicated the functionality of the methods. In order to make physiological conclusions to internalization and to increase the number of detected proteins, the number of isolated bacteria should be increased to at least about 1-2 million as done for GFP-based sorting (Schmidt et al., 2010b, Surmann et al., 2014b). Moreover, other than in the standard internalization protocol (Pförtner et al., 2013), NP-labeled bacteria were in stationary growth when infecting the eukaryotic cells. The impact of bacteria adapted to the limitations of stationary phase and of their extracellular, partly virulence-associated proteins, which were transferred to the cell culture during infection, should further be tested, since Schwartz and coworkers observed growth phase dependent internalization effects for *S. aureus* (Schwartz et al., 2009).

Both isolation methods (sorting *via* GFP-production or using NP-pre-labeling) are extremely useful for enriching bacterial cells and analyzing their proteome. The disadvantage of both approaches is that secreted proteins are washed away during sample preparation. However, the first contact of bacteria and the potential host cells is mediated by bacterial virulence factors which are released into the environment and which directly attack, attach to, and modulate the host cells. Thus, regulation of these proteins would give valuable information on the mechanism of *S. aureus* pathogenesis. Unfortunately, only few of these secreted virulence factors were covered in previous analyses (Schmidt et al., 2010b, Surmann et al., 2014b). Only those secreted proteins that are still attached to the bacteria could be analyzed. Within this study, proteome analysis of two million sorted bacteria resulted in identification and quantification of totally 1,450 staphylococcal proteins. Out of them less than 30 proteins could be assigned to extracellular function. In a proteomic analysis performed by

Attia and colleagues, only 22 staphylococcal proteins besides a prevailing number of mouse proteins could be covered from complete abscesses of mice infected with *S. aureus* isolates (Attia et al., 2013). However, several secreted virulence factors (LukD, LukE, LukS, HlgB, HlgC, Eap, and Emp) were identified among this very low number of bacterial proteins. In that study, total infected abscesses were excised by freezing and cutting slices, prepared for MS using lysostaphin and trypsin, and subsequently analyzed by gel-based LC-MS/MS. Data analysis was performed by spectral counting. Thus, it seems possible to capture extracellular proteins from complex samples. Still it is astonishing that only few cytosolic proteins were detected, although cell lysis was supported with lysostaphin. This leads to the assumption that the amount of secreted proteins might be quite high or that the number of bacterial cells was quite low. Maybe bacteria might have already been killed by immune cells but accumulated secreted proteins might have remained. In this thesis, phagosomes were isolated from infected host cells as it was already known – and proven by microscopy – that *S. aureus* HG001 resides inside phagosomes. In contrast to Attia and coworkers, here also many cytosolic proteins were detected. Abscesses are formed by host immune cells and comprise fibrin deposits enclosing the pathogen to protect the host organism from bacterial spreading (Cheng et al., 2011). Thus, it is more likely that bacteria will get killed inside abscesses formed by immune cells than inside phagosomes of non-professional phagocytic host cells where they were shown to survive.

Several protocols have been published for isolation of bacteria-containing phagosomes. They were employed to analyze the effect of intracellular pathogens and maturation stage-specific changes in phagosomal protein content. These protocols include magnetic bead-based assays (Steinhäuser et al., 2013) as well as density gradient centrifugation (Lührmann and Haas, 2000). Proteomic analyses of phagosomes and/or their respective pathogens upon separation from infected host cells have been published before including those containing *Mycobacterium avium*, *M. tuberculosis*, *Leishmania major, Legionella pneumophila,* and *L. hackeliae* (Desjardins, 2003, Mattow et al., 2006, Sturgill-Koszycki et al., 1994, Shevchuk et al., 2009, Steinhäuser et al., 2013).

After enriching phagosomes from infected host cells by density gradient centrifugation in this thesis, the percentage of identified secreted proteins in shotgun analysis could be increased after phagosome isolation (18 extracellular proteins of 547 proteins, 3%) compared to analysis of sorted bacterial cells (21 extracellular proteins of 1,445 proteins, 1%, Figure 59). Even if the total amount of identified and quantified staphylococcal proteins from isolated phagosomes amounted for only one third of those monitored from sorted bacteria, eleven secreted proteins were exclusively found in enriched phagosomes. Among them, interesting virulence factors such as lipase (Lip), α-hemolysin precursor (Hly), fibrinogen-binding protein-related protein SAOUHSC_01110, and truncated secreted von Willebrand factor-binding protein SAOUHSC_00814 as well as several hypothetical proteins were identified. This proves the functionality of the protocol and indicates that isolation of phagosomes indeed helps to capture secreted proteins which are located in the phagosomal lumen. However, the

actual number of quantified secreted proteins was not increased. More than 110 proteins in the database of the strain applied in this study were predicted to be extracellularly localized by PSORT (Nakai and Horton, 1999). The low number of detected secreted proteins might be due to several technical reasons. As a fact, the sorted bacteria from infected S9 cells were measured with a more sensitive device, the Q Exactive, and the isolated phagosomes with the Orbitrap-Velos. Furthermore, since the phagosomal membrane was not destroyed, more human proteins were expected in the isolated phagosomes than in the sorted bacterial samples. Besides proteins of the phagosomal membrane and lumen, also cytosolic proteins which might be attached to the phagosomal membrane are likely to be analyzed as well. Since the sorted bacteria were washed during isolation it was supposed that less human proteins would stick to the bacteria. These human contaminations likely complicate MS analysis. Efforts on optimizing phagosome separation from other eukaryotic cell compounds, for example by refining the gradient, could improve the results. In future, the number of detected secreted proteins might increase by application of more sensitive mass spectrometers. Furthermore, the new isolation protocol was combined with the sensitive MRM method and allowed quantification of important proteins of *S. aureus* which were not assessable in earlier approaches. Due to methodical limitation, not all possible 112 extracellular proteins were targeted by MRM, but in total 61 interesting proteins with impact on virulence of *S. aureus* and also few cytosolic proteins which served as “positive control” for the method were investigated. Finally, 17 extracellular proteins were distinctly identified and quantified by MRM. Out of these targeted proteins only ten extracellular proteins were additionally detected with shotgun MS. However, the two secreted proteins SsaA2 and IsaA, which were found significantly increased during internalization in the shotgun approach, were also distinctly increased in abundance in the MRM approach.

When performing internalization experiments, it is interesting to compare the effects of host cell contact to bacteria with the properties of bacteria grown in pure culture. Such a sample requires careful treatment in order to serve as a reliable control. First, proteomic changes of the bacteria should be caused by the internalization and not by the shift of the medium. Therefore, the special adapted prokaryotic minimal essential medium (pMEM) was employed which was developed from MEM and known requirements of *S. aureus* medium (Gertz et al., 1999) by Dr. Sandra Ernst and tested by Dr. Melanie Gutjahr within their PhD theses. Further, variances were minimized by analyzing not the bacteria in pure culture medium but those which had contact to the host cells and the serum but were not internalized. That way, direct differences between internalizing and non-internalizing bacteria were discovered. In contrast to the collaboration project with Dr. Yanina Lamberti where internalization effects of *B. pertussis* Tohama I were analyzed, the putative control bacteria were not exposed to the host. Probably the macrophages utilized would have taken up all bacteria. Miller and coworkers observed that *S. aureus* cells, which were exposed to macrophages but were not internalized, showed different levels for some proteins. For example the stringent response and SigB activation were increased; also proteins responsible for defense for oxidative

stress were more abundant in these non-adherent bacteria compared to bacteria which had no contact to eukaryotic cells (Miller et al., 2011). Also, the *B. pertussis* control was not treated with complete serum but BSA should mimic serum effects. Since proteome analyses revealed unexpected increased levels or proteins involved in protein synthesis such as ribosomal proteins which cannot be explained without further analyses, functional analysis was performed only for internalized bacteria over time. Similarly, the non-adherent *S. aureus* HG001 control which was sampled from A549 cell supernatant before killing extracellular bacteria by centrifugation was regarded critically. This treatment was different to sampling of internalized bacteria. It revealed many proteins with decreased amounts in bacteria internalized for 1.5 h which cannot be explained by protein degradation in 30 min. Therefore, sampling of the non-adherent control was further improved by adding Triton X-100 and sorting bacterial cells for more reliable results.

Advanced strategies in data analysis

Next to the general experimental setup, the number of identified and quantified proteins influences the physiological interpretation of proteome data. The more proteins from several pathways are covered, the more meaningful and complete is the picture gained from such studies. Usually, protein identification from classical shotgun proteome experiments is performed by database searches where measured spectra are assigned to peptides and then to proteins. These databases are available on public platforms such as UniProt and NCBI and are established from different researchers worldwide. A more specific method employs spectral libraries such as SpectraST (Lam et al., 2007). In an approach performed by Dr. Maren Depke and Dr. Stephan Michalik from our working group, such a database was established for *S. aureus* HG001 from more than 100 MS measurements (Depke et al., manuscript submitted). This spectral library was applied to analyze a complex sample of internalized bacteria after isolation from host cells. Again, bacteria were pre-labeled with NP according to the protocol described in this thesis. Exactness of identification was improved since spectra of the complex internalization sample could be directly compared with spectra that were acquired previously with the same strain and same mass spectrometer, and thus, the risk of false positive identifications of actually human host proteins was reduced in contrast to classical database analysis. However, combination with a classical database search is still recommended since not all genes are expressed under normal cultivation conditions and therefore, not all possible proteins can be covered by MS and in the subsequent spectral library. Incorporation of several search tools has already be shown to improve identification in proteome analyses (Shteynberg et al., 2013). The combined workflow of classical database and spectral library search applied in this study increased distinctly the number of identified and quantified proteins after internalization of GFP-expressing bacteria by human cell lines and bacterial cell sorting. The advances in data analysis and protein identification are obvious when comparing different studies which all applied a cell culture infection model and *S. aureus* as it is described in this thesis. In a first study bacterial proteins were digested with trypsin and analyzed in

an LTQ-Orbitrap mass analyzer. Thereby, 591 staphylococcal proteins were identified with an LTQ-Orbitrap mass spectrometer and 367 of them were quantified using SILAC (Schmidt et al., 2010b). This protocol was further improved by enhanced protease digestion after preceding lysis of the staphylococcal cell wall with lysostaphin (Pförtner et al., 2013). Applying the new digestion protocol and the Orbitrap Velos 824 proteins of *S. aureus* HG001 could be identified and quantified in a label-free approach within this thesis (Surmann et al., manuscript in preparation). Utilizing a newer and more sensitive mass spectrometer, the Q Exactive, Henrike Pförtner and coworkers were able to identify 1,302 bacterial proteins and quantify 980 of them after internalization of *S. aureus* HG001 and its isogenic *ΔsigB* mutant by the S9 cell line (Pförtner et al., 2014). In this thesis we now introduced a data analysis workflow combining classical database search, spectral library matching, and additional repeated search of non-matching spectra with more relaxed criteria (reSpect-algorithm, Positive Probability, Ltd., Isleham, United Kingdom). It allowed identification and label-free quantification of almost 50% of the entire *S. aureus* HG001 proteome since 1,443 bacterial proteins were quantified after isolation from infected A549, S9 or HEK 293 cells (Surmann et al., 2014b). The comprehensiveness of the spectral library can be increased further by analysis of mutant strains and bacteria cultivated with different stresses and in different media which might force the bacteria to express other genes encoding for not yet covered proteins. This would likely increase the number of detected proteins as well as improve exactness and control of additional database search.

Physiological interpretation of the acquired proteome data was possible due to the comparison and transfer of functional annotations between the database of strain *S. aureus* NCTC8325 and other bacteria. Thus, improved pathway analysis was possible while comparing proteome adaptation of *S. aureus* HG001 to different cell lines (Surmann et al., 2014b), Furthermore, comprehensive annotations were useful for choosing virulence factors of interest for MRM. These new functional annotations were also implemented in the AureoWiki platform. In an attempt to specify the *S. aureus* species' pan-genome (Greek: *pan* for "whole") more *S. aureus* strains will be considered for incorporation into the AureoWiki database. The pan-genome comprises all genes found in different strains of a species. It consists of two parts. The core-genome covers the genes present in all strains of the *S. aureus* species and the dispensable genes are in contrast present in only some strains and contribute to the diversity of a species (Medini et al., 2005). The strain specific dispensable genes might allow prediction of genes important for example in resistance or virulence mechanisms. It is expected that the pan-genome is open and subjected to extension because new genes will be discovered by sequencing of new strains. The pan-genome and the total AureoWiki-platform also allow comparison of gene functions in different strains. Meaning, even if some genes are not yet annotated in a certain *S. aureus* strain used for a proteomics experiment, genes are now compared over different strains and the pan-genome. If a targeted gene is characterized in another strain, functional characterization of the current experiment is possible as the characterization of one gene in one strain can most likely be transferred to another strain. Within the framework of the SFBTR34 the

gene characterizations and functional annotations are automated with sophisticated databases, but still not all genes are covered with that approach, and the results from the manual search of this thesis are still valuable information for functional genomics experiments. Thus, update of annotations of all genes of *S. aureus* HG001 from this thesis allowed more extensive functional characterization of *S. aureus* adaption to infection assays in this study and will provide the research community with a better functional comparison within several *S. aureus* strains on the AureoWiki platform.

Proteomic adaptation of internalized S. aureus HG001

S. aureus is able to infect several human organs (Wertheim et al., 2005). In the last years it became clear that this pathogen can be internalized by non-professional phagocytic host cells although it was for long time regarded as an extracellular pathogen (Ellington et al., 1999, Kintarak et al., 2004, Haslinger-Löffler et al., 2005, Sinha and Herrmann, 2005, Haslinger-Löffler et al., 2006, Garzoni et al., 2007, Schmidt et al., 2010b, Fraunholz and Sinha, 2012, Garzoni and Kelley, 2009). Since different organs can be affected by staphylococcal infections, quite a few internalization experiments were already performed employing diverse host cell lines as model systems for *S. aureus* infections (Haslinger-Löffler et al., 2005, Haslinger-Löffler et al., 2006, Schmidt et al., 2010b, Hudson et al., 1995, Kintarak et al., 2004, Almeida et al., 1996). It was reviewed that *S. aureus* can persist and replicate within non-professional phagocytic host cells (Fraunholz and Sinha, 2012). Within this thesis, the molecular mechanisms of *S. aureus* adaptation to the intracellular milieu of different host cell lines were analyzed on the proteome level. First, the time-resolved adaptations of *S. aureus* HG001 pMV158GFP to human alveolar epithelial A549 cells were investigated hourly during the first 6.5 h after infection. Second, the proteomic adaptation of this strain was compared after internalization by different cell lines. Additionally, the human bronchial epithelial S9 cell line and the human embryonic kidney HEK 293 cell line were employed as host models. Common and specific protein response patterns of *S. aureus* HG001 pMV158GFP upon internalization were examined at the selected sampling points 2.5 h and 6.5 h after infection. In a third approach, phagosomes from S9 cells infected with *S. aureus* HG001 pMV158GFP were enriched. Selected secreted and cell wall-associated virulence factors were identified and quantified 2.5 h and 6.5 h *p.i.* using the MRM method.

Microscopy approaches indicated that the strain used in this thesis was internalized by the three cell lines. Since only internalized bacteria should be investigated by mass spectrometry, the infection medium was replaced after one hour. The fresh medium contained lysostaphin, which kills extracellular bacteria but does not enter the host cells (Kumar, 2008, Schindler and Schuhardt, 1964). In order to compare the behavior of *S. aureus* HG001 pMV158GFP during internalization in different cell lines, first, the intracellular replication between 1.5 h and 6.5 h post-infection was recorded. Bacterial counting from lysed host cells revealed that the bacteria replicated inside A549, S9, and HEK 293 cells but to different extent. At the earliest sampling point (1.5 h *p.i.*), most bacteria were observed inside S9 cells. Inside this cell line, the bacterial number raised to three-fold until 6.5 h *p.i.* which confirms a previous study where the bacterial proteome adaptation to internalization by this cell line was examined in a time-resolved manner (Schmidt et al., 2010b). Inside A549 cells, the bacterial number increased likewise to the threefold amount but the total number of internalized *S. aureus* was little fewer. The highest number of internalized bacteria was measured inside HEK 293 cells 6.5 h after infection. Compared to the first sampling point 1.5 h *p.i.,* the number of intracellular *S. aureus* HG001 increased even nine fold. Interestingly, the first doubling was observed only between the first

four hours after infection. But within the next two hours the number increased fourfold. Thus, the adaptation of the bacteria inside the embryonic kidney cells preceded slower compared to the epithelial cell lines, and this difference in adaptation was expected to be reflected on molecular level.

In order to explain these different growth rates the host cell metabolome at the starting point of infection was investigated. Most essential amino acids and the carbon source glucose were present in similar amounts. Some metabolites were found in slightly different amounts. However, different supply of the measured nutrients seems not to be the only reason for differences in growth. Also other properties of the host, such as production of reactive oxygen species, secretion of factors which would alarm the immune system in tissue, and supply of not-measured elements such as iron or oxygen might explain the differences. Additional analysis of these and further factors would contribute to an extended understanding of the different intracellular behavior. Integrated OMICs approaches are powerful tools to investigate the complex changes in transcription, protein synthesis, and metabolism. Metabolome analyses are hampered, as it is not yet possible to distinguish between bacterial and host metabolites which might both be detected even after sorting of bacteria. Moreover, metabolites have a fast turnover which is reflected in an altered energy charge pointing to damaged cells (Atkinson, 1968), and thus, metabolite harvest needs to be very fast (Meyer et al., 2010). For this reasons, only host metabolites were determined at the starting point of infection in this study (Surmann et al., 2014b). A recent metabolome study revealed that even purified α-hemolysin changed the metabolite pattern of airway epithelial cells (Gierok et al., 2014). After treatment of S9 and 16HBE14o- cells for 2 h, increased levels of many extracellular metabolites were detected. In the same time, the abundance of intracellular metabolites decreased compared to the non-treated cells. Strongest changes were observed for glycine, glutamate, and aspartate (Gierok et al., 2014). These data led to the assumption that also internalized bacteria might cause changes in the intracellular metabolite pool. Since this could affect metabolic enzymes of host and pathogen, metabolomics of an infection model could complement proteome data in future.

Few transcriptome and proteome studies elucidating the response of *S. aureus* to internalization have been accomplished until now. In a pioneering study in 2007, Garzoni and colleagues investigated the adaptation of *S. aureus* after internalization by eukaryotic cells. They observed that *S. aureus* 6850 was able to persist for about two weeks inside human epithelial A549 cells (Garzoni et al., 2007). In addition, they analyzed the transcriptome of *S. aureus* 6850 in the initial hours (2 h and 6 h) after internalization and compared results to non-adherent bacteria. Interestingly, about 40% of all putative open reading frames (ORF) which were identified in the genome of *S. aureus* 6850 were found to be regulated, and thus, a profound adaptation was observed (Garzoni et al., 2007). Most of them were down-regulated over time. This was true for many genes involved in metabolic function, such as genes encoding for ribosomal proteins or proteins involved in ATP synthesis, and those responsible for nucleotide acid metabolism. Up-regulation was observed for genes involved in iron-regulation and response to oxidative stress. In a more recent study, the transcriptome profile of

methicillin-resistant *S. aureus* USA300 was analyzed in human abscesses and infected mouse kidneys (Date et al., 2014). The data revealed that transcriptional adaptations in both models were remarkably similar and included up-regulation of genes coding for multiple proteases and toxins as well as iron and peptide transporters. Moreover, specific influence of the global regulators *agrB* and *saeRS* on regulation of virulence associated genes *in vivo* was examined.

The proteome can give a comprehensive picture of the molecular reaction to different perturbations, since proteins are the key players of the metabolism and act in response to many stresses, such as oxidative stress, host immune response, iron starvation, and oxygen limitation. Thus, analyzing many proteins from intracellular bacteria (824 from *S. aureus* HG001 internalized by A549 cells in a time-resolved study and 1,443 bacterial proteins after internalization by A549, S9, and HEK 293 cells 2.5 h and 6.5 h *p.i.*) as performed in this thesis allowed elaborate analysis of many important influences and helped to understand this intracellular pathogen better. In this thesis, Voronoi-like treemaps [hierarchically organized data structure, which can be combined with functional classification systems such as the SEED (Overbeek et al., 2005)] were used to give an overview of metabolic effects between internalized sample and control or to compare the first and the last sampling point and show thus a general trend of regulation. Additional time-resolved bar charts provide a more detailed picture on the intracellular adaptation of *S. aureus* during the early hours of internalization by A459 cells. In consumption with the intracellular growth, increasing numbers of regulated proteins were observed between the first (1.5 h *p.i.*) and last (6.5 h *p.i.*) sampling point. General proteomic adaptations could be compared to transcriptome data of *S. aureus* 6850 internalized by A549 cells published previously (Garzoni et al., 2007). They observed differences between the non-adherent control bacteria and internalized *S. aureus* at similar sampling points to this thesis (2 h and 6 h *p.i.*). The proteome regulation results from this thesis are in contrast to that transcriptome study (Garzoni et al., 2007). There, differential gene expression compared to the control was found for 1,042 staphylococcal genes after 2 h and for 766 genes after 6 h of infection. Most of the genes were down-regulated during infection. In this thesis, more proteins were increased in level than decreased. Also during ongoing time of internalization, the number of proteins with higher abundance increased. Of course, due to their differences in nature, proteome and transcriptome data cannot be directly compared. Further, a response to infection on gene level does not have to be visible on proteome level. When comparing not single proteins but the protein classes, ribosomal proteins were decreased in both studies, and genes and proteins involved in iron acquisition and response to oxidative stress were likewise increased. Thus, the general physiological picture does not differ too much.

During internalization, the environment of the bacteria changed. *S. aureus* HG001 cells which were cultivated in shaking flask culture were then subjected to cell lines in tissues culture plates which were further incubated with 5% CO_2. It is likely that the intracellular oxygen supply is reduced compared to the pure culture. The nutrients have to be shared with the host and most likely fewer

metabolites are available. Further, the bacteria have to compete with the host for iron and have to defeat the immune response such as reactive oxygen species. The changed conditions might explain the hampered growth. Adaptations on proteome level were expected and indicated with the number of regulated proteins upon internalization. Along with that, physiological alterations of metabolic and virulence associated proteins were observed.

The obtained proteome results support the assumption of a decreased supply of oxygen for bacteria after internalization into host cells. *S. aureus* possesses two groups of terminal oxidases, CydBA and QoxABCD, which are expressed differentially depending on the oxygen supply. They generate a membrane potential and promote aerobic respiration (Götz and Mayer, 2013). The alternative oxidase CydBA which is preferably utilized under microaerobic conditions (Götz and Mayer, 2013) was found increased in abundance during internalization, whereas Qox which is the main oxidase in an aerobic milieu (Götz and Mayer, 2013) was decreased in level during internalization. Thus, protein regulation of the oxidases points to reduced oxygen supply inside the host. This reaction was found to be conserved inside A549, S9, and HEK 293 cells (Surmann et al., 2014b). The observed increase of fermentation enzymes especially inside A549 and HEK 293 cells indicates the supplementary utilization of fermentative enzymes under microaerobic conditions. Probably due to the harsher intracellular conditions, intracellular growth rate of *S. aureus* HG001 slowed down compared to bacteria cultivated in pure medium. In concert with this observation, decreased levels of bacterial ribosomal proteins were measured after infection by the three cell lines. But not only compared to the non-adherent control, also during ongoing time of internalization, decreased levels were detected. Therein this study agrees with the results from the transcriptome study by Garzoni and colleagues, and the proteome study by Schmidt and colleagues (Garzoni et al., 2007, Schmidt et al., 2010b). Further, the decreased levels of proteins involved in ribonucleotide reduction and *de novo* purine biosynthesis of internalized samples compared to the non-adherent control reflect the lower levels which are required at impaired growth rate. The adaptation to the new environment was accompanied with increased levels of proteins involved in some metabolic pathways. Some proteins of the TCA cycle were induced after internalization compared to the non-adherent control. However, time-resolved protein data of bacteria inside A549 cells show diverse regulation, increasing or decreasing levels during progressing internalization. This reorganization probably reflects a switch between energy sources due to the limited oxygen supply. Interestingly, cell type-dependent differences were observed for some TCA enzymes. Bacterial protein levels were similar inside A549 and S9 cells but some levels were increased for *S. aureus* enriched from HEK 293 cells. Since A549 and S9 cells are both lung epithelial cells it was expected that they provoke more similar bacterial adaptation reactions. A further pathway, which was modulated upon internalization, was cell wall biosynthesis. Many proteins involved in peptidoglycan biosynthesis were increased in level at later time of internalization compared to the first sampling point (1.5 h *p.i.*). This is in agreement with the first proteome approach of internalized *S. aureus* HG001 (Schmidt et al.,

2010b), and the observation is furthermore supported by the detection of the VraSR system's activity, which regulates cell wall biosynthesis (Kuroda et al., 2003). Levels of both sensor and regulator protein of this two-component-system were found to be increased starting from 3.5 h until 6.5 h after infection. This is an methodological advancement compared to the study published by Schmidt and colleagues which provided only increasing levels of the response regulator VraR but not the histidine kinase VraS (Schmidt et al., 2010b). Probably the more sensitive mass spectrometers and the improved digestion protocol led to this enhanced analysis. Activation of the VraSR system indicates the reorganization of the cell envelope as protection inside the host. Another cell surface associated protein that is controlled by the two component system is the protein export protein or also called foldase protein PrsA (Jousselin et al., 2012). This protein, which is involved in resistance to antibiotics targeting the cell wall, was found increased in levels triggered by internalization. Increased abundances were obtained by Schmidt and colleagues in 2010 with S9 cells as host, in the time-resolved proteome analysis of *S. aureus* HG001 internalized by A549 cells, and were, moreover, found to be a conserved reaction to internalization by the three cell lines S9, A549, and HEK 293.

Many staphylococcal proteins that play a role in infections of animals or cell cultures were reported to be influenced by the global transcriptional regulator SigB (Jonsson et al., 2004, Depke et al., 2012). It was already shown that SigB is activated upon internalization of *S. aureus* HG001 by S9 cells (Pförtner et al., 2014). The comparative analysis of *S. aureus* HG001 infection of the three different cell lines revealed that this activation is conserved upon internalization by A549 and HEK 293 cells as well (Surmann et al., 2014b). Five proteins that displayed clear increased levels upon internalization in the study performed by Henrike Pförtner (Asp23, SpoVG, ClfA, ClpL, and SAOUHSC_02665) showed also increased abundance 2.5 h after infection compared to the control inside all three host cell lines. However, the increase of protein YfkM which was reported by Pförtner and colleagues could not be confirmed in this comparative study which was here performed for three cell lines and three biological replicates each (Pförtner et al., 2014, Surmann et al., 2014b). Some adaptation reactions and reduced growth might also derive from nutrient starvation inside the host. The stringent response mechanism is a quick adaptation reaction to starvation of nutrients such as glucose or amino acids triggered by (p)ppGpp (Geiger et al., 2012). It provokes increased stress resistance, reduced growth, and altered metabolism. The bifunctional (p)ppGpp synthetase RSH (RelA and SpoT) as well as the two proteins RelP and RelQ which also control (p)ppGpp synthesis were described to be responsible for this emergency reaction in other bacteria and *S. aureus* (Geiger et al., 2014). In *S. aureus* the products of the three genes SAOUHSC_01742, SAOUHSC_00942, and SAOUHSC_02811 catalyze (p)ppGpp production (Geiger et al., 2010). In the internalization approach presented in this thesis, levels of RelP and RelQ increased early after infection. These two proteins were recently found to be responsible for adaptation to cell wall stress in *S. aureus* (Geiger et al., 2014). Since cell wall stress and modulation of peptidoglycan biosynthesis were observed in this thesis, the increased levels of RelP and RelQ upon internalization seem plausible. RSH was not

increased in level during ongoing internalization in this thesis. It was reported to be required during amino acid starvation, and induction of the *rsh* gene causes induction of the *ilv* and *leu*-operon encoding proteins involved in synthesis of branched-chain amino acids (Anderson et al., 2006, Geiger et al., 2012). Probably upon internalization by non-professional phagocytic host cells only a slight stringent response caused by cell wall stress was induced. The levels of the RSH homologue were even found decreased during ongoing infection and proteins involved in synthesis of branched-chain amino acids were not changed in level. Moreover, proteins involved in degradation of branched-chain amino acids were observed. Thus, in agreement with the metabolome data, many amino acids were present in sufficient intracellular amounts. Levels of enzymes involved in biosynthesis of other amino acids such as arginine, lysine, and aromatic amino acids were increased in bacteria harvested 2.5 h after internalization compared to non-adherent control bacteria (Surmann et al., 2014b). All amino acids as well as the carbon and energy source glucose were measured at the starting point of infection but later metabolome data were not available due to reasons mentioned above. Therefore, explanations of increased abundance of proteins involved in amino acid biosynthesis are speculative. For bacteria grown in pure culture it was shown that lysine might overtake the role as carbon source when glucose is no longer present (Liebeke et al., 2011). But such conclusions are not possible from this data of host cell-internalized staphylococcal samples.

In a recent study the importance of the element iron on the virulence of *S. aureus* USA300Δ*spa* was proposed (Stentzel et al., 2014). Results revealed as expected that under iron limitation proteins involved in iron acquisition were increased in level compared to bacteria grown without iron limitation. Further, decreased levels of superantigens and hemolysins were observed. Interestingly, when testing immunologic effect of *S. aureus* supernatant, more secreted proteins were bound by IgG when the bacteria were cultivated under iron-limitation (Stentzel et al., 2014). Maybe increased levels of adhesive iron dependent proteins IsdA and IsdB could have caused this effect. Iron is limited in the eukaryotic cells and needs to be released from host compounds. The preferred iron source of *S. aureus* is hemoglobin (Skaar et al., 2004b). Therefore, the pathogen possesses several heme-degrading enzymes such as IsdG and IsdI (Skaar et al., 2004a). Both monooxygenases were detected in increased levels in bacteria after internalization by A549, S9, and HEK 293 cells. IsdG might be more important for iron acquisition than IsdI which was found increased in internalized bacteria but to lesser extent. The cell wall associated iron transport associated domain-containing protein IsdA was not changed or even found in slightly lower levels in the shotgun approaches of analysis of internalized bacteria during ongoing infection. Three more related proteins, SAOUHSC_02430 (involved in iron binding), SAOUHSC_00749 (iron uptake transporter), and EfeM (iron transporter) were increased in level upon internalization. That iron metabolism is related with oxidative stress was already described comprehensively in two reviews (Cornelis et al., 2011, Andrews et al., 2003). Iron catalyzes formation of highly reactive hydroxyl radicals which could damage bacteria in a defense mechanism of eukaryotic cells to invaders. Commonly increased

protein classes upon internalization by all three cell lines were flavohaemoglobins, peptide methionine sulfoxide reductases (MsrA, MsrB), and superoxide dismutases (SodA, SodM). This notion indicates that *S. aureus* HG001 possesses several response mechanisms to oxidative stress. Flavohaemoglobins protect against nitrosative stress. MsrA was found to catalyze reduction of oxidized methionine (Singh and Moskovitz, 2003). The superoxide dismutases reduce superoxide anions, reactive oxygen species which are produced to kill pathogens after enclosure in a phagosomes (Karavolos et al., 2003).

Until here, adaptations of large sets of cellular proteins were described. However, it was investigated for example for the *Listeria* species that especially secreted proteins contribute to virulence of a strain (Trost et al., 2005). In the high resolution MS approach (Surmann et al., 2014b) only 1% of 1,450 detected staphylococcal proteins were assigned to extracellular location, more exactly, 21 detected out of 112 predicted by PSORT (Nakai and Horton, 1999). The biggest group of identified *S. aureus* proteins comprised cytoplasmic proteins with 65% followed by cytoplasmic membrane associated proteins with 18%. Becher and coworkers published a comprehensive study of the *S. aureus* proteome in 2009 (Becher et al., 2009). They proclaim extracellular proteins that are still bound to the cell wall or already secreted into extracellular space build the most important class of *S. aureus* proteins during infection because most of the proteins belonging to this classes contribute to virulence and pointed out the strain variability of the secreted virulence factors (Becher et al., 2009). In this thesis, some secreted and other virulence associated proteins of *S. aureus* HG001 were detected in a targeted approach from isolated phagosomes. From the selected secreted virulence factors, only γ-hemolysin subunit HlgC was found decreased over time. This pore-forming toxin was shown to destroy host cell membranes (Vandenesch et al., 2012). Levels of many extracellular virulence factors such as Geh, Lip, Atl, HlgB, Aur, LukeD, and LukE were not changed over time. Interestingly, other secreted proteins SsaA2, LytM, Efb, IsaA, SAOUHSC_02241, and SAOUHSC_02243 were found in increased abundance during ongoing infection. Interestingly and in contrast to the shotgun proteome data where the cell wall associated adhesin ClfA was first increased 2.5 h after internalization and decreased 6.5 h *p.i.*, this SigB-regulated protein was found to be increased between 6.5 h *p.i.* compared to 2.5 h after infection after MRM. Results from shotgun analyses indicated its production was stopped probably since adhesion was not necessary at later points in time. However, ClfA was found increased inside the phagosome. It could be accumulated extracellularly even when intracellular production stopped and/or the MRM approach is able to discover more exact data for this comparatively low abundant protein. This virulence factor was reported to protect internalized *S. aureus* against macrophage activation and modulates cytokine expression (Palmqvist et al., 2004). So it seems important for intracellular survival. Support is given by a study conducted by Loughman and coworkers which showed that ClfA is the dominant *S. aureus* adhesin preferably produced in stationary phase (Loughman et al., 2005) or here, when growth is reduced inside the host. The opposite was reported for ClfB (McAleese et al., 2001) and fibronectin

binding protein (Saravia-Otten et al., 1997) which were found increased inside growing *S. aureus*. Both proteins would be thus interesting targets for possible follow-up studies. The increase of many virulence factors is astonishing since the small colony variants, which can obviously persist for long time inside host cells, probably decrease their virulence in order to hide from the immune system (Tuchscherr et al., 2011). However, the SCV were observed to prevail intracellular after long time (Tuchscherr et al., 2011). Therefore, it would be interesting to analyze the whole proteome of internalized bacteria at later sampling points. For this purpose, the sampling and analysis must be further improved since microscopy pictures and first trials of cell sorting after 24 h (data not presented) revealed too few intracellular bacteria. Garzoni and coworkers observed likewise diminished intracellular number of *S. aureus* 6850 inside A549 cells between 6 h and 24 h after infection (Garzoni et al., 2007). Thus, the internalization setting itself must be enlarged first. But still these early results provide interesting information. In future it would be interesting to apply the protocol of phagosome isolation to mutants with deficiencies in regulatory genes such as *sigB, sarA* or *agr* since they are known to regulate several extracellular virulence factors (Ziebandt et al., 2001, Ziebandt et al., 2004, Kullik et al., 1998, Karlsson and Arvidson, 2002, Blevins et al., 2002).

The exclusively human pathogen *B. pertussis* was likewise found to be able to invade and persist inside non-professional phagocytic host cells, for example A549 cells (Lamberti et al., 2013). In a collaboration project with Dr. Yanina Lamberti, this pathogen was observed to survive inside macrophages for at least two days. Furthermore, iron dependent protein classes were discovered. Common and specific features of the proteome adaptations of the two bacteria *B. pertussis* Tohama I and *S. aureus* HG001 were observed. But besides the different properties of the microorganism one has to keep in mind that also the different types of host cells (macrophages as professional phagocytes *vs.* the non-professional phagocytic A549, S9, and HEK 293 cells) might influence the outcome as proposed in the mentioned review on host cell models (Eisenreich et al., 2013). Also the second sampling point of internalized *B. pertussis* was much later (48 h *p.i.*). Similar to internalized *S. aureus* HG001 abundance of ribosomal proteins decreased during ongoing time of infection. Proteins involved in peptidoglycan biosynthesis were increased over time in internalized *S. aureus* but not in internalized *B. pertussis*. This could be explained by their nature of the Gram-positive *S. aureus* and the Gram-negative *B. pertussis*. Common for both pathogens, proteins involved in iron acquisition from the host were induced during internalization. Since oxidative stress is linked to iron metabolism (Cornelis et al., 2011) also *B. pertussis* proteins responsible for oxidative stress defense were increased in level after iron limitation as well as upon internalization which was similar for internalized *S. aureus* HG001 (Surmann et al., 2014b). Also virulence proteins were altered in level in order to adapt to intracellular survival which is also accomplished by *S. aureus* during long term internalization (Löffler et al., 2014, Tuchscherr et al., 2010). Further proteins which were affected by iron limitation of *B. pertussis* in our study were enzymes involved in biofilm formation which contributes to infection and spreading within tissue. Literature reports offer different perspectives on

the influence of iron on biofilm formation. For example biofilm formation was enhanced in *L. pneumophila* under iron starvation (Hindré et al., 2008) but inhibited for *Vibrio cholera* (Mey et al., 2005). Taken together, iron limitation induced production of iron uptake systems, altered virulence, and led to changes that support host colonization, and these results were mainly reflected in internalized bacteria as well.

Host response to infection with S. aureus HG001

From the first days after birth, humans get almost permanently in contact with diverse microorganisms. Along with that, immunological reactions of the organism develop. Among the first species which human cells encounter are *Staphylococcus*, *Streptococcus*, *Enterococcus*, and *Enterobacter* (Wopereis et al., 2014, Jiménez et al., 2008). Some intracellular pathogens, among them *S. aureus*, are even able to invade mammalian cells and persist inside them (Garzoni and Kelley, 2009). Various physiological responses of these host cells caused by interaction with the internalized bacteria were reviewed extensively by Eisenreich and colleagues, 2013. These responses include multiple metabolic changes in the affected host which are even stronger when the pathogen replicates. For example, host cells change general metabolic reactions and try to prevent pathogens from stealing host cell metabolites. Further, they generate reactive oxygen species and/or nitrogen species as defense reaction. Metabolic adaptation effects caused by the intracellular pathogens *Salmonella enterica* serovar Typhimurium, *Mycobacterium tuberculosis*, *Listeria monocytogenes*, *Chlamydia spp*., *Coxiella burnetii*, and *Legionella pneumophila* were reviewed, and the choice of the host cell type was concluded to represent an important factor (Eisenreich et al., 2013). This thesis provides in addition data on host response of human epithelial cells to infection with *S. aureus* HG001 pMV158GFP. To summarize, contact of A549 cells to this pathogen leads to quick secretion of cytokines and remodeling of the immunoproteasome. Furthermore, S9 cells were observed to engulf *S. aureus* HG001 pJL76 inside LAMP-1-positive membranes. These phagosomes could be niches for the pathogen (Olivier et al., 2009, Schröder et al., 2006) or a trap where they get digested by phagolysosomal enzymes and killed with reactive oxygen species (Schwartz et al., 2009). In addition, hints of early apoptosis triggered by caspase-9 were observed.

In 2005, Moreilhon and coworkers reported the transcriptome response of human airway epithelial MM-39 cells (transformed human tracheal gland cell line) to exposure to *S. aureus* NCTC8325-4. They performed two experiments. First, bacteria cultivated in TSB were centrifuged, washed and subjected in cell culture medium to the eukaryotic cells (MOI 50 bacteria per host cell). Second, the centrifuged supernatant was diluted in cell culture medium prior to incubation of the MM-39 cells. The early host transcriptome response after 3 h was investigated using microarray techniques (Moreilhon et al., 2005). In contrast to that setup, in this thesis the epithelial A549 cells were exposed to an infection mix containing whole bacteria (MOI 25 bacteria per host cell) together with their secreted virulence factors which probably mimics best the physiological situation of a possible host. This became possible since the bacteria were already cultivated in adapted cell culture medium (pMEM) in order to minimize metabolic shifts (Schmidt et al., 2010b). Moreilhon and colleagues detected only 3% of infected MM-39 cells, much less than the here infected 20% of A549 cells. Their transcriptome analyses revealed up-regulation of several genes encoding for transcription regulators after internalization of bacteria but also to a higher extend after treatment with supernatant. Further, many genes encoding for proteins with inflammatory function such as the pro-inflammatory cytokines IL-1α,

IL-1β, IL-6, and IL-8 were clearly induced 3 h after incubation with the supernatant but almost not altered after internalization of bacteria for the same duration (Moreilhon et al., 2005). These stronger changes after incubation with bacterial supernatant than after contact with the whole bacteria probably indicate that especially secreted bacterial proteins induce cytokine secretion. Again, the pre-cultivation in TSB can play a role, since bacteria grown in rich medium secrete highest levels of protein, especially in the stationary phase (Antelmann et al., 2001). Furthermore, mostly anti-apoptotic gene were up-regulated in MM-39 cells 3 h after treatment with supernatant or whole bacteria (Moreilhon et al., 2005). The proteome adaptation of A549 cells to infection was already studied with the human respiratory syncytial virus (HRSV) as pathogen (Munday et al., 2010b). Host proteome analysis was accomplished using SILAC and LC-MS/MS. Additionally to this methods which were similarly applied in this thesis, Munday and colleagues separated a nuclear and cytosolic fraction, and pre-fractionated the proteins with a SDS-PAGE prior to LC-MS/MS analysis of each ten gel slices per fraction. The authors identified and quantified in total 904 host proteins, and the abundance of 112 of them was changed more than twice after infection compared to non-infected cells. With this increased methodological and time-consuming effort, they identified and quantified about 150 host proteins more compared to the results of A549 proteome analysis (737 proteins) performed in this thesis. In agreement to the results obtained for *S. aureus* HG001 infected A549 cells, also infection with HRSV caused changes in abundance of mitochondrial proteins of the host. Additional alterations were observed for proteins associated with respiratory complexes, the pathway of oxidative phosphorylation, and superoxide dismutase. Most proteins were identified in the pathways of cell death and gene expression. As expected, they observed activation of pathways of innate and adaptive immunity as well as anti-viral activity (Munday et al., 2010b). In another shotgun proteomics approach, Ventura and coworkers investigated host airway proteins which were attached to *S. aureus* 30 min and 6 h after intranasal inoculation of mice. Bronchoalveolar lavage was collected from each ten mice at both points in time. Bacteria were separated by centrifugation from the lavage, and host proteins were separated from the bacterial surface and analyzed by LC-MS/MS (Ventura et al., 2008b). About 500 host proteins were found to interact with *S. aureus* in the airways. More host proteins were detected 6 h after inoculation. Since many intracellular host proteins were found, the authors proposed that the bacteria were internalized by the airway cells or cell lysis happened before or during sampling. Remarkably, 105 (about 70 for each sampling point, some overlapping proteins) of the 513 totally identified proteins were associated with phagosomal functions. Other protein classes which were associated with the bacteria involved some extracellular host proteins with impact on inflammation, proteolysis, and transport. Additionally, hemoglobin was associated with *S. aureus* during early airway infection (Ventura et al., 2008b). The importance of iron acquisition for internalized bacteria was also shown in this thesis since involved bacterial proteins such as IsdA increased in level upon internalization. Hemoglobin was earlier described to be the preferred intracellular iron source of *S. aureus* (Skaar et al., 2004b).

In the frame of this thesis, the proteome of A549 cells was investigated after infection with *S. aureus* HG001 pMV158GFP. The limiting factor was the already mentioned low percentage of A549 cells which actually carried the pathogen (20%). The experiment was designed for sampling every hour after infection to provide the same conditions to host analysis as the previously described analysis of *S. aureus* HG001 proteome. Within that time, about 10^5 infected host cells were sorted. After 1.5 h infection the number was too low for stable mass spectrometry analysis. Therefore, the host cell response to *S. aureus* HG001 pMV158GFP infection was carried out hourly between 2.5 h and 6.5 h after infection. The number of quantified host proteins was even lower than the number of quantified staphylococcal proteins which were extracted from two million bacteria in the parallel experiment. In the future this number could be increased by allowing longer sorting time which would though be accompanied by including less sampling points. Further, application of more sensitive mass spectrometers as the Q Exactive for example and other data acquisition strategies such as the data-independent mode (Vowinckel et al., 2013, Gillet et al., 2012) might improve host cell proteomics. Nevertheless, among the 737 quantified host proteins, some differential abundant host proteins were observed between the three different sample types of A549 cells. First, it was interesting to observe a clear general difference between the proteomes of GFP-positive, GFP-negative, and control cells. Thus, one can conclude that even pure contact to the pathogen caused proteomic changes but internalized bacteria caused even more differential abundances of proteins compared to the control. Pathway analysis revealed changes in the EIF2 signaling pathway upon infection. This pathway was a little underrepresented inside the GFP-positive cells compared to the GFP-negative cells; the same was true for the pathway of ras-related nuclear protein (RAN) signaling. Proteins of the eukaryotic TCA cycle, as well as proteins belonging to the pathways of granzyme B signaling, the mitochondrial dysfunction and apoptosis signaling showed increased levels in GFP-positive A549 cells compared to GFP-negative and control cells. Nevertheless, interpretations only relying on the proteome data are critical since the percentage of identified proteins to the total number of proteins assigned to pathways was sometimes below 50%. In order to validate these proteome results and to enhance the physiological interpretation, follow-up experiments were performed for selected protein classes.

When pathogens such as *S. aureus* are recognized by the eukaryotic cells, the attacked cell will likely intend to alarm the immune system whose professional phagocytes can defend against pathogens more efficiently than non-professional phagocytes. Proteome results from this study show clear differences between A549 cells which carry bacteria, those, which do not after 1 h contact, and control A549 cells that were never exposed to *S. aureus*. These data propose communication also between infected and non-infected neighboring cells. Infected epithelial cells secrete cytokines, small molecular mediators of the immune system which for example recruit macrophages which could eliminate the intruder (Stadnyk, 1994). Even purified *S. aureus* virulence factors or compounds of the bacterial cell wall caused cytokine release from human epithelial cells (Räth et al., 2013, Cheon et al.,

2008). Early after infection (1.5 h *p.i.*) many cytokines were detected in distinct higher amount in supernatant of infected A549 cells compared to non-infected A549 cells. This could be caused by the exposure of epithelial cells to whole bacteria together with their secreted virulence factors which probably mimics most similar the physiological situation. In contrast, in a previously performed transcriptome approach early expression (3 h *p.i.*) of pro-inflammatory cytokine encoding genes (for IL-1α, IL-1β, IL-6, and IL-8) was only induced when the airway epithelial cells were treated with supernatant which accumulates virulence factors but not with whole washed bacteria (Moreilhon et al., 2005). However, the increase in level 1.5 h *p.i.* seems to be only the first reaction upon contact with the invader. Most levels of secreted cytokines decreased afterwards. Solely levels of IL-8, which presumably recruits leukocytes, increased steadily until 24.5 h after infection. It was shown before that already staphylococcal peptidoglycan induces secretion of this chemokine (Cheon et al., 2008). IL-8 was also the only cytokine which was detected in considerable levels in non-infected A549 cells but still to a lower extent compared to the infected cells. Interestingly, IL-8 and other chemokines were found to be secreted by A549 cells after stimulation with the serine protease trypsin (Sachse et al., 2006). Since this protease is applied in regular cultivation of the host cells, it is likely that it induces IL-8 expression even though trypsin is inactivated by serum compounds about 5-10 min after contact to the cells. The pro-inflammatory IL-6 was detected late after infection but became the second most abundant cytokine 24.5 h *p.i.*. In agreement with that observation, Räth and coworkers did not observe distinct levels of IL-6 after 6 h stimulation of A549 cells with purified α-hemolysin but measured pronounced amounts after likewise incubation of S9 and 16HBE14o- cells (Räth et al., 2013). S9 and 16HBE14o- (Cozens et al., 1994) cells both derived from bronchial epithelium which should encounter pathogens first whereas the A549 alveolar epithelial cells are located deeper inside the lung. Maybe this common place of origin causes more similarities in response to the virulence factor. Another similarity factor between S9 and 16HBE14o- is that both are immortalized cell lines and the A549 cell is a cancer cell line. Eisenreich and colleagues announced in their review that this property might also lead to different host responses to infection (Eisenreich et al., 2013). It would be interesting to measure the cytokine secretion by S9 (immortalized bronchial epithelial cells) and HEK 293 cells (immortalized embryonic kidney cells) as well from the same infection setup to support or disprove the hypothesis. But it is also likely that other virulence factors than α-hemolysin are required to stimulate IL-6 secretion in A549 cells which might be accumulated in sufficient amounts not before 24.5 h after infection. Levels of the macrophage activating IFN-γ stayed at high levels during the whole time course of infection. It promotes conversion of the proteasome to the immunoproteasome. The proteasome is a non-lysosomal ATP-dependent complex of proteases which collaborates with ubiquitin. It functions after assembling of several subunits which was already extensively reviewed (Coux et al., 1996, Kloetzel, 2004). As consequence, intracellular antigens are processed and can be presented in MHC I-complexes to immune cells (Kloetzel, 2004). IFN-γ triggers formation of the immunoproteasome i20S complex which contains three immunosubunits whose

synthesis is enhanced by the cytokine (Heink et al., 2005). This complex is developed faster than the regular proteasome and allows quick reaction of the immune system during infection, but comprises also a shorter half-life and is therefore highly regulated and can return to the normal situation when no longer required (Heink et al., 2005). In this study an induction of the three immunosubunits in A549 cells 6.5 h after infection with *S. aureus* HG001 compared to non-infected A549 cells was confirmed with an additional qRT-PCR experiment.

S. aureus found a way to hide from the immune system which allows long-term persistence inside non-professional phagocytes as so-called small colony variants (SCV). These altered phenotypes were associated with chronic staphylococcal diseases (Sendi and Proctor, 2009, Kahl et al., 1998). They can be mimicked in laboratory scale by mutations in the *hemB* (Kohler et al., 2003) or *menD* gene (Kohler et al., 2008). In a long-term study over 28 days, A549 cells were infected with two *S. aureus* strains (6850 and 628) (Tuchscherr et al., 2011). The percentage of intracellular SCV increased steadily during ongoing time of infection until about 90% after 28 days. To determine host inflammatory changes caused by SCV, the authors monitored cytokine secretion at later points in time starting from two days after infection. Compared to non-infected control mice, the secretion of IL-6, TNF-α, and IL-10 elevated during infection. However, after 14 days the cytokine levels decreased again until they were almost equal to those of the control (Tuchscherr et al., 2011). Thus, it seems that cytokine secretion was almost terminated when only SCV were present inside the host. Early cytokine secretion of A549 cells after infection with an isogenic *ΔmenD* SCV mutant of *S. aureus* HG001 pMV158GFP performed in the Bachelor's thesis of Jörn Steinke was compared to the data measured after infection with the wild-type performed in this thesis. In agreement with long-term mouse experiments (Tuchscherr et al., 2011), the *ΔmenD* mutant triggered almost no cytokine expression after infection. The levels were always below those of the wild-type-infected samples. The molecular background has yet to be determined. Since secreted proteins were shown to induce more genes involved in cytokine production than washed bacteria (Moreilhon et al., 2005), the extracellular proteome of the mutant and the wild-type are currently investigated.

Furthermore, SCV have been shown to survive and grow within phagosomes of infected endothelial cells (Schröder et al., 2006). As subtopic of this thesis, it was also investigated if *S. aureus* HG001 can survive inside phagosomes of epithelial cells. Fluorescence microscopy of infected S9 cells indicated that some bacteria were engulfed in LAMP-1-postive vesicles and some were not. Thus, several sub-populations of bacteria seem to reside inside the host. Since it was shown that *S. aureus* can prevent fusion of endosomes with lysosomes (Schnaith et al., 2007), it is possible that those bacteria also overdue in earlier stages of the phagosome such as early or late endosomes. Therefore, it would be informative to stain infected host cells with fluorescent antibodies of typical markers such as EEA1 or RAB5 for early endosomes and MPRD or RAB7 for late endosomes. When using different staining in one approach it might be possible to calculate proportions between the subpopulations. Proteome analysis of phagosomes from S9 cells detected

markers for all stages of phagosomal maturation. Only Niemann-Pick C1 protein (NPC1), which catalyzes vesicular trafficking in late endosomes and lysosomes, and lysosome associated membrane protein 1 (LAMP-1), a phagolysosomal marker, were found in higher levels during ongoing time of internalization. These results led to the assumption that a mixture of different maturation stages was present. Some subpopulations of the bacteria might replicate inside endosomes, others might be destroyed inside phagolysosomes and a further group could be present inside the cytosol. Shevchuk and coworkers observed in a comparative proteome study that the pathogens influence the phagosomal proteome. They identified differences after isolation of phagosomes from infected *Dictostelium discoideum* with the pathogenic *Legionella pneumophila* or the less virulent *L. hackeliae* (Shevchuk et al., 2009). Other pathogens including *Mycobacterium tuberculosis* (Ferrari et al., 1999), *L. pneumophila* (Vogel and Isberg, 1999), and *Brucella abortus* (Pizarro-Cerdá et al., 1998) were reported to possess virulence mechanisms preventing fusion of phagosomes with phagolysosomes since the phagosomes are the bacterial intracellular niche for replication and survival. *S. aureus* not only prevents phagosomes from fusion with lysosomes to prevent phagosomal digestion (Schnaith et al., 2007). Some strains can even evade the phagosomes. Recently, it was shown that *S. aureus* strains USA300 LAC, USA400 MW2, and 6850 require PSMα to escape from phagosomes (Grosz et al., 2014). Phagosomal escape and cytoplasmic replication was reported for other pathogens, too, such as *Shigella flexneri,* where IpaB was described to be the membrane-lysing toxin (High et al., 1992)*, Listeria monocytogenes* (Rabinovich et al., 2012), and *Rickettsia* spp. (Heinzen et al., 1999). Some virulent *S. aureus* strains which produce several pore-forming toxins such as the Panton-Valentine-Leukocidin (PVL) are able to kill host cells, among them also phagocytic neutrophils (Genestier et al., 2005) which would normally eliminate the bacteria. Thereby PVL stimulates mitochondria. Cytochrome C which is usually a mitochondrial protein is then released through the porous mitochondrial membrane. Once inside the cytosol, this protein causes activation of a cascade of cysteine-aspartate-proteases (caspases) which degrade the host cell during apoptosis. However, it is not always an advantage for the bacteria to kill their host. Inside non-professional phagocytic cells, *S. aureus* is able to survive and replicate (Schmidt et al., 2010b, Surmann et al., 2014b) and is secured from professional phagocytes of the immune system which would surely kill this bacterium. Infected eukaryotic cells are able to eliminate themselves and the invaded bacteria by apoptosis, programmed cell death. After their degradation they attract phagocytic cells which would remove dead host cells and enclosed bacteria. Therewith, they prevent contamination of neighbor cells and infection of whole tissues. In this study, caspase-9, a key player in apoptosis, was found induced after 2.5 h of infection but almost not detected after 6.5 h. Apoptosis induction by *S. aureus* is discussed controversially. Bantel *et al.* described activation of intrinsic cell death activation (Bantel et al., 2001) while Koziel *et al.* observed an induction of anti-apoptotic factors after infection of macrophages by *S. aureus* (Koziel et al., 2009). In a transcriptome study, treatment of epithelial MM-39 cells with supernatant of *S. aureus* NCTC8325-4 caused activation of genes encoding anti-apoptotic factors

during early treatment but up-regulation of apoptotic genes 8 h after incubation (Moreilhon et al., 2005). The data recorded in this thesis suggest an early effort of the infected A549 cells to eliminate the bacteria but later *S. aureus* HG001 seems to induce anti-apoptotic genes since the signal of active caspase-9 was decreased later on. Koziel and colleagues observed over-expression of BCL2 or MCL1 (Koziel et al., 2009) but they were, however, not present in our proteome data. Anti-apoptotic factors could prevent elimination by the host to enable intracellular persistence and survival. For pleural mesothelial cells, Mohammed and coworkers observed time- and MOI-dependent apoptosis induction after infection with *S. aureus*. In their study, they determined apoptosis by measuring DNA fragmentation. At their first sampling point 6 h after exposure to the bacteria, less than 10% cells were apoptotic no matter which MOI was employed. At an MOI of ten bacteria per host cell, which is closest to the MOI of 25 bacteria/host cell applied in this thesis, time-dependent increases until 40% of apoptotic cells were observed after 48 h (Mohammed et al., 2007). That might be similar for *S. aureus* HG001 internalized by A549 cells and could explain why only low amounts of caspases were detected in the early monitored time frame. This enzyme is preferably produced inside the apoptotic cells and does not seem to be an ideal marker of apoptosis when only a low percentage of host cells are actually affected.

Outlook

This thesis provides new techniques to separate and analyze bacterial proteins after infection. Further, it provides an insight on the host response to the *S. aureus* HG001 wild-type strain. Also the influence of the host on pathogen adaptation was investigated. The findings of this work provide information on host-pathogen interaction but also point to new questions which should be addressed in the future. The methods developed within the framework of this thesis might help answering them.

Bacterial cell counting using the Guava easyCyte^{TM} flow cytometer is now a standard procedure in our laboratory. GFP-expressing bacteria (pure bacterial culture and internalization experiment) or bacteria stained with a fluorescent dye (only pure bacterial culture) can now be counted precisely and much faster compared to earlier performed CFU plating. An upcoming challenge is the counting of non-GFP-expressing bacterial cells which derive from internalization workflows. As the now employed dye SYTO9 stains RNA and DNA, bacteria as well as host cell debris are labeled making it hard to distinguish the populations. Thus, at the moment different label strategies are tested.

The protocol for enrichment of NP-labeled bacteria is currently optimized by Maren Depke with the goal to apply it to non-fluorescent strains such as clinical isolates.

The newly annotated database of *S. aureus* NCTC8325 or HG001 provides information on the functions of many more genes compared to the previous state. It is not only the new standardized database used in our work group and collaborative projects but also a fundament of the recently developed AureoWiki platform which offers a comprehensive platform for researchers on *S. aureus* worldwide. The new annotations will be implemented in the currently developed pan-genome database covering many *S. aureus* strains.

The protocol for phagosome isolation was successfully applied to analyze phagosomal proteins of epithelial cell lines as well as secreted virulence factors of *S. aureus* HG001 wild-type. The protocol could be optimized in future for example by refining of the sucrose gradient by adding more phases in order to reduce the contamination of host proteins from other eukaryotic compartments. We now possess a possibility to quantify low abundant secreted proteins which could not be detected earlier. It would therefore be interesting to apply this protocol to isogenic mutants of regulators of virulence factors such as *sigB, sarA* or *agr* and to determine their actual impact on secreted protein expression.

The quantification of these low abundant secreted proteins benefited not only from the enrichment protocol, but also from the application of the highly sensitive MRM method. The knowledge about this method was successfully applied on collaboration projects to analyze also proteins of *Escherichia coli* and *B. pertussis* which already led to a publication and preparation of further manuscripts due to interesting findings and can be transferred to new projects.

Performing comparative infection experiments, it became evident that *S. aureus* behaves differently after internalization by different non-professional phagocytic cell lines. Here it was shown that the adaptation varies for some protein classes between lung epithelial cells and human embryonic kidney cells. The same protocol could be applied to macrophages in order to compare

results from bacteria internalized by professional phagocytes with those from internalization into non-professional phagocytes.

The modification of the internalization protocol allowed analyzing the host response to infection with the *S. aureus* HG001 wild-type strain. During early stage of infection, apoptosis was modulated, the immunoproteasome was activated, and several pro-inflammatory cytokines were secreted by the host which could probably stimulate immune cells such as macrophages and neutrophils in a more complex internalization setting. The activation of the innate immune response represents an important step of host defense against *S. aureus.* Thus, analysis of the combined response of epithelial cells and neutrophils to infection of epithelial cells by *S. aureus* generates the topic of a recently started PhD thesis in our group. To prevent elimination by the immune system, so-called small colony variants of *S. aureus* with changed phenotypes are able to hide within the cells. During his Bachelor's thesis Jörn Steinke already discovered that a mutation in the *menD* gene leads to a phenotype which prevents cytokine production from epithelial cells. In order to investigate the molecular explanation, comparative intracellular and extracellular proteome analyses of the *S. aureus* HG001 wild-type and the isogenic *ΔmenD* mutant were subject of a recent student's project under my supervision.

REFERENCES

ABU KWAIK, Y., EISENSTEIN, B. I. & ENGLEBERG, N. C. 1993. Phenotypic modulation by Legionella pneumophila upon infection of macrophages. *Infect Immun,* 61**,** 1320-9.

AGERER, F., LUX, S., MICHEL, A., ROHDE, M., OHLSEN, K. & HAUCK, C. R. 2005. Cellular invasion by *Staphylococcus aureus* reveals a functional link between focal adhesion kinase and cortactin in integrin-mediated internalisation. *J Cell Sci,* 118**,** 2189-200.

ALMEIDA, R. A., MATTHEWS, K. R., CIFRIAN, E., GUIDRY, A. J. & OLIVER, S. P. 1996. *Staphylococcus aureus* invasion of bovine mammary epithelial cells. *J Dairy Sci,* 79**,** 1021-6.

AMADO, I. R., VÁZQUEZ, J. A., GUERRA, N. P. & PASTRANA, L. 2013. Thermal resistance of Salmonella enterica, Escherichia coli and *Staphylococcus aureus* isolated from vegetable feed ingredients. *J Sci Food Agric*.

ANDERSON, K. L., ROBERTS, C., DISZ, T., VONSTEIN, V., HWANG, K., OVERBEEK, R., OLSON, P. D., PROJAN, S. J. & DUNMAN, P. M. 2006. Characterization of the *Staphylococcus aureus* heat shock, cold shock, stringent, and SOS responses and their effects on log-phase mRNA turnover. *J Bacteriol,* 188**,** 6739-56.

ANDREWS, S. C., ROBINSON, A. K. & RODRÍGUEZ-QUIÑONES, F. 2003. Bacterial iron homeostasis. *FEMS Microbiol Rev,* 27**,** 215-37.

ANTELMANN, H., TJALSMA, H., VOIGT, B., OHLMEIER, S., BRON, S., VAN DIJL, J. M. & HECKER, M. 2001. A proteomic view on genome-based signal peptide predictions. *Genome Res,* 11**,** 1484-502.

APPELBAUM, P. C. 2006a. MRSA--the tip of the iceberg. *Clin Microbiol Infect,* 12 Suppl 2**,** 3-10.

APPELBAUM, P. C. 2006b. The emergence of vancomycin-intermediate and vancomycin-resistant *Staphylococcus aureus*. *Clin Microbiol Infect,* 12 Suppl 1**,** 16-23.

APS, J. K., VAN DEN MAAGDENBERG, K., DELANGHE, J. R. & MARTENS, L. C. 2002. Flow cytometry as a new method to quantify the cellular content of human saliva and its relation to gingivitis. *Clin Chim Acta,* 321**,** 35-41.

ATKINSON, D. E. 1968. The energy charge of the adenylate pool as a regulatory parameter. Interaction with feedback modifiers. *Biochemistry,* 7**,** 4030-4.

ATTIA, A. S., CASSAT, J. E., ARANMOLATE, S. O., ZIMMERMAN, L. J., BOYD, K. L. & SKAAR, E. P. 2013. Analysis of the *Staphylococcus aureus* abscess proteome identifies antimicrobial host proteins and bacterial stress responses at the host-pathogen interface. *Pathog Dis*.

AVAL, P. S., WERNER, J., CERQUEIRA, A., BALFOUR-BOEHM, J. & ULANOVA, M. 2013. Piceatannol modulates lung epithelial cellular responses to Pseudomonas aeruginosa. *Inflamm Allergy Drug Targets,* 12**,** 297-307.

BANTEL, H., SINHA, B., DOMSCHKE, W., PETERS, G., SCHULZE-OSTHOFF, K. & JÄNICKE, R. U. 2001. alpha-Toxin is a mediator of *Staphylococcus aureus*-induced cell death and activates caspases *via* the intrinsic death pathway independently of death receptor signaling. *J Cell Biol,* 155**,** 637-48.

BANTSCHEFF, M., LEMEER, S., SAVITSKI, M. M. & KUSTER, B. 2012. Quantitative mass spectrometry in proteomics: critical review update from 2007 to the present. *Anal Bioanal Chem,* 404**,** 939-65.

BECHER, D., HEMPEL, K., SIEVERS, S., ZÜHLKE, D., PANÉ-FARRÉ, J., OTTO, A., FUCHS, S., ALBRECHT, D., BERNHARDT, J., ENGELMANN, S., VÖLKER, U., VAN DIJL, J. M. & HECKER, M. 2009. A proteomic view of an important human pathogen--towards the quantification of the entire *Staphylococcus aureus* proteome. *PLoS One,* 4**,** e8176.

BECKER, D., SELBACH, M., ROLLENHAGEN, C., BALLMAIER, M., MEYER, T. F., MANN, M. & BUMANN, D. 2006. Robust Salmonella metabolism limits possibilities for new antimicrobials. *Nature,* 440**,** 303-7.

BELOW, S., KONKEL, A., ZEECK, C., MÜLLER, C., KOHLER, C., ENGELMANN, S. & HILDEBRANDT, J. P. 2009. Virulence factors of *Staphylococcus aureus* induce Erk-MAP kinase activation and c-Fos expression in S9 and 16HBE14o- human airway epithelial cells. *Am J Physiol Lung Cell Mol Physiol,* 296**,** L470-9.

BERGMANN, S., SCHOENEN, H. & HAMMERSCHMIDT, S. 2013. The interaction between bacterial enolase and plasminogen promotes adherence of Streptococcus pneumoniae to epithelial and endothelial cells. *Int J Med Microbiol,* 303**,** 452-62.

BERNHARDT, J., MICHALIK, S., WOLLSCHEID, B., VÖLKER, U. & SCHMIDT, F. 2013. Proteomics approaches for the analysis of enriched microbial subpopulations and visualization of complex functional information. *Curr Opin Biotechnol,* 24**,** 112-9.

BEYNON, R. J., DOHERTY, M. K., PRATT, J. M. & GASKELL, S. J. 2005. Multiplexed absolute quantification in proteomics using artificial QCAT proteins of concatenated signature peptides. *Nat Methods,* 2**,** 587-9.

BLEVINS, J. S., BEENKEN, K. E., ELASRI, M. O., HURLBURT, B. K. & SMELTZER, M. S. 2002. Strain-dependent differences in the regulatory roles of sarA and agr in *Staphylococcus aureus*. *Infect Immun,* 70**,** 470-80.

BLOM, E. J., RIDDER, A. N., LULKO, A. T., ROERDINK, J. B. & KUIPERS, O. P. 2011. Time-resolved transcriptomics and bioinformatic analyses reveal intrinsic stress responses during batch culture of Bacillus subtilis. *PLoS One,* 6**,** e27160.

BLUEMLEIN, K. & RALSER, M. 2011. Monitoring protein expression in whole-cell extracts by targeted label- and standard-free LC-MS/MS. *Nat Protoc,* 6**,** 859-69.

BRIDSON, E. Y. & GOULD, G. W. 2000. Quantal microbiology. *Lett Appl Microbiol,* 30**,** 95-8.

BRUINS, M. J., JUFFER, P., WOLFHAGEN, M. J. & RUIJS, G. J. 2007. Salt tolerance of methicillin-resistant and methicillin-susceptible *Staphylococcus aureus*. *J Clin Microbiol,* 45**,** 682-3.

BUSCHOW, S. I., LASONDER, E., SZKLARCZYK, R., OUD, M. M., DE VRIES, I. J. & FIGDOR, C. G. 2012. Unraveling the human dendritic cell phagosome proteome by organellar enrichment ranking. *J Proteomics,* 75**,** 1547-62.

CHAIBENJAWONG, P. & FOSTER, S. J. 2011. Desiccation tolerance in *Staphylococcus aureus*. *Arch Microbiol,* 193**,** 125-35.

CHAMBERS, H. F. 1997. Methicillin resistance in staphylococci: molecular and biochemical basis and clinical implications. *Clin Microbiol Rev,* 10**,** 781-91.

CHELIUS, D. & BONDARENKO, P. V. 2002. Quantitative profiling of proteins in complex mixtures using liquid chromatography and mass spectrometry. *J Proteome Res,* 1**,** 317-23.

CHENG, A. G., DEDENT, A. C., SCHNEEWIND, O. & MISSIAKAS, D. 2011. A play in four acts: *Staphylococcus aureus* abscess formation. *Trends Microbiol,* 19**,** 225-32.

CHEON, I. S., WOO, S. S., KANG, S. S., IM, J., YUN, C. H., CHUNG, D. K., PARK, D. K. & HAN, S. H. 2008. Peptidoglycan-mediated IL-8 expression in human alveolar type II epithelial cells requires lipid raft formation and MAPK activation. *Mol Immunol,* 45**,** 1665-73.

CHO, S., PARK, S. G., LEE, D. H. & PARK, B. C. 2004. Protein-protein interaction networks: from interactions to networks. *J Biochem Mol Biol,* 37**,** 45-52.

CHOI, M., CHANG, C. Y., CLOUGH, T., BROUDY, D., KILLEEN, T., MACLEAN, B. & VITEK, O. 2014. MSstats: an R package for statistical analysis of quantitative mass spectrometry-based proteomic experiments. *Bioinformatics*.

CLARKE, S. R., ANDRE, G., WALSH, E. J., DUFRÊNE, Y. F., FOSTER, T. J. & FOSTER, S. J. 2009. Iron-regulated surface determinant protein A mediates adhesion of *Staphylococcus aureus* to human corneocyte envelope proteins. *Infect Immun,* 77**,** 2408-16.

CORNELIS, P., WEI, Q., ANDREWS, S. C. & VINCKX, T. 2011. Iron homeostasis and management of oxidative stress response in bacteria. *Metallomics,* 3**,** 540-9.

CORRIGAN, R. M., MIAJLOVIC, H. & FOSTER, T. J. 2009. Surface proteins that promote adherence of *Staphylococcus aureus* to human desquamated nasal epithelial cells. *BMC Microbiol,* 9**,** 22.

CORRIGAN, R. M., RIGBY, D., HANDLEY, P. & FOSTER, T. J. 2007. The role of *Staphylococcus aureus* surface protein SasG in adherence and biofilm formation. *Microbiology,* 153**,** 2435-46.

COUX, O., TANAKA, K. & GOLDBERG, A. L. 1996. Structure and functions of the 20S and 26S proteasomes. *Annu Rev Biochem,* 65**,** 801-47.

COZENS, A. L., YEZZI, M. J., KUNZELMANN, K., OHRUI, T., CHIN, L., ENG, K., FINKBEINER, W. E., WIDDICOMBE, J. H. & GRUENERT, D. C. 1994. CFTR expression and chloride secretion in polarized immortal human bronchial epithelial cells. *Am J Respir Cell Mol Biol,* 10**,** 38-47.

CRAMTON, S. E., GERKE, C., SCHNELL, N. F., NICHOLS, W. W. & GÖTZ, F. 1999. The intercellular adhesion (ica) locus is present in *Staphylococcus aureus* and is required for biofilm formation. *Infect Immun,* 67**,** 5427-33.

CUCARELLA, C., TORMO, M. A., KNECHT, E., AMORENA, B., LASA, I., FOSTER, T. J. & PENADÉS, J. R. 2002. Expression of the biofilm-associated protein interferes with host protein receptors of *Staphylococcus aureus* and alters the infective process. *Infect Immun,* 70**,** 3180-6.

DATE, S. V., MODRUSAN, Z., LAWRENCE, M., MORISAKI, J. H., TOY, K., SHAH, I. M., KIM, J., PARK, S., XU, M., BASUINO, L., CHAN, L., ZEITSCHEL, D., CHAMBERS, H. F., TAN, M. W., BROWN, E. J., DIEP, B. A. & HAZENBOS, W. L. 2014. Global gene expression of methicillin-resistant *Staphylococcus aureus* USA300 during human and mouse infection. *J Infect Dis,* 209**,** 1542-50.

DAVE, K., PALZKILL, T. & PRATT, R. F. 2014. Neutral β-Lactams Inactivate High Molecular Mass Penicillin-Binding Proteins of Class B1, Including PBP2a of MRSA. *ACS Med Chem Lett,* 5**,** 154-7.

DE ASTORZA, B., CORTÉS, G., CRESPÍ, C., SAUS, C., ROJO, J. M. & ALBERTÍ, S. 2004. C3 promotes clearance of Klebsiella pneumoniae by A549 epithelial cells. *Infect Immun,* 72**,** 1767-74.

DEPKE, M., BURIAN, M., SCHÄFER, T., BRÖKER, B. M., OHLSEN, K. & VÖLKER, U. 2012. The alternative sigma factor B modulates virulence gene expression in a murine *Staphylococcus aureus* infection model but does not influence kidney gene expression pattern of the host. *Int J Med Microbiol,* 302**,** 33-9.

DEPKE, M., SURMANN, K., HILDEBRANDT, P., JEHMLICH, N., MICHALIK, S., STANCA, S. E., FRITZSCHE, W., VÖLKER, U. & SCHMIDT, F. 2014. Labeling of the pathogenic bacterium *Staphylococcus aureus* with gold or ferric oxide-core nanoparticles highlights new capabilities for investigation of host-pathogen interactions. *Cytometry A,* 85**,** 140-50.

DESJARDINS, M. 2003. ER-mediated phagocytosis: a new membrane for new functions. *Nat Rev Immunol,* 3**,** 280-91.

DIAZ-RUIZ, R., RIGOULET, M. & DEVIN, A. 2011. The Warburg and Crabtree effects: On the origin of cancer cell energy metabolism and of yeast glucose repression. *Biochim Biophys Acta,* 1807**,** 568-76.

DOSSETT, J. H., KRONVALL, G., WILLIAMS, R. C. & QUIE, P. G. 1969. Antiphagocytic effects of staphylococcal protein A. *J Immunol,* 103**,** 1405-10.

DOVE, B. K., SURTEES, R., BEAN, T. J., MUNDAY, D., WISE, H. M., DIGARD, P., CARROLL, M. W., AJUH, P., BARR, J. N. & HISCOX, J. A. 2012. A quantitative proteomic analysis of lung epithelial (A549) cells infected with 2009 pandemic influenza A virus using stable isotope labelling with amino acids in cell culture. *Proteomics,* 12**,** 1431-6.

DREISBACH, A., OTTO, A., BECHER, D., HAMMER, E., TEUMER, A., GOUW, J. W., HECKER, M. & VÖLKER, U. 2008. Monitoring of changes in the membrane proteome during stationary phase adaptation of Bacillus subtilis using in vivo labeling techniques. *Proteomics,* 8**,** 2062-76.

DUMONT, A. L. & TORRES, V. J. 2014. Cell targeting by the *Staphylococcus aureus* pore-forming toxins: it's not just about lipids. *Trends Microbiol,* 22**,** 21-7.

DÖRRIES, K. & LALK, M. 2013. Metabolic footprint analysis uncovers strain specific overflow metabolism and D-isoleucine production of *Staphylococcus aureus* COL and HG001. *PLoS One,* 8**,** e81500.

EGAN, M., FLOTTE, T., AFIONE, S., SOLOW, R., ZEITLIN, P. L., CARTER, B. J. & GUGGINO, W. B. 1992. Defective regulation of outwardly rectifying Cl- channels by protein kinase A corrected by insertion of CFTR. *Nature,* 358**,** 581-4.

EICHSTAEDT, S., GÄBLER, K., BELOW, S., MÜLLER, C., KOHLER, C., ENGELMANN, S., HILDEBRANDT, P., VÖLKER, U., HECKER, M. & HILDEBRANDT, J. P. 2009. Effects of *Staphylococcus aureus*-hemolysin A on calcium signalling in immortalized human airway epithelial cells. *Cell Calcium,* 45**,** 165-76.

EISENREICH, W., HEESEMANN, J., RUDEL, T. & GOEBEL, W. 2013. Metabolic host responses to infection by intracellular bacterial pathogens. *Front Cell Infect Microbiol,* 3**,** 24.

ELLINGTON, J. K., REILLY, S. S., RAMP, W. K., SMELTZER, M. S., KELLAM, J. F. & HUDSON, M. C. 1999. Mechanisms of *Staphylococcus aureus* invasion of cultured osteoblasts. *Microb Pathog,* 26**,** 317-23.

ENG, J. K., JAHAN, T. A. & HOOPMANN, M. R. 2013. Comet: an open-source MS/MS sequence database search tool. *Proteomics,* 13**,** 22-4.

ENG, J. K., MCCORMACK, A. L. & YATES, J. R. 1994. An approach to correlate tandem mass spectral data of peptides with amino acid sequences in a protein database. *J Am Soc Mass Spectrom,* 5**,** 976-89.

FERNÁNDEZ-ARENAS, E., CABEZÓN, V., BERMEJO, C., ARROYO, J., NOMBELA, C., DIEZ-OREJAS, R. & GIL, C. 2007. Integrated proteomics and genomics strategies bring new insight into Candida albicans response upon macrophage interaction. *Mol Cell Proteomics,* 6**,** 460-78.

FERRARI, G., LANGEN, H., NAITO, M. & PIETERS, J. 1999. A coat protein on phagosomes involved in the intracellular survival of mycobacteria. *Cell,* 97**,** 435-47.

FIERRO-MONTI, I., RACLE, J., HERNANDEZ, C., WARIDEL, P., HATZIMANIKATIS, V. & QUADRONI, M. 2013. A novel pulse-chase SILAC strategy measures changes in protein decay and synthesis rates induced by perturbation of proteostasis with an Hsp90 inhibitor. *PLoS One,* 8**,** e80423.

FLOTTE, T. R., AFIONE, S. A., SOLOW, R., DRUMM, M. L., MARKAKIS, D., GUGGINO, W. B., ZEITLIN, P. L. & CARTER, B. J. 1993. Expression of the cystic fibrosis transmembrane conductance regulator from a novel adeno-associated virus promoter. *J Biol Chem,* 268**,** 3781-90.

FOERSTER, S., KACPROWSKI, T., DHOPLE, V. M., HAMMER, E., HERZOG, S., SAAFAN, H., BIEN-MÖLLER, S., ALBRECHT, M., VÖLKER, U. & RITTER, C. A. 2013. Characterization of the EGFR interactome reveals associated protein complex networks and intracellular receptor dynamics. *Proteomics,* 13**,** 3131-44.

FOURNIER, B., KLIER, A. & RAPOPORT, G. 2001. The two-component system ArlS-ArlR is a regulator of virulence gene expression in *Staphylococcus aureus*. *Mol Microbiol,* 41**,** 247-61.

FRAUNHOLZ, M. & SINHA, B. 2012. Intracellular *Staphylococcus aureus*: live-in and let die. *Front Cell Infect Microbiol,* 2**,** 43.

GALLIEN, S., DURIEZ, E. & DOMON, B. 2011. Selected reaction monitoring applied to proteomics. *J Mass Spectrom,* 46**,** 298-312.

GARCÍA-PÉREZ, B. E., MONDRAGÓN-FLORES, R. & LUNA-HERRERA, J. 2003. Internalization of Mycobacterium tuberculosis by macropinocytosis in non-phagocytic cells. *Microb Pathog,* 35**,** 49-55.

GARVIS, S., MEI, J. M., RUIZ-ALBERT, J. & HOLDEN, D. W. 2002. *Staphylococcus aureus* svrA: a gene required for virulence and expression of the agr locus. *Microbiology,* 148**,** 3235-43.

GARZONI, C., FRANCOIS, P., HUYGHE, A., COUZINET, S., TAPPAREL, C., CHARBONNIER, Y., RENZONI, A., LUCCHINI, S., LEW, D. P., VAUDAUX, P., KELLEY, W. L. & SCHRENZEL, J. 2007. A global view of *Staphylococcus aureus* whole genome expression upon internalization in human epithelial cells. *BMC Genomics,* 8**,** 171.

GARZONI, C. & KELLEY, W. L. 2009. *Staphylococcus aureus*: new evidence for intracellular persistence. *Trends Microbiol,* 17**,** 59-65.

GEIGER, T., FRANCOIS, P., LIEBEKE, M., FRAUNHOLZ, M., GOERKE, C., KRISMER, B., SCHRENZEL, J., LALK, M. & WOLZ, C. 2012. The stringent response of *Staphylococcus aureus* and its impact on survival after phagocytosis through the induction of intracellular PSMs expression. *PLoS Pathog,* 8**,** e1003016.

GEIGER, T., GOERKE, C., FRITZ, M., SCHÄFER, T., OHLSEN, K., LIEBEKE, M., LALK, M. & WOLZ, C. 2010. Role of the (p)ppGpp synthase RSH, a RelA/SpoT homolog, in stringent response and virulence of *Staphylococcus aureus*. *Infect Immun,* 78**,** 1873-83.

GEIGER, T., KÄSTLE, B., GRATANI, F. L., GOERKE, C. & WOLZ, C. 2014. Two small (p)ppGpp synthases in *Staphylococcus aureus* mediate tolerance against cell envelope stress conditions. *J Bacteriol,* 196**,** 894-902.

GENESTIER, A. L., MICHALLET, M. C., PRÉVOST, G., BELLOT, G., CHALABREYSSE, L., PEYROL, S., THIVOLET, F., ETIENNE, J., LINA, G., VALLETTE, F. M., VANDENESCH, F. & GENESTIER, L. 2005. *Staphylococcus aureus* Panton-Valentine leukocidin directly targets

mitochondria and induces Bax-independent apoptosis of human neutrophils. *J Clin Invest,* 115**,** 3117-27.

GERBER, S. A., RUSH, J., STEMMAN, O., KIRSCHNER, M. W. & GYGI, S. P. 2003. Absolute quantification of proteins and phosphoproteins from cell lysates by tandem MS. *Proc Natl Acad Sci U S A,* 100**,** 6940-5.

GIACHINO, P., ENGELMANN, S. & BISCHOFF, M. 2001. Sigma(B) activity depends on RsbU in *Staphylococcus aureus*. *J Bacteriol,* 183**,** 1843-52.

GIEROK, P., HARMS, M., RICHTER, E., HILDEBRANDT, J. P., LALK, M., MOSTERTZ, J. & HOCHGRÄFE, F. 2014. *Staphylococcus aureus* alpha-toxin mediates general and cell type-specific changes in metabolite concentrations of immortalized human airway epithelial cells. *PLoS One,* 9**,** e94818.

GIESE, B., DITTMANN, S., PAPROTKA, K., LEVIN, K., WELTROWSKI, A., BIEHLER, D., LÂM, T. T., SINHA, B. & FRAUNHOLZ, M. J. 2009. Staphylococcal alpha-toxin is not sufficient to mediate escape from phagolysosomes in upper-airway epithelial cells. *Infect Immun,* 77**,** 3611-25.

GILLASPY, A. F., WORREL, V., ORVIS, J., ROE, B. A., DYER, D. W. & IANDOLO, J. J. 2006. The *Staphylococcus aureus* NCTC 8325 genome. *In:* FISCHETTI, V. A., NOVICK, R., FERRETTI, J. J., PORTNOY, D. A. & ROOD, J. I. (eds.) *Gram-positive Pathogens.* Washington: ASM Press.

GILLET, L. C., NAVARRO, P., TATE, S., RÖST, H., SELEVSEK, N., REITER, L., BONNER, R. & AEBERSOLD, R. 2012. Targeted data extraction of the MS/MS spectra generated by data-independent acquisition: a new concept for consistent and accurate proteome analysis. *Mol Cell Proteomics,* 11**,** O111.016717.

GIRAUDO, A. T., CALZOLARI, A., CATALDI, A. A., BOGNI, C. & NAGEL, R. 1999. The sae locus of *Staphylococcus aureus* encodes a two-component regulatory system. *FEMS Microbiol Lett,* 177**,** 15-22.

GOKCE, E., SHUFORD, C. M., FRANCK, W. L., DEAN, R. A. & MUDDIMAN, D. C. 2011. Evaluation of normalization methods on GeLC-MS/MS label-free spectral counting data to correct for variation during proteomic workflows. *J Am Soc Mass Spectrom,* 22**,** 2199-208.

GORDON, R. J. & LOWY, F. D. 2008. Pathogenesis of methicillin-resistant *Staphylococcus aureus* infection. *Clin Infect Dis,* 46 Suppl 5**,** S350-9.

GRAHAM, F. L., SMILEY, J., RUSSELL, W. C. & NAIRN, R. 1977. Characteristics of a human cell line transformed by DNA from human adenovirus type 5. *J Gen Virol,* 36**,** 59-74.

GROSZ, M., KOLTER, J., PAPROTKA, K., WINKLER, A. C., SCHÄFER, D., CHATTERJEE, S. S., GEIGER, T., WOLZ, C., OHLSEN, K., OTTO, M., RUDEL, T., SINHA, B. & FRAUNHOLZ, M. 2014. Cytoplasmic replication of *Staphylococcus aureus* upon phagosomal escape triggered by phenol-soluble modulin α. *Cell Microbiol,* 16**,** 451-65.

GÖTZ, F. & MAYER, S. 2013. Both terminal oxidases contribute to fitness and virulence during organ-specific *Staphylococcus aureus* colonization. *MBio,* 4**,** e00976-13.

HAIR, P. S., ECHAGUE, C. G., SHOLL, A. M., WATKINS, J. A., GEOGHEGAN, J. A., FOSTER, T. J. & CUNNION, K. M. 2010. Clumping factor A interaction with complement factor I increases C3b cleavage on the bacterial surface of *Staphylococcus aureus* and decreases complement-mediated phagocytosis. *Infect Immun,* 78**,** 1717-27.

HARTLEIB, J., KÖHLER, N., DICKINSON, R. B., CHHATWAL, G. S., SIXMA, J. J., HARTFORD, O. M., FOSTER, T. J., PETERS, G., KEHREL, B. E. & HERRMANN, M. 2000. Protein A is the von Willebrand factor binding protein on *Staphylococcus aureus*. *Blood,* 96**,** 2149-56.

HASLINGER-LÖFFLER, B., KAHL, B. C., GRUNDMEIER, M., STRANGFELD, K., WAGNER, B., FISCHER, U., CHEUNG, A. L., PETERS, G., SCHULZE-OSTHOFF, K. & SINHA, B. 2005. Multiple virulence factors are required for *Staphylococcus aureus*-induced apoptosis in endothelial cells. *Cell Microbiol,* 7**,** 1087-97.

HASLINGER-LÖFFLER, B., WAGNER, B., BRÜCK, M., STRANGFELD, K., GRUNDMEIER, M., FISCHER, U., VÖLKER, W., PETERS, G., SCHULZE-OSTHOFF, K. & SINHA, B. 2006. *Staphylococcus aureus* induces caspase-independent cell death in human peritoneal mesothelial cells. *Kidney Int,* 70**,** 1089-98.

HEILMANN, C., HUSSAIN, M., PETERS, G. & GÖTZ, F. 1997. Evidence for autolysin-mediated primary attachment of Staphylococcus epidermidis to a polystyrene surface. *Mol Microbiol,* 24**,** 1013-24.

HEINK, S., LUDWIG, D., KLOETZEL, P. M. & KRÜGER, E. 2005. IFN-gamma-induced immune adaptation of the proteasome system is an accelerated and transient response. *Proc Natl Acad Sci U S A,* 102**,** 9241-6.

HEINRICHS, J. H., BAYER, M. G. & CHEUNG, A. L. 1996. Characterization of the sar locus and its interaction with agr in *Staphylococcus aureus*. *J Bacteriol,* 178**,** 418-23.

HEINZEN, R. A., GRIESHABER, S. S., VAN KIRK, L. S. & DEVIN, C. J. 1999. Dynamics of actin-based movement by Rickettsia rickettsii in vero cells. *Infect Immun,* 67**,** 4201-7.

HENDRIX, H., LINDHOUT, T., MERTENS, K., ENGELS, W. & HEMKER, H. C. 1983. Activation of human prothrombin by stoichiometric levels of staphylocoagulase. *J Biol Chem,* 258**,** 3637-44.

HERBERT, S., ZIEBANDT, A. K., OHLSEN, K., SCHÄFER, T., HECKER, M., ALBRECHT, D., NOVICK, R. & GÖTZ, F. 2010. Repair of global regulators in *Staphylococcus aureus* 8325 and comparative analysis with other clinical isolates. *Infect Immun,* 78**,** 2877-89.

HERMANN, I., RÄTH, S., ZIESEMER, S., VOLKSDORF, T., DRESS, R. J., GUTJAHR, M., MÜLLER, C., BEULE, A. G. & HILDEBRANDT, J. P. 2014. *Staphylococcus aureus*-hemolysin A Disrupts Cell-matrix Adhesions in Human Airway Epithelial Cells. *Am J Respir Cell Mol Biol*.

HIGH, N., MOUNIER, J., PRÉVOST, M. C. & SANSONETTI, P. J. 1992. IpaB of Shigella flexneri causes entry into epithelial cells and escape from the phagocytic vacuole. *EMBO J,* 11**,** 1991-9.

HINDRÉ, T., BRÜGGEMANN, H., BUCHRIESER, C. & HÉCHARD, Y. 2008. Transcriptional profiling of Legionella pneumophila biofilm cells and the influence of iron on biofilm formation. *Microbiology,* 154**,** 30-41.

HIRSCHHAUSEN, N., SCHLESIER, T., SCHMIDT, M. A., GÖTZ, F., PETERS, G. & HEILMANN, C. 2010. A novel staphylococcal internalization mechanism involves the major autolysin Atl and heat shock cognate protein Hsc70 as host cell receptor. *Cell Microbiol,* 12**,** 1746-64.

HOGEA, C., VAN EFFELTERRE, T. & CASSIDY, A. 2014. A model-based analysis: what potential could there be for a *S. aureus* vaccine in a hospital setting on top of other preventative measures? *BMC Infect Dis,* 14**,** 291.

HU, C., XIONG, N., ZHANG, Y., RAYNER, S. & CHEN, S. 2012. Functional characterization of lipase in the pathogenesis of *Staphylococcus aureus*. *Biochem Biophys Res Commun,* 419**,** 617-20.

HUDSON, M. C., RAMP, W. K., NICHOLSON, N. C., WILLIAMS, A. S. & NOUSIAINEN, M. T. 1995. Internalization of *Staphylococcus aureus* by cultured osteoblasts. *Microb Pathog,* 19**,** 409-19.

IBARRA, J. A., PÉREZ-RUEDA, E., CARROLL, R. K. & SHAW, L. N. 2013. Global analysis of transcriptional regulators in *Staphylococcus aureus*. *BMC Genomics,* 14**,** 126.

JANEWAY, C. A. & MEDZHITOV, R. 2002. Innate immune recognition. *Annu Rev Immunol,* 20**,** 197-216.

JEHMLICH, N., HÜBSCHMANN, T., GESELL SALAZAR, M., VÖLKER, U., BENNDORF, D., MÜLLER, S., VON BERGEN, M. & SCHMIDT, F. 2010. Advanced tool for characterization of microbial cultures by combining cytomics and proteomics. *Appl Microbiol Biotechnol,* 88**,** 575-84.

JIANG, R. D., SHEN, H. & PIAO, Y. J. 2010. The morphometrical analysis on the ultrastructure of A549 cells. *Rom J Morphol Embryol,* 51**,** 663-7.

JIMÉNEZ, E., MARÍN, M. L., MARTÍN, R., ODRIOZOLA, J. M., OLIVARES, M., XAUS, J., FERNÁNDEZ, L. & RODRÍGUEZ, J. M. 2008. Is meconium from healthy newborns actually sterile? *Res Microbiol,* 159**,** 187-93.

JONSSON, I. M., ARVIDSON, S., FOSTER, S. & TARKOWSKI, A. 2004. Sigma factor B and RsbU are required for virulence in *Staphylococcus aureus*-induced arthritis and sepsis. *Infect Immun,* 72**,** 6106-11.

JOOST, I., JACOB, S., UTERMÖHLEN, O., SCHUBERT, U., PATTI, J. M., ONG, M. F., GROSS, J., JUSTINGER, C., RENNO, J. H., PREISSNER, K. T., BISCHOFF, M. & HERRMANN, M. 2011. Antibody response to the extracellular adherence protein (Eap) of *Staphylococcus aureus* in healthy and infected individuals. *FEMS Immunol Med Microbiol,* 62**,** 23-31.

JOUSSELIN, A., RENZONI, A., ANDREY, D. O., MONOD, A., LEW, D. P. & KELLEY, W. L. 2012. The posttranslocational chaperone lipoprotein PrsA is involved in both glycopeptide and oxacillin resistance in *Staphylococcus aureus*. *Antimicrob Agents Chemother,* 56**,** 3629-40.

JUNGK, J., COMO-SABETTI, K., STINCHFIELD, P., ACKERMAN, P. & HARRIMAN, K. 2007. Epidemiology of methicillin-resistant *Staphylococcus aureus* at a pediatric healthcare system, 1991-2003. *Pediatr Infect Dis J,* 26**,** 339-44.

JUTRAS, I., HOUDE, M., CURRIER, N., BOULAIS, J., DUCLOS, S., LABOISSIÈRE, S., BONNEIL, E., KEARNEY, P., THIBAULT, P., PARAMITHIOTIS, E., HUGO, P. & DESJARDINS, M. 2008. Modulation of the phagosome proteome by interferon-gamma. *Mol Cell Proteomics,* 7**,** 697-715.

KAHL, B., HERRMANN, M., EVERDING, A. S., KOCH, H. G., BECKER, K., HARMS, E., PROCTOR, R. A. & PETERS, G. 1998. Persistent infection with small colony variant strains of *Staphylococcus aureus* in patients with cystic fibrosis. *J Infect Dis,* 177**,** 1023-9.

KAHL, B. C. 2014. Small colony variants (SCVs) of *Staphylococcus aureus*--a bacterial survival strategy. *Infect Genet Evol,* 21**,** 515-22.

KAPETANOVIC, R., NAHORI, M. A., BALLOY, V., FITTING, C., PHILPOTT, D. J., CAVAILLON, J. M. & ADIB-CONQUY, M. 2007. Contribution of phagocytosis and intracellular sensing for cytokine production by *Staphylococcus aureus*-activated macrophages. *Infect Immun,* 75**,** 830-7.

KARAVOLOS, M. H., HORSBURGH, M. J., INGHAM, E. & FOSTER, S. J. 2003. Role and regulation of the superoxide dismutases of *Staphylococcus aureus*. *Microbiology,* 149**,** 2749-58.

KARLSSON, A. & ARVIDSON, S. 2002. Variation in extracellular protease production among clinical isolates of *Staphylococcus aureus* due to different levels of expression of the protease repressor sarA. *Infect Immun,* 70**,** 4239-46.

KELLER, A., NESVIZHSKII, A. I., KOLKER, E. & AEBERSOLD, R. 2002. Empirical statistical model to estimate the accuracy of peptide identifications made by MS/MS and database search. *Anal Chem,* 74**,** 5383-92.

KELLER, A. & SHTEYNBERG, D. 2011. Software pipeline and data analysis for MS/MS proteomics: the trans-proteomic pipeline. *Methods Mol Biol,* 694**,** 169-89.

KERSEY, P., HERMJAKOB, H. & APWEILER, R. 2000. VARSPLIC: alternatively-spliced protein sequences derived from SWISS-PROT and TrEMBL. *Bioinformatics,* 16**,** 1048-9.

KIM, H. K., DEDENT, A., CHENG, A. G., MCADOW, M., BAGNOLI, F., MISSIAKAS, D. M. & SCHNEEWIND, O. 2010. IsdA and IsdB antibodies protect mice against *Staphylococcus aureus* abscess formation and lethal challenge. *Vaccine,* 28**,** 6382-92.

KINTARAK, S., WHAWELL, S. A., SPEIGHT, P. M., PACKER, S. & NAIR, S. P. 2004. Internalization of *Staphylococcus aureus* by human keratinocytes. *Infect Immun,* 72**,** 5668-75.

KLOETZEL, P. M. 2004. The proteasome and MHC class I antigen processing. *Biochim Biophys Acta,* 1695**,** 225-33.

KLOSE, J. 1975. Protein mapping by combined isoelectric focusing and electrophoresis of mouse tissues. A novel approach to testing for induced point mutations in mammals. *Humangenetik,* 26**,** 231-43.

KO, Y. P., LIANG, X., SMITH, C. W., DEGEN, J. L. & HÖÖK, M. 2011. Binding of Efb from *Staphylococcus aureus* to fibrinogen blocks neutrophil adherence. *J Biol Chem,* 286**,** 9865-74.

KOHLER, C., VON EIFF, C., LIEBEKE, M., MCNAMARA, P. J., LALK, M., PROCTOR, R. A., HECKER, M. & ENGELMANN, S. 2008. A defect in menadione biosynthesis induces global changes in gene expression in *Staphylococcus aureus*. *J Bacteriol,* 190**,** 6351-64.

KOHLER, C., VON EIFF, C., PETERS, G., PROCTOR, R. A., HECKER, M. & ENGELMANN, S. 2003. Physiological characterization of a heme-deficient mutant of *Staphylococcus aureus* by a proteomic approach. *J Bacteriol,* 185**,** 6928-37.

KONG, K. F., VUONG, C. & OTTO, M. 2006. Staphylococcus quorum sensing in biofilm formation and infection. *Int J Med Microbiol,* 296**,** 133-9.

KOZIEL, J., MACIAG-GUDOWSKA, A., MIKOLAJCZYK, T., BZOWSKA, M., STURDEVANT, D. E., WHITNEY, A. R., SHAW, L. N., DELEO, F. R. & POTEMPA, J. 2009. Phagocytosis of *Staphylococcus aureus* by macrophages exerts cytoprotective effects manifested by the upregulation of antiapoptotic factors. *PLoS One,* 4**,** e5210.

KULLIK, I., GIACHINO, P. & FUCHS, T. 1998. Deletion of the alternative sigma factor sigmaB in *Staphylococcus aureus* reveals its function as a global regulator of virulence genes. *J Bacteriol,* 180**,** 4814-20.

KUMAR, J. K. 2008. Lysostaphin: an antistaphylococcal agent. *Appl Microbiol Biotechnol,* 80**,** 555-61.

KURODA, M., KURODA, H., OSHIMA, T., TAKEUCHI, F., MORI, H. & HIRAMATSU, K. 2003. Two-component system VraSR positively modulates the regulation of cell-wall biosynthesis pathway in *Staphylococcus aureus*. *Mol Microbiol,* 49**,** 807-21.

KÖNIG, B., PRÉVOST, G. & KÖNIG, W. 1997. Composition of staphylococcal bi-component toxins determines pathophysiological reactions. *J Med Microbiol,* 46**,** 479-85.

LAM, H., DEUTSCH, E. W., EDDES, J. S., ENG, J. K., KING, N., STEIN, S. E. & AEBERSOLD, R. 2007. Development and validation of a spectral library searching method for peptide identification from MS/MS. *Proteomics,* 7**,** 655-67.

LAMBERTI, Y., GORGOJO, J., MASSILLO, C. & RODRIGUEZ, M. E. 2013. Bordetella pertussis entry into respiratory epithelial cells and intracellular survival. *Pathog Dis,* 69**,** 194-204.

LEE, P. K., DILL, B. D., LOUIE, T. S., SHAH, M., VERBERKMOES, N. C., ANDERSEN, G. L., ZINDER, S. H. & ALVAREZ-COHEN, L. 2012. Global transcriptomic and proteomic responses of Dehalococcoides ethenogenes strain 195 to fixed nitrogen limitation. *Appl Environ Microbiol,* 78**,** 1424-36.

LEVINE, A. J. & PUZIO-KUTER, A. M. 2010. The control of the metabolic switch in cancers by oncogenes and tumor suppressor genes. *Science,* 330**,** 1340-4.

LIANG, X., YAN, M. & JI, Y. 2009. The H35A mutated alpha-toxin interferes with cytotoxicity of staphylococcal alpha-toxin. *Infect Immun,* 77**,** 977-83.

LIEBEKE, M., DÖRRIES, K., MEYER, H. & LALK, M. 2012. Metabolome analysis of gram-positive bacteria such as *Staphylococcus aureus* by GC-MS and LC-MS. *Methods Mol Biol,* 815**,** 377-98.

LIEBEKE, M., DÖRRIES, K., ZÜHLKE, D., BERNHARDT, J., FUCHS, S., PANÉ-FARRÉ, J., ENGELMANN, S., VÖLKER, U., BODE, R., DANDEKAR, T., LINDEQUIST, U., HECKER, M. & LALK, M. 2011. A metabolomics and proteomics study of the adaptation of *Staphylococcus aureus* to glucose starvation. *Mol Biosyst,* 7**,** 1241-53.

LIEBER, M., SMITH, B., SZAKAL, A., NELSON-REES, W. & TODARO, G. 1976. A continuous tumor-cell line from a human lung carcinoma with properties of type II alveolar epithelial cells. *Int J Cancer,* 17**,** 62-70.

LINDSAY, J. A. 2007. Prospects for a MRSA vaccine. *Future Microbiol,* 2**,** 1-3.

LIVAK, K. J. & SCHMITTGEN, T. D. 2001. Analysis of relative gene expression data using real-time quantitative PCR and the 2(-Delta Delta C(T)) Method. *Methods,* 25**,** 402-8.

LOUGHMAN, A., FITZGERALD, J. R., BRENNAN, M. P., HIGGINS, J., DOWNER, R., COX, D. & FOSTER, T. J. 2005. Roles for fibrinogen, immunoglobulin and complement in platelet activation promoted by *Staphylococcus aureus* clumping factor A. *Mol Microbiol,* 57**,** 804-18.

LOWY, F. D. 1998. *Staphylococcus aureus* infections. *N Engl J Med,* 339**,** 520-32.

LÖFFLER, B., TUCHSCHERR, L., NIEMANN, S. & PETERS, G. 2014. *Staphylococcus aureus* persistence in non-professional phagocytes. *Int J Med Microbiol,* 304**,** 170-6.

LÜHRMANN, A. & HAAS, A. 2000. A method to purify bacteria-containing phagosomes from infected macrophages. *Methods Cell Sci,* 22**,** 329-41.

MAASS, S., SIEVERS, S., ZÜHLKE, D., KUZINSKI, J., SAPPA, P. K., MUNTEL, J., HESSLING, B., BERNHARDT, J., SIETMANN, R., VÖLKER, U., HECKER, M. & BECHER, D. 2011. Efficient, global-scale quantification of absolute protein amounts by integration of targeted mass spectrometry and two-dimensional gel-based proteomics. *Anal Chem,* 83**,** 2677-84.

MACCOSS, M. J., WU, C. C. & YATES, J. R. 2002. Probability-based validation of protein identifications using a modified SEQUEST algorithm. *Anal Chem,* 74**,** 5593-9.

MACLEAN, B., TOMAZELA, D. M., ABBATIELLO, S. E., ZHANG, S., WHITEAKER, J. R., PAULOVICH, A. G., CARR, S. A. & MACCOSS, M. J. 2010a. Effect of collision energy optimization on the measurement of peptides by selected reaction monitoring (SRM) mass spectrometry. *Anal Chem,* 82**,** 10116-24.

MACLEAN, B., TOMAZELA, D. M., SHULMAN, N., CHAMBERS, M., FINNEY, G. L., FREWEN, B., KERN, R., TABB, D. L., LIEBLER, D. C. & MACCOSS, M. J. 2010b. Skyline: an open source

document editor for creating and analyzing targeted proteomics experiments. *Bioinformatics,* 26**,** 966-8.

MALLICK, P., SCHIRLE, M., CHEN, S. S., FLORY, M. R., LEE, H., MARTIN, D., RANISH, J., RAUGHT, B., SCHMITT, R., WERNER, T., KUSTER, B. & AEBERSOLD, R. 2007. Computational prediction of proteotypic peptides for quantitative proteomics. *Nat Biotechnol,* 25**,** 125-31.

MANNA, A. & CHEUNG, A. L. 2001. Characterization of sarR, a modulator of sar expression in *Staphylococcus aureus*. *Infect Immun,* 69**,** 885-96.

MARSHALL, J. H. & WILMOTH, G. J. 1981. Pigments of *Staphylococcus aureus*, a series of triterpenoid carotenoids. *J Bacteriol,* 147**,** 900-13.

MATTOW, J., SIEJAK, F., HAGENS, K., BECHER, D., ALBRECHT, D., KRAH, A., SCHMIDT, F., JUNGBLUT, P. R., KAUFMANN, S. H. & SCHAIBLE, U. E. 2006. Proteins unique to intraphagosomally grown Mycobacterium tuberculosis. *Proteomics,* 6**,** 2485-94.

MAYA, S., INDULEKHA, S., SUKHITHASRI, V., SMITHA, K. T., NAIR, S. V., JAYAKUMAR, R. & BISWAS, R. 2012. Efficacy of tetracycline encapsulated O-carboxymethyl chitosan nanoparticles against intracellular infections of *Staphylococcus aureus*. *Int J Biol Macromol,* 51**,** 392-9.

MAZMANIAN, S. K., SKAAR, E. P., GASPAR, A. H., HUMAYUN, M., GORNICKI, P., JELENSKA, J., JOACHMIAK, A., MISSIAKAS, D. M. & SCHNEEWIND, O. 2003. Passage of heme-iron across the envelope of *Staphylococcus aureus*. *Science,* 299**,** 906-9.

MCALEESE, F. M., WALSH, E. J., SIEPRAWSKA, M., POTEMPA, J. & FOSTER, T. J. 2001. Loss of clumping factor B fibrinogen binding activity by *Staphylococcus aureus* involves cessation of transcription, shedding and cleavage by metalloprotease. *J Biol Chem,* 276**,** 29969-78.

MCCOURT, J., O'HALLORAN, D. P., MCCARTHY, H., O'GARA, J. P. & GEOGHEGAN, J. A. 2014. Fibronectin binding proteins are required for biofilm formation by community-associated methicillin resistant *Staphylococcus aureus* strain LAC. *FEMS Microbiol Lett*.

MCNAMARA, P. J., MILLIGAN-MONROE, K. C., KHALILI, S. & PROCTOR, R. A. 2000. Identification, cloning, and initial characterization of rot, a locus encoding a regulator of virulence factor expression in *Staphylococcus aureus*. *J Bacteriol,* 182**,** 3197-203.

MEDIAVILLA, J. R., CHEN, L., MATHEMA, B. & KREISWIRTH, B. N. 2012. Global epidemiology of community-associated methicillin resistant *Staphylococcus aureus* (CA-MRSA). *Curr Opin Microbiol,* 15**,** 588-95.

MEDINI, D., DONATI, C., TETTELIN, H., MASIGNANI, V. & RAPPUOLI, R. 2005. The microbial pan-genome. *Curr Opin Genet Dev,* 15**,** 589-94.

MELVIN, J. A., MURPHY, C. F., DUBOIS, L. G., THOMPSON, J. W., MOSELEY, M. A. & MCCAFFERTY, D. G. 2011. *Staphylococcus aureus* sortase A contributes to the Trojan horse mechanism of immune defense evasion with its intrinsic resistance to Cys184 oxidation. *Biochemistry,* 50**,** 7591-9.

MEY, A. R., CRAIG, S. A. & PAYNE, S. M. 2005. Characterization of Vibrio cholerae RyhB: the RyhB regulon and role of ryhB in biofilm formation. *Infect Immun,* 73**,** 5706-19.

MEYER, H., LIEBEKE, M. & LALK, M. 2010. A protocol for the investigation of the intracellular *Staphylococcus aureus* metabolome. *Anal Biochem,* 401**,** 250-9.

MILLER, M., DREISBACH, A., OTTO, A., BECHER, D., BERNHARDT, J., HECKER, M., PEPPELENBOSCH, M. P. & VAN DIJL, J. M. 2011. Mapping of interactions between human macrophages and *Staphylococcus aureus* reveals an involvement of MAP kinase signaling in the host defense. *J Proteome Res,* 10**,** 4018-32.

MOHAMMED, K. A., NASREEN, N. & ANTONY, V. B. 2007. Bacterial induction of early response genes and activation of proapoptotic factors in pleural mesothelial cells. *Lung,* 185**,** 355-65.

MOISAN, H., BROUILLETTE, E., JACOB, C. L., LANGLOIS-BÉGIN, P., MICHAUD, S. & MALOUIN, F. 2006. Transcription of virulence factors in *Staphylococcus aureus* small-colony variants isolated from cystic fibrosis patients is influenced by SigB. *J Bacteriol,* 188**,** 64-76.

MOREILHON, C., GRAS, D., HOLOGNE, C., BAJOLET, O., COTTREZ, F., MAGNONE, V., MERTEN, M., GROUX, H., PUCHELLE, E. & BARBRY, P. 2005. Live *Staphylococcus aureus* and bacterial soluble factors induce different transcriptional responses in human airway cells. *Physiol Genomics,* 20**,** 244-55.

MOSKOVITZ, J., SINGH, V. K., REQUENA, J., WILKINSON, B. J., JAYASWAL, R. K. & STADTMAN, E. R. 2002. Purification and characterization of methionine sulfoxide reductases from mouse and *Staphylococcus aureus* and their substrate stereospecificity. *Biochem Biophys Res Commun,* 290**,** 62-5.

MUNDAY, D. C., EMMOTT, E., SURTEES, R., LARDEAU, C. H., WU, W., DUPREX, W. P., DOVE, B. K., BARR, J. N. & HISCOX, J. A. 2010a. Quantitative proteomic analysis of A549 cells infected with human respiratory syncytial virus. *Mol Cell Proteomics,* 9**,** 2438-59.

MUNDAY, D. C., HISCOX, J. A. & BARR, J. N. 2010b. Quantitative proteomic analysis of A549 cells infected with human respiratory syncytial virus subgroup B using SILAC coupled to LC-MS/MS. *Proteomics,* 10**,** 4320-34.

NAKAI, K. & HORTON, P. 1999. PSORT: a program for detecting sorting signals in proteins and predicting their subcellular localization. *Trends Biochem Sci,* 24**,** 34-6.

NAQVI, S., SAMIM, M., ABDIN, M., AHMED, F. J., MAITRA, A., PRASHANT, C. & DINDA, A. K. 2010. Concentration-dependent toxicity of iron oxide nanoparticles mediated by increased oxidative stress. *Int J Nanomedicine,* 5**,** 983-9.

NESVIZHSKII, A. I., KELLER, A., KOLKER, E. & AEBERSOLD, R. 2003. A statistical model for identifying proteins by tandem mass spectrometry. *Anal Chem,* 75**,** 4646-58.

NICOD, L. P. 1993. Cytokines. 1. Overview. *Thorax,* 48**,** 660-7.

NIETO, C. & ESPINOSA, M. 2003. Construction of the mobilizable plasmid pMV158GFP, a derivative of pMV158 that carries the gene encoding the green fluorescent protein. *Plasmid,* 49**,** 281-5.

NIZET, V. 2007. Understanding how leading bacterial pathogens subvert innate immunity to reveal novel therapeutic targets. *J Allergy Clin Immunol,* 120**,** 13-22.

NOVICK, R. P. 2003. Autoinduction and signal transduction in the regulation of staphylococcal virulence. *Mol Microbiol,* 48**,** 1429-49.

NOVICK, R. P., ROSS, H. F., PROJAN, S. J., KORNBLUM, J., KREISWIRTH, B. & MOGHAZEH, S. 1993. Synthesis of staphylococcal virulence factors is controlled by a regulatory RNA molecule. *EMBO J,* 12**,** 3967-75.

O'FARRELL, P. H. 1975. High resolution two-dimensional electrophoresis of proteins. *J Biol Chem,* 250**,** 4007-21.

O'RIORDAN, K. & LEE, J. C. 2004. *Staphylococcus aureus* capsular polysaccharides. *Clin Microbiol Rev,* 17**,** 218-34.

OGSTON, A. 1882. Micrococcus poisoning. *J Anat Physiol.* [Online], 16.

OLIVIER, A. C., LEMAIRE, S., VAN BAMBEKE, F., TULKENS, P. M. & OLDFIELD, E. 2009. Role of rsbU and staphyloxanthin in phagocytosis and intracellular growth of *Staphylococcus aureus* in human macrophages and endothelial cells. *J Infect Dis,* 200**,** 1367-70.

OLSEN, J. V., ONG, S. E. & MANN, M. 2004. Trypsin cleaves exclusively C-terminal to arginine and lysine residues. *Mol Cell Proteomics,* 3**,** 608-14.

ONG, S. E., BLAGOEV, B., KRATCHMAROVA, I., KRISTENSEN, D. B., STEEN, H., PANDEY, A. & MANN, M. 2002. Stable isotope labeling by amino acids in cell culture, SILAC, as a simple and accurate approach to expression proteomics. *Mol Cell Proteomics,* 1**,** 376-86.

OTTO, A., BECHER, D. & SCHMIDT, F. 2014. Quantitative proteomics in the field of microbiology. *Proteomics,* 14**,** 547-65.

OTTO, M. 2013. Staphylococcal infections: mechanisms of biofilm maturation and detachment as critical determinants of pathogenicity. *Annu Rev Med,* 64**,** 175-88.

OTTO, M. 2014. Phenol-soluble modulins. *Int J Med Microbiol,* 304**,** 164-9.

OVERBEEK, R., BEGLEY, T., BUTLER, R. M., CHOUDHURI, J. V., CHUANG, H. Y., COHOON, M., DE CRÉCY-LAGARD, V., DIAZ, N., DISZ, T., EDWARDS, R., FONSTEIN, M., FRANK, E. D., GERDES, S., GLASS, E. M., GOESMANN, A., HANSON, A., IWATA-REUYL, D., JENSEN, R., JAMSHIDI, N., KRAUSE, L., KUBAL, M., LARSEN, N., LINKE, B., MCHARDY, A. C., MEYER, F., NEUWEGER, H., OLSEN, G., OLSON, R., OSTERMAN, A., PORTNOY, V., PUSCH, G. D., RODIONOV, D. A., RÜCKERT, C., STEINER, J., STEVENS, R., THIELE, I., VASSIEVA, O., YE, Y., ZAGNITKO, O. & VONSTEIN, V. 2005. The subsystems approach to genome annotation and its use in the project to annotate 1000 genomes. *Nucleic Acids Res,* 33**,** 5691-702.

PALMQVIST, N., PATTI, J. M., TARKOWSKI, A. & JOSEFSSON, E. 2004. Expression of staphylococcal clumping factor A impedes macrophage phagocytosis. *Microbes Infect,* 6**,** 188-95.

PANDEY, A. & MANN, M. 2000. Proteomics to study genes and genomes. *Nature,* 405**,** 837-46.

PASZTOR, L., ZIEBANDT, A. K., NEGA, M., SCHLAG, M., HAASE, S., FRANZ-WACHTEL, M., MADLUNG, J., NORDHEIM, A., HEINRICHS, D. E. & GÖTZ, F. 2010. Staphylococcal major autolysin (Atl) is involved in excretion of cytoplasmic proteins. *J Biol Chem,* 285**,** 36794-803.

PERKINS, D. N., PAPPIN, D. J., CREASY, D. M. & COTTRELL, J. S. 1999. Probability-based protein identification by searching sequence databases using mass spectrometry data. *Electrophoresis,* 20**,** 3551-67.

PFÖRTNER, H., BURIAN, M. S., MICHALIK, S., DEPKE, M., HILDEBRANDT, P., DHOPLE, V. M., PANÉ-FARRÉ, J., HECKER, M., SCHMIDT, F. & VÖLKER, U. 2014. Activation of the alternative sigma factor SigB of *Staphylococcus aureus* following internalization by epithelial cells - An in vivo proteomics perspective. *Int J Med Microbiol,* 304**,** 177-87.

PFÖRTNER, H., WAGNER, J., SURMANN, K., HILDEBRANDT, P., ERNST, S., BERNHARDT, J., SCHURMANN, C., GUTJAHR, M., DEPKE, M., JEHMLICH, U., DHOPLE, V., HAMMER, E., STEIL, L., VÖLKER, U. & SCHMIDT, F. 2013. A proteomics workflow for quantitative and time-resolved analysis of adaptation reactions of internalized bacteria. *Methods,* 61**,** 244-50.

PIZARRO-CERDÁ, J., MÉRESSE, S., PARTON, R. G., VAN DER GOOT, G., SOLA-LANDA, A., LOPEZ-GOÑI, I., MORENO, E. & GORVEL, J. P. 1998. Brucella abortus transits through the autophagic pathway and replicates in the endoplasmic reticulum of nonprofessional phagocytes. *Infect Immun,* 66**,** 5711-24.

PROCTOR, R. A., VON EIFF, C., KAHL, B. C., BECKER, K., MCNAMARA, P., HERRMANN, M. & PETERS, G. 2006. Small colony variants: a pathogenic form of bacteria that facilitates persistent and recurrent infections. *Nat Rev Microbiol,* 4**,** 295-305.

PÉRICHON, B. & COURVALIN, P. 2009. VanA-type vancomycin-resistant *Staphylococcus aureus*. *Antimicrob Agents Chemother,* 53**,** 4580-7.

RABINOVICH, L., SIGAL, N., BOROVOK, I., NIR-PAZ, R. & HERSKOVITS, A. A. 2012. Prophage excision activates Listeria competence genes that promote phagosomal escape and virulence. *Cell,* 150**,** 792-802.

RABINOVITCH, M. 1995. Professional and non-professional phagocytes: an introduction. *Trends Cell Biol,* 5**,** 85-7.

RECSEI, P. A., GRUSS, A. D. & NOVICK, R. P. 1987. Cloning, sequence, and expression of the lysostaphin gene from Staphylococcus simulans. *Proc Natl Acad Sci U S A,* 84**,** 1127-31.

ROOIJAKKERS, S. H., VAN WAMEL, W. J., RUYKEN, M., VAN KESSEL, K. P. & VAN STRIJP, J. A. 2005. Anti-opsonic properties of staphylokinase. *Microbes Infect,* 7**,** 476-84.

ROSSEAU, S., SELHORST, J., WIECHMANN, K., LEISSNER, K., MAUS, U., MAYER, K., GRIMMINGER, F., SEEGER, W. & LOHMEYER, J. 2000. Monocyte migration through the alveolar epithelial barrier: adhesion molecule mechanisms and impact of chemokines. *J Immunol,* 164**,** 427-35.

RÄTH, S., ZIESEMER, S., WITTE, A., KONKEL, A., MÜLLER, C., HILDEBRANDT, P., VÖLKER, U. & HILDEBRANDT, J. P. 2013. *S. aureus* haemolysin A-induced IL-8 and IL-6 release from human airway epithelial cells is mediated by activation of p38- and Erk-MAP kinases and additional, cell type-specific signalling mechanisms. *Cell Microbiol,* 15**,** 1253-65.

SACHSE, F., VON EIFF, C., STOLL, W., BECKER, K. & RUDACK, C. 2006. Induction of CXC chemokines in A549 airway epithelial cells by trypsin and staphylococcal proteases - a possible route for neutrophilic inflammation in chronic rhinosinusitis. *Clin Exp Immunol,* 144**,** 534-42.

SADIGHI AKHA, A. A., THERIOT, C. M., ERB-DOWNWARD, J. R., MCDERMOTT, A. J., FALKOWSKI, N. R., TYRA, H. M., RUTKOWSKI, D. T., YOUNG, V. B. & HUFFNAGLE, G. B. 2013. Acute infection of mice with Clostridium difficile leads to eIF2α phosphorylation and pro-survival signalling as part of the mucosal inflammatory response. *Immunology,* 140**,** 111-22.

SALEH, M., BARTUAL, S. G., ABDULLAH, M. R., JENSCH, I., ASMAT, T. M., PETRUSCHKA, L., PRIBYL, T., GELLERT, M., LILLIG, C. H., ANTELMANN, H., HERMOSO, J. A. & HAMMERSCHMIDT, S. 2013. Molecular architecture of Streptococcus pneumoniae surface

thioredoxin-fold lipoproteins crucial for extracellular oxidative stress resistance and maintenance of virulence. *EMBO Mol Med,* 5**,** 1852-70.

SARAVIA-OTTEN, P., MÜLLER, H. P. & ARVIDSON, S. 1997. Transcription of *Staphylococcus aureus* fibronectin binding protein genes is negatively regulated by agr and an agr-independent mechanism. *J Bacteriol,* 179**,** 5259-63.

SCHILLING, B., RARDIN, M. J., MACLEAN, B. X., ZAWADZKA, A. M., FREWEN, B. E., CUSACK, M. P., SORENSEN, D. J., BEREMAN, M. S., JING, E., WU, C. C., VERDIN, E., KAHN, C. R., MACCOSS, M. J. & GIBSON, B. W. 2012. Platform-independent and label-free quantitation of proteomic data using MS1 extracted ion chromatograms in skyline: application to protein acetylation and phosphorylation. *Mol Cell Proteomics,* 11**,** 202-14.

SCHINDLER, C. A. & SCHUHARDT, V. T. 1964. Lysostaphin: A new bacteriolytic agent for the *Staphylococcus*. *Proc Natl Acad Sci U S A,* 51**,** 414-21.

SCHMIDT, C., LENZ, C., GROTE, M., LÜHRMANN, R. & URLAUB, H. 2010a. Determination of protein stoichiometry within protein complexes using absolute quantification and multiple reaction monitoring. *Anal Chem,* 82**,** 2784-96.

SCHMIDT, F., SCHARF, S. S., HILDEBRANDT, P., BURIAN, M., BERNHARDT, J., DHOPLE, V., KALINKA, J., GUTJAHR, M., HAMMER, E. & VÖLKER, U. 2010b. Time-resolved quantitative proteome profiling of host-pathogen interactions: the response of *Staphylococcus aureus* RN1HG to internalisation by human airway epithelial cells. *Proteomics,* 10**,** 2801-11.

SCHMIDT, F., STROZYNSKI, M., SALUS, S. S., NILSEN, H. & THIEDE, B. 2007. Rapid determination of amino acid incorporation by stable isotope labeling with amino acids in cell culture (SILAC). *Rapid Commun Mass Spectrom,* 21**,** 3919-26.

SCHMIDT, F. & VÖLKER, U. 2011. Proteome analysis of host-pathogen interactions: Investigation of pathogen responses to the host cell environment. *Proteomics,* 11**,** 3203-11.

SCHMIDT, K. A., MANNA, A. C., GILL, S. & CHEUNG, A. L. 2001. SarT, a repressor of alpha-hemolysin in *Staphylococcus aureus*. *Infect Immun,* 69**,** 4749-58.

SCHNAITH, A., KASHKAR, H., LEGGIO, S. A., ADDICKS, K., KRÖNKE, M. & KRUT, O. 2007. *Staphylococcus aureus* subvert autophagy for induction of caspase-independent host cell death. *J Biol Chem,* 282**,** 2695-706.

SCHRÖDER, A., KLAND, R., PESCHEL, A., VON EIFF, C. & AEPFELBACHER, M. 2006. Live cell imaging of phagosome maturation in *Staphylococcus aureus* infected human endothelial cells: small colony variants are able to survive in lysosomes. *Med Microbiol Immunol,* 195**,** 185-94.

SCHWARTZ, J., LEIDAL, K. G., FEMLING, J. K., WEISS, J. P. & NAUSEEF, W. M. 2009. Neutrophil bleaching of GFP-expressing staphylococci: probing the intraphagosomal fate of individual bacteria. *J Immunol,* 183**,** 2632-41.

SENDI, P. & PROCTOR, R. A. 2009. *Staphylococcus aureus* as an intracellular pathogen: the role of small colony variants. *Trends Microbiol,* 17**,** 54-8.

SHEVCHUK, O., BATZILLA, C., HÄGELE, S., KUSCH, H., ENGELMANN, S., HECKER, M., HAAS, A., HEUNER, K., GLÖCKNER, G. & STEINERT, M. 2009. Proteomic analysis of Legionella-containing phagosomes isolated from Dictyostelium. *Int J Med Microbiol,* 299**,** 489-508.

SHTEYNBERG, D., DEUTSCH, E. W., LAM, H., ENG, J. K., SUN, Z., TASMAN, N., MENDOZA, L., MORITZ, R. L., AEBERSOLD, R. & NESVIZHSKII, A. I. 2011. iProphet: multi-level integrative analysis of shotgun proteomic data improves peptide and protein identification rates and error estimates. *Mol Cell Proteomics,* 10**,** M111.007690.

SHTEYNBERG, D., NESVIZHSKII, A. I., MORITZ, R. L. & DEUTSCH, E. W. 2013. Combining results of multiple search engines in proteomics. *Mol Cell Proteomics,* 12**,** 2383-93.

SIEPRAWSKA-LUPA, M., MYDEL, P., KRAWCZYK, K., WÓJCIK, K., PUKLO, M., LUPA, B., SUDER, P., SILBERRING, J., REED, M., POHL, J., SHAFER, W., MCALEESE, F., FOSTER, T., TRAVIS, J. & POTEMPA, J. 2004. Degradation of human antimicrobial peptide LL-37 by *Staphylococcus aureus*-derived proteinases. *Antimicrob Agents Chemother,* 48**,** 4673-9.

SILENCE, K., HARTMANN, M., GÜHRS, K. H., GASE, A., SCHLOTT, B., COLLEN, D. & LIJNEN, H. R. 1995. Structure-function relationships in staphylokinase as revealed by "clustered charge to alanine" mutagenesis. *J Biol Chem,* 270**,** 27192-8.

SINGH, V. K. & MOSKOVITZ, J. 2003. Multiple methionine sulfoxide reductase genes in *Staphylococcus aureus*: expression of activity and roles in tolerance of oxidative stress. *Microbiology,* 149**,** 2739-47.

SINHA, B., FRANCOIS, P., QUE, Y. A., HUSSAIN, M., HEILMANN, C., MOREILLON, P., LEW, D., KRAUSE, K. H., PETERS, G. & HERRMANN, M. 2000. Heterologously expressed *Staphylococcus aureus* fibronectin-binding proteins are sufficient for invasion of host cells. *Infect Immun,* 68**,** 6871-8.

SINHA, B., FRANÇOIS, P. P., NÜSSE, O., FOTI, M., HARTFORD, O. M., VAUDAUX, P., FOSTER, T. J., LEW, D. P., HERRMANN, M. & KRAUSE, K. H. 1999. Fibronectin-binding protein acts as *Staphylococcus aureus* invasin *via* fibronectin bridging to integrin alpha5beta1. *Cell Microbiol,* 1**,** 101-17.

SINHA, B. & HERRMANN, M. 2005. Mechanism and consequences of invasion of endothelial cells by *Staphylococcus aureus*. *Thromb Haemost,* 94**,** 266-77.

SKAAR, E. P., GASPAR, A. H. & SCHNEEWIND, O. 2004a. IsdG and IsdI, heme-degrading enzymes in the cytoplasm of *Staphylococcus aureus*. *J Biol Chem,* 279**,** 436-43.

SKAAR, E. P., HUMAYUN, M., BAE, T., DEBORD, K. L. & SCHNEEWIND, O. 2004b. Iron-source preference of *Staphylococcus aureus* infections. *Science,* 305**,** 1626-8.

SMITH, E. J., VISAI, L., KERRIGAN, S. W., SPEZIALE, P. & FOSTER, T. J. 2011. The Sbi protein is a multifunctional immune evasion factor of *Staphylococcus aureus*. *Infect Immun,* 79**,** 3801-9.

SONG, L., HOBAUGH, M. R., SHUSTAK, C., CHELEY, S., BAYLEY, H. & GOUAUX, J. E. 1996. Structure of staphylococcal alpha-hemolysin, a heptameric transmembrane pore. *Science,* 274**,** 1859-66.

STADNYK, A. W. 1994. Cytokine production by epithelial cells. *FASEB J,* 8**,** 1041-7.

STEINHÄUSER, C., HEIGL, U., TCHIKOV, V., SCHWARZ, J., GUTSMANN, T., SEEGER, K., BRANDENBURG, J., FRITSCH, J., SCHROEDER, J., WIESMÜLLER, K. H., ROSENKRANDS, I., WALTHER, P., POTT, J., KRAUSE, E., EHLERS, S., SCHNEIDER-BRACHERT, W., SCHÜTZE, S. & REILING, N. 2013. Lipid-labeling facilitates a novel magnetic isolation procedure to characterize pathogen-containing phagosomes. *Traffic,* 14**,** 321-36.

STENTZEL, S., CHI, V. H., WEYRICH, A. M., JEHMLICH, N., SCHMIDT, F., SALAZAR, M. G., STEIL, L., VÖLKER, U. & BRÖKER, B. M. 2014. Altered immune proteome of *Staphylococcus aureus* under iron-restricted growth conditions. *Proteomics*.

STRELKOV, S., VON ELSTERMANN, M. & SCHOMBURG, D. 2004. Comprehensive analysis of metabolites in Corynebacterium glutamicum by gas chromatography/mass spectrometry. *Biol Chem,* 385**,** 853-61.

STURGILL-KOSZYCKI, S., SCHLESINGER, P. H., CHAKRABORTY, P., HADDIX, P. L., COLLINS, H. L., FOK, A. K., ALLEN, R. D., GLUCK, S. L., HEUSER, J. & RUSSELL, D. G. 1994. Lack of acidification in Mycobacterium phagosomes produced by exclusion of the vesicular proton-ATPase. *Science,* 263**,** 678-81.

SURMANN, K., LAERMANN, V., ZIMMANN, P., ALTENDORF, K. & HAMMER, E. 2014a. Absolute quantification of the Kdp subunits of Escherichia coli by multiple reaction monitoring. *Proteomics,* 14**,** 1630-8.

SURMANN, K., MICHALIK, S., HILDEBRANDT, P., GIEROK, P., DEPKE, M., BRINKMANN, L., BERNHARDT, J., SALAZAR, M. G., SUN, Z., SHTEYNBERG, D., KUSEBAUCH, U., MORITZ, R. L., WOLLSCHEID, B., LALK, M., VÖLKER, U. & SCHMIDT, F. 2014b. Comparative proteome analysis reveals conserved and specific adaptation patterns of *Staphylococcus aureus* after internalization by different types of human non-professional phagocytic host cells. *Front Microbiol,* 5**,** 392.

TEGMARK, K., KARLSSON, A. & ARVIDSON, S. 2000. Identification and characterization of SarH1, a new global regulator of virulence gene expression in *Staphylococcus aureus*. *Mol Microbiol,* 37**,** 398-409.

THOMAS, D., CHOU, S., DAUWALDER, O. & LINA, G. 2007. Diversity in *Staphylococcus aureus* enterotoxins. *Chem Immunol Allergy,* 93**,** 24-41.

TROST, M., WEHMHÖNER, D., KÄRST, U., DIETERICH, G., WEHLAND, J. & JÄNSCH, L. 2005. Comparative proteome analysis of secretory proteins from pathogenic and nonpathogenic Listeria species. *Proteomics,* 5**,** 1544-57.

TUCHSCHERR, L., HEITMANN, V., HUSSAIN, M., VIEMANN, D., ROTH, J., VON EIFF, C., PETERS, G., BECKER, K. & LÖFFLER, B. 2010. *Staphylococcus aureus* small-colony variants are adapted phenotypes for intracellular persistence. *J Infect Dis,* 202**,** 1031-40.

TUCHSCHERR, L., MEDINA, E., HUSSAIN, M., VÖLKER, W., HEITMANN, V., NIEMANN, S., HOLZINGER, D., ROTH, J., PROCTOR, R. A., BECKER, K., PETERS, G. & LÖFFLER, B. 2011. *Staphylococcus aureus* phenotype switching: an effective bacterial strategy to escape host immune response and establish a chronic infection. *EMBO Mol Med,* 3**,** 129-41.

TWINE, S. M., MYKYTCZUK, N. C., PETIT, M. D., SHEN, H., SJÖSTEDT, A., WAYNE CONLAN, J. & KELLY, J. F. 2006. In vivo proteomic analysis of the intracellular bacterial pathogen, Francisella tularensis, isolated from mouse spleen. *Biochem Biophys Res Commun,* 345**,** 1621-33.

VAN DEN BERG, S., BOWDEN, M. G., BOSMA, T., BUIST, G., VAN DIJL, J. M., VAN WAMEL, W. J., DE VOGEL, C. P., VAN BELKUM, A. & BAKKER-WOUDENBERG, I. A. 2011. A multiplex assay for the quantification of antibody responses in *Staphylococcus aureus* infections in mice. *J Immunol Methods,* 365**,** 142-8.

VAN OOSTEN, M., SCHÄFER, T., GAZENDAM, J. A., OHLSEN, K., TSOMPANIDOU, E., DE GOFFAU, M. C., HARMSEN, H. J., CRANE, L. M., LIM, E., FRANCIS, K. P., CHEUNG, L., OLIVE, M., NTZIACHRISTOS, V., VAN DIJL, J. M. & VAN DAM, G. M. 2013. Real-time in vivo imaging of invasive- and biomaterial-associated bacterial infections using fluorescently labelled vancomycin. *Nat Commun,* 4**,** 2584.

VANDENESCH, F., LINA, G. & HENRY, T. 2012. *Staphylococcus aureus* hemolysins, bi-component leukocidins, and cytolytic peptides: a redundant arsenal of membrane-damaging virulence factors? *Front Cell Infect Microbiol,* 2**,** 12.

VAUDAUX, P., FRANCOIS, P., BISOGNANO, C., KELLEY, W. L., LEW, D. P., SCHRENZEL, J., PROCTOR, R. A., MCNAMARA, P. J., PETERS, G. & VON EIFF, C. 2002. Increased expression of clumping factor and fibronectin-binding proteins by hemB mutants of *Staphylococcus aureus* expressing small colony variant phenotypes. *Infect Immun,* 70**,** 5428-37.

VENTURA, C. L., HIGDON, R., HOHMANN, L., MARTIN, D., KOLKER, E., LIGGITT, H. D., SKERRETT, S. J. & RUBENS, C. E. 2008a. *Staphylococcus aureus* elicits marked alterations in the airway proteome during early pneumonia. *Infect Immun,* 76**,** 5862-72.

VENTURA, C. L., HIGDON, R., KOLKER, E., SKERRETT, S. J. & RUBENS, C. E. 2008b. Host airway proteins interact with *Staphylococcus aureus* during early pneumonia. *Infect Immun,* 76**,** 888-98.

VIZCAÍNO, J. A., DEUTSCH, E. W., WANG, R., CSORDAS, A., REISINGER, F., RÍOS, D., DIANES, J. A., SUN, Z., FARRAH, T., BANDEIRA, N., BINZ, P. A., XENARIOS, I., EISENACHER, M., MAYER, G., GATTO, L., CAMPOS, A., CHALKLEY, R. J., KRAUS, H. J., ALBAR, J. P., MARTINEZ-BARTOLOMÉ, S., APWEILER, R., OMENN, G. S., MARTENS, L., JONES, A. R. & HERMJAKOB, H. 2014. ProteomeXchange provides globally coordinated proteomics data submission and dissemination. *Nat Biotechnol,* 32**,** 223-6.

VOGEL, J. P. & ISBERG, R. R. 1999. Cell biology of Legionella pneumophila. *Curr Opin Microbiol,* 2**,** 30-4.

VOWINCKEL, J., CAPUANO, F., CAMPBELL, K., DEERY, M. J., LILLEY, K. S. & RALSER, M. 2013. The beauty of being (label)-free: sample preparation methods for SWATH-MS and next-generation targeted proteomics. *F1000Res,* 2**,** 272.

WANG, J. H., ZHANG, K., WANG, N., QIU, X. M., WANG, Y. B. & HE, P. 2013. Involvement of phosphatidylinositol 3-Kinase/Akt signaling pathway in β1 integrin-mediated internalization of *Staphylococcus aureus* by alveolar epithelial cells. *J Microbiol,* 51**,** 644-50.

WASINGER, V. C., CORDWELL, S. J., CERPA-POLJAK, A., YAN, J. X., GOOLEY, A. A., WILKINS, M. R., DUNCAN, M. W., HARRIS, R., WILLIAMS, K. L. & HUMPHERY-SMITH, I. 1995. Progress with gene-product mapping of the Mollicutes: Mycoplasma genitalium. *Electrophoresis,* 16**,** 1090-4.

WEBER, H., ENGELMANN, S., BECHER, D. & HECKER, M. 2004. Oxidative stress triggers thiol oxidation in the glyceraldehyde-3-phosphate dehydrogenase of *Staphylococcus aureus*. *Mol Microbiol,* 52**,** 133-40.

WERTHEIM, H. F., MELLES, D. C., VOS, M. C., VAN LEEUWEN, W., VAN BELKUM, A., VERBRUGH, H. A. & NOUWEN, J. L. 2005. The role of nasal carriage in *Staphylococcus aureus* infections. *Lancet Infect Dis,* 5**,** 751-62.

WERTHEIM, H. F., VOS, M. C., OTT, A., VAN BELKUM, A., VOSS, A., KLUYTMANS, J. A., VAN KEULEN, P. H., VANDENBROUCKE-GRAULS, C. M., MEESTER, M. H. & VERBRUGH, H. A. 2004. Risk and outcome of nosocomial *Staphylococcus aureus* bacteraemia in nasal carriers *versus* non-carriers. *Lancet,* 364**,** 703-5.

WHICHER, J. T. & EVANS, S. W. 1990. Cytokines in disease. *Clin Chem,* 36**,** 1269-81.

WOPEREIS, H., OOZEER, R., KNIPPING, K., BELZER, C. & KNOL, J. 2014. The first thousand days - intestinal microbiology of early life: establishing a symbiosis. *Pediatr Allergy Immunol,* 25**,** 428-38.

WU, H., DOWNS, D., GHOSH, K., GHOSH, A. K., STAIB, P., MONOD, M. & TANG, J. 2013. Candida albicans secreted aspartic proteases 4-6 induce apoptosis of epithelial cells by a novel Trojan horse mechanism. *FASEB J,* 27**,** 2132-44.

XIA, Q., WANG, T., TAUB, F., PARK, Y., CAPESTANY, C. A., LAMONT, R. J. & HACKETT, M. 2007. Quantitative proteomics of intracellular Porphyromonas gingivalis. *Proteomics,* 7**,** 4323-37.

YARWOOD, J. M., MCCORMICK, J. K. & SCHLIEVERT, P. M. 2001. Identification of a novel two-component regulatory system that acts in global regulation of virulence factors of *Staphylococcus aureus*. *J Bacteriol,* 183**,** 1113-23.

ZEITLIN, P. L., LU, L., RHIM, J., CUTTING, G., STETTEN, G., KIEFFER, K. A., CRAIG, R. & GUGGINO, W. B. 1991. A cystic fibrosis bronchial epithelial cell line: immortalization by adeno-12-SV40 infection. *Am J Respir Cell Mol Biol,* 4**,** 313-9.

ZIEBANDT, A. K., BECHER, D., OHLSEN, K., HACKER, J., HECKER, M. & ENGELMANN, S. 2004. The influence of agr and sigmaB in growth phase dependent regulation of virulence factors in *Staphylococcus aureus*. *Proteomics,* 4**,** 3034-47.

ZIEBANDT, A. K., WEBER, H., RUDOLPH, J., SCHMID, R., HÖPER, D., ENGELMANN, S. & HECKER, M. 2001. Extracellular proteins of *Staphylococcus aureus* and the role of SarA and sigma B. *Proteomics,* 1**,** 480-93.

ZYBAILOV, B., MOSLEY, A. L., SARDIU, M. E., COLEMAN, M. K., FLORENS, L. & WASHBURN, M. P. 2006. Statistical analysis of membrane proteome expression changes in Saccharomyces cerevisiae. *J Proteome Res,* 5**,** 2339-47.

CONTENT OF SUPPLEMENTARY MATERIAL

1. Supplementary_Material_01_Details of LC-MS-analysis.docx
   Information on parameters for LC-MS/MS analysis for the NP and the cell line comparison project.
2. Supplementary_Material_02_Genedata_Refiner_Workflow_identification_NP.pdf
3. Supplementary_Material_03_Genedata_Refiner_Workflow_quantification_NP.pdf
4. Supplementary_Material_04_Voronoi-like_treemaps.pdf
   Voronoi-like treemaps of Figure 37, 52, 53, and 64 are provided as pdf-file to allow zooming into pathways.
5. Supplementary_Material_Table_01_MRM_transitions_S_aureus_HG001.xlsx
   MRM transitions for targeted S. aureus HG001 proteins. The finally acquired list is presented. Precursor and product m/z data as well as optimized collision energies are given together with start and end retention times as the instrument was run in scheduled mode.
6. Supplementary_Material_Table_02_MRM_transitions_B_pertussis_Tohama_I.xlsx
   MRM transitions acquired to identify and relatively quantify proteins of B. pertussis Tohama I. A list of proteins, sequences, corresponding precursor-product pairs and collision energies is provided. All transitions were acquired to allow accurate identification. Only peptides detectable in all replicates were used for relative comparison in different samples and are highlighted in gray. For peptides written in bold letters additional MS/MS spectra are available for validation of peaks.
7. Supplementary_Material_Table_03_S_aureus_DB_NCTC8325_BLAST_HGW.xlsx
   The database of S. aureus HG001 was updated by strain comparisons in order to find functions of proteins for similar sequences. Additionally the source of the new functional annotation is provided. This database was used as the new in-house database for studies on S. aureus HG001.
8. Supplementary_Material_Table_04_S_aureus_proteins_quantified_from_infected_celllines.xlsx
   All staphylococcal proteins which could be quantified with unique peptides after internalization by A549, S9 or HEK 293 cells are listed. Mean values of median-normalized protein intensities from three BR of internalized samples (2.5 h and 6.5 h after infection) were related on the non-adherent (non-ad) control. Ratio values to the control <0.5 are highlighted in blue, ratio values to the control >2 are highlighted in red. Data that were not available are labeled “na” and highlighted in gray.
9. Supplementary_Material_Table_05_TEM_slides_A549_S_aureus_cell_counting.xlsx
   A549 cells infected with S. aureus HG001 were prepared for transmission electron microscopy (TEM). At three sampling points (2.5 h, 4.5 h, and 6.5 h p.i.) each two slices were analyzed by

TEM and infected and non-infected A549 cells as well as bacteria were counted. Average values, standard deviation and coefficient of variance (CV) are given. Values that were not available are labeled "na".

10. Supplementary_Material_Table_06_extracellular_metabolome_host.xlsx
    The extracellular metabolome was measured by ^{1}H-NMR in the supernatant of A549 (four BR), S9 (three BR), and HEK 293 (four BR) cells one hour after exposure to the cells. Average, standard deviation and coefficient of variation (CV) are given for each metabolite.
11. Supplementary_Material_Table_07_intracellular_metabolome_host.xlsx
    The intracellular metabolome of A549, S9, and HEK 293 cells was analyzed by GC-MS and LC-MS one hour after treatment with sterile infection mix. Average values, standard deviations and coefficient of variation (CV) from each four BR were calculated.
12. Supplementary_Material_Table_08_S_aureus_internalized_by_A549.xlsx
    Mean values of median-normalized protein intensities from three BR of S. aureus HG001 pMV158GFP internalized by A549 cells are displayed. Data were acquired hourly between 1.5 h and 6.5 h after infection and are normalized on the 1.5 h time-point. Ratio values to the 1.5 h point in time <0.5 are highlighted in blue, ratio values to the 1.5 h point in time >2 are highlighted in red.
13. Supplementary_Material_Table_09_the_SEED_functional_categories_S_aureus_HG001.xlsx
    List of S. aureus HG001 proteins assigned to functional categories in three levels according to the SEED (Overbeek et al., 2005) are displayed. This list was used for physiological interpretation of S. aureus proteome response to internalization by human cell lines.
14. Supplementary_Material_Table_10_S_aureus_HG001_proteins_in_isolated_phagosomes_shotgun.xlsx
    Five BR of proteome analysis of S. aureus HG001 pMV158GFP detected inside infected phagosomes from S9 cells are displayed. Shotgun results were complement with average values, standard deviation, coefficient of variation (CV), ratio data, fold changes, and p-values together with false discovery rate (FDR) determination. When no spectral counts were detected, "0" was replaced by "0.1". P-values and FDR <0.05 are highlighted in yellow. Regulated proteins are labeled "yes" and highlighted in green. Fold change values 6.5 h/2.5 h <-1.5 are highlighted in blue, those >1.5 in red.
15. Supplementary_Material_Table_11_PSORT_NCTC_8325_protein_localization.xlsx
    Localization of S. aureus proteins detected inside isolated phagosomes was performed using the PSORTb algorithm (Nakai and Horton, 1999).
16. Supplementary_Material_Table_12_PSORT_S_aureus_isolated_from_phagosomes_or_sorted_from_S9_cell_debris.xlsx
    Proteins of S. aureus HG001 pMV158GFP which were internalized by S9 cells were analyzed after isolation of phagosomes or sorting of bacteria from host cell debris. Information are

provided if proteins were quantified in one of the categories or not (na). Further the localization prediction according to the PSORTb algorithm (Nakai and Horton, 1999) are given in order to compare differences in percentage of protein classes depending on the localization.

17. Supplementary_Material_Table_13_B_pertussis_iron_limitation_spectral_counting.xlsx
    Spectral counts of B. pertussis Tohama I proteins measured during iron-supply and iron-limitation are displayed. Mean values and coefficient of variation (CV) of three BR are displayed as well as ratio data, p-values from student's t-test and q-values from multiple testing correction according to Benjamini-Hochberg are provided. P-values and q-values <0.05 are highlighted in yellow. Ratios between the conditions <0.66667 are highlighted in blue, ratios >1.5 are highlighted in red. Ratios that were not available were labeled "na" and highlighted in gray.
18. Supplementary_Material_Table_14_B_pertussis_internalized_spectral_counting.xlsx
    Spectral counts of B. pertussis Tohama I proteins measured from bacteria grown in DMEM and internalized bacteria 2 h and 48 h after infection are displayed. Mean values and coefficient of variation (CV) of three BR are displayed as well as ratio data, p-values from student's t-test and q-values from multiple testing correction according to Benjamini-Hochberg are provided. P-values and q-values <0.05 are highlighted in yellow. Ratios between the conditions <0.66667 are highlighted in blue, ratios >1.5 are highlighted in red.
19. Supplementary_Material_Table_15_normalized_SILAC_ratios_of_A549_proteins_infected_with_S_aureus.xlsx
    Mean values of median-normalized protein intensities from each three BR of three different treatment groups of A549 cells (non-infected control, GFP-positive A549 cells that were infected with S. aureus HG001 pMV158GFP, A549 cells non-carrying bacteria after contact) are displayed. Mean ratio data from three BR of normalized intensities of the sample related to the heavy labeled standard A549 cells are listed. Ratios between internalized samples and the heavy labeled control <0.83333 are highlighted in blue, ratios >1.2 are highlighted in red.
20. Supplementary_Material_Table_16_human_proteins_from_isolated_phagosomes_of_S_aureus_HG001-infected_S9_cells_shotgun.xlsx
    Five BR of proteome analysis of phagosomes isolated from human S9 cells infected with S. aureus HG001 pMV158GFP are displayed. Shotgun results were complemented with average values, standard deviation, coefficient of variation (CV), ratio data, fold changes, and p-values together with false discovery rate (FDR) determination. P-values and FDR <0.05 are highlighted in yellow. Regulated proteins are labeled "yes" and highlighted in green. Fold change values 6.5 h/2.5 h <-1.2 are highlighted in blue, those >1.2 in red.

PUBLICATIONS

Articles

Henrike Pförtner, Juliane Wagner, **Kristin Surmann**, Petra Hildebrandt, Sandra Ernst, Jörg Bernhardt, Claudia Schurmann, Melanie Gutjahr, Maren Depke, Nico Jehmlich, Vishnu Dhople, Elke Hammer, Leif Steil, Uwe Völker, Frank Schmidt.
A proteomics workflow for quantitative and time-resolved analysis of adaptation reactions of internalized bacteria.
Methods. 2013. 61:244-250. doi: 10.1016/j.ymeth.2013.04.009.

Maren Depke*, **Kristin Surmann***, Petra Hildebrandt, Nico Jehmlich, Stephan Michalik, Sarmiza E Stanca, Wolfgang Fritsche, Uwe Völker, Frank Schmidt.
Labeling of the pathogenic bacterium *Staphylococcus aureus* with gold or ferric oxide-core nanoparticles highlights new capabilities for investigation of host-pathogen interactions.
Cytometry Part A. 2014. 85:140-150. doi: 10.1002/cyto.a.22425.

Kristin Surmann*, Vera Laermann*, Petra Zimmann, Karlheinz Altendorf, Elke Hammer.
Absolute Quantification of the Kdp subunits of *Eschericha coli* by Multiple Reaction Monitoring.
Proteomics. 2014. 14:1630-1638. doi: 10.1002/pmic.201300563.

Kristin Surmann, Stephan Michalik, Petra Hildebrandt, Philipp Gierok, Maren Depke, Lars Brinkmann, Jörg Bernhardt, Manuela Gesell Salazar, Zhi Sun, David Shteynberg, Ulrike Kusebauch, Robert Moritz, Bernd Wollscheid, Michael Lalk, Uwe Völker, Frank Schmidt.
Comparative analysis reveals common and host cell specific proteome patterns of the adaptation of *Staphylococcus aureus* to internalization by different types of human non-professional phagocytic host cells.
Frontiers in Microbiology, Systems Microbiology. 2014. 5:392. doi: 10.3389/fmicb.2014.00392.

Maren Depke*, Stephan Michalik*, Alexander Rabe, **Kristin Surmann**, Lars Brinkmann, Nico Jehmlich, Jörg Bernhardt, Bernd Wollscheid, Zhi Sun, Robert Moritz, Uwe Völker, Frank Schmidt.
The *Staphylococcus aureus* proteotype resource.
Submitted to MCP, 02.10.2014.

Kristin Surmann, Marjolaine Simon, Petra Hildebrandt, Henrike Pförtner, Stephan Michalik, Sebastian Stentzel, Leif Steil, Vishnu M. Dhople, Jörg Bernhardt, Rabea Schlüter, Maren Depke, Philipp Gierok, Michael Lalk, Barbara Bröker, Frank Schmidt, Uwe Völker.
Proteomic characterization of the interplay of *Staphylococcus aureus* and human alveolar epithelial cells during infection.
In preparation.

Jimena Alvarez Hayes*, Yanina Lamberti*, **Kristin Surmann**, Frank Schmidt, Uwe Völker, Maria Eugenia Rodriguez.
Shotgun proteomic analysis of *Bordetella pertussis* response to iron availability.
In preparation.

* Both authors contributed equally.

Posters & Talks

Kristin Surmann, Manuel Liebeke, Britta Jürgen, Thomas Schweder, Michael Lalk.
Metabolomics of an industrial microorganism, *Bacillus licheniformis* under glucose starvation.
"Jahrestagung der Deutschen Pharmazeutischen Gesellschaft", Bonn, Germany, 08.10.-11.10.2008 [Poster]

Kristin Surmann, Sandra Scharf, Henrike Pförtner, Marc Burian, Frank Schmidt, Uwe Völker.
Characterization of the response of *Staphylococcus aureus* to the host cell environment *via* Multiple Reaction Monitoring (MRM).
"Host-pathogen interactions in bacterial infections", Alfried Krupp Wissenschaftskolleg Greifswald, Germany, 31.05.-03.06.2010 [Poster]

Kristin Surmann, Petra Hildebrandt, Henrike Pförtner, Vishnu M. Dhople, Frank Schmidt, Uwe Völker.
Characterization of the response of *Staphylococcus aureus* to the host cell environment: Enrichment and analysis of secreted *S. aureus* proteins by isolation of phagosomes.
"Jahrestagung der Vereinigung für Allgemeine und Angewandte Mikrobiologie", Karlsruhe, Germany, 03.04.-06.04.2011 [Poster]

Kristin Surmann
Characterization of the response of *Staphylococcus aureus* to the host cell environment: Enrichment and analysis of *S. aureus* proteins by isolation of phagosomes.
"Summer school in Functional Genomics of Microorganisms of Alfried Krupp Wissenschaftskolleg Greifswald, Mini-Symposium: Molecular Microbiology, Health and Diseases", Tel Aviv University, Tel Aviv, Israel, 29.05.-03.06.2011 [Talk]

Frank Schmidt, Maren Depke, Sandra Scharf, Petra Hildebrandt, Elke Hammer, Melanie Gutjahr, **Kristin Surmann**, Juliane Wagner, Henrike Pförtner, Vishnu M. Dhople, Jörg Bernhardt, Michael Hecker, Ulrike Mäder, Uwe Völker.
Global analysis of the response of *Staphylococcus aureus* to internalization into human epithelial cells: an integrated, time-resolved functional genomics approach.
"HUPO 10th Annual World Congress", Geneva, Switzerland, 04.09.-07.09.2011 [Poster]

Kristin Surmann, Marjolaine Simon, Petra Hildebrandt, Henrike Pförtner, Vishnu M. Dhople, Rabea Schlüter, Jörg Bernhardt, Frank Schmidt, Uwe Völker.
Proteomic characterization of host pathogen interactions during internalization of *S. aureus* by A549 cells.
"Jahrestagung der Vereinigung für Allgemeine und Angewandte Mikrobiologie", Tübingen, Germany, 18.03.-21.03.2012 [Poster]

Kristin Surmann, Marjolaine Simon, Petra Hildebrandt, Vishnu M. Dhople, Rabea Schlüter, Henrike Pförtner, Jörg Bernhardt, Frank Schmidt, Uwe Völker.
Proteomic characterization of host pathogen interactions during internalization of *S. aureus* HG001 by A549 cells.
"6th European Summer School in Proteomic Basics", Brixen, Italy, 19.08.-25.08.2012 [Poster], [awarded FEBS (Federation of European Biochemical Societies) travel grant]

Frank Schmidt, Maren Depke, Sandra Ernst, Marjolaine Simon, Danny Kägebein, Petra Hildebrandt, **Kristin Surmann**, Henrike Pförtner, Vishnu Dhople, Jörg Bernhardt, Stephan Fuchs, Stephan Michalik, Uwe Völker.
The response of *Staphylococcus aureus* to internalization into three different human cell lines: a time-resolved proteomics study.
"9th Siena Meeting, From Genome to Proteome: Open Innovations", Siena, Italy, 26.08.-30.08.2012 [Talk]

Frank Schmidt, Maren Depke, Sandra Ernst, Marjolaine Simon, Danny Kägebein, Petra Hildebrandt, **Kristin Surmann**, Henrike Pförtner, Vishnu Dhople, Jörg Bernhardt, Stephan Fuchs, Stephan Michalik, Uwe Völker.
The response of *Staphylococcus aureus* to internalization into three different human cell cines: a time-resolved proteomics study.
"HUPO 11th Annual World Congress", Boston, USA, 09.09.-14.09.2012 [Talk]

Kristin Surmann, Stephan Michalik, Henrike Pförtner, Marjolaine Simon, Petra Hildebrandt, Vishnu M. Dhople, Rabea Schlüter, Jörg Bernhardt, Sebastian Stentzel, Barbara Bröker, Uwe Völker, Frank Schmidt.
Characterization of host pathogen interactions during internalization of *Staphylococcus aureus* HG001 by A549 cells.
"Proteomics Forum 2013", Berlin, Germany, 17.03.-21.03.2013 [Poster]

Kristin Surmann, Marjolaine Simon, Maren Depke, Petra Hildebrandt, Henrike Pförtner, Sebastian Stentzel, Stephan Michalik, Vishnu Dhople, Jörg Bernhardt, Rabea Schlüter, Leif Steil, Barbara Bröker, Uwe Völker, Frank Schmidt.
In deep characterization of the host pathogen interaction during internalization of *Staphylococcus aureus* by A549 cells.
"HUPO 12th Annual World Congress", Yokohama, Japan, 14.09.-18.09.2013 [Talk]

Kristin Surmann, Marjolaine Simon, Petra Hildebrandt, Henrike Pförtner, Stephan Michalik, Vishnu M. Dhople, Frank Schmidt, Uwe Völker.
Proteomic characterization of the interplay of *Staphylococcus aureus* and human lung epithelial cells during infection.
"65. Jahrestagung der Deutschen Gesellschaft für Hygiene und Mikrobiologie (DGHM) e.V.", Rostock, Germany, 22.09.-25.09.2013 [Talk]
Maren Depke, **Kristin Surmann**, Petra Hildebrandt, Nico Jehmlich, Stephan Michalik, Sarmiza E Stanca, Wolfgang Fritsche, Uwe Völker, Frank Schmidt.
Labeling of *Staphylococcus aureus* with fluorescent or para-magnetic nanoparticles highlights new capabilities for following host-pathogen interactions.
"23rd Annual Conference of the German Society for Cytometry", Dresden, Germany, 09.10.-11.10.2013 [Talk]

Kristin Surmann, Stephan Michalik, Petra Hildebrandt, Philipp Gierok, Maren Depke, Lars Brinkmann, Jörg Bernhardt, Manuela Gesell Salazar, Zhi Sun, David Shteynberg, Ulrike Kusebauch, Robert Moritz, Benrd Wollscheid, Michael Lalk, Uwe Völker, Frank Schmidt.
Comparative analysis of the adaptation of *Staphylococcus aureus* to internalization by different types of human nonprofessional phagocytic host cells.
"4. Gemeinsame Konferenz von DGHM und VAAM", Dresden, 05.10.-08.10.2014 [Poster]

Emina Cudic, **Kristin Surmann**, Elke Hammer, Sabine Hunke.
The role of the Cpx-system within the envelope stress systems in *Escherichia coli* analyzed by MRM and co-localization studies.
“4. Gemeinsame Konferenz von DGHM und VAAM“, Dresden, 05.10.-08.10.2014 [Poster]

Jörg Bernhardt, Stephan Fuchs, Henry Mehlan, Andreas Otto, Stephan Michalik, **Kristin Surmann**, Stefan Weiß, Linus Backert, André Henning, Alexander Herbig, Kay Nieselt, Michael Hecker, Katharina Riedel, Uwe Völker, Ulrike Mäder.
*Aureo*Wiki - the repository of the *Staphylococcus aureus* research and annotation community.
“4. Gemeinsame Konferenz von DGHM und VAAM“, Dresden, 05.10.-08.10.2014 [Poster]

Presenting author

DANKSAGUNG

- An erster Stelle möchte ich mich sehr herzlich bei Prof. Dr. Uwe Völker für die Vergabe des sehr interessanten Themas sowie für zahlreiche hilfreiche Diskussionen und Ratschläge bedanken. In seiner Arbeitsgruppe bekam ich die Möglichkeit vielfältige Methoden zu erlernen, sowie auch durch Teilnahme an interessanten Konferenzen und Betreuung von Studenten mein Wissen zu erweitern und zu vertiefen.
- Weiterhin geht ein großer Dank auch an Dr. Frank Schmidt für seine Unterstützung während der gesamten Doktorarbeit, das Korrekturlesen der Arbeit und viele gute Ideen, die die Arbeit vorangebracht und stets mit neuen Projekten bereichert haben.
- Bei Dr. Elke Hammer bedanke ich mich für die Ermöglichung der Mitarbeit in Kooperationsprojekten aber auch für viele gute, hilfreiche Ratschläge sowie Geduld und Unterstützung beim Kdp-Paper.
- Besonderer Dank gebührt meinem Büro-Mitbewohner Dr. Vishnu M. Dhople, der mir mit seiner unerschöpflichen Geduld nicht nur bei der Lösung vielfältiger Probleme mit LC und MS half, sondern mir auch immer mit einem guten Rat zur Seite stand.
- Dr. Petra Hildebrandt danke ich herzlich für die unzähligen FACS-Analysen, für die Vermittlung ihres Wissens in der Zellkultur und der Durchflusszytometrie, die mir die Hintergründe der GUAVA-Analysen näher gebracht haben.
- Lars Brinkmann und Dirk Lewerentz danke ich für die Hilfe bei immer wieder neuen Problemen mit dem Computer.
- Ich danke auch Dr. Manuela Gesell Salazar und Annette Murr für die unermüdlichen Anstrengungen die Proteomanalysen zum Vergleich der Zelllinien trotz Widerstands der Q Exactive schließlich doch erfolgreich durchzuführen.
- Bei allen aktuellen und ehemaligen Mitgliedern und Gästen der Funktionellen Genomforschung möchte ich mich für das stets gute Arbeitsklima, sowie kleinere und größere Hilfen im Arbeitsalltag bedanken.
- Hervorheben möchte ich Dr. Nico Jehmlich, Dr. Leif Steil, Dr. Stefan Weiß und Dr. Stephan Michalik, die mir oft bei der Datenauswertung halfen. Weiterhin danke ich Anja Wiechert, Ashley Haluck-Kangas, Danny Kägebein, Henrike Pförtner, Janine Gumz, Jörn Steinke, Kirsten Bartels, Dr. Maren Depke, Marjolaine Simon, Marc Schaffer, Nicole Normann und Dr. Praveen Kumar Sappa für Unterstützung im Labor.
- Ganz besonders herzlich möchte ich mich bei meinen lieben fleißigen Korrekturlesern Dr. Maren Depke, Dr. Sarah Foerster und Christian Hentschker bedanken, die diese Arbeit damit sehr verbessert haben.
- Ich danke auch Kollegen aus anderen Greifswalder Arbeitsgruppen, die mir mit speziellen Analysen aushalfen: Dr. Rabea Schlüter (TEM), Philipp Gierok (Metabolom), Dr. Jan Pané-

Farré (konfokale Fluoreszenzmikroskopie), Jörg Bernhardt (Treemaps), Sebastian Stenzel (Durchführung einiger Western Blots).

- Den Mitarbeitern im Forschungszentrum Borstel um Dr. Norbert Reiling, Dr. Christine Steinhäuser und Katrin Seeger danke ich für die Möglichkeit einige Zeit in ihren Laboren zu arbeiten und mein Wissen zur Phagosomenisolierung zu erweitern.
- Dr. Sarmiza E. Stanca und Dr. Wolfgang Fritsche, den Kooperationspartnern im Nanopartikel-Projekt, danke ich für die Bereitstellung der Partikel.
- Den Kooperationspartnern aus Seattle Dr. Zhi Sun, Dr. David Shteynberg, Dr. Ulrike Kusebauch und Prof. Dr. Robert L. Moritz danke ich für die komplexe Datenauswertung und Zusammenarbeit beim Zelllinienpaper.
- Auch den Osnabrücker Kooperationspartnern Prof. Dr. Sabine Hunke und Emina Ćudić sowie Prof. Dr. Karlheinz Altendorf und Dr. Vera Laermann, ebenso Dr. Yanina Lamberti von der Universität La Plata in Argentinien, danke ich für die gute Zusammenarbeit und das Vertrauen, dass sie mir entgegen brachten, ihre Proben mittels MRM zu vermessen.
- Die Arbeit wurde unter anderem mit Hilfe der Graduiertenschule „A Functional Genomics Approach to Infection Biology“ der Alfried Krupp von Bohlen und Halbach-Stiftung, dem Graduiertenkolleg GRK1870BacRes sowie dem SFB Transregio 34 finanziert und unterstützt.
- Der größte Dank gebührt natürlich meiner Familie, meinen Freunden und meinem Freund, die mich während des Studiums und der Promotionszeit unterstützt und in den richtigen Momenten immer wieder motiviert oder abgelenkt haben.